Elemental Composition in Monocytes in response to Anti-Malarial Drugs and Hemozoin

by

Tamara Ann Hiltunen

(neé Cannon)

B. Sc. (Hons) (Natal)

Submitted in fulfilment of the

academic requirements for the degree of

Master of Science

in

Biochemistry

in the

School of Molecular and Cellular Biosciences

University of Natal

Pietermaritzburg

September 2003

PREFACE

The experimental work described in this dissertation was carried out in the Department of Biochemistry, University of Natal, Pietermaritzburg from January 2001 to October 2002 under the supervision of Professor J. P. D. Goldring.

These studies represent original work by the author and have not been submitted in any other form to another university. Where use was made of the work of others, it has been duly acknowledged in the text.

Tamara Hiltunen
September 2003

ABSTRACT

Every year there are approximately 300 million new cases of malaria with 2 million deaths. The majority of deaths occur in African children between the ages of 1 and 4 years and are caused by the parasite *Plasmodium falciparum*. Approximately R90-million is spent by the South African government each year to control malaria. Peripheral blood monocytes are the first line of defence during infection and they perform many functions, such as phagocytosis, intracellular and extracellular killing by the generation of reactive oxygen intermediates and the production of cytokines. During malaria infection some of these functions are suppressed or elevated by phagocytosis of hemozoin, fever conditions (heat shock) and the presence of anti-malarial drugs in the bloodstream of the patient. Under normal conditions phospholipase A_2 (PLA_2) is down regulated by heat shock protein 70 (HSP70) but in severe malaria PLA_2 is elevated. Two antigenic peptides were selected from the highly conserved human HSP70 and HSC70 proteins. Anti-peptide antibodies raised in chickens were affinity purified and were able to recognize the free peptide in an ELISA and the native proteins in human and canine heat shocked lymphocyte lysates on western blots. Antibodies against HSP70 detected two major proteins at 70 kDa and 33 kDa, which are most likely native HSP70 and a possible breakdown product of HSP70 respectively. The anti-HSC70 antibodies detected two proteins, an as yet unidentified 100 kDa protein and the 70 kDa HSC70. Due to the monocytes being activated during the isolation procedure, HSP70 was expressed at both 37°C and 44°C in this study. Electron-probe X-ray microanalysis enables determination of the elemental composition of any sample under the electron microscope. When the electron beam interacts with a specimen, X-rays are generated and can be used to identify and quantify the elements in the cell. Canine monocytes were analysed using this technique after incubation with therapeutically relevant concentrations of anti-malarial drugs, β-hematin and under fever conditions. The concentrations of the elements in normal canine monocytes were: Na (518.2 mmoles/kg), Mg (199.1 mmoles/kg), P (439.7 mmoles/kg), S (316.3 mmoles/kg), Cl (279.7 mmoles/kg), K (204 mmoles/kg) and Ca (81.3 mmoles/kg). All the drugs (quinine, chloroquine, primaquine, pyrimethamine, artemisinin, tetracycline, doxycycline, dapsone and suramin), phagocytosis of latex beads and β-hematin as well as heat shock, altered the elemental concentrations of canine monocytes in a unique way. Quinine, artemisinin and

suramin were the most influential drugs in altering the concentrations of elements in the cells. Suramin substantially increased the concentration of Ca (356%) after 18 h and decreased K concentration (64%) after 18 h. Quinine decreased the concentrations of Na (47%), Cl (70%), and K (67%). The concentrations of P (52%) and Ca (72%) were increased by quinine after 10 min. Artemisinin induced small increases in Mg (21%) and K (38%) concentrations within 10 min and large increases in the concentrations of Na (291%) and Cl (389%) after 18 h. Chloroquine induced a large increase in S (212%). Quinine induced major changes after 10 min whereas artemisinin, suramin chloroquine induced huge changes after 18 h. Although artemisinin did increase the concentrations certain elements after 10 min, it was by much smaller amounts than after 18 h. Quinine, suramin and pyrimethamine altered the P/K ratios by the greatest margins whereas artemisinin had no significant effect. The P/K ratio was increased by quinine (348%) after 10 min and suramin (261%) after 18 h. Pyrimethamine decreased the P/K ratio after 18 h by 49%. The findings suggest that further investigations into the alterations in the elemental concentrations of monocytes by anti-malarial drugs, fever and hemozoin may lead to a greater understanding of the influence of these conditions in a patient during a malaria infection and its treatment.

ACKNOWLEDGMENTS

I would like to express my appreciation to the following people for their invaluable contributions to this dissertation:

Prof. Dean Goldring, for all his support, endless ideas and faith in my ability to make this project work, even after numerous technical failures.

Dr. Alice Warley, for her help and guidance with the EPXMA calibration and quantification. Especially for taking a day out of her holiday in SA to help me.

Dr. Tanya Hughes and the Scottsville Society for the Prevention of Cruelty to Animals (SPCA), for providing canine blood whenever I needed it.

The EM unit staff – Vijay Bandu, Belinda White, Cilla Donnelly, Helen Roberts & Tony Bruton, for guidance in using the equipment in the unit, amongst many other things.

My lab colleagues, for discussions, laughter and support – Christina Thobakgale, Pamela Mkhize, Brendan Meyer, Tim Smallie, Ike Achilonu, Laura Huson & Habtom Habte.

To the secretaries and lab technicians for ordering or helping me find the required chemicals – Jenny Schwartz, Janine Jeary, Melody Webber, Denzil Lakay & Yegan Pillay.

The National Research Foundation & the University of Natal Research Fund for financial assistance that made this study possible.

My parents for their love and support.

To my husband Daryn, for laughter, love & fun, as well as his infinite support and patience.

Finally, to all my friends, near and far, for simply being there when needed.

LIST OF TABLES

LIST OF FIGURES

ABBREVIATIONS

aa	amino acid
A_{280}	absorbance at 280 nm
A_{405}	absorbance at 405 nm
ABTS	2,2'-azino-di-(3-ethyl)-benzthiozoline sulfonic acid
AEBSF	4-(2-aminoethyl)-benzenesulfonyl fluoride
ATP	adenosine triphosphate
BCIP	5-bromo-4-chloro-3-indolylphosphate
bis	N,N'-methylenebisacrylamide
BSA	bovine serum albumin
C-terminal	carboxy terminal
CD	cluster determinant
CPD	citrate-phosphate-dextrose
Da	dalton(s)
DAB	3,3'-diaminobenzidine
ddH_2O	distilled, deionised water
DDT	dichlorodiphenyltrichloroethane
DF	dilution factor
dH_2O	distilled water
DHFR	dihydrofolate reductase
DMF	dimethylformamide
DMSO	dimethylsulphoxide
DNA	deoxyribonucleic acid
DPX	distrene dibutyl phthalate xylene
DTT	dithiothreitol
E	extinction coefficient
E64	N-[(L-3-*trans*-carboxyoxiran-2-carbonyl)-L-leucyl]-amido(4-guanidino)butane
EDTA	ethylenediaminetetraacetic acid, disodium salt
ELISA	enzyme-linked immunosorbent assay
EPXMA	electron probe X-ray microanalysis
ESEM	environmental scanning electron microscope

EXAFS	extended X-ray absorption fine structure
FCA	Freund's complete adjuvant
FCS	fetal calf serum
FIA	Freund's incomplete adjuvant
FP	ferriprotoporphyrin IX
g	relative centrifugal force
GPI	glycosylphosphatidylinositol
h	hour(s)
HEPES	N-2-hydroxyethylpiperazine-N'-2-ethanesulphonic acid
HRG	histidine rich glycoprotein
HNE	4-hydroxy-trans-nonenal
HRP	histidine rich protein
HRPO	horseradish peroxidase
HSC70	heat shock cognate protein 70
HSP70	heat shock protein 70
iNOS	inducible nitric oxide synthase
iRBC	infected red blood cell (malaria)
ICAM	intercellular adhesion molecule
IFN	interferon
IgG	immunoglobulin G
IgY	immunoglobulin Y
IL	interleukin
IR	infra-red spectrum
kDa	kilodalton(s)
LAM	leucocyte adhesion molecule
LFA	leucocyte function antigen
LPS	lipopolysaccharide(s)
min	minute(s)
mRNA	messenger ribonucleic acid
mTHF	methylene-tetrahydrofolate
MBS	m-maleimidobenzoyl-N-hydroxysuccinimide ester

MDL	minimum detection limit
MEC	molecular exclusion chromatography
MHC	major histocompatibility complex
MIF	migration inhibitory factor
MPO	myeloperoxidase
MW	molecular weight
N-terminal	amino terminal
NBT	nitroblue tetrazolium
NOX	nitric oxide synthase
PABA	para-aminobenzoic acid
PAGE	polyacrylamide gel electrophoresis
PBS	phosphate buffered saline
PEG	polyethylene glycol
PLA_2	phospholipase A_2
PKC	protein kinase C
PMN	polymorphonuclear leucocyte
PMSF	phenylmethylsulfonyl fluoride
®	registered trademark
RBC	red blood cell
RNA	ribonucleic acid
RNI	reactive nitrogen intermediates
ROI	reactive oxygen intermediates
RPMI	Roswell Park Memorial Institute
RT	room temperature
s	second(s)
SDS	sodium dodecyl sulfate
SDS-PAGE	sodium dodecyl sulfate polyacrylamide gel electrophoresis
SEM	scanning electron microscope
™	trademark
TBS	Tris buffered saline
TEM	transmission electron microscope

TEMED	N,N,N',N'-tetramethylethylenediamine
TH	helper T-lymphocytes
TNF-α	tumor necrosis factor-α
Tris	2-amino-2-(hydroxymethyl)-1,3-propandiol
U	unit of enzyme activity
UV	ultraviolet
VCAM	vascular cellular adhesion molecule

TABLE OF CONTENTS

CHAPTER 1

INTRODUCTION

1.1 MALARIA

Every year there are approximately 300 -500 million new cases of malaria with between 1.5 and 2.7 million deaths (Carosi and Castelli, 1997); to put this value into perspective a person dies of malaria every 12 seconds (Butler *et al.*, 1997; Philips, 2001). The majority of deaths occur in African children between the ages of 1 and 4 years. Approximately R90-million is spent by the South African government each year to control malaria, this includes treatment of people who have contracted the disease as well as buying DDT to spray infected areas (Health Systems Trust news article, 2001).

Protozoal parasites of the *Plasmodium* genus are responsible for the disease in a wide range of vertebrates, but four morphologically distinct species (*P. falciparum, P. vivax, P. ovale* and *P. malariae*) infect humans (Collins and Paskewitz, 1995). The most morbidity and mortality is caused by *P. falciparum*.

Female mosquitoes of the genus *Anopheles* are the vectors of the malaria parasites, with nearly 20% of the 500 plus described species implicated in transmission of the parasites (Collins and Paskewitz, 1995). The transmission of malaria is dependent on climate and geography and coincides with the rainy season (Coetzee *et al.*, 2000; Petney, 2001).

1.1.1 Life cycle of malaria parasites

The life cycle of the malaria parasite comprises of stages in invertebrate and vertebrate host's, as well as intracellular and extracellular developmental stages. The intricacy of the host response to infection by these parasites is not surprising considering the complexity of the organism's life cycle (Figure 1.1).

The bite of an infected anopheline mosquito initiates the infection, with motile sporozoites being injected into the bloodstream (Deans and Cohen, 1983). The sporozoites remain in the bloodstream for 30 min prior to entering hepatic parenchyma cells (Wernsdorfer, 1980). Here they become multinucleated hepatic schizonts, wherein many thousands of tiny invasive merozoites develop. After approximately one week after infection, the liver cells rupture and release more than 30,000 merozoites, in a *P. falciparum* infection, into the hepatic capillaries (Knell, 1991). The merozoites invade erythrocytes within a few minutes of their release, where they appear as a ring shape (Wernsdorfer, 1980). The merozoite now becomes an erythrocytic trophozoite that ingests and digests hemoglobin. The trophozoite accumulates hemozoin as it grows and divides into a schizont (Knell, 1991). During *P. falciparum* malaria, the trophozoites and schizonts are usually absent from the peripheral blood as they are sequestered within the deep vascular beds (Newton *et al.*, 2000). Erythrocytic schizonts rupture periodically, with the periodicity depending on the species; each blood cell releases 10 – 20 merozoites and these invade new erythrocytes (Noble and Noble, 1982; Deans and Cohen, 1983). At the same time hemozoin is also released. The clinical manifestations of malaria, such as the shivering and sweating stages coincide, with the erythrocytic cycle of the parasite (Sherry *et al.*, 1995). A number of merozoites, after invading a new erythrocyte differentiate into gametocytes.

Sexual reproduction occurs when the gametocytes are ingested into the gut of the mosquito and are transformed into gametes (Wernsdorfer, 1980; Noble and Noble, 1982). The zygote elongates and becomes an actively mobile ookinete, which enters the invertebrates' gut epithelium. It comes to rest under the basal lamina, forming an oocyst. The oocyst's cytoplasm divides to form sporozoites. When these emerge they migrate to the host's salivary glands, where they penetrate the cells until they reach the lumina of the salivary duct (Wernsdorfer, 1980). Here they remain until the mosquito feeds again and the cycle begins once more.

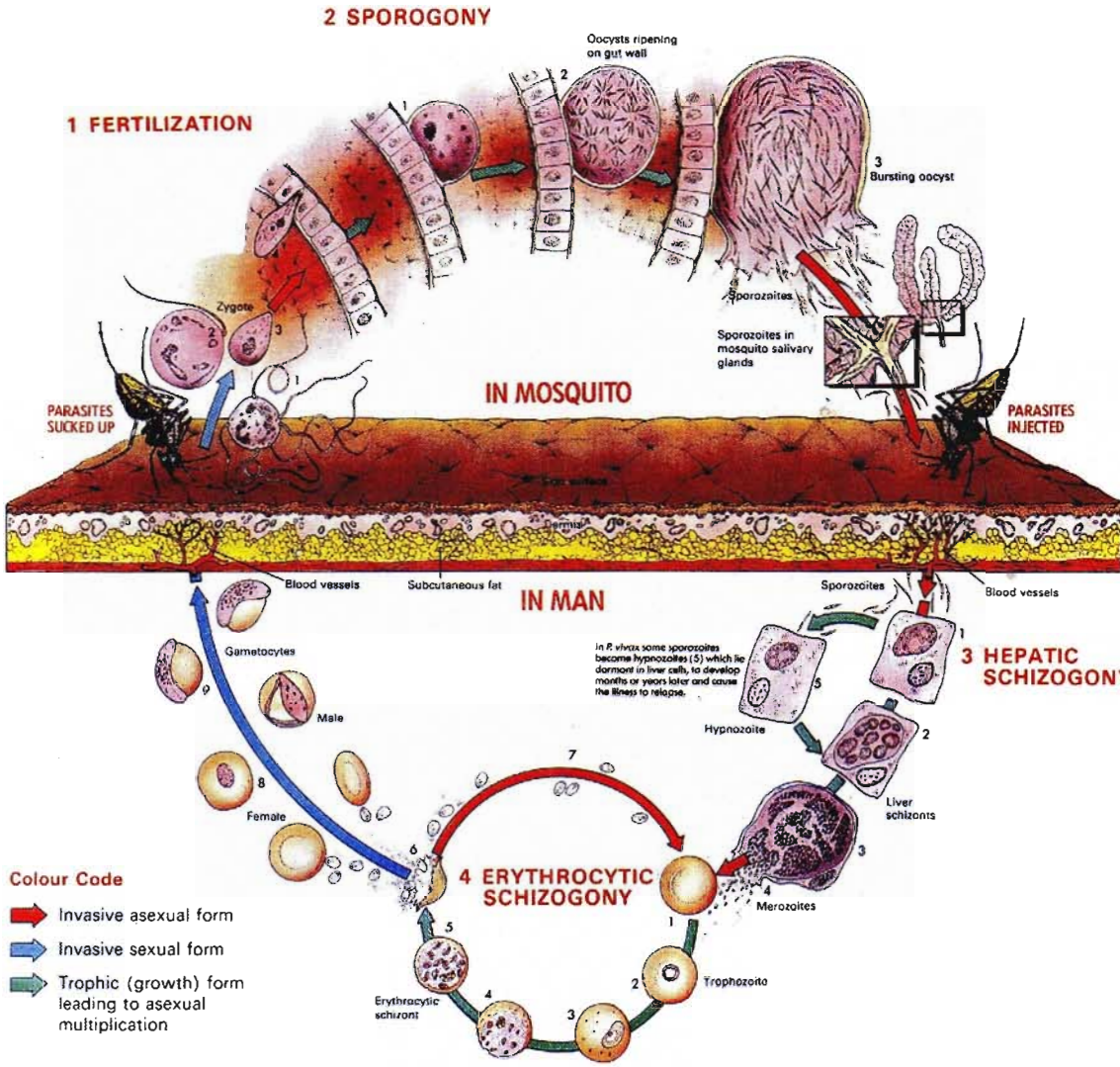

Figure 1.1 The life cycle of *Plasmodium* malaria parasites. Adapted from Knell (1991).

1.1.2 The malaria problem

On August 16, 1897 the Surgeon-Major Ronald Ross dissected an *Anopheles* mosquito, that had previously fed on a malaria patient (Schmidt and Roberts, 1989). He found the malaria parasites in the stomach lining of the insects. That day he wrote in his notebook:

> This day designing God
> Hath put into my hand
> A wondrous thing. And God
> Be praised. At this command
> I have found they secret deeds
> Oh million-murdering Death
>
> I know that this little thing
> A myriad men will save -
> Oh death where is they sting?
> Thy victory oh Grave?

Ross thought that they had conquered malaria by finding the mosquito stages of the infection. But that was 106 years ago, and we are still no closer to conquering malaria. Of great concern today is the resurgence of malaria, when in the early 60s it was nearly completely eradicated. Some of the reasons are mentioned in Table 1. However, the technological age and the increase in the gap between poverty stricken and 'wealthy' nations can be seen as some of the most important man-made factors. The increase in resistance of the malarial parasites to the drugs used in treatment of malaria (Rosenblatt, 1999) and the resistance of vectors to insecticides are also other contributors.

Average global temperatures are predicted to rise by 1.5 - 6°C by 2100, which will ultimately impact the geographical distribution of malaria (Patz and Reisen, 2001). The minimum temperature required for *Plasmodium falciparum* and vector development is between 15 and 18°C.

Table 1.1 Reasons for the resurgence of malaria.

Man-made	Complacency and laxity in anti-malarial campaigns
	Conflicts and wars
	Deteriorating health systems
	Poverty
	Malnutrition
	Overcrowding
	Human encroachment on forest and other 'frontier lands'
Parasite	Drug resistance
Vector	Insecticide resistance
	Ban on DDT
Environment	Global warming – increased breeding and life span of the insect vector
	Unusual El Niño type weather conditions
Jet age	Shrinking world – spread of malaria from endemic areas to all other parts of the world

1.2 ANTI-MALARIAL DRUGS

A relatively small number of drugs against malaria are available today. Drugs are used in two capacities, for prophylaxis and for treatment of the disease. Some may be used for both. There are different classes of drug activity (Figure 1.2). Drugs in current use are either based on natural products, such as quinine (Figure 1.3A), artemisinin (Figure 1.3H) and its derivatives, or drugs introduced as a result of research during the 1940s and 1950', such as chloroquine (Figure 1.3B), primaquine (Figure 1.3C) and pyrimethamine (Figure 1.3d) (Breckenridge and Winstanely, 1997). However, since then there have been no really promising anti-malarial drugs with the exception of more artemisinin derivatives.

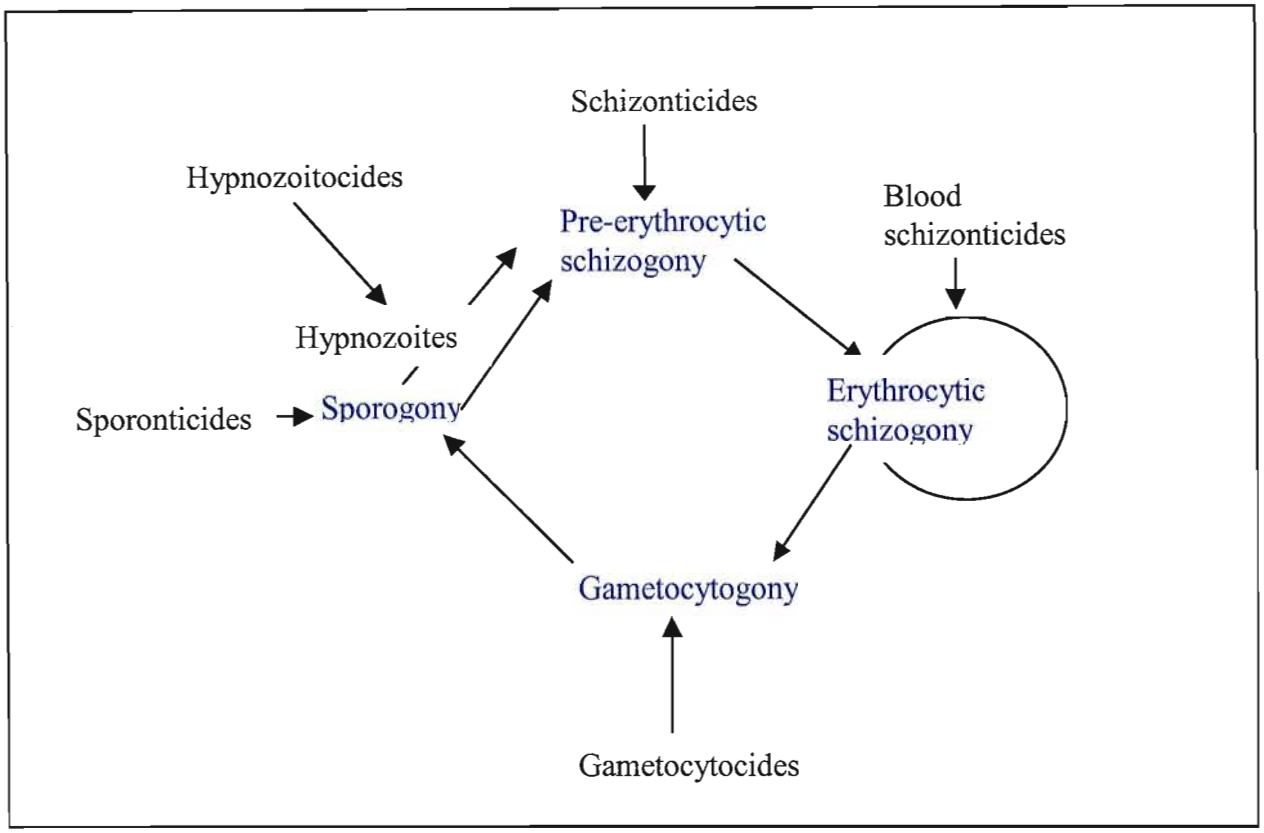

Figure 1.2 Anti-malarial drug activity in relation to the plasmodial life cycle. Drug activity is indicated in black and the plasmodial life cycle is indicated in blue. Adapted from Wernsdorfer (1997).

Briefly, blood schizonticides interfere with erythrocyte schizogony. Since this part of the cycle is when the clinical manifestations appear, they are important in treatment. Gametocytocides affect the gametocytes at any stage in their development; thus far there are none against *P. falciparum* (Wernsdorfer, 1997). The drugs acting against any form within the invertebrate host and thus preventing transmission are known as sporonticides. Hypnozoitocides are anti-relapse drugs as they act against the "latent" hypnozoites. Lastly, the tissue schizontocides affect the schizonts within the hepatocytes (Wernsdorfer, 1997). A number of these activities may be exerted by one drug.

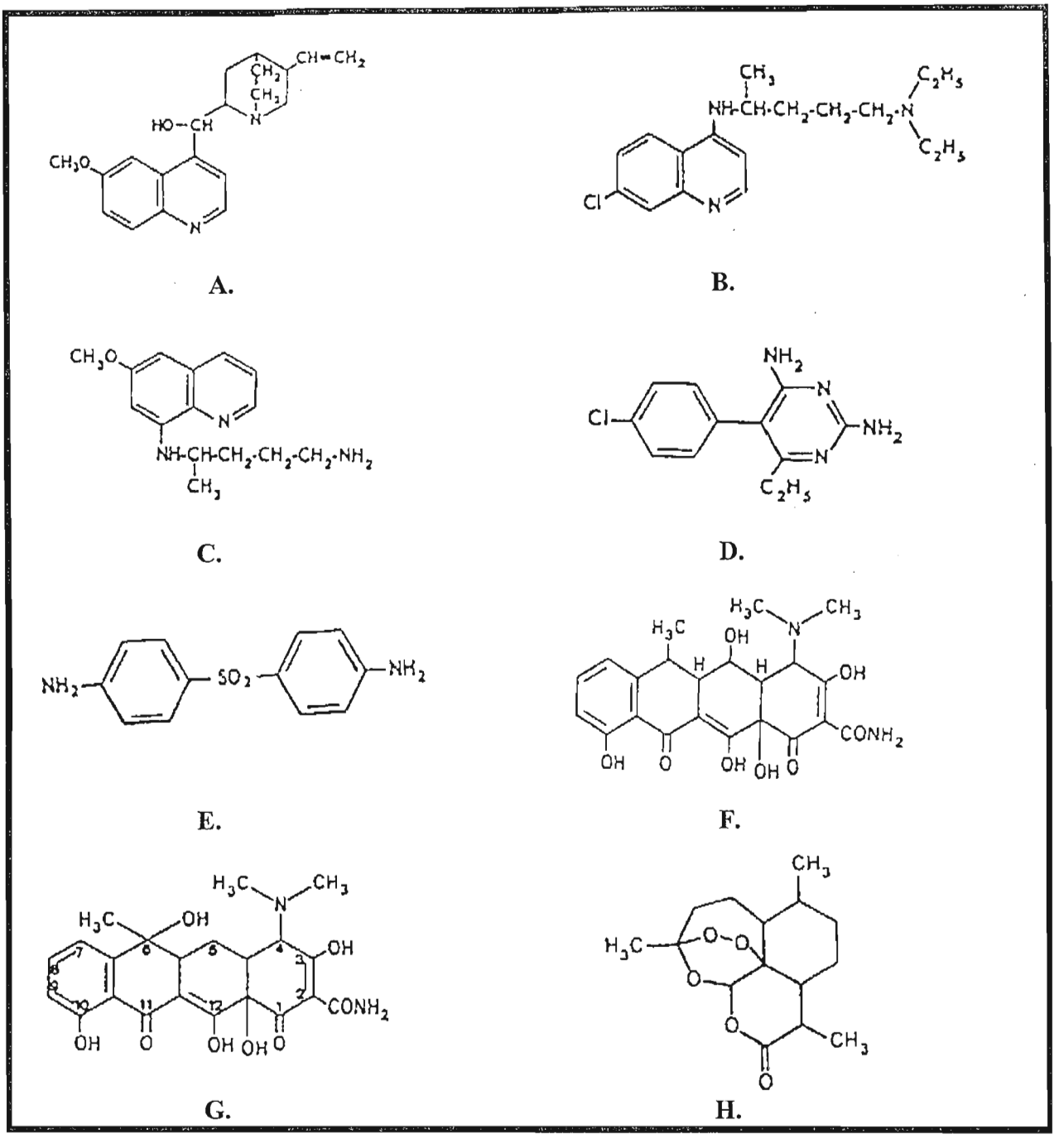

Figure 1.3 Structures of the anti-malarial drugs utilized in this study: A. quinine; B. chloroquine; C. primaquine; D. pyrimethamine; E. dapsone; F. doxycycline; G. tetracycline; H. artemisinin. Adapted from Wernsdorfer (1997).

In the last decade, drug resistance has been developing worldwide. Resistance has been defined as the 'ability of a parasite strain to survive and / or multiply despite the administration

and absorption of a drug given in doses equal to or higher that those usually recommended but within tolerance of the subject' (Bloland and Ettling, 1999).

To put the treatment of malaria into perspective here is a quote from White (1996):
"Mother Nature gave us cinchona alkaloids and qinghaosu. World War II led to the introduction of chloroquine, chloroguanide (proguanil), and eventually amodiaquine and pyrimethamine. The war in Vietnam brought mefloquine and halofantrine. These drugs are all we have available now to treat malaria. It is difficult to see where the next generation of anti-malarial drugs will come from...there is little pharmaceutical industry interest in developing new anti-malarial drugs; the risks are great, but the returns on investment are low... If drug resistance in *P. falciparum* continues to increase at the current rate, malaria may become untreatable in parts of Southeast Asia by the beginning of the next Millennium."

1.2.1 4-Quinolines and related drugs - quinine

The chemical name of quinine is 6-methoxy-α-(5-vinyl-2-quinuclidyl)-4-quinolinemethanol (Figure 1.3A), and it is the main alkaloid extracted from the bark of the *Cinchona* tree (Wernsdorfer, 1997). In the 1650s Jesuit priests used it as an anti-pyretic (Van Beek and Piette, 2001). It was only in 1820, that the alkaloid quinine was isolated from the bark (Crum and Gable, 2000). Its mode of action is blood schizonticidal and it has a very high activity against all human malaria parasites. Parasite protein metabolism is where the drug is thought to exert an effect. Quinine is also a K-channel blocker and this may be another mechanism of action (Maruyama *et al.*, 1994). Quinine is used today intravenously to treat severe and complicated malaria, particularly multi-drug resistant *P. falciparum* (Wernsdorfer, 1997; Raynes, 1999; Skinner-Adams and Davis, 1999). Resistance to quinine has been reported in Southeast Asia, South America and Africa, despite this clinical failure is unusual outside of Southeast Asia (Winstanley, 2000).

Some of the major side effects of quinine treatment include rash, thrombocytopaenia, hemolytic-uremic syndrome or disseminated intravascular coagulation (Crum and Gable, 2000).

1.2.2 4-Aminoquinolines - chloroquine

Chloroquine (Figure 1.3B) is the most widely used of all the anti-malarial drugs (Winstanley, 2000). It is a man-made drug with the chemical formula of 7-chloro-4-(4'-diethylamino-1'-methylbutylamino)quinoline (Wernsdorfer, 1997). It is a blood schizonticidal drug that appears to inhibit the enzymes within the food vacuole of the parasite, as well as hemozoin formation. How it does this is a matter of debate and there are numerous hypotheses, some of which will be discussed. Thus far the proposed mechanisms of chloroquine action include: 1. intercalation with parasite DNA, 2. inhibition of heme-dependent parasite protein synthesis and, 3. inhibition of heme-polymerization (Padmanaban and Ranarajan, 2000).

Electron microscopy studies revealed that there are morphological changes within the food vacuole of *P. falciparum* after treatment with quinoline drugs. These include swelling of the vacuole, vesiculation, pigment clumping (Pandey and Chauhan, 1998; Sullivan, 2002) and accumulation of undigested hemoglobin; these changes indicate inhibition of the normal functioning of the food vacuole (Sullivan Jr *et al.*, 1996b; Raynes, 1999).

Chloroquine is a diprotic weak base that has a pKa_1 of 8.1 and a pKa_2 of 10.2 (Raynes, 1999). It moves down the pH gradient between the acidic digestive vacuole of the parasite and the extracellular matrix (Figure 1.4). Chloroquine is able to diffuse across membranes and accumulate in the food vacuole in its unprotonated form. When the drug enters the acidic milieu of the food vacuole it is protonated and becomes membrane impermeable and hence trapped inside the organelle (Ginsburg *et* al., 1999; Weber *et al.*, 2000). Due to being a weak base, chloroquine is able to achieve a concentration in the food vacuole 1000 – 5000 times that of the external concentration of 10 – 100 nM (Foley and Tilley, 1997; Sullivan, 2002). Evidence from the laboratory of Hawley *et al.* (1998) suggests that a regulator of anti-malarial activity is the extent of drug accumulation in the food vacuole. It has been suggested that within resistant strains of *P. falciparum*, there is an impaired membrane bound proton pump that increases the pH of the food vacuole, resulting in a decrease in the accumulation of chloroquine (Figure 1.4) (Raynes, 1999).

A Na^+/H^+ exchanger has also been implicated in the uptake of chloroquine by infected erythrocytes (Figure 1.4). Using an inhibitor that binds to the Na^+ binding site of the exchanger, the accumulation of chloroquine was decreased. This evidence suggested that chloroquine is transported by the Na^+ binding domain of the exchanger into the parasite, in exchange for protons (Raynes, 1999). However, Bray *et al.* (1998) showed with Na^+-free medium that chloroquine is not directly exchanged for protons by the plasmodial Na^+/H^+ exchanger (Bray *et al.*, 1999).

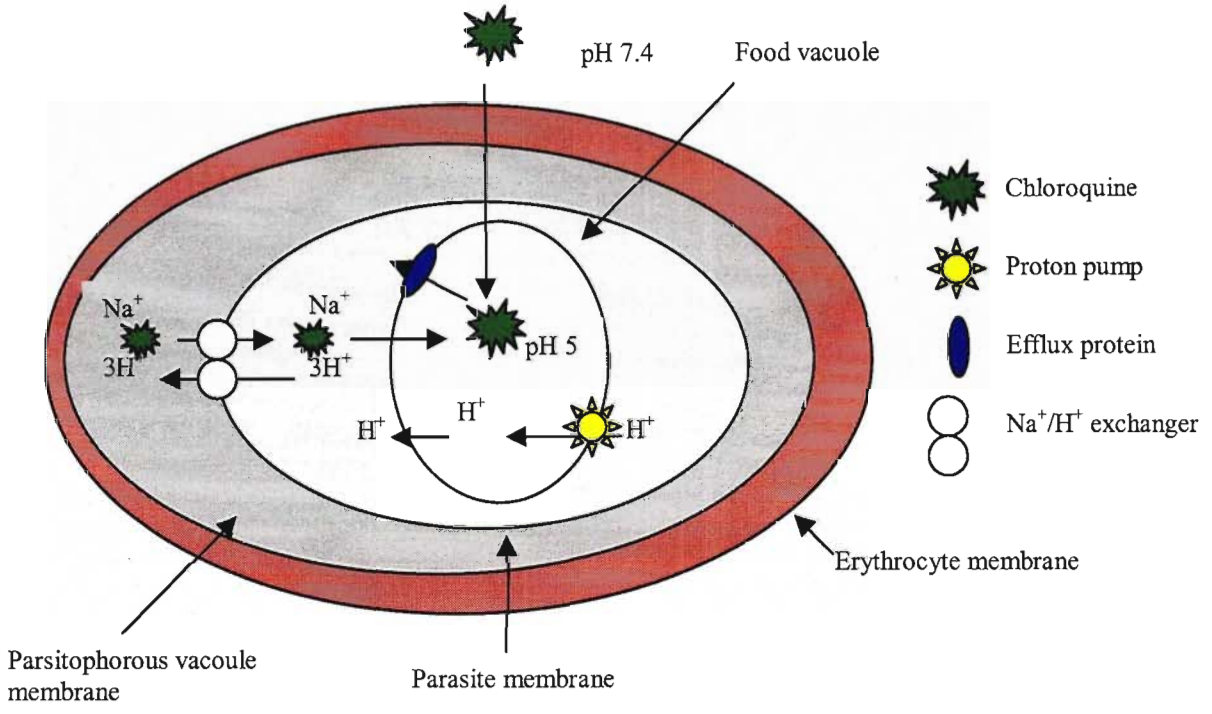

Figure 1.4 Movement of chloroquine and other quinolines in and out of the food vacuole. A mechanism proposed by Raynes (1999).

In chloroquine resistant malaria the drug may be pumped directly out of the food vacuole by a drug efflux protein or more specifically an ATP-dependent P-glycoprotein (Raynes, 1999). This idea was supported by the finding of a gene in *P. falciparum* (*pfmdr 1*), which is homologous to the mammalian multi-drug resistant (MDR) gene that encodes for this protein (Winstanley, 2000). Resistant parasites have also been found to accumulate chloroquine less avidly than non-resistant strains (Winstanley, 2000; Sullivan, 2002). Dua *et al.* (2000) found

evidence to support the hypothesis that resistance to chloroquine comes about from a reduction in the accumulation of the drug in the parasite.

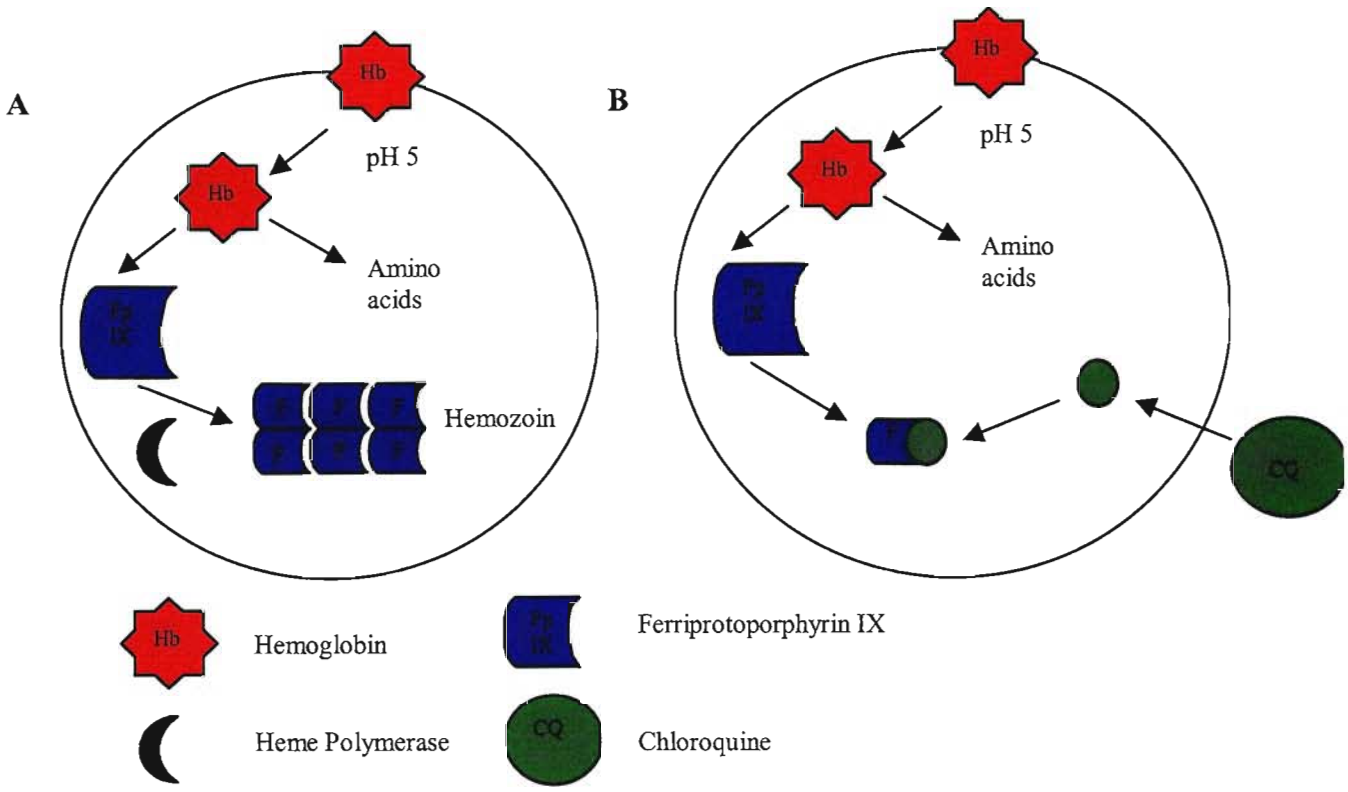

Figure 1.5 Proposed mechanism of chloroquine action on malarial parasites. A. After hemoglobin digestion, ferriprotoporphyrin IX (FpIX) is released. This is detoxified by polymerization into hemozoin, a reaction proposed to be catalyzed by a "heme polymerase". **B.** Chloroquine accumulates in the food vacuole, where it is thought to inhibit the polymerization of heme and thus lead to a build up of the toxic molecule (Foley and Tilley, 1997).

Independent of the way chloroquine enters the food vacuole, it will still have the same mechanism of action. It is believed by some that it is an inhibitor of hemoglobin uptake and digestion (Raynes, 1999).

Chloroquine treatment irreversibly impairs the uptake of lysosomal acid hydrolases as well as affecting the recycling of receptors necessary for this function. Since chloroquine is a base,

when it accumulates in the vacuole it increases the pH, which decreases the activity of the enzymes present. Ultimately, digestion of hemoglobin is inhibited. Alternatively, the sequestration of heme may be inhibited by chloroquine terminating hemozoin polymers prematurely, thus leading to a build up of unpolymerized heme (Figure 1.5) (Sullivan Jr *et al.*, 1996b; Raynes, 1999; Egan *et al.*, 2000). This is probably due to the drug binding to the heme with a K_d as low as 10^{-8} (Egan *et al.*, 1994; Meshnick, 1996; Sullivan Jr *et al.*, 1996b). Zhang *et al.* (1999) found that chloroquine caused a dose-dependent accumulation of hemozoin in the membrane fraction of infected cells, which may correlate with parasite killing via the production of ions that permeabilize the membrane. Egan *et al.* (2000) proposed that the 4-aminoquinoline nucleus of chloroquine is required to bind to ferriprotoporphyrin IX; the 7-chloro group inhibits the formation of β-hematin and the basic amino acid side chain is involved in the drug's accumulation in the parasite's food vacuole.

Chloroquine intercalates with DNA and many groups believe that this explains its anti-malarial activity (Foley and Tilley, 1998). The drug also inhibits DNA replication and RNA synthesis at high concentrations. However, the ability of chloroquine to kill the malaria parasite by this means has been questioned, since it interacts more strongly with GC-rich DNA and the malarial genome is AT-rich (Foley and Tilley, 1998).

Chloroquine has been the most widely used anti-malarial drug for clinical treatment of malaria. However, in recent years it has lost its efficacy due to resistance caused by indiscriminate use as an over-the-counter drug in many countries (Pandey and Chauhan, 1998). Malaria parasites that are chloroquine resistant are killed only by very high levels of the drug. However, it was noted by Orjih and Fitch (1993) that with an increase in drug concentration there is an increase in the amount of hemozoin produced even when the parasitemia is reduced.

1.2.3 8-Aminoquinolines – primaquine

This compound is known as 6-methoxy-8-(4'-amino-1'methylbutylamino) quinoline (Figure 1.3C) that has tissue and blood schizonticidal activity (Wernsdorfer, 1997) and gametocidal activity. Primaquine is not used routinely for *P. falciparum* malaria (Winstanely, 2000). The

drug interacts with hemozoin but does not inhibit hemozoin polymerization (Ridley *et al.*, 1997). Primaquine undergoes extensive but rapid metabolism by oxidative deamination, with a carboxylic acid (carboxyprimaquine) being formed (Na Bangchang *et al.*, 1992). Like chloroquine, primaquine has weak lysosomotrophic base properties (Schwartz *et al.*, 1985). Primaquine has been found to inhibit the mitochondrial respiration of the malaria parasite via oxidation reduction of ubiquinones and to disrupt the synthesis of pyrimidines (López-Antuñano, 1999). Due to its toxicity and the fact that it can cause methemeaglobinaemia, it is used only in treatment, not as a prophylactic.

1.2.4 Dihydrofolate reductase inhibitors - pyrimethamine

Pyrimethamine (Figure 1.3D) has blood schizonticidal activity. It inhibits the enzyme dihydrofolate reductase (DHFR) (EC 1.5.1.4) by competing with higher affinity than the enzyme's substrate for binding to the active site. Chemically, the drug is known as 2,4-diamino-5-p-chlorophenyl-6-ethylpyrimidine (Wernsdorfer, 1997). During normal DNA synthesis, 2'-deoxyribosyluracil monophosphate is converted to 2'-deoxyribosylthymine monophosphate, which is accomplished by methylene-tetrahydrofolate (mTHF) donating a methyl group. The resulting oxidized dihydrofolate is reduced to replenish the pool of mTHF with the rate limiting step in the reduction being catalyzed by DHFR (Winstanley, 2000). The antifolate drugs bind into the hydrophobic active site pocket of DHFR by hydrophobic interactions and hydrogen bonding (Warhurst, 1998).

Resistance to this drug is very high unless it is used in conjunction with the dihydropterate synthase inhibitor sulfadoxine, but resistance to this combination therapy is already widespread (Basco *et al.*, 1994; Juckett, 1999). Unlike the resistance to the quinoline anti-malarials, the resistance to DHFR inhibitors arises when a spontaneous single point mutation in the genes encoding these enzymes (*dhfr*) occurs (Warhurst, 1998; Newton and White, 1999). In Africa these point mutations can be found on *dhfr* at positions 108, 51 and 59, whereas in Southeast Asia a mutation often occurs at position 164 (Macreadie *et al.*, 2000; Winstanley, 2000). Some *P. falciparum* lines in culture have developed an alternate way to bypass the blockage in the folate pathway by these drugs (Macreadie *et al.*, 2000), by making use of external folates, either as folic acid or folininc acid.

1.2.5 Sulfones - dapsone

Dapsone (4,4'-diaminodiphenylsulfone) (Figure 1.3E) was initially used to treat streptococcal infections but due to the large doses required and the subsequent side effects, its use was reduced. In the 1940s it was shown to exert antimycobacterial activity and it became the mainstay of leprosy treatment for many years (Wolf *et al.*, 2000a). It was found to have anti-malarial activity when dapsone-treated leprosy patients were observed to be notably more resistant to malarial infections (Paniker and Levine, 2001). Dapsone is an inhibitor of dihydropteroate synthase and enhances the activity of dihydrofolate reductase inhibitors. It impairs folate synthesis by competing with para-aminobenzoic acid (PABA) for the active site of dihydropteroate synthetase (Wolf *et al.*, 2000a; Paniker and Levine, 2001). Polymorphonuclear phagocyte adherence is inhibited by dapsone (Tingle *et al.*, 1998). Dapsone is a blood schizonticide with moderate activity against *P. falciparum.*

1.2.6 Antibiotics – tetracycline and doxycycline

These include the teracyclines, which are broad spectrum antibiotics that are active against gram-positive and gram-negative bacteria, as well as *Chlamydia*, *Mycoplasma*, rikettsia, spirochetes and some protozoa (Klein and Cunha, 2001). Both tetracycline and doxycycline are used as prophylactics for mefloquine-resistant *Plasmodium falciparum* malaria (Smilack, 1999; Klein and Cunha, 2001).

Tetracycline (4-dimethylamino-1, 4, 4a, 5, 5a, 6, 11, 12a-octahydro- 3, 6, 10, 12, 12a pentahydroxy-6-methyl-1, 11-dioxo-2-naphthacenecarboxamide) (Figure 1.3G) is used to treat malaria resistant to 4-aminoquinolines (Wernsdorfer, 1997). It acts on mitochondria by depressing the activity of dihydroroate dehydrogenase from the pyrimidine pathway, probably by inhibiting synthesis of the enzyme (Pradines *et al.*, 2000).

Doxycycline (4-dimethylamino-1, 4, 4a, 5, 5a, 6, 11, 12a,-octahydro-3, 5, 10, 12, 12a pentahydroxyl-6-methyl-1, 11-dioxo-2-naphthacenecarboxamide) (Figure 1.3F) is a broad-spectrum antibacterial agent that has blood and tissue schizonticidal activity against *P. falciparum*. It is a member of the tetracycline group that is thought to inhibit chelation of Ca^{2+}

and protein synthesis (Wernsdorfer, 1997). Juckett (1999) mentions that doxycycline attacks both the preerythrocytic and erythrocytic phase of the *Plasmodium* life cycle through ribosomal inhibition. It also depletes the levels of deoxynucleoside and nucleoside 5'-triphosphates (Pradines *et al.*, 2000).

1.2.7 Artemisinin and derivatives

Artemisinin or qinghaosu is an endoperoxide sesquiterpene trioxane lactone found in *Artemisia annua* (sweet wormwood) (Basco and Le Bras, 1993; Bradley, 2000). It has a unique structure (Figure 1.3H) and lacks the nitrogen containing heterocyclic ring, found in most anti-malarials used today (Dhingra *et al.*, 2000). The peroxide moiety appears to be responsible for artemisinin's potent anti-malarial activity (Jung, 1994). Its medicinal use was first described in the "52 Prescriptions" unearthed in 168 BC (Hien and White, 1993). Several derivatives have been developed because artemisinin itself is very insoluble; these include arteether, artemether, sodium (Na) artesunate and dihydro-artemisinin (Skinner *et al*, 1996, Edwards *et al.*, 1997; Wernsdorfer, 1997). Artemether is a methyl ether of the parent compound and Na-artesunate is its Na-hemisuccinyl ester. These derivatives are 20 – 100 times more active than the parent compound (Hien and White, 1993).

These all exert potent blood schizonticidal activity although they have different stage specificity within erythrocytic schizogony (Skinner *et al.*, 1996), exerting their anti-malarial effects during the ring and early trophozoite stages (Van Agtmael *et al.*, 1999). These drugs also significantly reduce the number of gametocytocytes in the blood (Philips, 2001). Parasite clearance from the blood is more rapid by these drugs than any other anti-malarial drugs, even at nanomolar concentrations (Dhingra *et al.*, 2000). Artemisinin-type drugs are so potent that the parasite load can be reduced by a factor of 10^4 in a single dose (Philips, 2001). Artemisinin and its derivatives are effective against multi-drug resistant strains of *P. falciparum* (Lloyd, 1999). The only disadvantage currently known is the appearance of recrudescence when these drugs are given in short course monotherapy which is used since they clear parasites within 48 hours (Van Agtmael *et al.*, 1999).

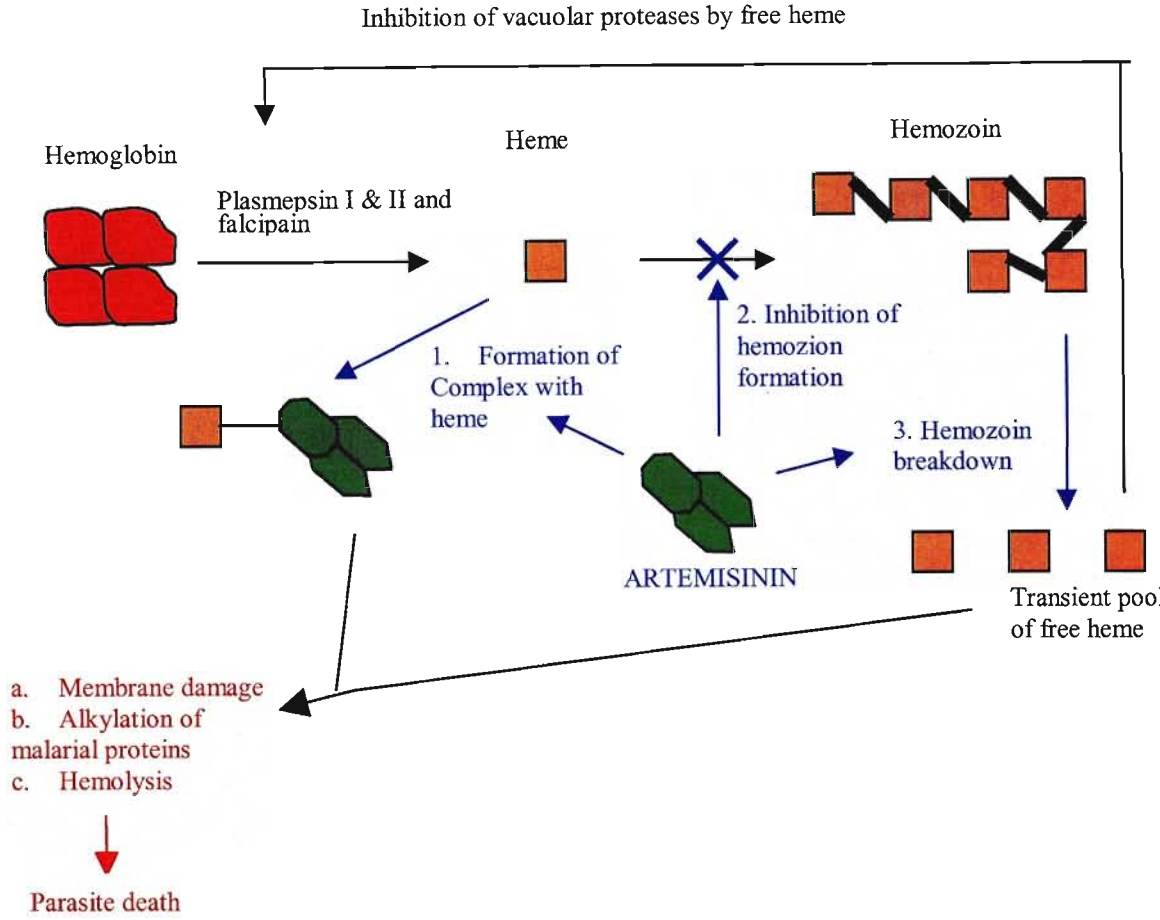

Figure 1.6 Proposed mechanism of action of artemisinin and related drug compounds. Adapted from Pandey *et al.* (1999).

There are three stages to the mechanism of action of artemisinin (Figure 1.6). These involve the generation of free oxygen radicals and an unstable radical of the drug, when the endoperoxide bridge is cleaved by intra-parasitic iron (Basco and Le Bras, 1993; Pandey *et al.*, 1999; Dhingra *et al.*, 2000; Olliaro *et al.*, 2001). This causes selective alkylation and bonding to parasite proteins and ultimately hemolysis (Wernsdorfer, 1997). Antioxidants or free radical scavengers such as catalase, dithiothreitol (DTT), ascorbate and α-tocopherol block the anti-malarial activity of artemisinin and its derivatives (Dhingra *et al.*, 2000). The catabolism of hemoglobin may also be inhibited as well as heme polymerization (Pandey *et al.*, 1999). Meshnick *et al.* (1991) noticed that hemozoin reacted with artemisinin to form an adduct of

approximate molecular weight 914 Da. Hong *et al.* (1994) also showed that artemisinin concentrated in hemozoin by covalently binding to the heme.

Brewer *et al.* (1994) found that intravenous injection of high doses of arteether and artemether into dogs and rats resulted in progressive cardio-respiratory collapse and fatal neurotoxicity (Price *et al.,* 1999). A study performed using human subjects taking oral doses of artemisinin, showed that absorption and elimination are both rapid, and at therapeutic concentrations there was little evidence of neurotoxicity (Duc *et al.*, 1994). Price *et al.* (1999) found that artesunate and artemether are well tolerated by human subjects with no attributable neurotoxicity, cardiotoxicity or allergic reactions, even when used in combination with mefloquine.

1.2.8 Combination therapy

The logic behind combination therapy is that the probability of resistance developing simultaneously to two anti-malarial drugs, with different mechanisms of action, is very low; approximately 1 in 10^{12} treatments (Bloland *et al.*, 2000). The effect of any combination therapy is enhanced by the inclusion of artemisinin or one of its derivatives, since these drugs reduce parasite load more rapidly than any other anti-malarial. Combination therapy may be a very promising treatment for treating malaria, as it may reduce the selection and transmission of resistant parasites. A major problem is that resistance may not be inhibited, since the malaria parasite and its lifecycle are so complex.

Chloroquine/doxycycline combination therapy was found to be effective against chloroquine resistant *P. falciparum* malaria in patients in northeastern Irian Jaya, Indonesia (Taylor *et al.*, 2001).

1.2.9 Suramin – a trypanocidal drug

Suramin or Germanin® was synthesized in 1916 by Bayer AG (Leverkusen, Germany) for the treatment of trypanosomiasis (Schiller *et al.*, 1994). It is the hexasodium salt of 8,8'-[Carbonylbis[imino-3,1-phenylenecarbonylimino(4-methyl-3,1-phenylene)carbonylimino]]bis-1,3,5-naphthalenetrisulfonic acid (Figure 1.7). Suramin has been found to inhibit reverse

transcriptase *in vitro* as well as other cellular enzymes such as DNA polymerase, terminal deoxynucleotidyl transferase, protein kinase C and ATPase (Schiller *et al.*, 1994). Suramin induces multiple effects on Ca homeostasis in cells (Emmick *et al.*, 1994).

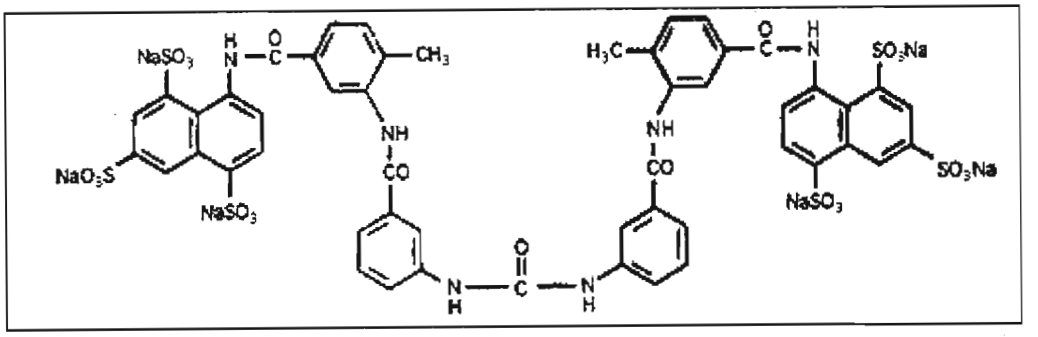

Figure 1.7 Structure of the trypanocidal drug, suramin.

1.3 THE MALARIAL PIGMENT, HEMOZOIN

1.3.1 Formation of hemozoin

Malaria parasites digest 60 - 80% of the host hemoglobin while they are growing inside erythrocytes (Goldie *et al.*, 1990; Dorn *et al.*, 1995; Francis *et al.*, 1997). Normally hemoglobin comprises 95% of the cytosolic protein of the red blood cell. The amino acids derived from hemoglobin degradation are incorporated into parasite proteins. The proteolysis of hemoglobin may be essential for parasite survival, since *Plasmodium* has limited de novo amino acid synthesis (Francis *et al.*, 1997).

Hemoglobin is converted from a ferrous (Fe^{2+}) to a ferric (Fe^{3+} or methemeoglobin) form in erythrocytes, and hemozoin is in the ferric state (Akompong *et al.*, 2000). Thus hemoglobin may be oxidized upon entering the favorable conditions of the acidic food vacuole. Digestion occurs in the acidic vacuole, by two aspartic (plasmepsins I and II) and one cysteine (falcipain) proteases (Hawley *et al.*, 1998) (Figure 1.8). The intravacuolar pH is estimated to be pH 4.5 – 5.2 (Francis *et al.*, 1997; Kirk, 2001; Ziegler *et al.*, 2001). The three vacuolar enzymes which have been isolated, all have sharp pH optima close to the normal physiological pH of the food

vacuole (Olliaro and Goldberg, 1995). A metallopeptidase, falcilysin, was discovered by Eggleson *et al.* (1999), which is active after the plasmepsins and falcipain.

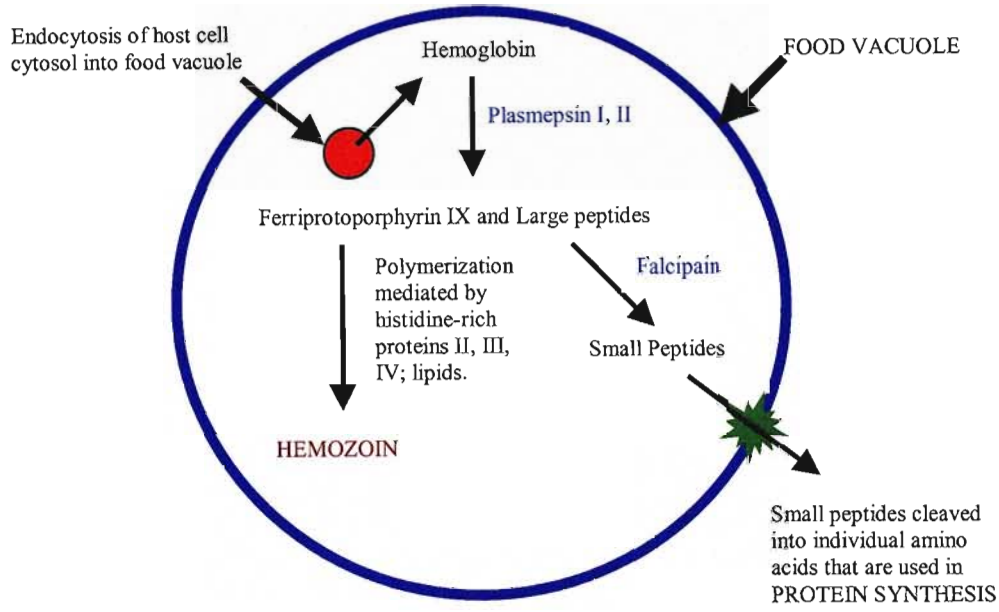

Figure 1.8 The pathways of hemoglobin digestion and hemozoin formation in the food vacuole of *Plasmodium falciparum* parasites. Adapted from Raynes (1999).

The toxic heme [Fe(III)protohemeatoporphyrin-IX] released during digestion is sequestered into hemozoin, an insoluble crystalline heme coordination polymer (Bohle *et al.*, 1997). This is an insoluble pigment (Goldie *et al.*, 1990) that consists of polymerized Fe (III) protohemeatoporphyrin-IX subunits (Dorn *et al.*, 1995) (Figure 1.9). The estimated concentration of heme in the parasite food vacuole can reach as high as 400 mM. At these levels, if the heme was still free, metabolic functioning would be disrupted via peroxidation of membranes, inhibition of enzymes and the generation of oxidative free radicals (Ziegler *et al.*, 2001).

The catabolism of hemoglobin and the formation of hemozoin are highly organized processes that are designed to produce amino acids for *de novo* protein synthesis, as well as to prevent

the build up and release of toxic heme (Figure 1.8). Free heme has a number of biochemical consequences that include membrane lysis and protease inhibition (Berger *et al.*, 1995; Bohle *et al.*, 1997). Malaria parasites do not have heme oxygenases so they are unable to cleave the heme into an open chain tetrapyrrole (Slater *et al.*, 1991; Berger *et al.*, 1995; Bohle *et al.*, 1997). Hemozoin formation was initially believed to be an enzyme-mediated process with heme polymerase being the mediator. However, when Dorn *et al.* (1995) treated parasite lysates with extreme heat, low temperatures for long periods of time and proteinase digestion, there was no significant decrease in the polymerization of heme, indicating that this is likely to be an autocatalytic chemical process and not enzyme catalysis (Dorn *et al.*, 1995; Ridley *et al.*, 1997; Sullivan, 2002). Other evidence exists in that β-hematin which is similar in structure to hemozoin, can form spontaneously under the conditions prevailing in the food vacuole (Egan *et al.*, 1994; Sullivan *et al.*, 1996; Egan *et* al., 2001; Sullivan, 2002). Hemozoin itself is capable of supporting heme polymerization. But there must be another mechanism as prior to hemoglobin digestion there is no hemozoin.

Phospholipids have been found to promote the polymerization of heme and could thus play a role in hemozoin formation in the malarial parasite (Bendrat *et al.*, 1995). Sullivan Jr. *et al.* (1996a) hypothesized that histidine-rich protein II (HRP II) could bind heme in the digestive vacuole. It has a repetitive sequence, that is similar to the heme binding motif of human histidine-rich glycoprotein (HRG), and thus may play a role in hemozoin formation (Pandey *et al.*, 1999).

1.3.2 Structure of hemozoin

Hemozoin has been found to be composed of 65% protein, 16% ferriprotoporphyrin-IX (hematin), 6% carbohydrate and trace amounts of nucleic acids and lipids (Goldie *et al.*, 1990). β-Hematin [Fe(III)-protoporphyrin-IX]$_2$, a synthetic product, is chemically, spectroscopically and chrystallographically identical to hemozoin (Pagola *et al.*, 2000; Egan *et al.*, 2001). Hemozoin is thought to consist of polymeric heme units (Figure 1.9) linked by a bond between the ferric iron of one heme and a proprionate carboxylate side chains (Fe^{3+}-O) (Slater *et al.*, 1991; Berger *et al.*, 1995; Ridley *et al.*, 1995).

Hemozoin may play a significant role in the physiology of malaria infection by interfering with phagocyte function once ingested and thus ultimately suppressing the host immunological response (Schwarzer *et al.*, 1998). It has also been implicated in the action of a number of anti-malarial drugs (Arese and Schwarzer, 1997).

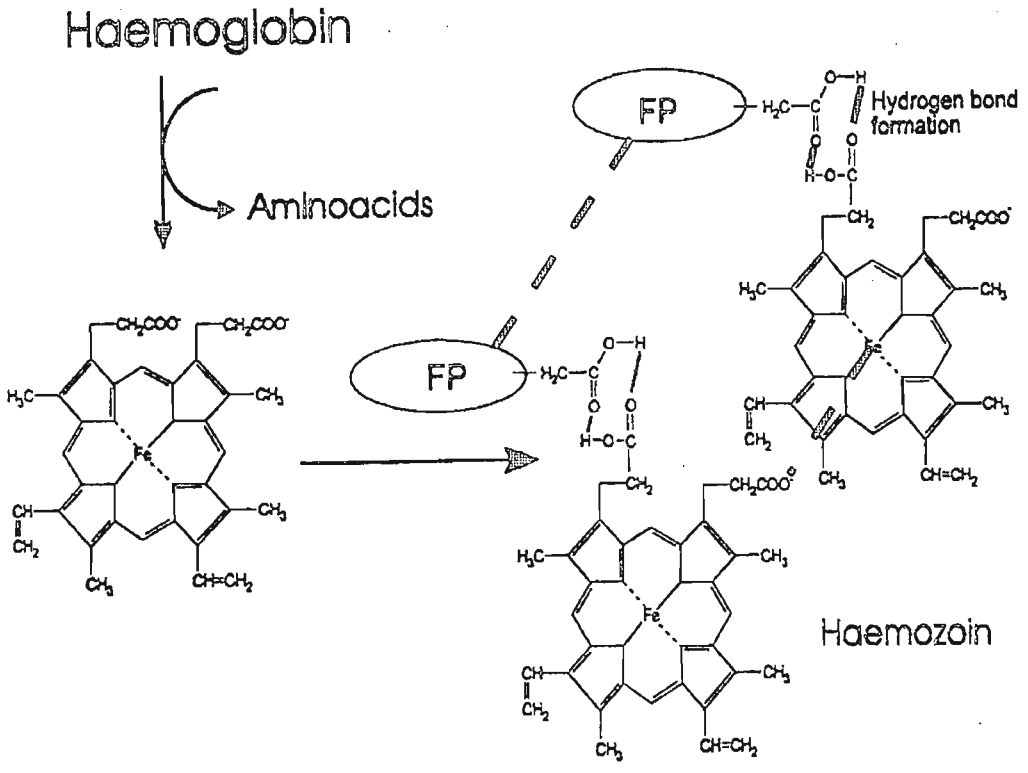

Figure 1.9 Structure of heme and hemozoin (ferriprotoporphyrin IX). Ferriprotoporphyrin IX (FP) is represented by an oval ring in the second hemozoin polymer. The dashed line shows the chelation of the iron atom with the proprionic acid side chain. The dimeric structure is thought to be formed by hydrogen bonds forming between the remaining proprionic functional groups (Raynes, 1999).

1.3.3 Targets for anti-malarial drugs

The sequestration of heme derived from hemoglobin may be critical to the survival and maturation of the parasites, hence this may represent an important target for anti-malarial drugs (Bendrat *et al.*, 1995). Drugs such as methylene blue, artemisinin and the quinolines are

thought to exert their pharmacological effects on the heme released during hemoglobin degradation (Padmanaban and Rangarajan, 2000). However, their mechanisms of action are open to a great deal of debate as many have been proposed.

Falcipain and plasmepsin inhibitors are also potential anti-malarials (Francis *et al.*, 1997). It has been shown that blocking the cathepsin-L like cysteine proteinase, plasmepsin I, is lethal to the parasite (Rosenthal *et al.*, 1991; Ziegler *et al.*, 2001). Plasmepsin II cannot compensate for the loss of plasmepsin I (Ziegler *et al.*, 2001). Inhibition of falcipain with a variety of cysteine proteinase inhibitors results in a marked swelling of the digestive vacuole, accumulation of undigested hemoglobin and parasite death.

Before new drugs can be developed we need to have an understanding of the mechanisms of action of the drugs that are used today, as well as the mechanisms employed by the parasites to resist these drugs.

1.4 MONONUCLEAR PHAGOCYTES

The mononuclear phagocyte system (MPS) comprises monoblasts in the bone marrow, promonocytes, peripheral blood monocytes and tissue macrophages (Auger and Ross, 1992). Mononuclear phagocytes are primitive cells, which are phylogenetically related to cells found in primitive life forms.

1.4.1 Morphology

Macrophages are large cells with a diameter measuring 25 – 50 nm. They have an irregular shape with either a round or kidney-shaped nucleus. Within the cytoplasm are many fine granules and azurophilic granules (Beelen *et al.*, 1989; Auger and Ross, 1992). Monocytes are smaller cells (12 – 15 μm diameter) but they have a large nucleus which is kidney-shaped. The cytoplasmic components are similar to those of macrophages (Auger and Ross, 1992).

1.4.2 Metabolism and organization

During differentiation the composition and metabolism of mononuclear phagocytes is altered. Changes may be increases in the number of mitochondria, the activity of mitochondrial

enzymes and cellular respiration and an increase in the respiratory burst in response to receptor-ligand interactions (Auger and Ross, 1992). The respiratory burst involves increased oxygen consumption and metabolism of glucose via the hexose monophosphate shunt. The activity of a membrane bound oxidase complex is altered by the respiratory burst, and molecular oxygen (O_2) is reduced to the superoxide (O_2^{2-}). The superoxide is converted to hydrogen peroxide (H_2O_2) and hydroxyl (OH^-) radicals, which are referred to as reactive oxygen intermediates (ROI) (Auger and Ross, 1992). Interferon-γ (IFN-γ) and migration inhibitory factor (MIF) can induce an increased respiratory burst *in vitro*. The respiratory burst is decreased markedly when monocytes mature into macrophages. There are a number of hydrolytic enzymes found within these cells, such as lysozyme, acid phosphatase, β-glucuronidase, N-acetyl-glucosamines, α-napthyl butyrate esterase and peroxidase (Auger and Ross, 1992).

1.4.3 Functions

Phagocytes provide the first defense against invading microbes. Mononuclear phagocytes are more efficient than neutrophils when the pathogen is large or the burden is large. They thus play a major role in the defense against microorganisms such as viruses, bacteria, fungi and protozoa (Auger and Ross, 1992). Microbicidal functions are mediated by reactive oxygen intermediates. The phagocytes kill microorganisms by both oxygen-dependent and independent mechanisms.

Secretions contain not only enzymes but other biologically active molecules, such as enzyme and cytokine inhibitors; complement components; reactive oxygen intermediates, arachidonic acid intermediates; coagulation factors, cytokines and many others (Rook, 1989; Segal, 1989; Auger and Ross, 1992). The cytokines that are secreted include tumor necrosis factor (TNF), interleukin-1 (IL-1) and interleukin-6 (IL-6).

Antigens are processed within these cells after uptake to generate peptides that are expressed on one of two glycoproteins, class I or II, of the major histo-compatibility complex (MHC). $CD8^+$ and $CD4^+$ T cells are activated once they recognize the presented peptides. When activated, the $CD8^+$ T cells secrete IFN-γ, which subsequently activates inducible nitric oxide

synthase (iNOS) and this induces the L-arginine dependent nitric oxide pathway (Good and Doolan, 1999). During malaria infection, T cell responses are generally suppressed (Plebanski and Hill, 2000). Intracellular parasites such as *Plasmodia* have evolved a mechanism to avoid the host immune response, by living within the host's cells, where the immune products such as antibodies and complement are unable to reach them (Sadick, 1992).

1.4.4 Effect of malaria on mononuclear phagocytes

1.4.4.1 Phagocytosis

The first line of defense in malaria is provided by phagocytic cells. Monocytes recognize parasite-infected red blood cells as non-self cells and attack them by phagocytosis and by intracellular and extracellular killing with reactive oxygen intermediates (Schwarzer *et al.*, 1992; Fiori *et al.*, 1993). Phagocytic activity is maximal at the beginning of infection but thereafter it declines with repeated malarial episodes (Schwarzer *et al.*, 1992). Phagocytosis is mediated by Fc and complement receptors and by phosphatidylserine-dependent ingestion. Malaria pigment (hemozoin) and infected red blood cells are avidly phagocytosed by host monocytes and tissue macrophages, where the pigment has been found to suppress the ability of these cells to elicit respiratory burst and to block the further phagocytosis of microorganisms and damaged erythrocytes (Francis *et al.*, 1997; Scorza *et al.*,1999). The acidic conditions in the lysosomes of the monocyte induces the release of free iron from hemozoin, and this interferes with the phagocytic capacity of the cells (Leitner and Krzych, 1997). The most highly active of phagocytes are inhibited to a greater extent than less effective phagocytes, since they would have phagocytosed more hemozoin. Thus hemozoin has been implicated as the major depressor of cell induced immunity that is commonly seen in malarial infections (Sherry *et al.*, 1995; Scorza *et al.*,1999). Monocytes that have previously phagocytosed trophozoite infected red blood cells, are unable to neutralize bacteria, fungi and tumor cells (Schwarzer *et al.*, 1992). Incapacitation of monocytes is only one aspect of immune suppression in malaria (Fiori *et al.*, 1993).

The amount of phagocytosed hemozoin in monocytes may reflect the sequestered pathogenic parasite burden during *Plasmodium falciparum* infection and ultimately disease severity

(Metzger *et al.*, 1995; Phu *et al.*, 1995). The presence of hemozoin in monocytes is also be a marker of recent malaria in patients with negative blood films.

1.4.4.2 Cytokine production

The response of the host immune system to infection with malarial parasites involves both humoral and cellular mechanisms that include the actions of a large number of cytokines. Thuma *et al.* (1996) mention that the ability of macrophages to be stimulated by interferon-gamma (IFN-γ), secreted by TH-1 cells is reduced under the prolonged stimulation of the immune system by malaria. The phagocytes ability to destroy the malarial parasites by nitric oxide generation is concomitantly reduced.

During malarial infections, hemozoin is not only found within the parasites but also in many tissues throughout the host, but predominantly in monocytes (Sullivan *et al.*, 1996). Erythrocytes that have been parasitized and thus contain hemozoin are either phagocytosed by leucocytes or at schizogony crystals of hemozoin are released into the bloodstream. As much as 200 μmol of hemozoin may be liberated into the bloodstream of a *P. falciparum* infected patient at schizogony with an underlying synchronous parasitemia of 1% (Sherry *et al.*, 1995).

Hemozoin has also been shown to induce the production and secretion of pyrogenic cytokines, namely TNF-α (Kwaitkowski, 1993), and two macrophage-derived inflammatory mediators (MIP-1α and MIP-1β) in human peripheral blood monocytes and murine macrophages (Sherry *et al.*, 1995). These may mediate the recurrent bouts of fever that are characteristic of a malarial infection. The increased levels of TNF-α and interleukin-1β (IL-1β) secreted by monocytes and macrophages, may be responsible for the anemia seen in many patients, since they are powerful inhibitors of erythroid differentiation (Mohan *et* al., 1995; Arese and Schwarzer, 1997; Wickramasinghe and Abdalla, 2000). IL-2 production is actively inhibited in monocytes that have phagocytosed hemozoin (Scorza *et al.*, 1999).

Macrophage migration inhibitory factor (MIF) is released by macrophages after phagocytosis of infected red blood cells or hemozoin (Martiney *et al.*, 2000). MIF acts as a counter

regulator of glucocorticoid activity, induces TNF-α secretions in macrophages and works with IFN-γ to promote nitric oxide formation. This factor may also be involved in malarial anaemia as it inhibits erythropoiesis.

IL-6 and interleukin 1α (IL-1α) levels are also increased in malaria, although their plasma levels follow the rise and fall of parasitemia in the blood (Picot *et al.*, 1993; Turrini *et al.*, 1993).

1.4.4.3 Surface receptors of endothelial cells and parasite sequestration.

Major histo-compatibility complex class II (MHC class II), intracellular adhesion molecule 1 (ICAM-1/ CD54) and p150,95 integrin (CD11c) expression is impaired in hemozoin loaded monocytes (Schwarzer *et al.*, 1998). Hemozoin loading does not affect the expression of MHC class I, the IgG receptors (CD16, CD32, CD64), the complement CR3 receptor (CD11b), the complement C3b/C4b receptor (CD35) and a vascular adhesion molecule 1 (VCAM-1/CD36) on monocytes (Schwarzer *et al.*, 1998). In diseases such as malaria, upregulation of MHC class II for antigen processing is important to ensure adequate helper T-cell development, as is the upregulation of ICAM-1 which contributes to the capacity of monocytes to adhere and stimulate T-cell proliferation by reinforcing the signal from the T-cell receptor. Hemozoin downregulation of ICAM-1 may explain the defective T-cell response in malaria (Schwarzer *et al.*, 1998).

Increased TNF and IL-1 secretions have been implicated in the upregulation of endothetilial cell surface receptors such as ICAM-1 (McGilvray *et al.*, 2000). This leads to the sequestration of circulating cells, such as monocytes and infected erythrocytes, expressing the leukocyte function antigen 1 (LFA-1/ CD11a/ CD18) (Senaldi *et al.*, 1994; Warrell, 1997; Newton *et al.*, 2000). LFA-1 is also upregulated after exposure of the leukocytes to hemozoin (Pichyangkul *et al.*, 1997). Ultimately, the sequestration of monocytes along with other leukocytes will lead to capillary clogging which may lead to pathological conditions. This has been noted in cerebral malaria where TNF levels are extremely high (Patnaik *et al.*, 1994).

Parasite glycosylphosphatidylinositol toxin (GPI) when released into the blood leads to the upregulation of ICAM-1, VCAM-1, E-selectin as well as cytokines and nitric oxide synthase (NOX) (Schofield *et al.*, 1996; Tachado *et al.*, 1996).

1.4.4.4 Reactive oxygen intermediate production and the enzymes involved.

Hemozoin may be inert but once it enters the phagocytes phagolysosome it may become harmful since it is a powerful generator of radicals. Free radicals are generated by aggregated ferric heme; unsaturated fatty acids and small amounts of free heme liberated by the acidic conditions and hydrogen peroxide (H_2O_2) (Arese and Schwarzer, 1997). Elemental iron catalyzes the formation of highly reactive hydroxyl radical (•OH) or oxidants of similar reactivity from hydrogen peroxide via the Fenton reaction ($H_2O_2 + Fe^{2+} \rightarrow Fe^{3+} + OH^- +$ •OH). The hydroxyl radical initiates a range of toxic reactions including peroxidation of biological membranes, damage to DNA (Wilson and Britigan, 1998), functional impairment (Schwarzer *et al.*, 1992) and the derangement of antigen processing and presentation (Schwarzer *et al.*, 1998). Lipid peroxidation is associated with a variety of pathological events, including changes in the bilayer properties, reduction of membrane fluidity and inactivation of membrane bound enzymes (Omodeo-Salè *et al.*, 1998).

Elevated concentrations of lipoperoxides have been located within hemozoin loaded cells; these are short lived, labile compounds that produce short chain aldehydes upon degradation of fatty acids. Unsaturated fatty acids, such as arachidonic and linolenic acid, yield an open chain hydroxyaldehyde degradation product named 4-hydroxy-trans-nonenal (HNE) (Arese and Schwarzer, 1997). The levels of this compound are elevated markedly in the hemozoin containing cells. HNE is an electrophylic alkylating agent that reacts with thiols and amino groups and thus inhibits a number of enzymes by blocking the reactive sites or other essential groups (Schwarzer *et al.*, 1996; Arese and Schwarzer, 1997). Protein kinase C (PKC), which is involved in phagocytosis and the oxidative burst (Turrini *et al.*, 1993), is inhibited by concentrations of HNE between 10 – 100 μm. The inhibition is due to the numerous thiol groups present on the enzyme, which have to be in the reduced state before it can function normally (Schwarzer *et al.*, 1996). Schwarzer *et al.* (1993) found that membrane-associated

PKC is irreversibly inactivated, after a brief activation, in human monocytes that had phagocytosed hemozoin. Low micromolar concentrations of hemozoin inhibited IFN-γ-mediated MHC class II expression (Schwarzer *et al.*, 1998).

One of the major phagocyte functions inhibited by hemozoin loading is the respiratory burst, that is controlled by the activity of NADPH oxidase (NOX) (Schwarzer and Arese, 1996; Arese and Schwarzer, 1997). NOX is under the control of PKC but it appears that it is inhibited by damage inflicted to the cytosolic subunits by free radicals.

Arese and Schwarzer (1997) posed two important yet unanswered questions. Why is hemozoin not toxic while in the parasite's food vacuoles? Why is the heme oxygenase from monocytes and macrophages not able to destroy the hemozoin heme?

1.4.4.5 Redox status of monocytes

The cell redox state may be modified by the phagocytosis of hemozoin or by the inevitable iron overload via the accumulation of iron-rich molecules. Transcription factors such as AP-1 and NF-kB/NF-IL6, that are involved in the regulation of the expression of the genes which control cytokines and adhesion molecules, are influenced by the redox status of the cell (Taramelli *et al.*, 1998).

1.4.5 Immunomodulatory action of anti-malarial drugs

1.4.5.1 Phagocytosis

Therapeutic concentrations of tetracycline, chloroquine, quinine and dapsone inhibited phagocytic activity in rhesus monkey (*Macaca mulatta*) monocytes (Prasad *et al.*, 1984). Opsonization and phagocytosis of infected red blood cells is inhibited by therapeutically relevant concentrations of quinine, chloroquine and artemether (Shalmiev *et al.*, 1996). When the infected red blood cells were opsonized prior to treatment with the drugs, phagocytosis was not inhibited. Shalmiev *et al.* (1996) concluded that the anti-malarial drugs affected the affinity of the IgG for infected red blood cells. Quinine did not noticeably affect phagocytosis

of latex beads by macrophages or their viability, even at concentrations as high as 200 μM (Maruyama *et al.*, 1994).

1.4.5.2 Intracellular organelles

The 4-aminoquinolines, 8-aminoquinolines and derivatives accumulate within the acidic food vacuole of the malaria parasite where they may increase the pH. Leukocytes have an acidic lysosomal system and these drugs also become trapped in millimolar concentrations in these organelles (Schwartz *et al.*, 1985; Gabay *et al.*, 1994). The pH of the lysosome is increased from pH 4.8 to pH 6.5, and this results in the swelling of the organelle as well as the inhibition of the lysosomal acid hydrolases and ultimately of degradation of proteins and glycosaminoglycans (Riches *et al.*, 1981; Wolf *et al.*, 2000b). Also, during treatment with chloroquine the number of lysosomes increases and their density decreases (Mackenzie, 1983). Vesicle fusion and exocytosis of cell products is diminished by chloroquine, probably through the modification of clathrin.

Chloroquine, primaquine and quinine inhibit esterase activity in leucocytes (Markovic *et al.*, 1988). However, these drugs had no inhibitory effect on the activity of peroxidase, alkaline phosphatase, acid phosphatase and β-glucuronidase. An accumulation of myeloid bodies also occurs, which results in decreased phagocytosis, chemotaxis and overall cell functioning (Van Beek and Piette, 2001). The majority of these effects have been observed at concentrations far exceeding those found in the blood of patients during treatment.

Primaquine potently inhibits membrane transport from the endosome to the plasma membrane (Van Weert *et al.*, 2000). Transferrin receptor recycling is inhibited by 1 mM primaquine. The secretory pathway from the trans-Golgi network (TGN) is inhibited with by primaquine. The drug may alter the physical properties of the membranes, thus interfering with the budding and fusion process.

Artemisinin concentrates in the acidic food vacuole. Morphological changes in the mitochondria, ribosomes and the endoplasmic reticulum and, much later in treatment the destruction of the digestive vacuole membrane has been observed at high concentrations

(Olliaro and Goldberg, 1995; Van Agtmael *et al.*, 1999). Artemisinin rapidly decomposes in medium containing peroxidase activity, thus indicating its instability in the presence of these enzymes and may likely contribute to changes seen in cells containing these enzymes (Dhingra *et al.*, 2000).

Dapsone has been found to inhibit lysosomal enzymes in polymorphonuclear leucocytes and it also stabilizes lysosomes by its potent antioxidant activity (Wolf *et al.*, 2000b). However, there have been numerous reports of dapsone inducing agranulocytosis, with a reduction in the number of peripheral granulocytes from 2 – 7.7 x 10^9 to 0.5 x 10^9 (Coleman, 2001).

Suramin accumulates in the secondary lysosomes of monocytes and inhibits the fusion of the phagosome with the lysosome (Schiller *et al.*, 1994).

1.4.5.3 Cytokine production

Macrophages treated with quinine, chloroquine, proguanil, mefloquine or halofantrine prior to stimulation were used by Picot *et al.* (1993). It was found that the secretions of TNF and IL-6 were suppressed by chloroquine in a dose-dependent manner (Kremsner *et al.*, 1993; Van den Borne, *et al.*, 1997; Karres *et al.*, 1998; Seth *et al.*, 1999), but the other drugs had no effect. Chloroquine also suppresses the production of interferon-γ (IFN-γ) in stimulated peripheral blood monocytes (Van den Borne, *et al.*, 1997). It is believed that TNF secretion is dependent on intracellular iron metabolism and that chloroquine inhibits its secretion by interfering with iron homeostasis (Picot *et al.*, 1993).

Chloroquine has been shown to inhibit the secretion of IL-1 and IL-2 and antigen presentation by helper cells and to depress the cytotoxicity of natural killer cells as well as displaying anti-inflammatory properties (Karres *et al.*, 1998; Wolf *et al.*, 2000b). The inhibition of pro-inflammatory cytokines is most likely at the transcription level (Karres *et al.*, 1998) and may be related to chloroquine intercalating with DNA.

Seth *et al.* (1999) observed that chloroquine upregulated the production of a number of inflammatory cytokine genes such as those for interleukin-1 receptor agonist (IL-1Ra), IL-1α,

IL-1β, IL-6, IL-12p40 and interferon-γ (IFN-γ). IL-1Ra levels are also enhanced during viral infections, but it's role during infection has yet to be ascertained. It has been shown that chloroquine enhances the severity of the symptoms and mortality observed during infection with the Semliki forest virus and encephalomycordartis virus (Seth *et al.*, 1999). Chloroquine also increases the viral titres in various organs.

Quinine, at concentrations capable of blocking the K-channels, inhibits cell proliferation and protein synthesis in human T-lymphocytes (Maruyama *et al.*, 1994). K-channels may be involved in cytokine production, which will thus be blocked by quinine.

Dapsone suppresses the expression of TNF-α mRNA as well as levels of TNF-α secreted by monocytes stimulated with lipopolysaccharide (LPS) (Miyachi, 2000).

Suramin has been found to inhibit the activity of TNF-α through a direct action on the cytokine rather than its receptors (Grazioli *et al.*, 1992). Alzani *et al.* (1993) demonstrated that the drug dissociates the quaternary structure of TNF-α.

1.4.5.4 Reactive oxygen intermediates

Chloroquine induces the activity of iNOS and thus increases the amount of nitric oxide produced. DNA and RNA biosynthesis is blocked, as is DNA replication and RNA transcription as chloroquine intercalates with DNA between adjacent base pairs (Van Beek and Piette, 2001). Kremsner *et al.* (1993) found that chloroquine significantly inhibited the production of reactive nitrogen intermediates (RNI) by murine macrophages, without affecting the production of reactive oxygen intermediates (ROI). However, these experiments were conducted at concentrations of chloroquine that greatly exceeded those normally found in patient blood. Quinine, at concentrations within the therapeutic range, significantly reduced the synthesis of reactive nitrogen intermediates without having any effects on reactive oxygen intermediate production (Kremsner *et al.*, 1993). Artemisinin was also found to effect a significant decrease in the production of reactive nitrogen intermediates, but this occurred at concentrations higher than therapeutic levels.

Endogenous H_2O_2 is produced by liver microsomes during the oxidation of NADPH. This process is enhanced by a number of drugs, including arteether and artelinic acid, but dihydroartemisinin had no effect (Leskovac and Peggins, 1992).

Dapsone has anti-inflammatory effects on PMNs. In normal PMNs activation leads to a cascade of reactions which ultimately releases reactive oxygen intermediates. However, dapsone directly inhibits the myeloperoxidase-peroxide-halide system of the PMNs by promoting the formation of an inactive form of myeloperoxidase (Wolf *et al.*, 2000a). Thus the conversion of H_2O_2 to hypochlorous acid is prevented. The extracellular xanthine oxidase system is also disrupted by dapsone (Paniker and Levine, 2001).

Tetracyclines inhibit reactive oxygen intermediate generation by PMNs and they also reduce PMN chemotaxis (Miyachi, 2000).

1.4.5.5 Surface receptors

Anti-malarial drugs at therapeutic concentrations have been found to reduce expression of monocyte receptors that ultimately affect the immune response and cytoadherence of the cells (Goldring and Nemaorani, 1999). Monocyte surface receptor expression as well as cytokine secretion, is also altered by anti-inflammatory and anti-oxidant drugs such as dexamethasone, cortisol, probucol, ambroxol, danazol and staurosporine (Goldring and Ramoshebi, 1999).

During *P. falciparum* malaria, trophozoite infected red blood cells adhere to non-infected red blood cells in a phenomenon known as 'rosetting' (David *et al.*, 1988). This is thought to enhance the ability of the parasites to invade the surrounding red cells when the schizonts rupture. Therapeutic concentrations of artemisinin, chloroquine, primaquine, pyrimethamine and quinine disrupt the rosettes (Goldring *et al.*, 1999), with artemisinin and quinine being the most effective and chloroquine being the least effective.

The expression of various surface receptors on monocytes and the phagocytic capacity of monocytes were found to be inhibited by suramin (Schiller *et al.*, 1994). However, Goldring

and Nemoarani (1999) found that suramin had minimal inhibition (<10%) on the expression of monocyte surface receptors.

1.4.5.6 Other effects

Quinine is used as a blocker of K^+ channels and has been found to modify phospholipid metabolism, by increasing phosphatidylserine and phosphatidylinositol synthesis, but decreasing the synthesis of phosphatidylcholine and phosphatidylethanolamine (Pelassy *et al.*, 1992). Primaquine inhibits liver microsomal cytochrome P450-dependent enzymes (Na Bangchang *et al.*, 1992). Chloroquine is used in laboratory technique for typing red blood cells since it has the ability to split antigen-antibody complexes (Wolf *et al.*, 2000b).

1.5 HEAT SHOCK RESPONSE IN MONOCYTES

1.5.1 The heat shock response

All organisms from bacteria to man when exposed to elevated temperatures or fever exhibit the phenomenon known as the "heat shock response" (Polla, 1988; Donati *et al.*, 1991). Various other stresses such as oxidative injury, heavy metals, ethanol, amino acid analogues, uncouplers of oxidative phosphorylation, steroid hormones and proinflammatory cytokines also induce the heat shock response (Maresca and Kobayashi, 1994; Polla *et al.*, 1995). The heat shock response can be characterized by three specific events: the specific and transient induction of heat shock gene expression; preferential expression of the heat shock protein (HSP)-coding mRNAs, and a blockade of normal protein translation and the induction of thermotolerance (Donati *et al.*, 1991).

The HSPs are classified according to molecular weight, with the HSP70 family consisting of both constitutive (HSC70) and inducible (HSP70) proteins (Polla *et al.*, 1995). The proteins in the HSP70 family are a highly conserved ubiquitous group of proteins (Miao *et al.*, 1997). When the HSP70 sequences from 24 divergent eukaryotic and prokaryotic species were compared, the most distantly related species were at least 45% identical in sequence (Miao *et al.*, 1997). They are able to bind short stretches of polypeptides and prevent the aggregation of unfolded proteins. Heat shock proteins are more commonly known as chaperones because of

their roles in protein translation, folding and proteolysis under normal physiological conditions.

1.5.2 Heat shock cognate protein – 70 (HSC70)

The majority of the HSP70s are abundantly and constitutively expressed under normal growth conditions (Miao *et al.*, 1997). However, their expression may be increased by fever (elevation of temperature) or other stresses. HSC70 is part of a large chaperonin complex, which facilitates protein renaturation, and it chaperones proteins for membrane translocation (Hightower and Leung, 1997). In unstressed cells HSC70 is distributed in the cytoplasm and nucleus but, in cells that are heat shocked, both HSC70 and the newly expressed HSP70 increase in the nucleus (Hightower and Leung, 1997) close to the chromosomes (Velazquez *et al.*, 1980). During the recovery stage after heat shock, both HSC70 and HSP70 redistribute in the cytoplasm. The HSC70 sequences are more conserved in the C-terminal region than those of HSP70, which is most likely due to evolutionary constraints due to their different functions.

1.5.3 Heat shock protein – 70 (HSP70)

HSP70 has been implicated in a number of cellular functions, such as DNA replication, binding of proteins in the endoplasmic reticulum, translocating proteins across intracellular organelle membranes and clathrin-uncoating ATPase (Donati *et al.*, 1991). These functions require HSP70 to bind to unfolded proteins in an ATP-dependent manner. However, the actual role of HSP70 in stressed cells is not clearly defined but it has been implicated in thermotolerance (Hightower and Leung, 1997). The structure of HSP70 consists of two domains: an N-terminal ATPase domain and a C-terminal peptide binding domain (Feige and Polla, 1994).

1.5.4 Heat shock protein expression in monocytes

When monocytes phagocytose a particle they generate large amounts of reactive oxygen intermediates (Polla *et al.*, 1991). It is believed that the increased production of reactive oxygen intermediates is detrimental to phagocytic cells and thus these cells are protected from

oxidative injury by the heat shock response (Clerget and Polla, 1990; Donati *et al.*, 1991; Fincato *et al.*, 1991; Jacquier-Sarlin *et al.* 1994). Oxygen free radicals generated in the presence of hemoglobin-derived iron are involved in the induction of the heat shock response during erythrophagocytosis (Clerget and Polla, 1990). The generation of hydroxyl radicals (•OH) in the presence of iron released from oxidized hemoglobin by the Haber-Weiss metal catalyzed reaction may induce the expression of heat shock proteins in monocytes (Clerget and Polla, 1990; Jacquier-Sarlin *et al.* 1995). However, phagocytosis of latex beads did not induce O_2^- production or detectable alterations in the synthesis of proteins. Heat shock proteins may also be induced by the presence of abnormal proteins as a result of the reactive oxygen intermediates altering protein structure and inducing breaks in the DNA strand (Polla and Kantengwa, 1991). Heat shock in monocytes was found by Polla *et al.* (1995) to selectively modulate the activity of enzymes without altering phagocytosis and microbial killing. NADPH oxidase activity was decreased and superoxide dismutase (SOD) activity was increased by heat shock. HSP70 expression in monocytes inhibits the production of IL-1β and TNF-α in the cells (Njemini *et al.*, 2002; Njemini *et al.*, 2003). Heat shock proteins have been found to protect monocytes from TNF-α induced lysis (Polla and Kantengwa, 1991; Jacquier-Sarlin *et al.*, 1994).

1.5.5 Heat shock protein 70, phospholipase A_2 and malaria

The inflammatory reaction is characterized by phospholipase A_2 (PLA_2) activity induced by pro-inflammatory cytokines (Il-1 and TNFα) (Pruzanski and Vadas, 1991; Vadas *et al.*, 1991) (Figure 1.9). PLA_2 is part of a calcium-dependent family of enzymes that cleave the *sn*-2 bond of diacylphospholipids, freeing fatty acids and monoacylphospholipids (Diccianni *et al.*, 1990). TNF-α activated PLA_2 (Clark *et al.*, 1988) induces the release of arachidonic acid from membrane phospholipids (Jäättelä, 1993). However, HSP70 has been found to inhibit the TNF-α induced activation of PLA_2 without interfering with the signal transduction pathways or receptor binding (Figure 1.9). PLA_2 activity can also be altered by local anesthetics, anti-malarial drugs, antibiotics, polyamines, anti-psychotics (Diccianni *et al.*, 1990) and anti-inflammatory glucocorticoids (Hoeck *et al.*, 1993).

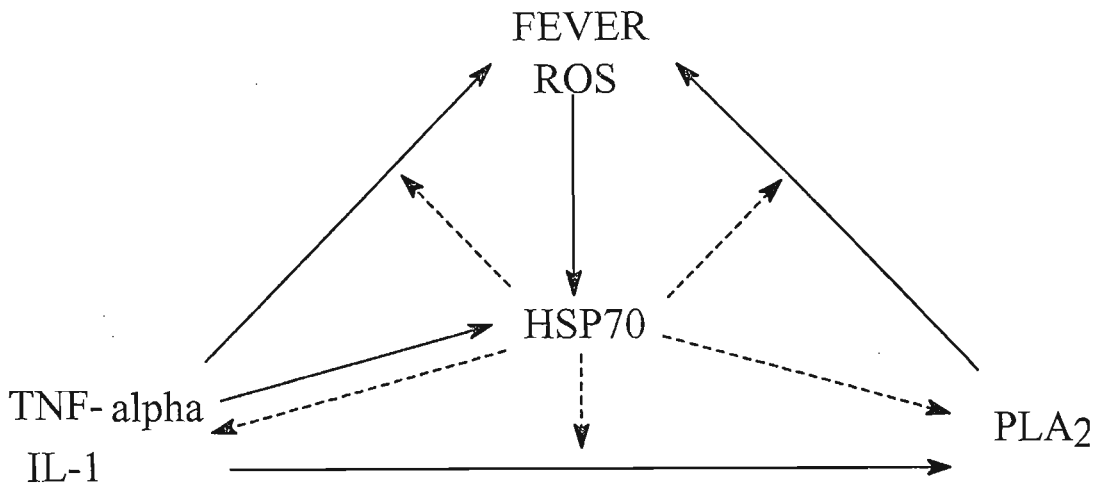

Figure 1.9 Schematic representation of the role of heat shock protein 70 in terminating the inflammatory response. TNF-α (tumor necrosis factor-α); IL-1 (interleukin-1); ROS (reactive oxygen intermediates); HSP70 (heat shock protein 70) and PLA_2 (phospholipase A_2). Stimulation of the inflammatory response is indicated by —— and inhibition by - - - .

In patients with *P. falciparum* malaria, serum levels of TNF-α and PLA_2 were elevated (Vadas *et al.*, 1992; Vadas *et al.*, 1993). Elevated levels of secretory PLA_2 have been implicated in the pathogenesis of numerous diseases such as collagen vascular disease, acute pancreatitis, Crohn's disease, septic shock, adult respiratory distress syndrome (ARDS) and multiple sclerosis (Vadas and Pruzanski, 1986). Since HSP70 has been implicated in inhibiting TNF-α induced activation of PLA_2 in cells, why does HSP70 not inhibit the activation of PLA_2 during malaria? HSPs are generally regarded as intracellular molecules but they can be released into the extracellular compartments and serum (Pockley, 2001). HSP70 binds to human monocytes and CD14 with high affinity and subsequent activation of the monocyte. Pro-inflammatory cytokines (IL-1β, IL-6 and TNF-α) are induced by the CD14-dependent interaction (Asea *et* al., 2000; Kuppner *et* al., 2001; Pockley, 2001). Thus the increased levels of TNF-α in serum would most likely lead to elevated levels of serum PLA_2. Polla (1991) suggests that host HSP may be induced during cerebral malaria and thus would play a role in protecting the brain tissue from damage.

1.6 X-RAY MICROANALYSIS

1.6.1 What is X-ray microanalysis?

Literally, microanalysis is the analysis of "very small' samples by any technique available but the term actually has a much narrower meaning. Electron-probe X-ray microanalysis (EPXMA) enables one to determine the elemental composition of any sample under either the scanning electron microscope (SEM) or the transmission electron microscope (TEM) (Warley, 1997). This technique is able to detect low concentrations with its minimum detection limits (MDLs) below 1% and in the very best cases 0.1%. This technique enables one to correlate the elemental content with specific structural features using qualitative or quantitative digital mapping (Warley, 1997).

1.6.2 Principles of the technique

When the electron beam enters the sample, a number of interactions occur, but the only one of interest in X-ray microanalysis is the generation of X-rays. These X-rays contain information about the elemental content of a specific region that is being irradiated. There are two mechanisms in which X-rays are produced (Figure 1.11).

X-rays are generally produced as a result of the rearrangement of the orbiting electrons, after an incident electron from the electron beam has ejected an inner shell electron from an atom (Warley, 1997). This results in an ionized but unstable state and an electron from an outer shell will move to the inner shell to stabilize the atom. Since this electron has moved from a high-energy state to a low energy state it loses the excess energy as an X-ray photon (Warley, 1997). The energy of this emitted photon is equivalent to the difference between the energy of the two shells. X-rays may also be produced when the incident electrons pass the nucleus and are slowed down and thus lose energy. The X-rays emitted by the atom are distinct and characteristic of the element emitting it: ultimately a number of peaks are produced, each representing the different elements.

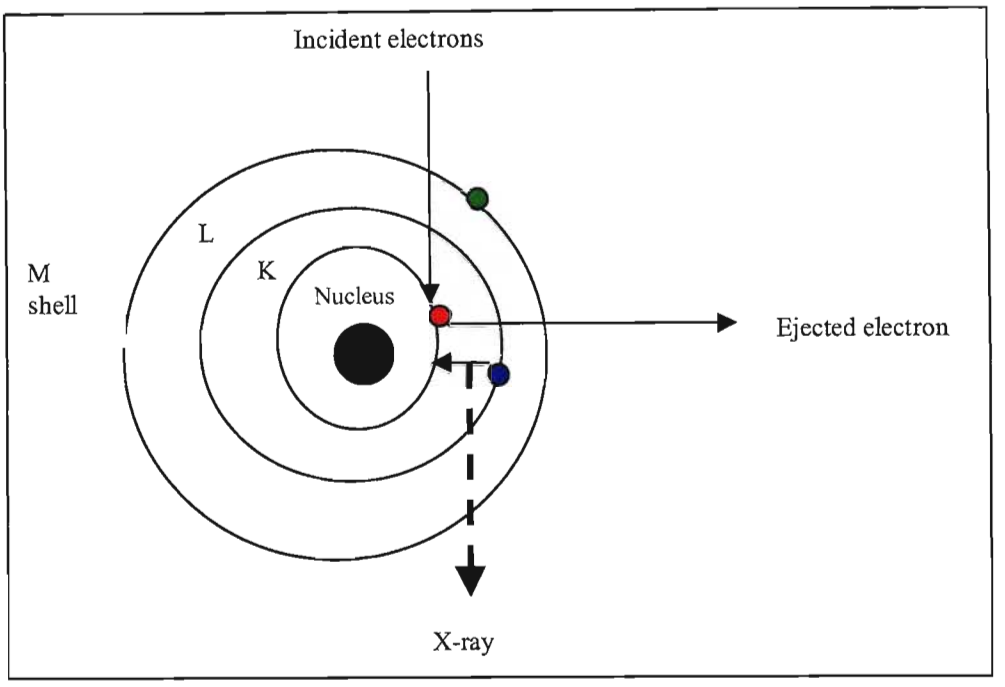

Figure 1.11 Model of an atom showing the production of X-rays. An electron in the incident beam may have sufficient energy to eject an inner electron: another electron in an outer orbital with higher energy moves to fill the vacated position. The excess energy is emitted as an X-ray (Warley, 1997).

The major difficulties associated with the preparation of biological samples, apart from the development of appropriate standards (Warley, 1990), is the preservation of the chemical composition of the cell without altering ultrastructural details (Fishman *et al.*, 1985). In an ideal situation, studies should be made on fresh, hydrated specimens but due to the vacuum present in the microscopes as well as the interaction of the electron beam, severe mass loss occurs (Warley and Skepper, 2000). The composition of standards should generally resemble the specimen closely, i.e. they are based on proteins as the organic matrix and are, either cryo-frozen or embedded in resin before sectioning.

1.6.3 X-ray microanalysis and monocytes

Fishman *et al.* (1985) determined the elemental composition of normal blood cells, namely monocytes, neutrophils, lymphocytes and platelets. They found that nucleus-containing cells

had a high phosphorous content, and platelelets, monocytes and neutrophils had elevated levels of sulfur. This is thought to be due to the cytoplasmic granules that contain sulfated glycosamines. Monocytes and neutrophils yield similar high peaks for phosphorous and sulfur (Fishman *et al.*, 1985). Monocytes yield higher peaks for sodium, chlorine and calcium. Since it is possible to distinguish types of cells by their different elemental content or spectra, it should be possible to distinguish activated, drug treated, hemozoin- or infected erythrocyte-fed monocytes from normal monocytes. Monocytes occur naturally and are easily isolated, and easily prepared for EM by cryofixation and cryosectioning (Warley *et al.*, 1994). Cells may even be cultured on gold grids covered with a pioloform film and laminin, especially since monocytes are known for their ability to adhere to surfaces (Warley *et al.*, 1994; Skepper *et al.*, 1999).

1.6.4 X-ray microanalysis and malaria

To date only one X-ray microanalysis study has been done on malarial parasites and drugs. The normal erythrocyte maintains a high intracellular K and a low intracellular Na concentration, with the [Na] / [K] being ~ 0.12 (Kirk, 2001). In infected red blood cells the [Na] / [K] was greatly altered to ~ 11.6, a 100 fold change indicating that the normal Na and K gradients may be lost (Lee *et al.*, 1988).

The only related approach to have been used is soft X-ray microscopy, which involves the bombardment of the specimens with X-rays (Magowan *et al.*, 1997). This technique does offer high spatial resolution, as well as being a novel way to approach the intraerythrocytic development of *Plasmodium*. Utilizing this technique gave new insight into the complex relationship between the host and the parasite, similarly the use of X-ray microanylsis may offer new insights in a number of areas including the interaction and effects of *Plasmodial* by-products and parasite-infected erythrocytes on monocytes, as well as the immunomodulatory effects of anti-malarial drugs on monocytes. The detection of alterations in elemental contents and distributions in parasites brought about by anti-malarial drugs, may also provide new insights.

1.7 OBJECTIVES OF THE PRESENT STUDY

- The initial aims of this study were to isolate monocytes from either human or canine blood and assess their yield, viability and functional integrity.
- Trypan blue exclusion was used to determine the viability and number of the cells.
- Phagocytosis of latex beads and the staining for peroxidase and alkaline phosphatase activity, would give a clear indication of the functional integrity of the isolated monocytes.
- Due to the difficulty of isolating hemozoin from malaria parasites, β-hematin was synthesized from hematin. The synthesized β-hematin structure was confirmed by scanning electron microscopy and EPXMA.
- The phagocytic ability of the isolated monocytes will be further investigated using unopsonized β-hematin.
- Prior to examining the monocytes using EPXMA on the transmission electron microscope, the grid, film and elemental correction factors were determined.
- The cells were analysed and individual elemental concentrations of Na, Mg, P, S, Cl, K and Ca were calculated and statistically evaluated using the Mann-Whitney U-test.
- The major focus of the study will be to examine the effects of anti-malarial drugs (quinine, chloroquine, primaquine, pyrimethamine, dapsone, doxycycline, tetracycline and artemisinin); the trypanocidal drug, suramin; fever and β-hematin phagocytosis on the elemental concentrations of monocytes.
- It was hypothesized that the elemental concentrations within monocytes, would be altered by the experimental conditions applied.
- Monocytes express heat shock proteins in response to malarial fever. Peptides from two heat shock proteins, HSP70 and HSC70 that were most likely to elicit an immune response in immunized chickens were identified and synthesized.

- The antibody production was evaluated using an ELISA coated with the peptide and western blot with the native protein. If the antibodies detected and differentiated between HSP70 and HSC70, the effects of anti-malarial drugs on the expression of heat shock proteins in the presence or absence of β-hematin or heat shock would be examined.

CHAPTER 2

GENERAL MATERIALS AND METHODS

2.1 MATERIALS

The majority of the chemicals utilized in this study were from BDH (Poole, England), Merck (Darmstadt, Germany), Roche Diagnostics GmbH (Mannheim, Germany) or Sigma (St. Louis, USA), and were of analytical grade. The low molecular weight markers and nitrocellulose Hybond-C were from Amersham Pharmacia Biotech (USA). Bovine serum albumin (BSA), 2,2'-azino-di-(3-ethyl)-benzthiozoline sulfonic acid (ABTS), nitroblue tetrazolium (NBT), 5-bromo-4-chloro-3-indolylphosphate (BCIP) were from Roche Diagnostics GmbH (Mannheim, Germany). Giemsa stain, Histopaque®-1077, RPMI-1640, 1M HEPES buffer (N-2-hydroxyethylpiperazine-N'-2-ethanesulphonic acid), cell culture filtration units (0.45 μm), latex beads (polystyrene 0.760 μm), 3,3'-diaminobenzidine (DAB), m-maleimidobenzoyl-N-hydroxysuccinimide ester (MBS) and 5,5'-dithiobis-(-2-nitrobenzoic acid) (Ellman's reagent) were from Sigma (St. Louis, USA). Other chemicals from Sigma were hematin, artemisinin, chloroquine, quinine, pyrimethamine, primaquine, dapsone, trypan blue, ponsceau S, pepstatin A, 1,10-phenanthroline, iodoacetic acid and N-[(L-3-*trans*-carboxyoxiran-2-carbonyl)-L-leucyl]-amido(4-guanidino)butane (E64). Pefabloc [4-(2-aminoethyl)benzenesulfonylfluoride (AEBSF)] and phenylmethylsulfonyl fluoride (PMSF) were from Boehringer Mannheim, GmbH, Germany. Tetracycline HCl and doxycycline HCl were from ICN Biomedicals Inc. (Ohio, USA). Jackson Immunoresearch Laboratories Inc. (Westgrove, P. A., USA) supplied the horseradish peroxidase linked rabbit anti-chicken IgY. Fetal calf serum was from Delta Bioproducts (Kempton Park, South Africa). Sigma Genosys (St. Louis, USA) synthesized the synthetic peptides, HSP and HSC. Maxisorp™ surface 96 well ELISA plates were from Nunc-Immuno™ (Denmark). The Sulfolink® affinity matrix was from Pierce (Rockford, USA). The gold grids (100 square mesh) and LR white resin were from Agar Scientific LTD (Essex, UK). Dimethylsulfoxide was from Fluka Chemie (GmbH, Switzerland). Heparinized vacutainers, sleeves and needles were from BD vacutainer systems (Plymouth, UK). Petri dishes were from Sterilin (Biddy Sterilin LTD, Staffs, UK) and Corning Incorporated (USA). Canine blood was obtained through Dr Tanya Hughes of the Pietermaritzburg SPCA and

human blood was donated by a healthy male volunteer. Distilled water (dH_2O) was from a Milli-Ro® 15 water purification system (Millipore, Marlboro, USA) and deionised water (ddH_2O) was from a Milli-Q Plus ultra-pure water system (Millipore, Marlboro, USA) with a minimum resistivity of 18MΩ.cm. Scanning of images was performed using the Scanmaker 8700 (Microtek) scanner. All scanned images and digital pictures of cells under the light microscope were captured using analySIS® Version 3.0 (Soft Imaging Systems, GmbH, Germany). X-ray spectra were collected using the EDAX® DX-4 bDX Biological Thin System Version 2.30 (EDAX International, Mahwah, USA).

2.1.1 Ethical approval

Ethical approval was obtained from the University of Natal Ethics Committee to inject chickens with peptide rabbit albumin conjugates. The ethics reference number was U.NATAL.AE/Goldring/01/07.

2.2 ISOLATION OF MONOCYTES

In 1968, Boyum described methods for the isolation of mononuclear cells from circulating blood. These cells are one of the easiest blood cells to isolate since they adhere to plastics and glass, whereas the remaining non-adherent blood cells are washed off. Blood was collected in heparinized vacutainers, since monocytes isolated from EDTA and citrate-phosphate-dextrose (CPD) anti-coagulated blood showed very poor adhesion as well as loss of phagocytic activity (Bussolino *et al.*, 1987). Wynne and Moore (1982) mention that one of the disadvantages of isolating monocytes using heparin as an anticoagulant is that platelets become "stickier" and large numbers of platelets may contaminate the monocyte preparations. This can be avoided by washing the cover slips thoroughly. The procedure utilizes Histopaque®-1077 which is a solution of polysucrose and sodium diatroate, adjusted to a density of 1.077±0.001 g/ml. This solution facilitates the rapid recovery of viable mononuclear cells from small volumes of blood. The anti-coagulated blood is layered on to the Histopaque®-1077. During centrifugation the erythrocytes and granulocytes are aggregated by polysucrose and rapidly sediment while the monocytes and other mononuclear cells remain at the plasma interface (Figure 2.1). RPMI-1640 medium was developed by Moore *et al.* (1967) at Roswell Park

Memorial Institute. This medium is used for the culturing of normal and neoplastic leukocytes. The isolation procedure outlined here is adapted from Goldring *et al.* (1992).

2.2.1 Materials

Phosphate buffered saline (PBS), pH 7.2. NaCl (8 g), KCl (0.2 g), $Na_2HPO_4.2H_2O$ (1.15 g) and KH_2PO_4 (0.2 g) were dissolved in 900 ml ddH_2O, the pH was adjusted to 7.2 with NaOH and made up to 1 l. The solution was aliquoted into smaller volumes, sterilized by autoclaving and kept refrigerated at 4°C.

Heat inactivated fetal calf serum (FCS). Fetal calf serum was aliquoted into 10 ml sterile tubes and heated to 60°C for 30 min.

N-2-hydroxyethylpiperazine-N'-2-ethanesulphonic acid (HEPES) buffer (1 M), pH 7.5. Purchased from Sigma (St. Louis, USA)

Complete RPMI 1640 medium (25 mM HEPES; 5% FCS). RPMI 1640 medium powder (10.64 g) was dissolved in 900 ml sterile ddH_2O by stirring. If required, the pH was adjusted to pH 4 with HCl to aid in dissolving the powder. Once dissolved, the pH is increased to pH 7.2 with NaOH and Na_2CO_3 (2 g) is added and stirred until dissolved. The pH was adjusted to within 0.1 - 0.3 pH units of pH 7.2, the volume was adjusted to 1 l. HEPES buffer (25 ml) and heat inactivated fetal calf serum (50 ml) was added. This solution was filter sterilized through 0.45μm acetate filters into sterilized bottles.

2.2.2 Procedure

Canine or human blood was drawn using heparinized vacutainers or sterile tubes containing heparin (25 U/ml). The blood was inverted a number of times to ensure complete mixing of the anticoagulant heparin. The tubes were kept on ice. The blood was diluted 1:1 with sterile cold PBS. For a 13 ml polyallomer ultracentrifuge tube, 10 ml of the blood:PBS solution was carefully layered onto 3 ml of Histopaque®-1077 (d = 1.077). The tubes were centrifuged in the Beckman preparative ultracentrifuge with a SW 40 Ti swinging bucket rotor (2000 *g* 25 min, 8°C). The buffy coat that contains the lymphocytes (2^{nd} layer) was removed and diluted

with cold PBS (Figure 2.1). The tubes were centrifuged (250 *g*, 10 min, 8°C). The pellet was resuspended in PBS and recentrifuged (250 *g*, 10 min, 8°C). These steps remove any excess Histopaque that may have a negative impact on any further experiments. The final pellet was resuspended in complete RPMI 1640 medium (2 ml). The cell suspension (1 ml/coverslip ~ $1x10^6$ cells) was placed on 22x22 mm cover slips previously sterilized at 120°C overnight or sterile 35 mm petri dishes. The cover slips in petri dishes or the petri dishes were incubated at 37°C for 2 h in a humidified atmosphere with 5% CO_2. Non-adherent cells were removed by thoroughly washing the cover slips or petri dishes in warm complete RPMI 1640 medium.

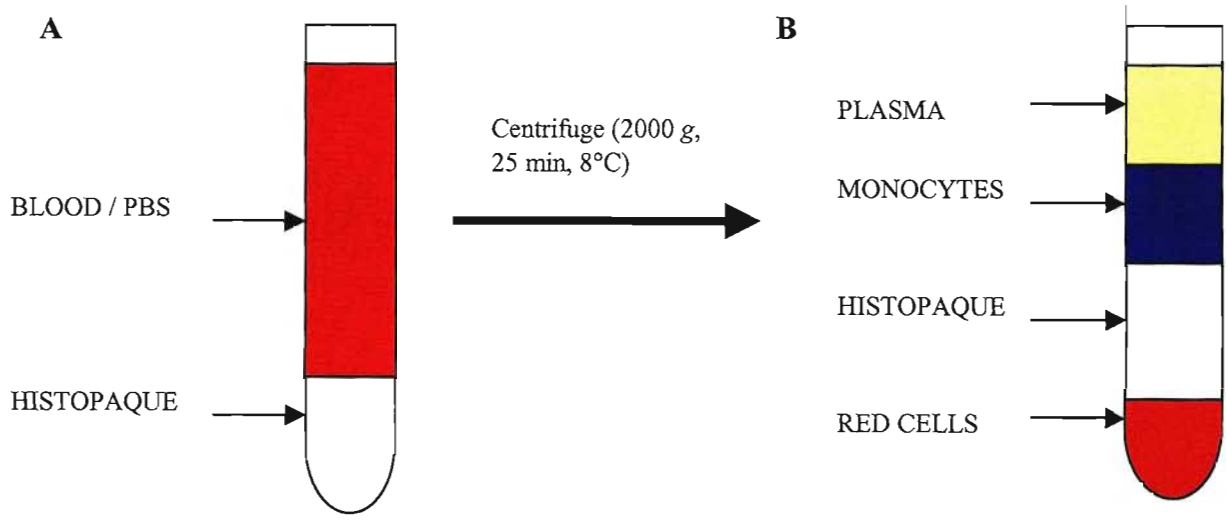

Figure 2.1 Diagrammatic representation of the separation of blood into its components before and after centrifugation through the Histopaque®- 1077 density gradient. (A) Prior to centrifugation the blood/PBS mixture was layered on to the Histopaque®-1077. **(B)** After completion of centrifugation four layers are visible: the plasma layer, monocyte layer, the histopaque layer and the red blood cell layer.

2.3 VIABILITY AND COUNTING ASSAYS

Trypan blue has been used in viability assays since 1956 (Martel *et al.*, 1974). It is an acid dye of the dis-azo group (Gurr, 1960) that is actively excluded from viable cells due to its negative charge, but it readily enters and stains dead cells because the outer membrane is no longer intact. Thus dead cells are stained blue. This allows an estimation of the number of viable

cells present. A haemocytometer is an etched glass chamber with raised sides that will hold the cover slip exactly 0.1mm above the chamber floor. The volume under the cover slip will always be the same and is known.

2.3.1 Materials

Trypan blue stock solution [0.4% (w/v) in 0.81% (w/v) NaCl and 0.06% (w/v) K_2HPO_4]. Trypan blue (0.04 g), NaCl (0.081 g) and K_2HPO_4 (0.006 g) were dissolved in ddH_2O in a final volume of 100 ml. The solution was sterilized through an acetate filter (0.22 μm pore size) into a bottle sterilized by autoclaving and stored at 4°C.

2.3.2 Procedure

An aliquot of the cell suspension (50 μl) obtained as described in Section 2.2 was diluted with PBS (450 μl), mixed with trypan blue stock solution (500 μl) in a 1.5 ml Eppendorf microfuge tube and incubated for 15 min at RT. A small volume was aspirated using a clean Pasteur pipette and dispensed into a haemocytometer by capillary action until both chambers were full but not overflowing. The cell numbers and the percentage of viable cells were estimated using the following calculations.

Dilution factor (DF) = 20

Total no. viable cells = [average no. viable cells x DF x 10^4]x volume of resuspended pellet

Total no. cells = [average no. cells x DF x 10^4] x volume of resuspended pellet

Viability = [Total no. viable cells / Total no. cells] x 100

2.4 GENERAL STAINING OF MONOCYTES

Monocytes can be identified by their morphology, their ability to phagocytose and their surface molecules (Stachura, 1989). In order to visualize and identify monocytes or any cells they must be stained. There are many stains to choose from. Giemsa is one of the most widely used of the blood cell stains. The nucleus is stains dark purple with the cytoplasm stained lightly. Different types of blood cells are stained differently by giemsa and thus one is able to differentiate between them. Methyl green is a counter stain, which stains the whole cell a light green. This is useful when in enzyme cytochemistry where the cells' enzymes, such as alkaline phosphatase or peroxidase, cleave a substrate into a precipitating product and thus visualize where the enzyme is localized.

2.4.1 Giemsa and methyl green staining of monocytes

Giemsa stain is a mixture of methylene blue and the azurs in different combinations with eosin Y (Gurr, 1960). Thus different brands may vary in the combinations of the component dyes present. Giemsa is traditionally used for staining blood smears for cells and parasites, particularly malaria. The nuclei of stained leucocytes are a reddish purple with the cytoplasms being a pale pink.

Methyl green is a bluish-green basic dye of the triphenylmethane group (Gurr, 1960). It is a widely used nuclear stain for both plant and animal material, and occasionally as a cytoplasmic stain. Methyl green stains DNA as it occurs in the nuclei, but it will not stain depolymerised DNA or RNA. In the present study it was used as a general stain where both the nuclei and cytoplasm were stained a light green.

2.4.1.1 Materials

Giemsa staining solution. Dilute stock stain solution (1 ml) in ddH_2O (20 ml).

2% Methyl green. Methyl green (2 g) was dissolved in dH_2O (100 ml).

2.4.1.2 Procedure

Monocytes on glass cover slips (Section 2.2) were air dried and immediately fixed in methanol (100%) for 30 s and air-dried. They were stained, with the cell side of the cover slip on the stain solution, either for 15 min at RT for the giemsa stain or 5 min for 2% methyl green. The cover slips were rinsed in three changes of distilled water and air-dried, followed by mounting onto slides with DPX (distrene dibutyl phthalate xylene) mountant.

2.4.2 Detecting alkaline phosphatase and peroxidase activity in monocytes

Alkaline phosphatase is a zinc-containing metalloenzyme that catalyses the hydrolysis of an ortho-phosphoric monoester to yield an alcohol and an orthophosphate. Phosphatase has been localized in the primary lysosomes of promonocytes and mature monocytes (Van Noorden and Frederiks, 1992). The detection of this enzyme involves the indoxyl-tetrazolium salt method. In the case of substrates containing an indoxyl or indolylamine group, such as 5-bromo-4-chloro-3-indolyl phosphate (BCIP), a colourless dehydro-indigo is generated instead of blue indigo. The electrons liberated during the dehydro-indigo formation reduce a tetrazolium salt such as nitroblue tetrazolium (NBT) to form formazan (reduced NBT dye), which in this case is a purple precipitate (Van Noorden and Frederiks, 1992). According to Absolom (1986) neutrophils are positive for the histochemical reaction for alkaline phosphatase while monocytes are negative. On the other hand Van Noorden and Frederiks (1992), as mentioned before state that alkaline phosphatase is present in monocytes.

Peroxidases are heme-containing enzymes that oxidize a variety of xenobiotics by hydrogen peroxide (O'Brien, 2000). Plant peroxidases consist of 300 amino acids (aa) and the heme is non-covalently bound, whereas mammalian peroxidases are much larger (576 – 738 aa) and the heme is covalently bound. The peroxidase of interest in neutrophils and other leukocytes is myeloperoxidase (MPO), which is localized in the lysosomes (O'Brien, 2000). MPO functions by oxidising chloride to produce strong oxidants (e.g. hypochlorous acid) that kill microorganisms. Promonocytes contain peroxidase in primary lysosomes and the more mature promonocytes develop a second population of granules, which are peroxidase negative. As monocytes mature the peroxidase activity is decreased (Stachura, 1989). Several chromogens

have been used to localize peroxidase activity, the most common being 3,3'-diaminobenzidine (DAB). The light-brown water soluble DAB acts as a hydrogen and electron donor and becomes oxidized to form a water insoluble precipitate (Van Noorden and Frederiks, 1992). The use of 4-chloro-1-naphthol was explored in the present study but it was found not to stain monocytes.

2.4.2.1 Materials

50 mM Tris-HCL, pH 9.5. Tris base (3.03 g) was dissolved in 450 ml dH_2O, the pH was adjusted with HCl and made up to a final volume of 500 ml with dH_2O.

50 mM Tris-HCL, 5 mM $MgCl_2$, pH 9.5. $MgCl_2$ (25 µl of a 1 M solution) was made up to 500 ml with 50 mM Tris-HCL (pH 9.5).

70% (v/v) Dimethylformamide (DMF). DMF (700 µl) was made up to 1 ml with dH_2O.

Alkaline phosphatase substrate solution. 5-Bromo-4-chloro-3-indolyl phosphate (BCIP) (0.003 g) was dissolved in 1 ml DMF and nitroblue tetrazolium (NBT) (0.006 g) was dissolved in 70% (v/v) DMF (1 ml). These two solutions were mixed and made up to 20 ml with 50 mM Tris-HCL, 5 mM $MgCl_2$ (pH 9.5).

50 mM Tris-HCL, pH 7.3. Tris base (0.6 g) was dissolved in 90 ml dH_2O, the pH was adjusted to 7.3 with HCl, and the solution was made up to a final volume of 100 ml with dH_2O.

Peroxidase substrate solution [39 mM 3,3'-diaminobenzidine (DAB), in 50 mM Tris-HCl (pH 7.3) with H_2O_2 (0.01%)]. DAB (0.011 g) was dissolved in 20 ml 50 mM Tris-HCl (pH 7.3) and H_2O_2 (2 µl). Immediately prior to use.

2.4.2.2 Procedure

Monocytes were isolated according to the procedure outlined in Section 2.2. After removal of the non-adherent cells the cover slips were incubated with either the alkaline phosphatase or the peroxidase substrate solutions for 30 min. The cover slips were rinsed in dH_2O and stained as described in Section 2.4.1.2.

2.5 MONOCYTE PHAGOCYTOSIS OF UNOPSONIZED LATEX BEADS AND β-HEMATIN

Phagocytosis is the most important defence mechanism in all species in the animal kingdom and today it still remains the principal way of disposing of invading pathogens (Van Oss, 1986; Oppenheim and Leonard, 1989). Monocytes are the second line of defence after neutrophils but both are highly phagocytic cells. Phagocytosis may be halted by lowering the temperature to 0°C (Wright, 1986). The binding of particles occurs, but pseudopods cannot be extended and invagination of the plasma membrane does not occur. When measuring phagocytosis *in vitro*, it is important to distinguish between adhering particles and those that have been ingested.

Heme is detoxified by the malaria parasite in a unique process to hemozoin. Hemozoin is not identical to β-hematin, as hemozoin is hematin associated with a protein (Goldie *et al.*, 1990). When comparing the two compounds using elemental composition, extended X-ray absorption fine structure (EXAFS) and the infra-red spectrum (IR) they were very similar (Slater *et al.*, 1991). The X-ray powder diffraction pattern obtained for hemozoin and β-hematin were almost indistinguishable. Since the molecules are very similar, β-hematin is a good substitute for the study of cell interactions with hemozoin. β-Hematin was synthesized according to the method used by Slater *et al.* (1991) and Taramelli *et al.* (1995), with minor modifications.

Monocytes are activated when incubated with the supernatants of parasite cultures, which contain malarial pigment or hemozoin (Abdalla and Wickramasinge, 1985). Taramelli *et al.* (1995) found that certain functions in monocytes are inhibited by the phagocytosis of hemozoin. Hemozoin phagocytosis has also been found to inhibit the expression of MHC

Class II antigen, CD54, CD11c and LAM-1 and increases the expression of CD11b (Pichyangkul *et al.*, 1997; Schwarzer *et al.*, 1998). Malarial pigment was later found to be a hematin derivative hemozoin. It was noted that hematin was responsible for inhibiting the production of nitric oxide and TNF-α (Taramelli *et al.*, 1995). Sherry *et al.* (1995) estimated that approximately 200 μmol hemozoin could be released into the blood stream of a malaria patient at schizogony, that is with a 1% underlying synchronous parasitemia. Pichyangkul *et al.* (1994) used β-hematin as a substitute for hemozoin in phagocytosis experiments. Latex beads are also phagocytosed by monocytes but they do not appear to alter the functioning of the cells. Latex beads were used as a control for phagocytosis (Schwarzer *et al.*, 2001).

2.5.1 Materials

0.1 M NaOH. NaOH (0.4 g) was dissolved in dH_2O (100 ml).

49 mM acetic acid. Acetic acid (1.4 ml) was added to dH_2O (490 ml) and made up to 500 ml with dH_2O.

0.2 M sodium carbonate (Solution A). Na_2CO_3 (4.24 g) was made up to 200 ml with dH_2O.

0.2 M sodium hydrogen carbonate (Solution B). $NaHCO_3$ (3.36 g) was made up to 200 ml with dH_2O.

0.1 M sodium bicarbonate buffer, pH 9.1. Solution A (10 ml) was titrated with solution B to pH 9.1 and made up to 200 ml with dH_2O.

200 μM β-hematin solution. β-hematin (1 mg) was suspended in ddH_2O (1 ml). This mixture (126 μl) was made up to 1 ml with RPMI complete medium (Section 2.2.1).

Phosphate buffer [100 mM sodium phosphate, 0.02% NaN_3, pH 7.6]. $NaH_2PO_4.H_2O$ (13.8 g) and NaN_3 (0.2 g) were dissolved in ddH_2O. The pH was adjusted to 7.6 with NaOH and made up to 1 l with ddH_2O.

Latex beads (1 μm). Purchased from Sigma chemicals as a 10% (w/v) solution in sterile water.

0.1% (w/v) Latex bead solution. Latex beads in solution (10 μl) were made up to 1 ml using complete RPMI medium (Section 2.2.1).

2.5.2 Procedure

Hematin (600 μmol or 0.03 g) was dissolved in 0.1 M NaOH (80 ml). The porphyrin was precipitated by addition of 49 mM acetic acid. The suspension was heated overnight at 70°C, and the precipitate was washed four times with dH_2O. Unreacted hematin was removed by extracting the precipitate twice for 3 h in 0.1 M sodium bicarbonate buffer. The remaining insoluble material was recovered by centrifugation (20 000 *g*, 10 min, RT) (Sigma 3K20) and washed four times with dH_2O. The insoluble β-hematin was recovered by centrifugation (20 000 *g*, 5 min, RT). After a final wash in 70% ethanol, the β-hematin was air dried and weighed. The hematin and the β-hematin were mounted onto carbon stubs and viewed in a Philips environmental scanning electron microscope (ESEM) under a large field detector. This allowed for the comparison of the crystal structure of the compounds. X-ray microanalysis was also performed on the ESEM at 2000x magnification, accelerating voltage of 20 kV and a spot size of 4.

Monocytes were isolated as per the protocol in Section 2.2. After removal of the nonadherent cells, the 0.1% latex bead solution or the 200 μM β-hematin solution (1 ml) was placed on each of the cover slips. The cells were incubated at 37°C for 30 min in a humidified atmosphere containing 5% CO_2. The cover slips were rinsed in dH_2O and stained with giemsa or methyl green as described in Section 2.4.1.

2.6 ELECTRON MICROSCOPY AND ELECTRON PROBE X-RAY MICROANALYSIS OF MONOCYTES

The transmission microscope is used for viewing particles smaller than a few tenths of a micrometer in diameter. Resolution in the light microscope is limited by the wavelength of the light being larger than the particle examined. The electron beam gives greater resolving power

than the light microscope and hence higher magnifications are possible. The electrons are produced by a tungsten filament operating in a vacuum and the electron beam is focused by electromagnets. In the TEM the electrons pass through the specimen and then l on a fluorescent screen where the image is visualized (Jones *et al.*, 1994). Electron probe X-ray microanalysis (EPXMA) is a technique that enables determination of the elemental composition of a specimen in the TEM (Warley, 1997). When the electron beam interacts with the specimen, X-rays are generated and carry information about the composition of elements in the cell.

2.6.1 Preparation of the cell pellet

2.6.1.1 Materials

Phosphate buffered saline (PBS), pH 7.2. See Section 2.2.1 for preparation.

0.2 M K_2HPO_4. K_2HPO_4 (34.8 g) was made up to 1 l with dH_2O.

0.2 M KH_2PO_4. KH_2PO_4 (27.2 g) was made up to 1 l with dH_2O.

0.2 M K-phosphate buffer, pH 6.8. Equal volumes of 0.2 M K_2HPO_4 and 0.2 M KH_2PO_4 were mixed to make 0.2 M phosphate buffer. The pH was 6.8.

2.6.1.2 Procedure

Monocytes were isolated as outlined (Section 2.2). The adherent cells were removed with 1 ml ice cold PBS and scraping of the petri dish with the rubber end of a syringe plunger. The cell suspension was placed into an Eppendorf tube. This process was repeated three times. The Eppendorfs were centrifuged in a Heraeus Biofuge Pico desktop centrifuge (400 *g*, 5 min, RT). The cell pellets were resuspended in a small volume of 0.2 M phosphate buffer and combined into one Eppendorf tube and recentrifuged (400 *g*, 5 min, RT). The monocyte pellet was resuspended in 0.2 M phosphate buffer.

2.6.2 Fixing and resin embedding of the monocyte cell pellet

Without careful preparation of the cells being studied, the ultrastructural detail is rendered meaningless. The main purpose of chemical fixation is to preserve the cells in a lifelike state (Jones *et al.*, 1994). Primary fixation involves the use of paraformaldehyde and glutaraldehyde and is probably the most important step, in that it fixes and stabilizes proteins. Osmium tetroxide acts as post fixative and is an excellent lipid stabilizer and contrasting agent. It reacts with both proteins and lipids, thus the contrast of lipoprotein cell membranes and fatty inclusions are intensified (Weakley, 1981). Osmium tetroxide fixes by reacting with the double bonds in lipids and thus crosslinks neighbouring molecules. Thereafter it reacts with the polar groups of lipids. It appears to crosslink proteins via SS and SH groups. The high water content in tissues and cells usually hinders subsequent preparation so the water needs to be removed. Dehydration involves a series of organic solvents decreasing in water content (Jones *et al.*, 1994). Embedding involves infiltrating the specimen with a solid medium (resin) that will support it during sectioning. There are many types of resins available but the current trend has been to move away from hydrophobic resins to the hydrophilic resins. In the present study LR-White was utilized. This has been found to give better morphology and, in the case of immunocytochemistry, retention of antigenicity. The only disadvantage of using a hydrophilic resin is that scrupulous attention must be paid to the technical procedure in order to obtain high quality results.

2.6.2.1 Materials

Paraformaldehyde [16% (w/v)]. Paraformaldehyde (16 g) was dissolved in ddH_2O (100 ml) and heated to 60°C. Saturated NaOH was added drop wise to the solution until clearing occurred.

Paraformaldehyde [8% (w/v)] in 0.1 M phosphate buffer. Paraformaldehyde [50 ml of 16% (w/v)] was mixed with an equal volume of 0.2 M phosphate buffer (Section 2.6.1.1).

Paraformaldehyde [2% (w/v)] in 0.1 M phosphate buffer. Paraformaldehyde [1 ml of 8% (w/v)] was diluted with 1 ml ddH_2O. 0.2 M phosphate buffer (200 µl; Section 2.6.1.1) was diluted with 1.5 ml ddH_2O. The two solutions were mixed.

Paraformaldehyde [8% (w/v)] / Glutaraldehyde [0.2% (v/v)] in 0.1 M phosphate buffer. Paraformaldehyde [50 ml of 16% (w/v)] and glutaraldehyde [600 µl of 25% (v/v)] was mixed with 0.2 M phosphate buffer (50.6 ml; Section 2.6.1.1).

0.2 M Glycine. Glycine (0.113 g) was dissolved in 100 ml PBS (Section 2.2.1), aliquoted into Eppendorf tubes and stored at -20°C.

Gelatin solution [10% (w/v)]. Gelatin (1 g) was dissolved in 1 ml ddH_2O, with heating until clear and stored at 37°C until required.

Osmium tetroxide stock solution [4% (w/v)]. For safety reasons, this was prepared by the electron microscopy unit staff.

Osmium tetroxide working solution [2% (w/v)]. 0.2 M Phosphate buffer (1 ml; Section 2.6.1.1), 4% osmium tetroxide stock solution (2 ml) and ddH_2O (1 ml) were mixed together to prepare a working solution, which was used immediately.

2.6.2.2 Procedure

The monocyte suspension (500 µl from Section 2.6.1.2) was mixed with an equal volume of 8% paraformaldehyde / 0.2% glutaraldehyde in 0.1 M phosphate buffer for 2 h at RT. The cells were gently pelleted by centrifugation in a Heraeus Biofuge Pico desktop centrifuge at (400 *g*, 5 min, RT). The supernatant was removed and replaced with 8% paraformaldehyde in phosphate buffer and incubated overnight at 4°C. The cells were pelleted and the supernatant removed. The cells were resuspended in 0.2 M glycine (1 ml), incubated for 15 min at RT, repelleted and the supernatant discarded. A further 1 ml 0.2 M glycine was added and the pellet was resuspended and allowed to quench for 30 min. The cells were recentrifuged and the supernatant removed. The warmed gelatin solution (1 ml) was added and the pellet resuspended and incubated for 1 h at 37°C. The cells were spun down and the gelatin supernatant aspirated. Fresh gelatin solution (100 µl) was added and allowed to solidify on ice for 20 min. The gelatin pellet was removed from the Eppendorf using a needle and cut into

cubes. The cubes were osmicated using 2% osmium tetroxide for approximately 30 min or until they appeared brown. The osmium tetroxide was removed and the cubes washed twice in 0.2 M phosphate buffer for 15 min. The cubes were taken through a dehydration series of: 30% ethanol (5 min); 50% ethanol (5 min); 70% ethanol (5 min); 90% ethanol (5 min) and 100% ethanol (2 x 5 min). LR white resin (1 part) was mixed with 100% ethanol (1 part) and incubated with the pellet for 30 min. This solution was removed and replaced with 2 parts LR white resin, 1 part 100% ethanol and incubated for 30 min. LR white resin was added and incubated for 30 min: the resin was changed and left overnight. The cubes and fresh resin were added to the gelatin capsules and were allowed to polymerise at 45 - 50°C for 24 h. The polymerised resin was removed from the capsule and prepared for sectioning by cutting the tip off and mounting it on a perspex stub. The stub was then trimmed and ultra thin sections (100 nm) cut on a LKB Ultratome III using a glass knife.

2.6.3 Heavy metal staining of ultra thin sections

Many factors affect contrast within the electron microscope and of these the four most important are the thickness of the specimen, accelerating voltage, aperture size and the presence of heavy metal atoms in the specimen (Weakley, 1981). The atoms present in biological material are mainly of low atomic number: hydrogen (1); carbon (6); nitrogen (7); oxygen (8); phosphorous (15) and sulfur (16). Thus the electron scattering ability of these light elements is very small. Heavy metal salts are useful as contrast-increasing stains. Generally heavy metal cations form complexes with negatively charged groups in the cells while the ions of lead and uranium bind to oxygen. Uranyl acetate has strong affinities for nucleic acids, but also acts as a general stain for proteins (Weakley, 1981). It is thought that the uranium ions attach to the PO_4^{2-} groups of nucleic acids and some proteins. Lead citrate adds contrast to nucleic acids, membranes and glycogen. Lead also attaches to osmium compounds bound to the cellular components during fixing. The lead attaches to the OH groups of carbohydrates and RNA phosphate groups. These two stains give contrast and details on the ultrastructure of the sectioned cells.

2.6.3.1 Materials

Uranyl acetate [2% (w/v)]. Uranyl acetate (1 g) was dissolved in ddH_2O. A drop of 95% ethanol was added to lower the surface tension. The solution was kept in the dark and refrigerated.

Lead citrate. $Pb(NO_3)$ (1.33 g) and $Na_3(C_6H_5O_7).2H_2O$ (1.76 g) were dissolved in 30 ml CO_2 free ddH_2O (freshly boiled or vacuum degassed) by shaking vigorously for 1 min then intermittently every 30 min, to give a milky white solution. 1 N NaOH (8 ml) (1 g NaOH made up to 25 ml with CO_2 free ddH_2O) was added to the solution, which turns. The solution was made up to 50 ml with CO_2 free ddH_2O. Lead citrate is CO_2 sensitive and should be stored in the dark and in a sealed bottle. For safety reasons this reagent was made up by the staff of the electron microscopy unit.

2.6.3.2 Procedure

Drops of 2% uranyl acetate solution were placed on a clean waxed petri dish. Grids were inverted with the section side down on the surface of the drop. The specimens were allowed to stain for 10 min. The grid was removed and washed with a stream of dH_2O. The excess water was removed by touching the grid on a piece of filter paper. A teaspoon of pure sodium hydroxide pellets was placed in a second clean, waxed petri dish. Drops of the lead citrate solution were placed in the petri dish and the staining was carried out as for the 2% uranyl acetate. The grids were washed with dH_2O and dried as above.

2.6.4 Preparation of grids for EPXMA

TEM grids are made from a wide variety of materials and come in many patterns depending on the application. Typically the grids are 3.05 mm in diameter, made of copper and contain holes, which are very precisely calibrated with between 100 and 1000 holes per 25 mm. Due to copper being toxic to cells, gold was used in the present study as it is a neutral metal which has little to no effect on the viability of growing cells (Warley *et al.*, 1994). The cells are far too small to fit on the grid without falling through so the grid must be coated. The coating process involves placing a very thin film of a plastic compound (formvar) over the entire grid.

2.6.4.1 Materials

Acetic acid [20% (v/v)]. Acetic acid (20 ml) was added to dH_2O (80 ml).

Formvar solution [0.2% (w/v)]. Formvar (0.2 g) was dissolved in 100 ml dehydrated chloroform.

2.6.4.2 Procedure

The gold grids were cleaned by sequentially sonicating in chloroform, 100% ethanol, dH_2O (x2), 20% acetic acid, dH_2O (x2), 100% ethanol and dH_2O (x2). The grids were allowed to dry before being used. Clean microscope slides were dipped into the formvar solution and the excess solution was drained off onto tissue paper. The slides were allowed to dry and, using a sharp blade, the edges of the slide were cleared of formvar. The slide was carefully dipped into distilled water at an angle of + 45°, allowing the formvar to float off. The gold grids were placed on the floating formvar. Using another clean slide the grids and the formvar were picked up and allowed to dry. Once dry, three formvar-coated gold grids were placed in alternate wells of an ELISA plate lid (Figure 2.2). The grids on the lid were sterilized under UV light in a vertical Biohazard laminar flow cabinet (Faster; BH-2000 S/D) for 20 min.

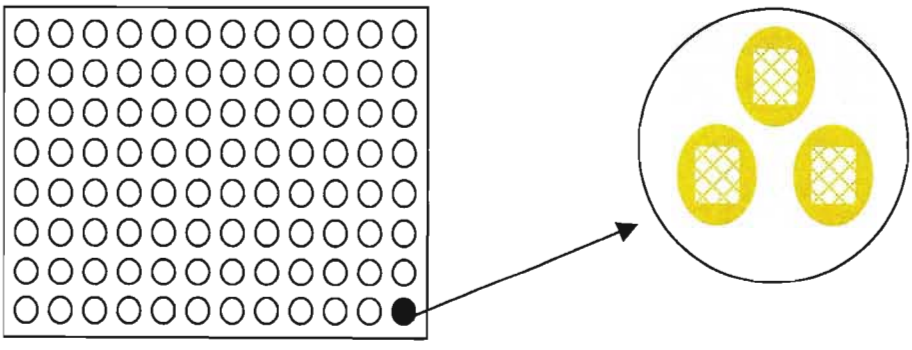

Figure 2.2 Schematic representation of the ELISA plate lid and the placement of the formvar coated grids for the culture of monocytes in preparation for EPXMA.

2.6.5 Preparation of monocytes for EPXMA

Cells such as monocytes can be cultured on grids since they adhere to plastic (formvar) and they grow in monolayers. Even though a small number of cells may be present per grid, this is all that is required for EPXMA. According to Warley *et al.* (1994) this is an ideal method for measuring elemental concentrations, fluxes and for studying the effects of drugs on a given cell type. The cells were washed in sterile ultra pure water to remove the medium as this was found by Warley *et al.* (1994) to be better than 0.3 M sucrose or 0.15 M sodium acetate. Liquid nitrogen is suitable and convenient to use for rapid freezing of cell monolayers. In the present study a freeze dryer capable of handling electron microscope grids was not available, so resort was made to air-drying. Air-drying is the simplest method for the preparation of cells, but the specimens shrink and their structure is disrupted. This technique is not suitable if ultrastructural details are required but when the total elemental content of the cell is of interest it is very successful (Chandler, 1977; Warley, 1997). Therapeutic concentrations for all the drugs used were from Goldring and Nemaorani (1999) and Goldring *et al.* (1999).

2.6.5.1 Materials

Phosphate buffered saline (PBS), pH 7.2. See Section 2.2.2 for preparation.

Complete RPMI 1640 medium [25 mM HEPES; 5% FCS]. See Section 2.2.2 for preparation

Quinine stock solution (200 µg/ml). Quinine (1 mg) was dissolved in 1 ml dimethylsulfoxide (DMSO) and made up to 5 ml with sterile ddH_2O.

Therapeutic quinine working solution (15 µg/ml). Quinine stock solution (375 µl) was made up to 5 ml with complete RPMI medium.

Chloroquine stock solution (100 µg/ml). Chloroquine (1 mg) was dissolved in 1 ml DMSO and made up to 10 ml with sterile ddH_2O.

Therapeutic chloroquine working solution (0.2 µg/ml). Chloroquine stock solution (20 µl) was made up to 10 ml with complete RPMI medium.

Artemisinin stock solution (100 µg/ml). Artemisinin (1 mg) was dissolved in 1 ml DMSO and made up to 10 ml with sterile ddH_2O.

Therapeutic artemisinin working solution (0.4 µg/ml). Artemisinin stock solution (40 µl) was made up to 10 ml with complete RPMI medium.

Primaquine stock solution (100 µg/ml). Primaquine (1 mg) was dissolved in 1 ml DMSO and made up to 10 ml with sterile ddH_2O.

Therapeutic primaquine working solution (0.15 µg/ml). Primaquine stock solution (31 µl) was made up to 20 ml with complete RPMI medium.

Pyrimethamine stock solution (100 µg/ml). Pyrimethamine (1 mg) was dissolved in 1 ml DMSO and made up to 10 ml with sterile ddH_2O.

Therapeutic pyrimethamine working solution (0.15 µg/ml). Pyrimethamine stock solution (31 µl) was made up to 20 ml with complete RPMI medium.

Dapsone stock solution (1 mg/ml). Dapsone (1 mg) was dissolved in 1 ml with sterile ddH_2O.

Therapeutic dapsone working solution (3 µg/ml). Dapsone stock solution (30 µl) was made up to 10 ml with complete RPMI medium.

Doxycycline stock solution (1 mg/ml). Doxycycline HCl (1 mg) was dissolved in 1 ml with sterile ddH_2O.

Therapeutic doxycycline working solution (3 µg/ml). Doxycycline stock solution (30 µl) was made up to 10 ml with complete RPMI medium.

Tetracycline stock solution (1 mg/ml). Tetracycline HCl (1 mg) was dissolved in 1 ml with sterile ddH_2O.

Therapeutic tetracycline working solution (3 μg/ml). Tetracycline stock solution (30 μl) was made up to 10 ml with complete RPMI medium.

Suramin stock solution (1 mg/ml). Suramin (1 mg) was dissolved in 1 ml with sterile ddH_2O.

Therapeutic suramin working solution (20 μg/ml). Suramin stock solution (100 μl) was made up to 5 ml with complete RPMI medium.

DMSO working solution. DMSO was made up to 5 ml with sterile ddH_2O, and 1.86 ml of this solution was made up to 5 ml with complete RPMI medium.

200 μM β-hematin solution. See Section 2.5 for preparation

0.1% Latex bead solution. See Section 2..5 for preparation

2.6.5.2 Procedure

Monocytes were isolated as described in Section 2.2. The adherent cells were removed with 1 ml ice cold PBS and scraping the petri dish with the rubber end of a syringe. The cell suspension was placed into an Eppendorf tube. This process was repeated three times. The Eppendorfs were centrifuged in a Heraeus Biofuge Pico desktop centrifuge (400 *g*, 5 min, RT). The cell pellets were resuspended in a small volume of cold PBS and combined into one Eppendorf tube and recentrifuged. The monocyte pellet was resuspended in warm complete RPMI medium, the volume corresponding to 100 μl for every three formvar coated gold grids in the ELISA plate lid (Figure 2.2). The cells were allowed to adhere to the grids at 37°C for 2 h in a humidified atmosphere with 5% CO_2. The medium was removed and the experimental conditions were applied to canine monocytes (Table 2.1). The grids were gently washed in sterile ddH_2O and air-dried or frozen in liquid nitrogen.

Table 2.1 Experimental conditions applied to monocytes adhering to gold grids.

Drug or conditions	Concentration	Biologically relevant levels	Time				
			0 min	10 min	30 min	2 h	18 h
Control (No drug)	Medium only	-	√	√			√
Quinine	15 µg/ml	Therapeutic	√	√			√
Chloroquine	0.2 µg/ml	Therapeutic	√	√			√
Artemisinin	400 ng/ml	Therapeutic	√	√			√
Primaquine	153 ng/ml	Therapeutic	√	√			√
Pyrimethamine	155 ng/ml	Therapeutic	√	√			√
Dapsone	3 µg/ml	Therapeutic	√	√			√
Doxycycline	3 µg/ml	Therapeutic	√	√			√
Tetracycline	3 µg/ml	Therapeutic	√	√			√
Suramin	20 µg/ml	Therapeutic	√	√			√
DMSO	20% (v/v)	Max Dilution	√	√			√
Hemozoin	200 µM	'Normal level'	√	√			√
Latex beads	0.1% (v/v)	-	√	√			√
Incubated 37°C	Medium only	No Heat Shock	√	√	√	√	
Incubated 44°C	Medium only	Heat Shock	√	√	√	√	

2.6.6 Grid and film correction for quantitative EPXMA

For quantitative analysis of specimens using the peak to continuum method, the contribution of the grid and the film to the continuum must be taken into account and corrected for. If this is not done concentrations will be grossly over estimated. An uncoated gold grid was analysed by X-ray microanalysis in a Philips CM120 transmission electron microscope equipped with an EDAX detector fitted with a 10 µm beryllium window. Ten spectra (Figure 2.3) were obtained at 80 kV, spot size 200 nm, specimen tilted to + 20° and a live time of 100 s. The number of counts under each peak were determined using the spectra obtained.

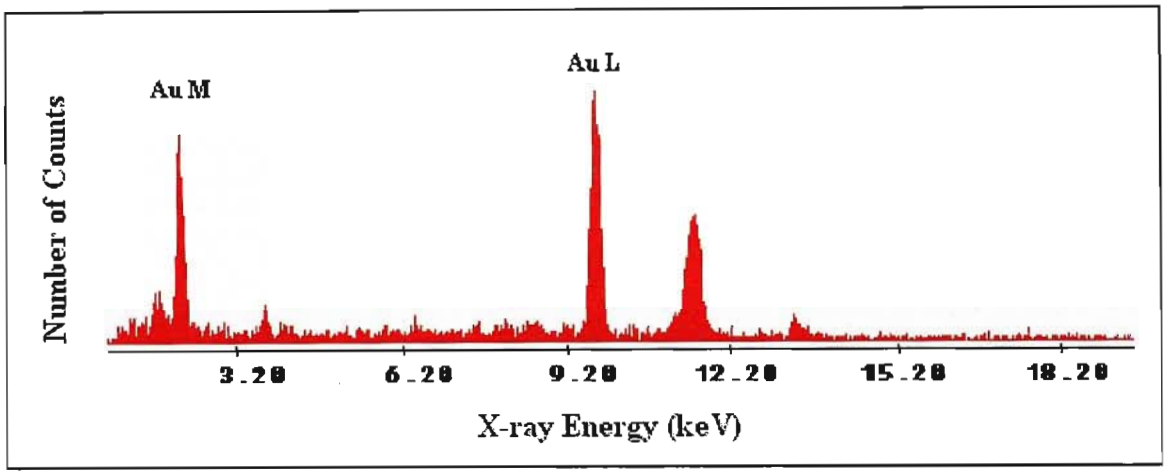

Figure 2.3 X-rays produced by irradiation of a gold (Au) grid either coated with formvar or uncoated. The spectrum collected between 0 and 18 keV, shows the L and M families of peaks. The M family occurs at 2.123 and 2.205 keV and the L family consists of Lα (9.71 keV), Lβ (11.44 keV), Lγ (13.38 keV), which are clearly defined peaks.

Using the following formulas the grid correction factors for the microscope were calculated and an average taken.

$k_x = C_x.W/ P_x$

C_x = Concentration of x
P_x = Net peak intensity
W = Continuum (4.2 – 6.2)
k_x = Calibration constant

Thus Grid correction factor = W/P_{Au}

P_{Au} = Net peak intensity Au
W = Continuum (4.2 – 6.2)

The average of all the grid correction factors was 0.38. The actual grid correction was calculated from the specimens being analysed and again an average taken. The formula for the grid correction is:

Grid correction for sample = 0.38 x P_{Au}

P_{Au} = Net peak intensity Au in sample

The film correction was carried out on the each sample, with an area devoid of cells being measured three times on each grid. The film correction was calculated using the following formula:

$$\text{Film correction} = W_{Film} - \text{Grid correction}$$

W_{Film}	= Continuum of specimen film

For most of the grids analysed the film correction corresponded to approximately 564.

2.6.7 Efficiency of sodium with respect to potassium for quantitative EPXMA

Sodium and potassium occur in the compound sodium potassium tartrate in a 1:1 ratio, thus the concentration is the same, and thus so should the peaks and calculated concentrations. This is not the case, however, as the detector's efficiency decreases with atomic number. This chemical enables us to correct for sodium.

2.6.7.1 Materials

Sodium potassium tartrate solution. A few crystals of $NaKC_4O_6H_4.4H_2O$ were dissolved in sterile ddH_2O.

2.6.7.2 Procedure

A drop of the sodium potassium tartrate solution was placed on a formvar coated gold grid and allowed to dry. The grid was analysed and spectra (Figure 2.4) obtained using X-ray microanalysis in the TEM and the number of counts under each peak determined. The Na peak is much smaller than the K even though they are in a 1:1 ratio, due to the efficiency of the detector diminishing with decreasing atomic number. The efficiency was calculated using the following formula:

$$\% \text{ efficiency of Na} = (P_{Na}/P_K) \times 100$$

The efficiency of Na with respect to K was calculated to be 15%.

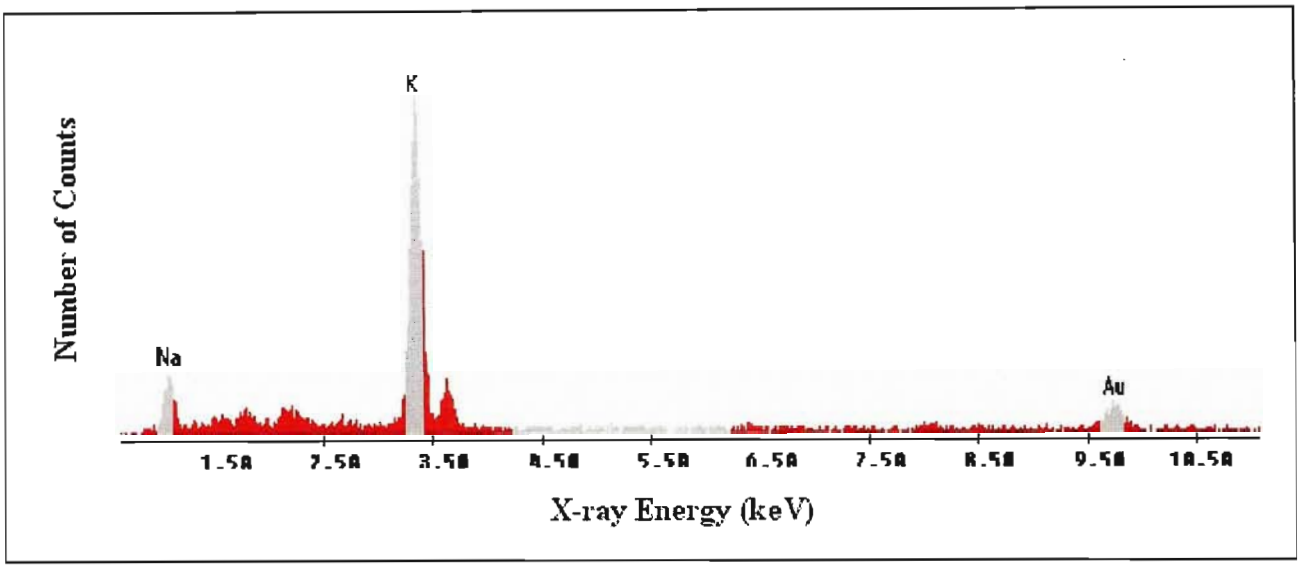

Figure 2.4 X-rays produced by irradiation of sodium potassium tartrate on a formvar coated gold grid. The spectrum collected between 0 and 10.5 keV, shows the Na, K and Au peaks, which are of different intensities.

2.6.8 Relative detector efficiency for quantitative EPXMA

The relative detector efficiency can be determined in a similar way to Section 2.6.7 but using an isoatomic solution containing the elements Na, Mg, P, S, Cl, K and Ca. The number of counts increase with increasing atomic number, with the exception of chlorine that is labile under the electron beam in this preparation. Thus the detectors efficiency for all the elements Na, Mg, P, S, Cl, and Ca can be determined with respect to K, these efficiencies are determined as a percentage and using K's correction factor the remaining correction factors can be determined. The isoatomic solution was sprayed onto the plastic film-covered grid. There are two main problems that may be encountered in preparing and analysing the fluids. One is the formation of large crystals of solute in the droplets as they dry and the second is the loss of elements during analysis. Ideally, the dried crystals should be small and have a homogenous appearance (Warley, 1997)

2.6.8.1 Materials

Isoatomic Solution. $MgSO_4.7H_2O$ (0.5 g), NaCl (0.12 g), KH_2PO_4 (0.28 g) and $Ca(NO_3)_2.4H_2O$ (0.48 g) were dissolved in sterile ddH_2O (250 ml).

2.6.8.2 Procedure

The isoatomic solution was sprayed onto the formvar coated gold grids using an atomizer. The grids were allowed to dry in a clean atmosphere. Once dry, they were coated with a thin layer of carbon. Spectra were collected from each whole droplet (Figure 2.5) and the number of counts under each peak determined. The counts for each element were normalized against K to give the relative detector efficiency with respect to K. The number of counts increases with increasing atomic number. The correction factors for each element were calculated using the known correction factor for K (K_k = 298). Cl was calculated by extrapolation from the curve (Figure 2.6) as it is extremely labile in this preparation and the correction factor would be distorted. The correction factors are listed in Table 2.2.

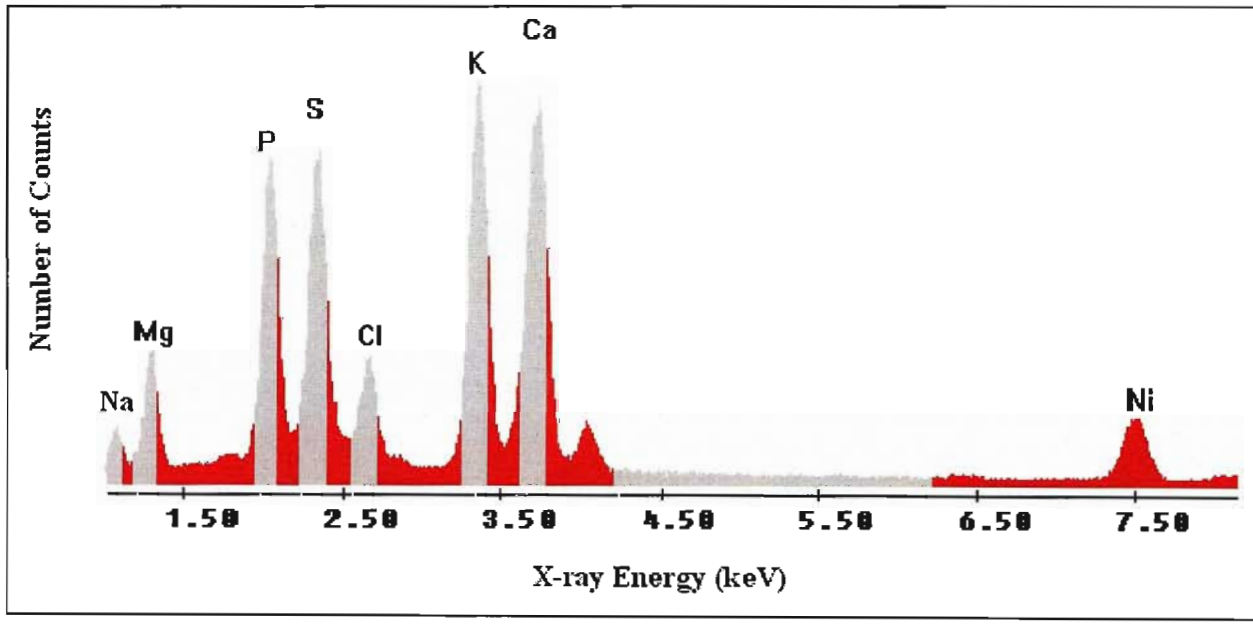

Figure 2.5 A typical spectrum produced by irradiation of isoatomic droplets containing the elements sodium, magnesium, phosphorous, sulfur, chlorine, potassium and calcium.

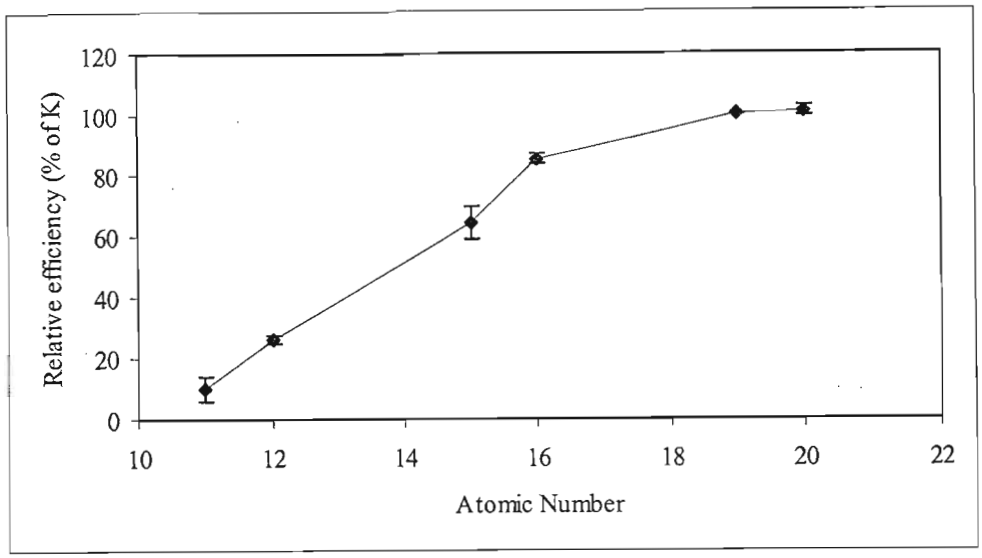

Figure 2.6 Relative efficiency of the EDAX detector system, with respect to the element potassium, plotted against atomic number as determined by the analysis of isoatomic droplets. The analyses were carried out at 80 kV, spot size 200 nm, specimen tilted to + 20° and with a live time of 100 s. Each point is the mean of ten analyses and each bar represents standard deviation of the mean.

Table 2.2 Elemental correction factors for quantitative EPXMA.

Element	Atomic Number	Correction factor (k_x)
Na	11	1490
Mg	12	1064
P	15	438
S	16	359
Cl	17	331
K	19	298
Ca	20	292

2.6.9 EPXMA analysis of monocytes

The handling of the specimen prior to analysis and the operation of the microscope during analysis will affect the results obtained. The specimen can become contaminated with elements from the environment during preparation and analysis, thus it is important to work in a clean environment and handle specimens as little as possible. Sources of contamination from the environment include dust; dirty glassware (various elements); sweat (Na, Cl); vacuum oils (Si, Cl, S); desiccants (Si, P, Ca, Cl, Cu, S); talcum powders (Al, Ca, Mg, Si, Zn) and adhesive

tape (Cl) (Warley, 1997). The optimal conditions of accelerating voltage, apertures, probe current, probe size, duration of analysis and magnification are determined and adhered to throughout analysis of the specimens.

2.6.9.1 Procedure

Monocytes on grids prepared in Section 2.6.5.2 were analysed in a Philips CM120 transmission electron microscope equipped with an EDAX detector fitted with a 10 μm beryllium window. Ten spectra per grid were obtained at 80 kV, spot size 200 nm, specimen tilted to + 20° and a live time of 100 s. The number of counts under each peak were determined and using the correction factors for each element (Table 2.2) and the continuum for each reading, the concentration in mmole/kg dry weight was calculated.

$$C_x = k_x.P_x/W$$

C_x = Concentration of x
P_x = Net peak intensity
W = Continuum (4.2 – 6.2)
k_x = Calibration constant

The P:K ratios were also calculated as these are a useful indicator of fluxes in the cell. The results were subjected to statistical analysis to determine any significant differences in the concentrations of elements (Na, Mg, P, S, Cl, K and Ca) in the monocytes. Statistical significance was determined using a Mann-Whitney U-test; a value of $p < 0.05$ was considered statistically significant.

2.7 HEAT SHOCK PROTEIN PEPTIDE SELECTION AND ANTIBODY PRODUCTION

2.7.1 Selection of peptides

The antigenic properties of synthetic peptides are interesting as they are able to mimic the antigenic sites of proteins (Van Regenmortel *et al.*, 1988). By breaking a protein down into smaller parts, knowledge about that specific protein can be gained using antibodies which the corresponding synthetic peptides can elicit. The anti-peptide antibodies generally react with the native protein from which the peptides were originally developed. Synthetic peptides are usually sequential or continuous epitopes since they are a defined sequence of amino acid

residues linked by peptide bonds (Van Regenmortel *et al.*, 1988). Conformational epitopes consist of a group of amino acid residues that are brought together by the folding of the protein and are not adjacent. A prerequisite for the development of peptides is knowledge of the DNA sequence or the amino acid sequence. This information enables prediction of the location of sequential epitopes in the protein.

Predict7 is a programme, which incorporates four prediction factors: hydrophilicity, flexibility, surface probability and antigenicity (Cármenes *et al.*, 1989). Hydrophilicity is considered an important factor since hydrophilic amino acid residues are generally on the exterior of the folded protein where they can interact with water (Van Regenmortel *et al.*, 1988). Hopp and Woods (1981; 1983) showed that hydrophilic segments correspond to sequential epitopes. Hydrophilic peptides are also more likely to be soluble for coupling reactions (Harlow and Lane, 1988). Thus, for the purpose of prediction, only the highest peaks on the hydrophilicity peaks were considered. Flexibility of the peptides is an important factor, as this allows different conformations to form and ultimately one will form that is the same as that in the protein. Flexible peptides will also be easier to couple to a carrier protein without disrupting the folding. Surface probability is related to hydrophilicity, as antibodies can only access the external surface of the protein (Van Regenmortel *et al.*, 1988).

Another selection criterion is the sequence variability, i.e. where the protein of interest is not similar in sequence to any known protein. It has been found in families with homologous proteins with highly conserved sequences, such as heat shock protein 70 (HSP70) and heat shock cognate protein 70 (HSC70), that regions of sequence variability correspond to the location of antigenic epitopes (Van Regenmortel *et al.*, 1988). Peptides consisting of 10 – 15 amino acid residues are easy to synthesize, and purify and yield satisfactory anti-sera. Peptide fragments can be conjugated to a carrier protein and immunized, and the antibodies produced can be tested against the native protein. A positive result is indicative that the peptide approximated to an epitope on the target protein (Van Regenmortel *et al.*, 1988).

2.7.1.1 Predict7

The amino acid sequences of human heat shock protein 70 (HSP) and heat shock cognate protein 70 (HSC) were obtained from Swiss Prot (http://www.expasy.ch). The accession number for human HSP is P08107 and human HSC is P11142. The sequences were entered into the Predict7 programme. The programme was utilized to find regions where all the prediction factors had high probabilities and 7 suitable regions were found for HSP and 10 for HSC.

2.7.1.2 Similarity searches

All the suitable peptide regions were run through a similarity search programme, BLAST2.0, on the Swiss Prot website. The number of suitable peptide regions was narrowed down to one for HSC and six for HSP. Sequences were also compared with those of chicken (*Gallus gallus*) proteins to determine percentage similarity since these proteins are highly conserved between species and this was the animal of choice for immunisation of the peptides. The HSP70 and HSC70 sequences were aligned, to determine where areas of non-similarity were. These were found in the C-terminal 110 amino acids and those peptides that were similar between these two proteins were not considered. Stressgen makes monoclonal antibodies against both the proteins of interest and in their catalogue they use a region between amino acids 436 and 503 for HSP only and for antibodies that recognized both HSP and HSC they use between amino acids 503 and 640. These regions were found to have high similarity between human and mouse proteins. The selected peptides are indicated in Table 2.3. The HSP peptide (1761.99 Da) and the HSC peptide (1689.96 Da) were synthesized by Sigma Genosys (St. Louis, USA).

Table 2.3 Peptide sequences selected to elicit anti-heat shock protein antibodies. Selected peptide sequences, with the corresponding amino acid number in the parent protein and the similarities between human and chicken heat shock and heat shock cognate proteins.

Peptide Sequence	Protein (Human)	AA No.	Similarity between sequences			
			Human		Chicken	
			HSP70	HSC70	HSP70	HSC70
KINDEDKQKILDKC	HSC	561-574	66%	100%	ND	82%
CLAEKDEFEHKRKE	HSP	586-598	100%	73%	73%	ND

2.7.2 Conjugation of peptides to rabbit albumin with MBS

To produce antibodies against small peptides, it is important to intensify their immunogenicity by coupling them to protein carriers (Van Regenmortel *et al.*, 1988). The peptides chosen in Section 2.7.1 have many lysine residues (K), thus glutaraldehyde cannot be used to conjugate the peptide to the carrier protein. Neither can carbodiimide be used, as there are many aspartic- (D) and glutamic acids (E). The HSC peptide has a cysteine on its C-terminus and the HSP peptide has had a cys residue added to its N-terminus, enabling conjugation with m-maleimidobenzoyl-N-hydroxysuccinimide ester (MBS). MBS is a heterobifunctional reagent that crosslinks peptides to carrier proteins through cysteines and free amino groups (Harlow and Lane, 1988). MBS reacts with the carrier protein first, by acylating the amino groups via the active N-succinimide ester, followed by the formation of a thioester bond through addition of a thiol group to the double bond of the maleimide (Van Regenmortel *et al.*, 1988; Hermanson, 1996). The peptide thiol groups are reduced by dithiothreitol (DTT). Ellman's reagent (5,5'-dithio-bis-(2-nitrobenzoic acid) is a compound used for the qualitative determination of sulfhydryls in solution. The disulfide in Ellman's reagent undergoes disulfide exchange with free sulfhydryls, such as those on the reduced peptides, to form a mixed disulfide and release one molecule of the chromogenic substance 5-sulfido-2-nitrobenzoate, which has an intense yellow colour (Hermanson, 1996).

The carrier was chosen with the following criteria in mind: availability of reactive sites, size, solubility, immunogenicity, commercial availability and cost. The conjugates of choice were

bovine serum albumin (BSA), ovalbumin and rabbit albumin. BSA is used routinely in the blocking steps for ELISAs and western blots and so would be unsuitable as the carrier, and ovalbumin is also unsuitable as the animal of choice for immunization is the chicken. Thus the carrier of choice was rabbit albumin. The MBS and rabbit albumin, and the peptides and DTT were separated from each other, respectively, on a gel exclusion column, which separates particles according to their size.

2.7.2.1 Materials

MEC buffer [100 mM phosphate buffer, 0.02% (m/v) NaN_3, pH 7]. $NaH_2PO_4.2H_2O$ (13.8 g) was dissolved in 900 ml dH_2O, the pH was adjusted to 7 with NaOH, NaN_3 (0.1 g) was then added and the solution made up to 1 l with dH_2O.

Reducing buffer [100 mM Tris-HCl, 1 mM Na_2EDTA, 0.02% (m/v) NaN_3, pH 8]. Tris base (1.21 g) and Na_2EDTA (0.037 g) were dissolved in 90 ml dH_2O, the pH was adjusted to 8 with HCl and made up to 100 ml with dH_2O.

Ellman's reagent buffer [100 mM Tris-HCl, 10 mM Na_2EDTA, 0.1% SDS, pH 8]. Tris base (1.21 g), Na_2EDTA (0.37 g) and SDS (0.1 g) were dissolved in 90 ml dH_2O, the pH was adjusted to 8 with HCl and made up to 100 ml with dH_2O.

10 mM dithiothreitol (DTT). DTT (7.71 mg) was dissolved in reducing buffer (5 ml).

Ellman's reagent. Ellman's reagent [5,5'-dithiobis-(2-nitrobenzoic acid)] (10 mg) was dissolved in Ellman's reagent buffer (2.5 ml).

Phosphate buffered saline (PBS), pH 7.2. See Section 2.2.1 for preparation

2.7.2.2 Procedure

Each peptide (4 mg) was dissolved in 100 µl DMSO and made up to 1 ml with reducing buffer. 10 mM DTT (1 ml) was added and allowed to incubate for 1.5 h at 37°C. The reduced peptide was separated from the DTT on a Sephadex-G10 column. To test for the reduced

peptide 10 µl eluant was added to 10 µl Ellman's reagent. The yellow samples indicated tubes containing the reduced peptide which were pooled. The amount of rabbit albumin carrier, was calculated for each peptide with HSC requiring 4 mg and HSP requiring 3.9 mg, thus a total of 7.9 mg of rabbit albumin was used and dissolved in 1.25 ml PBS. *m*-Maleimidobenzoyl-N-hydroxysuccinimide ester (MBS) (1.5 mg) was dissolved in 300 µl DMF and 450 µl PBS. The carrier protein and the MBS were combined and incubated at RT for 30 min with stirring. Unreacted MBS was separated from the carrier on a Sephadex G-25 column; the A_{280} of the eluant indicated where the carrier eluted. The reduced peptides were combined with the appropriate volume of the MBS-activated carrier (HSC – 2.04 ml; HSP – 1.96 ml) and incubated for 3 h at RT. The peptide-carrier conjugates were separately aliquoted into 4 equal volumes and stored in the freezer.

2.7.3 Immunization of chickens

Antibody production normally requires the use of laboratory animals (rabbits, mice, rats or guinea pigs) or larger animals (horses, sheep or goats). The procedure involves two steps, both of which causes distress or pain to the animals: the immunization itself and the bleeding, which is a prerequisite for antibody production (Schade *et al.*, 1999). The use of chickens for antibody production, as opposed to mammals, represents a refinement in that there is no longer the necessity to bleed the chickens, as the antibodies are packaged in the eggs. Chickens also produce much larger amounts of antibodies [50 – 100 mg IgY per egg (5-7 eggs/week)] than laboratory rodents (200 mg IgG per 40 ml bleed), so the number of animals used can also be reduced. Another advantage of using chickens to make antibodies against mammalian proteins or peptides is that birds are evolutionary distant from mammals, thus a good response will be elicited.

Classical immunization procedures can be used for synthetic peptides since there is usually no problem in raising antibodies as they are good immunogens. The adjuvant most commonly used to enhance the humoral response is Freund's complete adjuvant (FCA), which contains heat-killed *Mycobacterium tuberculosis* cells and mineral oil. Further inoculations use Freund's incomplete adjuvant (FIA), which consists only of mineral oil. It is essential to immunize more than one animal, as it has been commonly observed that animals receiving the

same immunogen and immunization regimen produce antisera with completely different characteristics (Van Regenmortel *et al.*, 1988).

2.7.3.1 Materials

Phosphate buffered saline (PBS), pH 7.2. See Section 2.2.1 for preparation

Freund's complete adjuvant. Purchased from Sigma (St. Louis, USA).

Freund's incomplete adjuvant. Purchased from Sigma (St. Louis, USA).

2.7.3.2 Procedure

An equal amount of Freund's complete adjuvant was added to the peptide-rabbit albumin conjugate and triturated. Trituration was considered complete when a small drop of the mixture, placed in dH_2O, remained a tight 'ball'. Using half the syringe volume per chicken, i.e. 1 ml and 1.2 ml for the chickens immunized with the HSP conjugate and the HSC conjugate, respectively, the chickens were immunized in both sides of the breast muscle. Boosters were administered on weeks 2, 4 and 6 used Freund's incomplete adjuvant. Prior to immunization, non-immune eggs were collected and after immunization all eggs until week 16 were collected for the isolation of IgY.

2.7.4 Chicken antibody (IgY) isolation

Several methods can be utilized for the extraction of IgY from egg yolk, but the method of choice involves the precipitation of the protein using polyethylene glycol (PEG) (Polson *et al.*, 1985). PEG is a non-ionic polymer available in a number of molecular weights from 400 to 20 000 (Boyer, 1993). PEG 6 000 was originally used by Polson *et al.* (1964). It is a mild precipitating agent that fractionally precipitates proteins by exclusion from water. The method involves successive precipitations at 3.5% PEG, to remove the vitellins and lipids, and 12% PEG to precipitate the IgY (Polson *et al.*, 1980). An advantage of using PEG is that, because it does not alter the ionic strength, there is no need to dialyse the antibodies. One of the greatest advantages of PEG over other precipitation techniques is its ability to fractionate proteins

according to size (Boyer, 1993). The procedure is also very mild and results in very little denaturation of the antibodies (Page and Thorpe, 1998).

2.7.4.1 Materials

100 mM Na-phosphate buffer, 0.02% (m/v) NaN_3, pH 7.6. $NaH_2PO_4.H_2O$ (13.8 g) was dissolved in 950 ml dH_2O, the pH was adjusted to 7.6 with NaOH, NaN_3 (0.2 g) was added and the solution was made up to 1 l with dH_2O.

2.7.4.2 Procedure

Egg yolks were separated from egg whites and carefully washed under running water. The yolk sac was broken and the volume of the yolk determined in a measuring cylinder. Two volumes of 100 mM Na-phosphate buffer (pH 7.6) were added and mixed in. Polyethylene glycol (PEG) was added to 3.5% (m/v) and dissolved gently. The vitellin precipitate was removed by centrifugation (4 420 *g*, 30 min, RT), and the supernatant filtered through absorbent cotton wool to remove the lipid fraction. The PEG concentration was increased by 8.5% to 12%, and mixed in thoroughly and the solution was centrifuged (12 000 *g*, 10 min, RT). The pellet was dissolved in a volume of 100 mM Na-phosphate buffer (pH 7.6) equal to that of the yolk volume. The PEG concentration was increased to 12%, mixed and centrifuged (12 000 *g*, 10 min, RT). The final IgY pellet was dissolved in 1/6 the original yolk volume of 100 mM Na-phosphate buffer (pH 7.6). The concentration of IgY was determined by measuring the A_{280} of a 1/50 dilution and using the extinction coefficient for IgY ($E_{280}^{1mg/ml} = 1.25$) and the following formula :

$$[IgY] = [(A_{280} / 1.25) \times 50] \text{ mg/ml}$$

The efficiency of the IgY isolation was determined by SDS-PAGE (Section 2.7.7).

2.7.5 Enzyme-linked immunosorbent assay (ELISA) to determine anti-peptide antibody titre

ELISAs are the most widely used immunoassays and are usually carried out in 96 well microtitre plates (Thorpe and Kerr, 1994). These assays are simple, robust, versatile, accurate and sensitive. They combine the specificity of antibodies with the sensitivity of a simple spectrophotometric enzyme assay by using antibodies coupled to enzymes that are easily assayed (Burrin, 1994). This technique may be used to measure the ability of peptides to elicit an immune response (Van Regenmortel *et al.*, 1988). As the outcome of immunizations is often unpredictable, it is important to frequently monitor the titre of antibodies to establish when it peaks. This is, however, more important when the animal that has been immunized has to be bled, but in the case of chicken IgY it is done solely to determine when the antibody titre peaks.

The antigens or, as in this case, the peptides were adsorbed directly onto the plastic wells of the microtitre plate. The coating concentration of the peptide are very important. At a higher concentration the binding is more rapid but when too much has bound it can lead to weak binding (Thorpe and Kerr, 1994). Commonly concentrations used are 1- 5μg/ml. Peptides of 15 residues or more adsorb to the plastic of a microtitre plate, although smaller peptides have been shown to bind (Van Regenmortel *et al.*, 1988). The temperature should also remain constant to avoid edge effects. The majority of antigens bound to the plate retain their immunological and biological activity. The antigens are effectively aggregated and thus lower affinity interactions may be favoured more than in solution. Due to this lower affinity, antibodies may be detected (Thorpe and Kerr, 1994).

The plates are blocked with fat free milk to eliminate 'non-specific' binding of proteins later in the assay. This step is very important, as antibodies used in the detection steps are particularly prone to 'non-specific' binding. If the plates are washed before the blocking step there should be no detergent in the wash buffer (Thorpe and Kerr, 1994), whereas after the blocking step detergent should be present. Washing the plates is important to remove free peptides. The detergent (Tween 20) blocks hydrophobic interactions and acts as a wetting agent. After washing, the bound antigen is detected with the addition of a specific enzyme linked antibody,

such as horseradish peroxidase (HRPO)-linked rabbit anti-chicken IgY. Upon addition of a substrate, the enzyme produces a coloured product that can be quantified spectrophotometrically. When using HRPO, the buffers, with the exception of the stopping buffer, should not contain azide as this inhibits the enzyme.

A positive control should always be used to ensure that all the reagents are working. Negative controls such as a non-immune primary antibody are also important to check for non-specific binding (Kemeny and Chantler, 1988; Thorpe and Kerr, 1994).

2.7.5.1 Materials

Phosphate buffered saline (PBS), pH 7.2. See Section 2.2.1 for preparation

Bovine serum albumin – PBS (BSA-PBS) [0.5% (m/v)]. BSA (0.5 g) was dissolved in 100 ml PBS.

PBS-Tween [0.1% (v/v)]. Tween 20 (1 ml) was made up to a litre in PBS.

0.15 M citrate-phosphate buffer, pH 5.0. A solution of citric acid.H_2O (21.0 g/l) was titrated with a solution of $Na_2HPO_4.2H_2O$ (35.6 g/l) to pH 5.0.

Substrate solution [0.05% (m/v) ABTS and 0.0015% (v/v) H_2O_2 in citrate phosphate buffer]. 2,2'-azino-di-(3-ethyl)-benzthiozoline sulfonic acid (ABTS; 7.5 mg) and H_2O_2 (7.5 µl) were dissolved in citrate-phosphate buffer, pH 5.0 (15 ml) per ELISA plate.

Stopping buffer [citrate-phosphate-0.1% (m/v) NaN_3]. NaN_3 (0.1 g) was made up to 100 ml in citrate-phosphate buffer.

2.7.5.2 Procedure

Peptides or rabbit albumin were coated at a concentration of 1 µg/ml in PBS (150 µl, 16 h, 4°C). The wells were blocked with 0.5% BSA-PBS (200 µl, 1 h, 37°C) to prevent non-specific binding of proteins. The plates were washed three times with 0.1% PBS-Tween.

Serial two-fold dilutions starting from 100 µg/ml anti-peptide antibody were prepared on the plate in 0.5% BSA-PBS and incubated (100 µl, 2 h, 37°C). The plates were washed three times with 0.1% PBS-Tween. Horseradish peroxidase linked rabbit anti-chicken IgY secondary antibody, at a dilution of 1:30 000 in 0.5% BSA-PBS was added to the wells and incubated (120 µl, 1 h, 37°C). The plates were washed with 0.1% PBS-Tween three times. Substrate solution (150 µl) was added to each well and the green colour was developed in the dark against the background of the controls for approximately 15 min. Adding the stopping buffer (50 µl) stopped the reaction and the A_{405} of each well was measured on a Titretek ELISA plate reader.

2.7.6 Affinity purification of anti-peptide antibodies

Affinity chromatography is a powerful procedure that is commonly used to purify antibodies present in sera or polyclonal antibody preparations (Page and Thorpe, 1998). Pure antigen, which in this case are the peptides HSP and HSC, are linked covalently to a solid support matrix. The polyclonal antibodies pass through the matrix and the anti-peptide antibodies bind to the peptides. The unbound antibodies are removed with washing and the specific antibodies are eluted using a low pH buffer, which in some cases may lead to the loss of the antibodies activity. High affinity antibodies may also remain bound to the column even under those conditions and this may ultimately lead to the column losing its antigen binding capacity (Harlow and Lane, 1988). The advantage of this technique is that specific antibodies can be isolated from a polyclonal antibody mixture. The large amount of antigen required and the harsh eluting conditions are the major disadvantages (Harlow and Lane, 1988).

The peptides HSC and HSP were activated using DTT and then coupled to a sulfolink® affinity column. Free cysteine was used to block the unbound sites on the column, which would otherwise interfere with the purification of the antibodies.

The anti-peptide antibodies in a polyclonal antibody solution were cycled through the peptide affinity matrix. The peptide specific antibodies bind to the matrix and the remaining antibodies pass straight through the column or are washed out during the washing step. The specific anti-peptide antibodies are eluted with a low pH buffer, which interferes with the bonds between

the peptide and antibody and hence elute the specific antibody. The only disadvantage with this technique is some of the highly specific antibodies may remain bound to the column (Harlow and Lane, 1988).

2.7.6.1 Materials

Tris buffer [50 mM Tris-HCl, 5 mM Na_2EDTA, pH 8.5]. Tris base (0.6 g) and Na_2EDTA (0.185 g) was dissolved in dH_2O (90 ml), the pH was adjusted to 8.5 with HCl and made up to 100 ml with dH_2O.

10 mM Dithiothreitol (DTT). See Section 2.7.2 for preparation

Sulfolink® affinity column. Purchased from Pierce (Rockford, USA)

50 mM Cysteine, 50 mM Tris-HCl, 5 mM Na_2EDTA, pH 8.5. Cysteine (8.78 mg) was dissolved in Tris buffer (1 ml).

1 M NaCl, 0.05% (w/v) NaN_3, pH 7.6. NaCl (5.84 g) was dissolved in 90 ml dH_2O, the pH was adjusted to 7.6 with HCl, NaN_3 (0.05 g) was added and the solution was made up to 100 ml with dH_2O.

100 mM Na-phosphate buffer, 0.02% (m/v) NaN_3, pH 7.6. See Section 2.7.4.1 for preparation

100 mM Na-phosphate buffer, 0.02% (m/v) NaN_3, pH 6.5. $NaH_2PO_4.H_2O$ (13.8 g) was dissolved in 950 ml dH_2O, the pH was adjusted to 7.6 with NaOH, NaN_3 (0.2 g) was added and the solution was made up to 1 l with dH_2O.

0.1 M Glycine-HCl, 0.02% (m/v) NaN_3, pH 2.8. Glycine (7.5 g) was dissolved in 950 ml dH_2O, the pH was adjusted to 2.8 with HCl, NaN_3 (0.2 g) was added and the solution was made up to 1 l with dH_2O.

1 M Na-phosphate buffer, 0.02% (m/v) NaN_3, pH 8.5. $NaH_2PO_4.H_2O$ (13.8 g) was dissolved in 90 ml dH_2O, the pH was adjusted to 8.5 with NaOH, NaN_3 (0.02 g) was added and the solution was made up to 100 ml with dH_2O.

2.7.6.2 Procedure

The peptide (10 mg) was dissolved in DMSO (100 µl) and Tris buffer, pH 8.5 (400 µl), to this was added 10 mM DTT (500 µl). The peptide-DTT mixture was incubated for 1.5 h at 37°C. The DTT and the peptide were separated on a Sephadex G-10 column. To test for the reduced peptide 10 µl eluant was added to 10 µl Ellman's reagent and the yellow samples indicated the tubes containing the peptide: these were pooled. Sulfolink® (4 ml of 50% slurry) was washed with six column volumes of Tris buffer (pH 8.5) and the reduced peptide was added to the gel. The gel was mixed for 15 min at RT and incubated for 30 min at RT without mixing. The buffer was drained and the column washed with three column volumes of Tris buffer (pH 8.5). 50 mM cysteine (2 ml) was added to the gel, mixed for 15 min at RT and incubated for 30 min with out mixing. The column was drained and washed with 16 column volumes of 1 M NaCl, 0.5% NaN_3 (pH 7.6) followed by 2 column volumes of 100 mM Na-phosphate buffer (pH 7.6). The column was packed and washed with 100 mM Na-phosphate buffer (pH 6.5). The antibody solution (max 70 ml) was circulated through the column overnight. The column was washed with several column volumes of the 100 mM Na-phosphate buffer (pH 6.5). The bound antibodies were eluted with 0.1 M glycine-HCl (pH 2.8). Fractions of 900 µl were collected and neutralized with 100 µl of the 1 M Na-phosphate buffer (pH 8.5). The A_{280} of all fractions was read and those with absorbance values above 0.2 were retained. The column was washed with 100 mM Na-phosphate buffer (pH 6.5) for several hours. The affinity-purified antibodies were tested using an ELISA (Section 2.7.5) and compared to those prior to purification.

2.7.7 Sodium dodecyl sulfate polyacrylamide gel electrophoresis (SDS-PAGE)

Electrophoresis is defined as the separation of charged particles through a molecular sieving gel towards an electrode of opposite charge, under the influence of an externally applied electric field. Laemmli (1970) developed sodium dodecyl sulfate gel electrophoresis or SDS-PAGE, since native PAGE could not distinguish between the effects of size, shape and charge

on electrophoretic mobility. The gel is formed by the free radical polymerisation of acrylamide and the cross linking agent N,N'-methylene-bis-acrylamide. The polymerisation is controlled by an initiator – catalyst system of ammonium persulfate and N,N,N',N'-tetramethylethylenediamine (TEMED) (Boyer, 1993). The molecular weights of proteins can be determined if an anionic detergent, sodium dodecyl sulfate (SDS) and 2-mercaptoethanol, a disulfide reducing agent is present. SDS disrupts the proteins secondary, tertiary and quaternary structure to produce a negatively charged linear polypeptide and the 2-mercaptoethanol reduces any disulfide bridges in a protein (Boyer, 1993). Thus proteins can be separated according to size, as they are all linear and negatively charged. The smaller proteins move through the SDS-PAGE gel faster than the larger proteins.

For the protein bands to be well resolved, the starting band of the sample needs to be as narrow as possible. The protein band diffusion must also be minimized. These two criteria are fulfilled in a discontinuous system. This system has two gel layers, a stacking gel and a resolving or running gel where the buffers used to prepare the two gels are of different pH. The stacking gel has a lower acrylamide concentration and hence larger pores. The sample and stacking gel buffers contain Tris-HCl at a pH of 6.8, whereas the Tris-HCl running gel buffer and the Tris-glycine electrode buffer are at pH 8.8 and 8.3 respectively. The glycine ions at pH 6.8 are poorly dissociated with a small negative charge and poor mobility. The proteins are thus stacked tightly between the highly mobile chloride ions and the glycine ions. At the resolving gel interface, the increase in pH causes the glycine ions to dissociate further and hence increase their mobility. The glycine ions pass the proteins and leave them to unstack at a constant pH in a uniform voltage gradient. The resolving gel thus separates the proteins according to their size by means of molecular sieving.

The most popular general staining procedures are based on the use of non-polar, sulfated triphenylmethane Coomassie stains developed for the textile industry. Coomassie brilliant blue is most frequently used and requires an acidic environment for electrostatic reactions between the dye molecules and the amino groups of the proteins (Dunn, 1987).

SDS-PAGE was used in the present study to determine the purity of IgY isolated from chicken eggs (Section 2.7.4), as well as to separate the proteins in monocyte or lymphocyte heat shock lysates (Section 2.7.9) for western blotting (Section 2.7.8).

2.7.7.1 Materials

Monomer solution [(30% m/v) acrylamide, 2.7% (m/v) Bis-acrylamide]. Acrylamide (73 g) and bis-acrylamide (2 g) were dissolved and made up to 250 ml with ddH_2O. The solution was filtered through Whatman No.1 filter paper and stored in an amber coloured bottle at 4°C.

Running gel buffer [1.5 M Tris-HCl, pH 8.8]. Tris (45.37 g) was dissolved in approximately 200 ml, the pH was adjusted to 8.8 with HCL and made up to 250 ml. The solution was filtered through Whatman No.1 filter paper.

Stacking gel buffer [500 mM Tris-HCl, pH 6.8]. Tris (3 g) was dissolved in dH_2O (40 ml), the pH was adjusted to 6.8 with HCl and made up to 100 ml. The solution was filtered through Whatman No.1 filter paper.

10% SDS (m/v). Sodium dodecyl sulfate (SDS, 10 g) was made up to 100 ml with dH_2O.

Initiator [10% (m/v) ammonium persulfate]. Ammonium persulfate (0.2 g) was made up to 2 ml with dH_2O.

Tank buffer [250 mM Tris-HCl, 192 mM glycine, 0.1% (m/v) SDS, pH 8.3]. Tris (15 g) and glycine (72 g) were dissolved and made up to 5 l with dH_2O. Prior to use 2.5 ml of 10% SDS was added to 250 ml.

Reducing treatment buffer [125 mM Tris-HCl, 4% (m/v) SDS, 20% (v/v) glycerol, 10% (v/v) 2-mercaptoethanol, pH 6.8]. Stacking gel buffer (2.5 ml), 10% SDS (4 ml), glycerol (2 ml) and 2-mercaptoethanol (1 ml) were made up to 10 ml with dH_2O.

Non-reducing treatment buffer [125 mM Tris-HCl, 4% (m/v) SDS, 20% (v/v) glycerol, pH 6.8]. Stacking gel buffer (2.5 ml), 10% SDS (4 ml), glycerol (2 ml) were made up to 10 ml with dH_2O.

Molecular mass markers. Standards for molecular mass determination were: phosphorylase b (94 kDa), bovine serum albumin (67 kDa), ovalbumin (43 kDa), carbonic anhydrase (30 kDa), soybean trypsin inhibitor (20.1 kDa) and α-lactalbumin (14.4 kDa). Lyophilised markers (Amersham Pharmacia Biotech, USA) were reconstituted in either the non-reducing buffer or the reducing buffer (100 µl) and heated at 100°C for 5 min for Coomassie staining or immunoblotting. For silver staining, the reconstituted markers were diluted 1:50 in the appropriate treatment buffer.

Coomassie stain stock solution [1% (m/v) Coomassie blue R-250]. Coomassie blue R-250 (1 g) was dissolved in dH_2O (100 ml) by stirring for 1 h at RT. The solution was filtered through Whatman No. 1 filter paper.

Coomassie staining solution [0.125% (m/v) Coomassie blue R-250, 50% (v/v) acetic acid]. Coomassie stain stock solution (62.5 ml) was mixed with methanol (250 ml) and acetic acid (50 ml), and made up to 500 ml with dH_2O.

Destaining solution I [50% (v/v) methanol, 10% (v/v) acetic acid]. Methanol (500 ml) was mixed with acetic acid (100 ml) and made up to 1 l with dH_2O.

Destaining solution II [7% (v/v) acetic acid, 5% (v/v) methanol]. Acetic acid (70 ml) was mixed with methanol (50 ml) and made up to 1 l with dH_2O

2.7.7.2 Procedure

The Bio-Rad mini-PROTEAN II® electrophoresis cell was used for SDS-PAGE and was assembled as described in the manufacturer's manual. This involved cleaning the glass plates, spacers, combs and casters with soap and ethanol (95%). After cleaning, the equipment was rinsed in ddH_2O. The inner glass plates (7.3x10.2 cm) and the outer glass plates (8.3x10.2 cm)

were positioned in the caster, separated by 1.5 mm polyethylene spacers. The running gel solution (Table 2.4) was run into the space between the glass plates to approximately 3 cm below the top edge of the outer glass plate. Distilled water was overlaid on top of the running gel to exclude oxygen that inhibits polymerisation. The running gel was allowed to polymerise at RT. Once the gel had polymerised (this was indicated by an interface between the water and gel appearing), the water was removed and the stacking gel (Table 2.4) overlaid till the top of the outer glass plate. A 10 or 15 well comb was inserted to form the sample loading wells, the stacking gel was allowed to polymerise at RT and, once polymerised, the wells were rinsed out with dH_2O. Tank buffer, containing SDS, was poured into the upper and lower electrode compartments. Samples for reducing gels were combined with an equal volume of reducing treatment buffer and incubated in a boiling water bath for 90 s before they were placed on ice. For non-reducing gels the samples were combined with half their volume of non-reducing treatment buffer before loading. Bromophenol blue (5 µl), a marker dye that migrates at the buffer front, was added to each sample prior to loading. Suitable amounts of protein (at least 1 µg of protein per band for Coomassie staining) were loaded into each well. The gel unit was connected to a power pack and run at 18 mA per gel until the dye front was 0.5 cm from the bottom of the gel.

The gels were removed and placed in the appropriate stain for visualisation, either silver or Coomassie, or the gel was prepared for immunoblotting. When the Coomassie stain was used, the gel was placed in the Coomassie stain solution for 4 h. The stain was removed and the gel was rinsed in dH_2O before the addition of destain I, overnight. The gel was placed in destain II to complete destaining.

Table 2.4 Reagents for two SDS-PAGE gels.

Reagent	Running gel (12.5%)	Stacking gel (4.0%)
Monomer solution	6.25 ml	0.94 ml
Running gel buffer	3.75 ml	-
Stacking gel buffer	-	1.75 ml
10% SDS	150 µl	70 µl
Initiator solution	75 µl	35 µl
TEMED	7.5 µl	15 µl
ddH_2O	4.75 ml	4.3 ml

2.7.8 Western blotting

Proteins of interest were separated by Laemmli (1970) SDS-PAGE (Section 2.4.7.2), electro-blotted and immobilized on nitrocellulose. Nitrocellulose is a matrix with high binding affinity for proteins and can bind as much as 80 – 100 $\mu g/cm^2$. The immobilized proteins were detected by immunological procedures. Thus the native heat shock proteins found in monocytes or lymphocytes can be immobilized on nitrocellulose and detected with the anti-peptide antibodies.

The procedure used was that described by Towbin *et al.* (1979). Methanol was used in the transfer buffer to enhance the hydrophobic binding of the protein-SDS complexes to the nitrocellulose. The nitrocellulose was blocked with non-fat milk to prevent further 'non-specific' binding of detection reagents. The antibody was allowed to react with the immobilized antigen or protein of interest; this reaction is detected by an enzyme-linked secondary antibody (e.g. goat anti-chicken IgY-horse radish peroxidase conjugate), which catalyses a reaction with a precipitating substrate (4-chloro-1-napthol) to yield a coloured band on the nitrocellulose membrane.

In the present study, western blotting was used to determine if the anti-peptide antibodies produced in chickens recognize the native HSC or HSP proteins in human or canine lymphocytes.

2.7.8.1 Materials

Blotting buffer. Tris (27.23 g) and glycine (64.8 g) were dissolved in 3.5 l of dH_2O, and 900 ml of methanol was added. The volume was made up to 4.5 l with dH_2O. Prior to use, 10% (m/v) SDS (4.5 ml, Section 2.7.7.1) was added.

Ponceau S stain. Ponceau S [0.1% (m/v)] was prepared in glacial acetic acid [1% (v/v)].

Tris buffered saline [TBS: 20 mM Tris, 200 mM NaCl, pH 7.4]. Tris (2.42 g) and NaCl (11.69 g) were dissolved in 950 ml dH_2O, the pH adjusted to 7.4 with HCl and made up to 1 l.

Bovine serum albumin – TBS (BSA-TBS) [3% (m/v)]. BSA (3 g) was dissolved in 100 ml TBS.

Bovine serum albumin – TBS (BSA-TBS) [0.5% (m/v)]. BSA (0.5 g) was dissolved in 100 ml TBS.

4-Chloro-1-napthol HRPO substrate stock solution. 4-Chloro-1-napthol (0.03 g) was dissolved in methanol (10 ml).

4-Chloro-1-napthol HRPO substrate working solution. 4-Chloro-1-napthol HRPO substrate stock solution (2 ml) and H_2O_2 (4 µl) were made up to 10 ml with TBS.

2.7.8.2 Procedure

After SDS-PAGE, one gel was stained to show position of the protein bands while the other was used for blotting. Nitrocellulose was cut to a similar size to the gel and was carefully floated onto blotting buffer before being totally immersed. The nitrocellulose was sandwiched with the gel lying squarely on top of it, between three pieces of Whatman No. 4 filter paper and two pieces of scotchbrite foam. The entire sandwich was immersed in the blotting buffer and placed in the blotting apparatus with the nitrocellulose on the anodal side of the gel. The apparatus was filled with blotting buffer and the cooling system was set up before the power pack was connected. Blotting was carried out at 200 mA for 16 h. When blotting was complete, the gel and the nitrocellulose were removed from the sandwich. The nitrocellulose was stained with Ponceau S to determine if the transfer was successful, where the molecular weight markers were positioned and also so that the nitrocellulose may be cut into smaller pieces. The nitrocellulose was destained with the addition of NaOH. The blotted nitrocellulose was air dried for 1.5 h and blocked with 3% BSA-TBS (1 h, RT). It was washed with TBS (3x5 min, RT) and incubated with the primary antibody in 0.5% BSA-TBS for 2 h at RT. Following washing in TBS (2x5 min, RT), the blot was incubated with the horseradish peroxidase linked rabbit anti-chicken IgY secondary antibody, at a dilution of 1:50 000 in 0.5% BSA-PBS for 1 h at RT. Again the blot was washed in TBS (3x5 min, RT) and immersed in the 4-chloro-1-napthol HRPO substrate working solution and reacted in the dark

at RT until bands were clearly visible. The strip was washed with dH_2O and dried between filter paper.

2.7.9 Detection of heat shock proteins in lymphocyte cell lysates using western blotting

Lymphocytes contain heat shock proteins, both the constitutive heat shock protein 70 (HSC70) and the inducible heat shock protein 70 (HSP70). These proteins were released from inside the cell by using an anionic detergent, sodium dodecyl sulfate (SDS), and 2-mercaptoethanol. An inhibitor cocktail was also incorporated to inhibit any proteolytic enzymes released under the lysis conditions. The lysate proteins were separated by SDS-PAGE before being electro-blotted onto nitrocellulose. The specificity of the anti-peptide antibodies was determined by probing the blot for the heat shock proteins.

Two temperatures were used for the purposes of this study, 37°C and 44°C. In the case of 37°C, this is the normal body temperature and hence is a normal control but constitutive HSC70 will be expressed in the lymphocytes. At 44°C, HSP70 expression will be induced. Thus using the anti-peptide antibodies for the respective protein, there should be differences in the expression of the two proteins at different temperatures.

Lymphocytes also contain proteolytic enzymes such as elastase, cathepsins, collagenase and myelinase, to name but a few (Auger and Ross, 1992). Cathepsin D has been found to hydrolyse *E. coli* DnaK or HSP70 into many smaller peptides, with there being no ATPase N-terminal domain fragments larger than 20 kDa (Sehorn *et al.*, 2002). A number of fragments greater than 20 kDa were sequenced and were from the C-terminal domain of HSP70, i.e. the region of interest in this study. Thus in order to detect the protein at 70 kDa protease inhibitors and specifically cathepsin D inhibitors must be used. However, if no inhibitors are used and the anti-peptide antibodies detect bands above 20 kDa, the antibodies can be considered specific for the C-terminal domain of HSP70.

An inhibitor cocktail was used to ensure a range of different families of proteases were inhibited. Phenylmethylsulfonyl fluoride (PMSF) is a general, irreversible inhibitor of serine proteases (Salvesen and Nagase, 1989). A specific irreversible inhibitor of serine proteases is

AEBSF (4-(2-Aminoethyl)benzenesulfonylfluoride). This compound inhibits chymotrypsin, kallikrein, plasmin, thrombin, trypsin and related thrombolytic enzymes. It is also a more stable, non-toxic alternative to PMSF. Benzamidine is a reversible inhibitor of trypsin and trypsin-like enzymes. E64 (N-(L-3-*trans*-carboxyoxiran-2-carbonyl)-L-leucyl]-amido(4-guanidino)butane) is an irreversible cysteine protease inhibitor that has no effect on cysteine residues of other proteins. It is specific for the active site where the *trans* epoxide group is thought to alkylate the active site cysteine. Iodoacetate is a cysteine protease inhibitor that alkylates the sulfydryl groups of the enzyme (Salvesen and Nagase, 1989). Metalloproteinases are classified as such because of the presence of a metal ion (usually zinc), which participates in catalysis (Salvesen and Nagase, 1989). Disodium EDTA is a reversible metalloprotease inhibitor that chelates with the Zn. 1,10-Phenanthroline is preferred as an inhibitor of metalloproteinases as it has a much higher stability constant for Zn (Salvesen and Nagase, 1989). Pepstatin A is an inhibitor of aspartic proteases and reversibly inhibits cathepsin D, cathepsin E, pepsin and renin. (Salvesen and Nagase, 1989).

If cathepsin D cleaves human and canine HSP70 and pepstatin A is present, there should be no small protein bands recognized at 30 kDa. However, the other protease inhibitors used are precautionary in case any other enzymes are capable of degrading HSP70.

2.7.9.1 Materials

Phosphate buffered saline (PBS), pH 7.2. See Section 2.2.1 for preparation

Complete RPMI 1640 medium {25 mM HEPES; 5% FCS}. See Section 2.2.1 for preparation

10% (m/v) SDS. See Section 2.7.7.1 for preparation

Reducing treatment buffer. See Section 2.7.9.1 for preparation

0.2 M Phenylmethylsulfonyl fluoride (PMSF). PMSF (29 mg) was dissolved in dry propanol (1 ml).

0.1 M Na_2-EDTA. Na_2-EDTA (37 mg) was dissolved in ddH_2O (1 ml).

0.1 M Benzamidine. Benzamidine (16 mg) was dissolved in ddH_2O (1 ml).

Pepstatin stock solution (1 mg/ml). Pepstatin (1 mg) was dissolved in methanol (1 ml).

1 M 1,10-phenanthroline. 1,10-Phenanthroline (0.198 g) was dissolved in ethanol (1 ml).

50 mM E-64. N-[(L-3-*trans*-carboxyoxiran-2-carbonyl)-L-leucyl]-amido(4-guanidino)butane (E64; 1.8 mg) was dissolved in ddH_2O (100 µl).

1 M Iodoacetic acid. Iodoacetic acid (0.208 g) dissolved in ddH_2O (1 ml).

Pefabloc [AESBF; 4-(2-aminoethyl)benzenesulfonylfluoride stock solution (1 mg/ml)]. Pefabloc (1 mg) was dissolved in dry propanol (1 ml).

Inhibitor cocktail. 0.2 M PMSF (5 µl), 0.1 M Na_2-EDTA (50 µl), 0.1 M benzamidine (10 µl), pepstatin stock solution (10 µl), 1 M 1,10-phenanthroline (2 µl), 50 mM E-64 (8 µl), 1 M iodoacetic acid (10 µl) and pefabloc stock solution (10 µl) were mixed together and made up to 1 ml with ddH_2O.

2.7.9.2 Procedure

The blood was prepared as in Section 2.2 but the final lymphocyte pellet was resuspended in 2 ml warm complete RPMI medium, and divided into two 1 ml samples in Eppendorf tubes. The first tube was incubated at 37°C and the other at 44°C, both for 2 h. The tubes were placed on ice for 5 min and the cells were pelleted by centrifugation (400 *g*, 5 min, RT). The pellet was resuspended in PBS and centrifuged (400 *g*, 5 min, RT). This was repeated twice to remove proteins that may be present in the medium. The final cell pellet was resuspended in 10% SDS (50 µl) and thereafter reducing treatment buffer (250 µl). For inhibition of proteases, the inhibitor cocktail (15 µl) was added but this was not the case for all samples as a comparison between uninhibited and inhibited was required. The samples were boiled for 5

min to reduce the viscosity. Immediately after boiling the samples were put on ice to cool, and once cool, a further 15 µl of the inhibitor cocktail was added. These samples were loaded directly on to an SDS-PAGE gel (Section 2.7.7) and western blotted (Section 2.7.8), to determine if the anti-peptide antibodies recognized human lymphocyte expressed heat shock protein 70 (HSP) or heat shock cognate protein 70 (HSC) and determine the level of reactivity between the anti-peptide antibodies and canine lymphocyte expressed HSP and HSC.

CHAPTER 3

ISOLATION AND CHARACTERIZATION OF MONOCYTES

3.1 INTRODUCTION

In this chapter the isolation of monocytes and their characterization using different staining, histochemical, morphological and functional assays will be detailed. Isolated cells were stained with methyl green or giemsa stain. Based on the nature of staining, the type of cell could be identified. The presence of enzymes localized within vesicles in the cytoplasm of monocytes, such as alkaline phosphatase and peroxidase, were detected with histochemical techniques. Transmission electron microscopic analysis of monocytes enabled the determination of the presence of monocytes morphologically. The functional assays involved the determination of phagocytic activity using latex beads or β-hematin. β-hematin was synthesized from hematin and the ultrastructural differences between the two compounds were examined using scanning electron microscopy and X-ray microanalysis.

3.2 ISOLATION AND STAINING OF MONOCYTES

Monocytes were isolated using the Histopaque®-1077 method. The monocyte layer (Figure 2.1) obtained after the initial centrifugation was more clearly defined in human blood separations than canine blood. The difference in separation maybe due to interspecies differences in monocyte densities. Austin *et al.* (1985) suggest that some techniques, which yield good monocyte preparations from human blood, do not work well with dog blood. The average viability of the cells as determined by the trypan blue exclusion assay was 96% for both canine and human cells. Thus 96% of all cells counted retained their membrane integrity through the isolation procedure. Monocytes are characterized by their ability to adhere to glass and plastics. To confirm the identity of adherent cells, the coverslips were stained with methyl green or giemsa. The methyl green serves as a stain to confirm the presence of cells as it stains the entire cell, that is the nucleus and cytoplasm, as indicated in Figure 3.1A. Giemsa is more specific in that it stains the nucleus more darkly than the cytoplasm. The adherent isolated cells have the distinctive horseshoe shaped nucleus of monocytes (Figure 3.1B). The general staining techniques confirmed the presence of adherent monocytes.

A

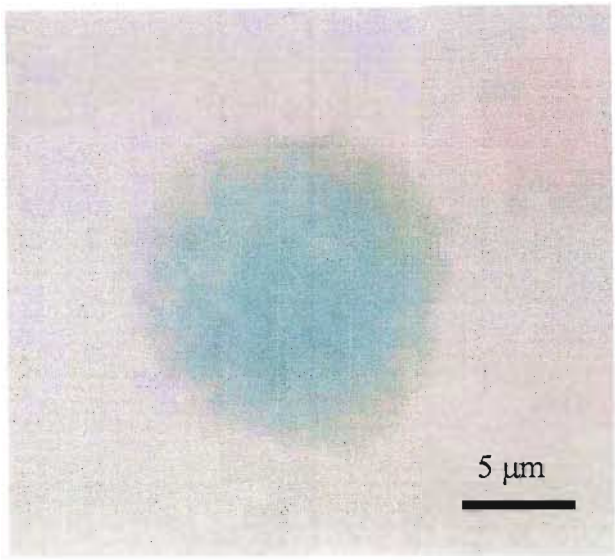

B

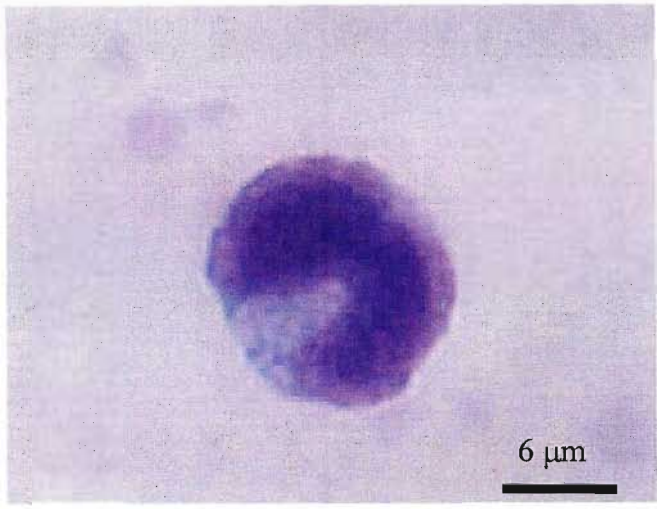

Figure 3.1 Staining of canine monocytes with giemsa and methyl green. Monocytes were fixed with methanol and stained with **(A)** methyl green for 5 min or **(B)** giemsa for 15 min. After staining the coverslips were mounted and viewed at 1000x magnification.

3.3 DETECTION OF ALKALINE PHOSPHATASE ACTIVITY IN MONOCYTES

Alkaline phosphatase was found to be active in the isolated canine monocytes (Figure 3.2), indicated by dark purple staining in numerous cytoplasmic granules (Figure 3.2A). There is diffuse enzyme activity in the cytoplasm as indicated by light purple staining. This is clearly visible in Figure 3.2B. The light general staining of the cytoplasm with methyl green is almost completely overlaid with the light purple product (Figure 3.2B). Human monocytes showed similar staining patterns to the canine monocytes (data not shown).

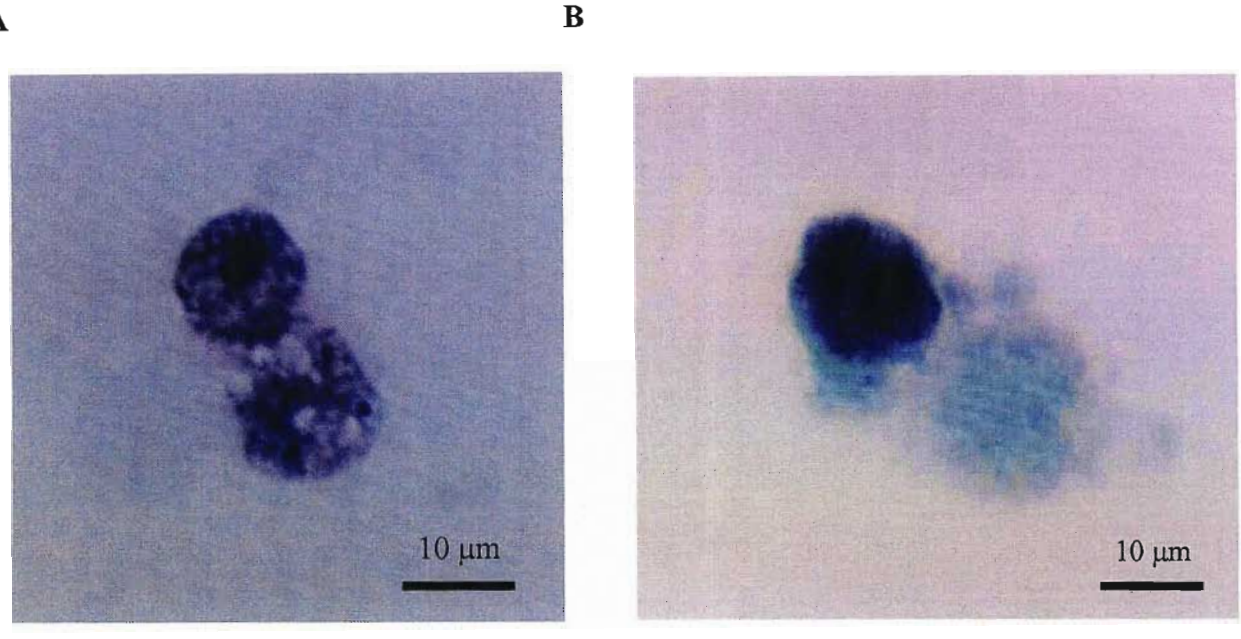

Figure 3.2 Alkaline phosphatase activity in canine monocytes. Peripheral blood monocytes were incubated with alkaline phosphatase substrate (BCIP/NBT) for 30 min before being washed and fixed with methanol. **(A)** No counter stain or **(B)** counterstained with methyl green for 5 min. After staining the coverslips were mounted and viewed at 1000x magnification.

3.4 DETECTION OF PEROXIDASE ACTIVITY IN MONOCYTES

Peroxidase activity was detected in isolated canine monocytes (Figure 3.3). The brown staining in the cells shows the peroxidase activity localized in cytoplasmic granules (Figure 3.3). There are numerous granules that have stained positively (Figure 3.3A) and there is very

little staining in the cytoplasm outside the granules. However, in Figure 3.3B there is a lysed cell and in this case there is enzyme activity in the cytoplasm. This suggests that in this preparation the granules were also lysed. Human cells showed similar staining patterns to their canine counterparts (data not shown).

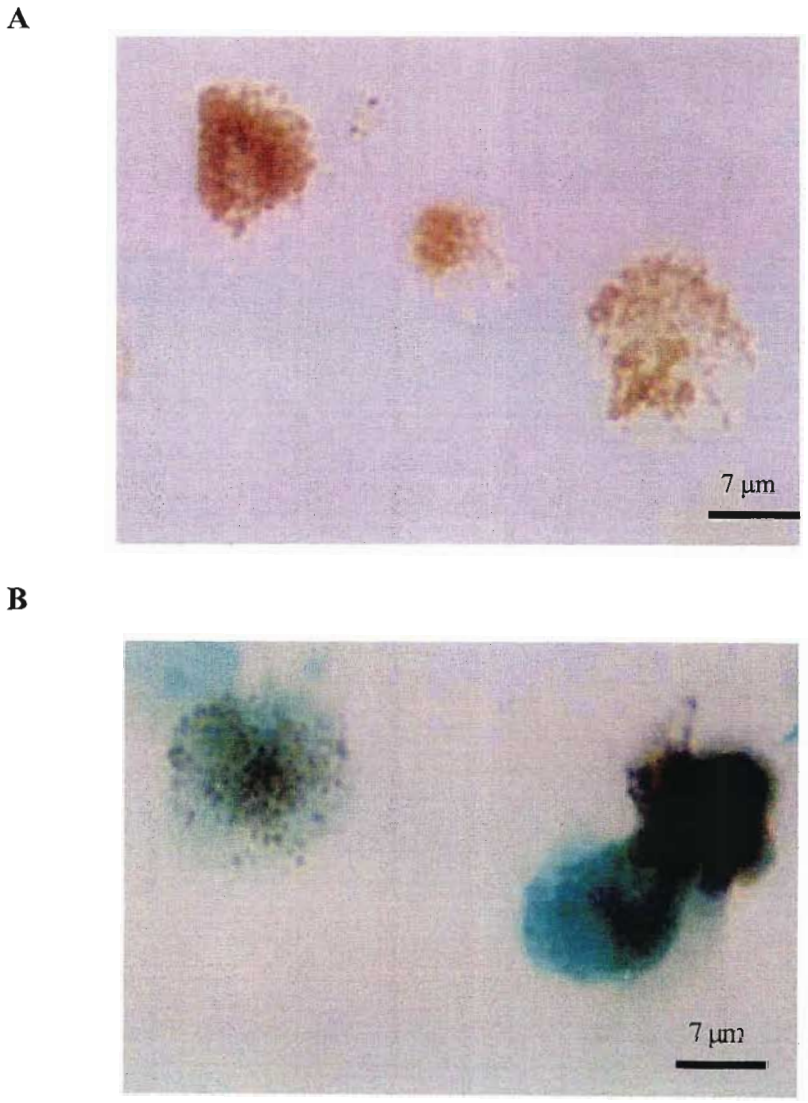

Figure 3.3 Peroxidase activity in canine monocytes. Peripheral blood monocytes were incubated with peroxidase substrate (DAB), washed and fixed with methanol. **(A)** Without counter stain or **(B)** counterstained with methyl green for 5 min. After staining the coverslips were mounted and viewed at 1 000x magnification.

3.5 TRANSMISSION ELECTRON MICROSCOPY OF MONOCYTES

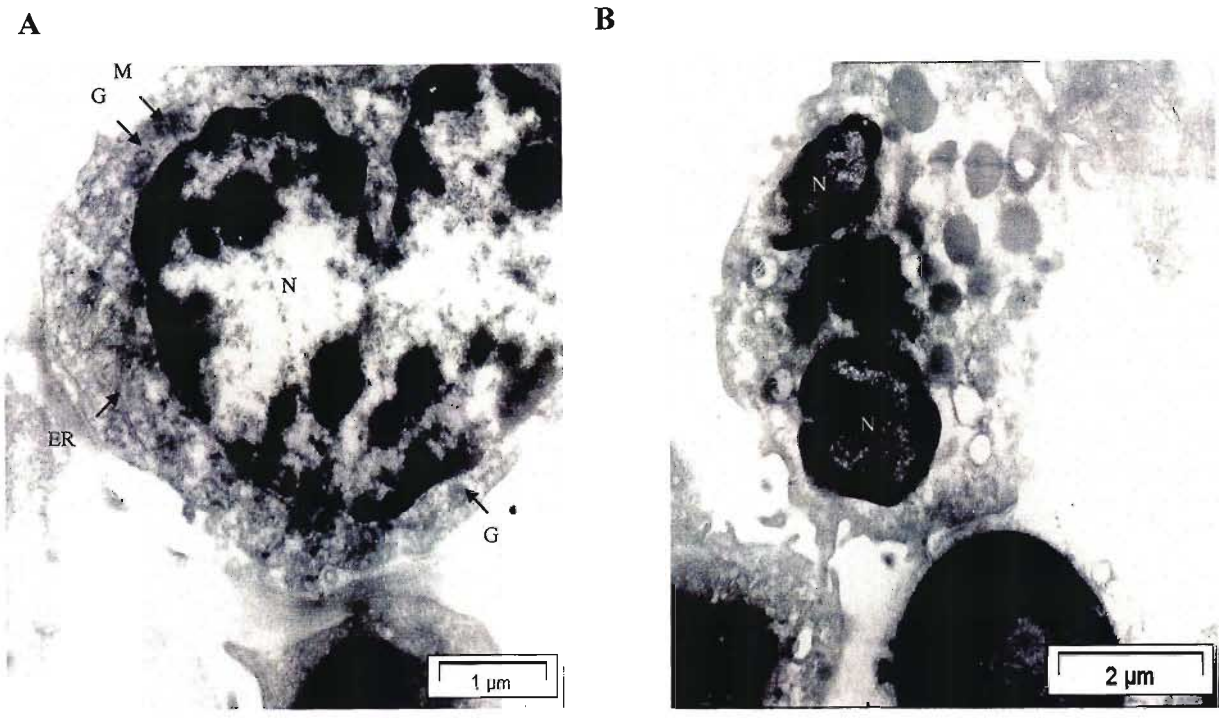

Figure 3.4 Transmission electron micrograph of canine monocytes. Peripheral blood monocytes were fixed, embedded in gelatin, osmicated, dehydrated and embedded in LR white resin. Ultrathin sections were cut from the embedded cells, and stained with uranyl acetate and lead citrate. **(A)** Monocyte sectioned through the nucleus (magnification 13 000x; Bar = 1 µm) or **(B)** different perspective of a sectioned monocyte (magnification 9 500x; Bar = 2 µm). The arrows indicate each organelle: mitochondria (M), granules (G) and endoplasmic reticulum (ER). An N indicates the nucleus.

The monocyte in Figure 3.4A is sectioned in the 'traditional view', showing the horseshoe shaped nucleus which is also visible when the cells have been giemsa stained (Figure 3.1B). In comparison to the giemsa stained monocytes, this micrograph gives more ultrastructural details such as the granules, mitochondria and the endoplasmic reticulum. Figure 3.4B does not show good ultrastructural detail but it illustrates how different a monocyte may look when the cell is sectioned at a different angle. The cell has been sectioned through the two lobes of the nucleus and looks like a different type of cell.

3.6 MONOCYTE PHAGOCYTOSIS OF UNOPSONIZED LATEX BEADS AND β-HEMATIN

3.6.1 Monocyte phagocytosis of unopsonized latex beads

A

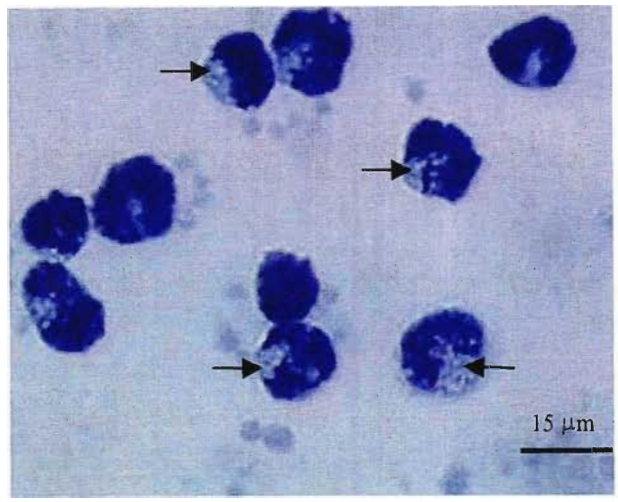

B

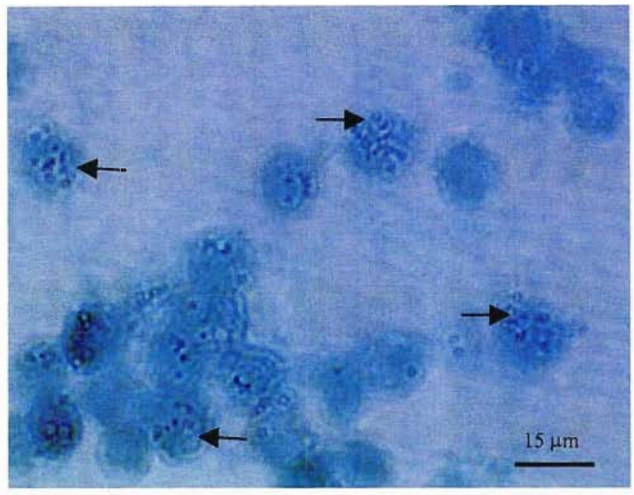

Figure 3.5 Canine monocyte phagocytosis of unopsonized latex beads. Peripheral blood monocytes were incubated with latex beads (0.1% w/v) for 30 min before washing, fixing with methanol and stained with **(A)** giemsa for 15 min or **(B)** methyl green for 5 min. After staining the coverslips were rinsed, dried, mounted and viewed at 400x magnification. The arrows indicate ingested latex beads.

The isolated monocytes (72%) were phagocytically active, as indicated by large quantities of ingested unopsonized latex beads in the monocytes (Figure 3.5). The giemsa stained monocytes (Figure 3.5A) showed darkly stained nuclei as in Figure 3.1 but the cytoplasm appears to be filled with latex beads. In the case of the methyl green stained monocytes the beads appear to be localized in distinct areas but the nucleus cannot be differentiated from the cytoplasm (Figure 3.5B). The methyl green stain is useful to determine whether the cells had in fact ingested the beads. In the case of giemsa, which is a much darker stain, it can be determined where the beads have been localized.

3.6.2 Synthesis and analysis of β-hematin

Even though β-hematin was synthesized from hematin, the crystal structures and the X-ray spectra are different. Hematin comprises large crystals that at a magnification of 12 000x have a smooth surface (Figure 3.6A). The β-hematin also has large crystals, but under the same magnification as the hematin it is evident that they are composed of numerous small crystals (Figure 3.7A). This confirms that the acid and temperature conditions applied in Section 2.5 altered the chemical and ultrastructure of the hematin. Both compounds contain the common elements iron, carbon and oxygen as determined by X-ray microanalysis. Hematin contained trace amounts of chlorine and potassium (Figure 3.6B), whereas β-hematin contained trace amounts of aluminum and silicon (Figure 3.7B). As β-hematin is elementally similar to hematin the C, O and Fe content would be similar between the two compounds, as was found experimentally. The additional elements such as K and Cl in the hematin may be by-products from the extraction procedure used to prepare hematin by the supplier. The Al and Si would most likely be artifacts from the synthesis of β-hematin. The figures presented here serve to indicate that a change in crystal structure has occurred during the conversion of hematin to β-hematin.

A

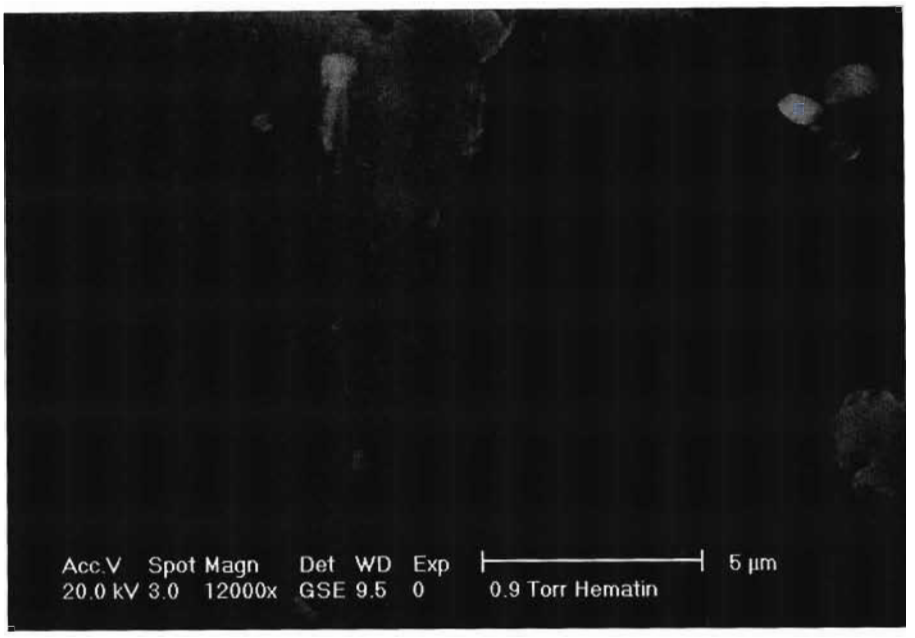

B

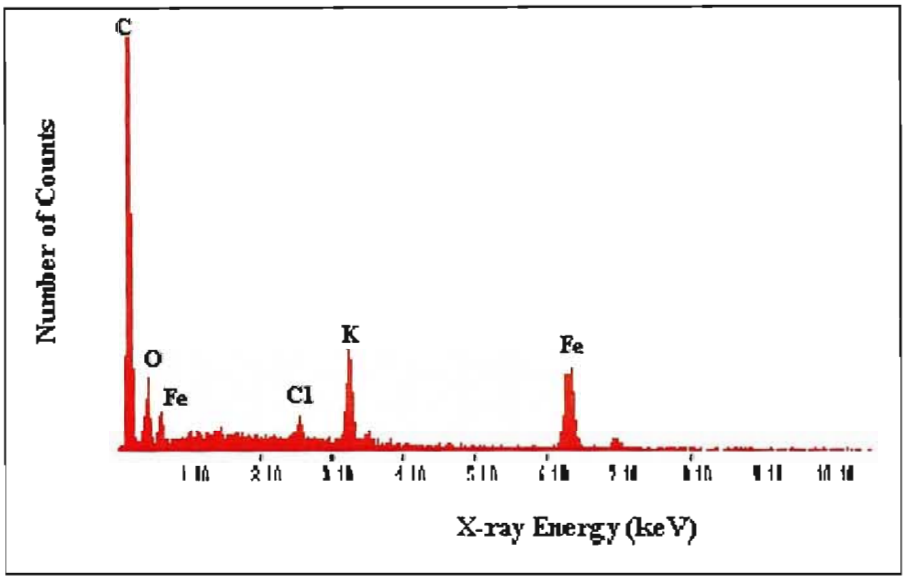

Figure 3.6 Scanning electron micrograph of hematin and corresponding X-ray spectrum. Hematin was mounted on a carbon stub and viewed in a Philips environmental scanning electron microscope fitted with a large field detector. **(A)** The crystal structure of hematin viewed and photographed at a magnification of 12 000x under an accelerating voltage of 20 kV. **(B)** The X-ray spectrum obtained at a magnification of 2 000x with a spot size of 4 for 150 s.

A

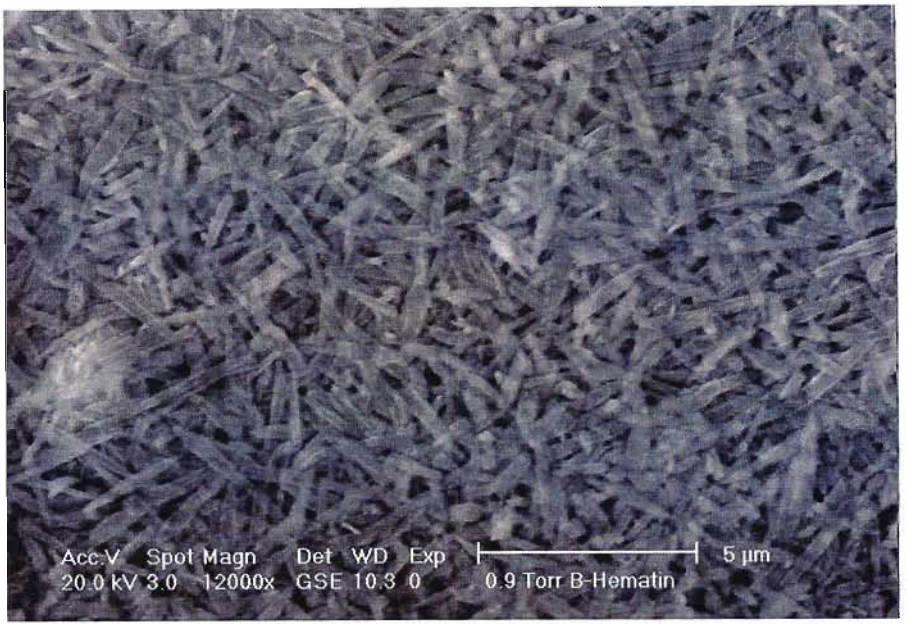

B

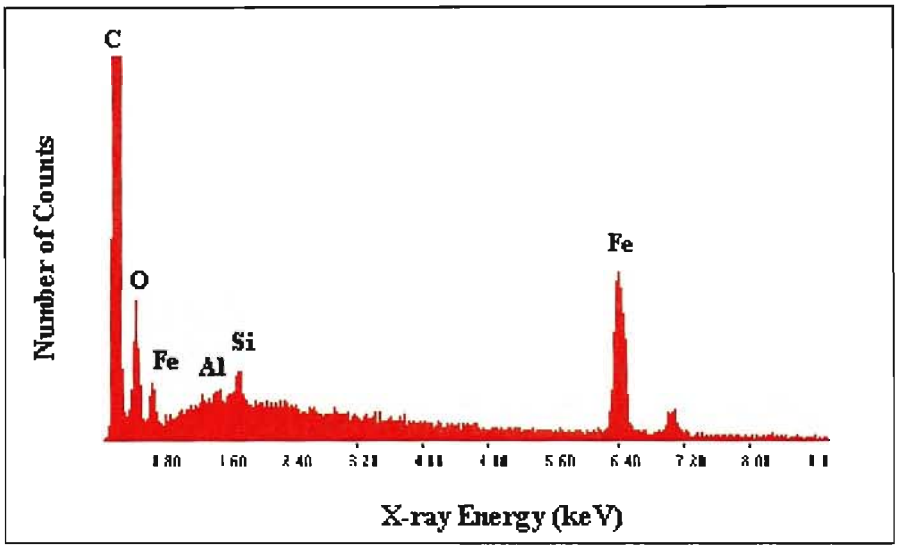

Figure 3.7 Scanning electron micrograph of β-hematin and corresponding X-ray spectrum. β-Hematin was mounted on a carbon stub and viewed in a Philips environmental scanning electron microscope fitted with a large field detector. **(A)** The crystal structure of β-hematin viewed and photographed at a magnification of 12 000x under an accelerating voltage of 20 kV. **(B)** The X-ray spectrum obtained at a magnification of 2 000x with a spot size of 4 for 150 s.

3.6.3 Monocyte phagocytosis of β-hematin

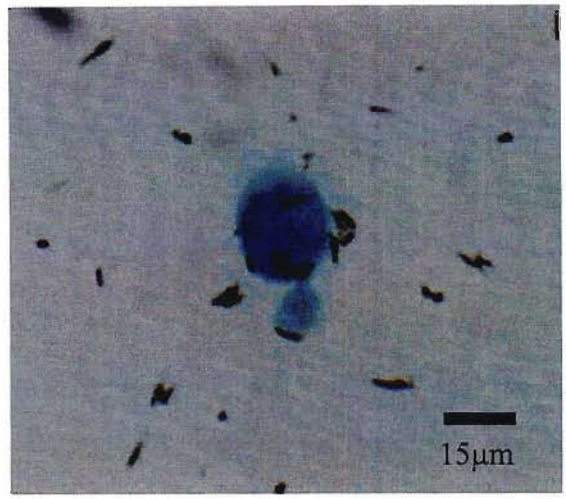

Figure 3.8 Canine monocyte phagocytosis of β-hematin. Canine peripheral blood monocytes were incubated with β-hematin for 30 min before washing, fixing with methanol and stained with methyl green. After staining, the coverslips were rinsed, dried, mounted and viewed at 1000x magnification.

The isolated monocytes (70.5%) phagocytosed unopsonized β-hematin (Figure 3.8). There were also numerous crystals adhering to the surface membrane of the monocytes. In comparison to the latex bead phagocytosis (Figure 3.5), there were fewer β-hematin crystals present in the monocytes after 30 min than there were beads. The difference in size of the particles, with unopsonised latex beads being 1 μm and β-hematin being between 0.7 and 3.85 μm, as well as the difference in chemical nature and structure between latex beads and β-hematin may account for the variance in phagocytosis of the compounds.

3.7 DISCUSSION

Monocytes are part of the first line of cellular defense against invading pathogens and disease, especially in a disease such as malaria (Asch, 1991; Roitt, 1997). These very important cells of the immune system were isolated from human and canine peripheral blood using a density gradient of Histopaque®-1077 as well as adherence to glass cover slips. A

series of experiments were performed to confirm the identity, viability and functionality of the isolated monocytes. It was noticed that during the density gradient centrifugation of the blood, the human monocyte layer was more clearly defined than the canine monocytes. This is most likely due to interspecies differences in the density of the respective cells, with the human cells having a density closer to that of the Histopaque®-1077 gradient, which averages 1.077 g/ml. Thiem *et al.* (1988) isolated canine monocytes using two techniques. The first using the method described by Boyum (1968) and the second employing hypertonic conditioning followed by Percoll density gradient centrifugation. The gradient was adjusted to 390 – 410 mosm/kg with the addition of crystalline sodium chloride. Using the second technique they obtained a greater yield and purity than obtained using the first method. De Almeida *et al.* (2000) also found that a hyperosmolar Percoll density gradient (d = 1.064 g/ml) improved the purity of isolated human monocytes. Austin *et al.* (1985) found that techniques utilized to isolate monocytes from human blood do not always work well with dog blood, especially Percoll gradients. They also suggest that Histopaque®-1077 type gradients, which yield mixed leukocyte populations, have been used successfully in dogs, but methods for further separation are not well established. In the present study, adherence rather than a Percoll density gradient was used as a second step to improve the purity of the monocytes isolated using a Histopaque®-1077 gradient.

The presence of cells adherent to glass cover slips was confirmed using methyl green staining (Figure 3.1A). The adherence of the cells served to confirm that they were monocytes (Miller and Stevenson, 1986). De Almeida *et al.* (2000) suggest that monocyte adherence is the most common purification method for monocytes but it does have a few disadvantages. There is high lymphocyte contamination within the first hour of adherence. Another disadvantage is the possible transient activation of the cells by the glass or by the methods used to detach the monocytes (Austin *et al.*, 1985).

The identity of the cells as monocytes was established using giemsa stain, which shows an easily-identifiable purple horseshoe shaped nucleus (Figure 3.1B) (Auger and Ross, 1992). Transmission electron microscopy yielded a similar result to the giemsa stain identifying an isolated cell nucleus with the shape of a horseshoe (Figure 3.4A). If, however, the cell is cut

at a different angle, then the cell can appear to have a different shaped nucleus (Figure 3.4B). This technique is very good for the identification of the ultrastructure of cells, but for the identification of cells it is often laborious and time consuming. The giemsa staining technique is much quicker and easier.

Monocytes act by phagocytosing pathogens and destroying them with enzymes and reactive oxygen intermediates (Roitt, 1997). Alkaline phosphatase and peroxidase activities were detected in the granules and, to a lesser extent, in the cytoplasm of the isolated canine monocytes (Figure 3.2; Figure 3.3). Peroxidase is present in monocytes (Krakowka and Wallace, 1983), but the activity of the enzymes decreases with the maturation of the cells (Stachura, 1989; Cribb *et al.*, 1990). There are many contradictory findings with regard to the presence of alkaline phosphatase in monocytes; Van Noorden and Frederiks (1992) state that it is present whereas Absolom (1986) and Murata *et al.* (1993) state that it is not present. Of interest, however, Murata *et al.* (1993) studied canine monocytes and neutrophils infected with *Hepatozoon canis* and they examined infected and uninfected cells for alkaline phosphatase, peroxidase and esterases. They found uninfected canine monocytes had no alkaline phosphatase or peroxidase activity; the only enzyme they found active was the alpha naphthol acetate esterase. Initially in the present study, when examining peroxidase activity in the monocytes, 4-chloro-1-naphthol substrate solution was utilized and no enzyme activity was noted (data not shown). However, when using a different substrate solution, DAB, enzyme activity was visualized (Figure 3.3). This shows that the substrate used can affect the apparent presence or absence of a particular enzyme. Unfortunately, Murata *et al.* (1993) did not describe the methods or substrates they used, they only refer to other investigators work, which is written in Japanese. In the case of alkaline phosphatase, Absolom (1986) used naphthol AS-BI phosphate as a substrate to detect alkaline phosphatase, which yielded a negative result. In light of these discrepancies in the literature a more conclusive enzyme to examine would have been the monocyte specific, nonspecific α-naphthyl acetate esterase (Stachura, 1989).

Monocytes are phagocytic cells (Auger and Ross, 1992), and the phagocytosis of latex beads is a functional way to confirm monocyte identity. Phagocytosis has to be selective to avoid

ingesting 'self' cells. The occurrence is dependent on two criteria. Firstly, the surface of the particle should be rough. Secondly, natural substances generally have an electronegative surface charge, as do the phagocytes, thus they will repel each other (Guyton, 1982). Dead tissue and foreign materials generally have an electropositive charge and hence can be ingested. In the natural system, phagocytosis is enhanced by opsonization, i.e. coating of an antigen with an opsonin which can be an antibody or C3b (Roitt, 1997). In this case unopsonized latex beads were used, as the β-hematin was also unopsonized, thus unopsonized latex beads were an appropriate control. The latex beads and the β-hematin also carry an electropositive charge, which would be expected to aid in ingestion. The isolated cells phagocytosed a number of unopsonized latex beads in 30 min (Figure 3.5).

The role of monocytes in malaria is the major focus of this study. The malaria parasite produces hemozoin as a result of the breakdown of hemoglobin from infected red blood cells. Monocytes have been shown to avidly phagocytose hemozoin *in vivo* (Phu *et al.*, 1995) and *in vitro* (Schwarzer *et al.*, 1999). The cells are unable to digest hemozoin and thus the phagocytosed hemozoin remains in the monocyte for a long time. It has been shown that phagocytosed hemozoin alters monocyte function. The cells failed to produce an oxidative burst, were unable to repeat the phagocytic cycle (Schwarzer *et al.*, 1992) and unable to kill ingested bacteria, fungi and tumor cells (Schwarzer *et al.*, 1999).

Hemozoin is difficult to isolate from the malaria parasite and so a chemically synthesized β-hematin with chemical characteristics similar to hemozoin was used. β-Hematin was synthesized from hematin using an alkali-acid-temperature technique (Slater *et al.*, 1991; Taramelli *et al.*, 1995). Scanning electron micrographs and X-ray spectra were taken to monitor any changes that had occurred during the treatment of hematin. The hematin and β-hematin have different shaped crystals. Their X-ray spectra are similar with the exception of elements derived from the preparation processes (Figure 3.6; Figure 3.7). Egan *et al.* (2001) examined the mechanism of β-hematin formation and in one experiment observed the changes in the external appearance of these materials. Hematin was found to consist of 'large angular particles with a smooth surface' that ranged in size from 3 to 50 μm. This is consistent with the electron micrograph of hematin depicted in Figure 3.6A. The surface of β-hematin was

described by Egan *et al.* (2001) as a 'mass of small clearly discernible crystals' of approximately 150 to 350nm long. This is consistent with the electron micrograph of the synthesized β-hematin depicted in Figure 3.7A.

The monocytes were able to phagocytose the β-hematin, although to a lesser extent than the unopsonised latex beads. As previously mentioned, hemozoin or β-hematin 'fed' monocytes are unable to repeat the phagocytic cycle. The monocytes phagocytosing latex beads would be unmodified and hence able to phagocytose many more particles than the monocytes phagocytosing β-hematin. Shaw and Anderson (1984) found that monocytes phagocytosed more latex beads than *Candida albicans* particles and they suggested that this was due to the considerable size difference, as well as differences on the external surface. It would be possible to redo the same experiments with latex beads and β-hematin opsonized with antibodies. Thus it could be determined if the β-hematin is more avidly phagocytosed because it is unable to exert its effects on the monocytes due to the presence of the bound anti-hemozoin antibodies which can be obtained from malaria patients. Biswas *et al.* (2001) detected antibodies against hemozoin in patients infected with *P. falciparum* malaria. These antibodies were mainly IgM types, which appeared to have an anti-disease effect.

These experiments served to confirm the presence of monocytes that are functionally active as determined by the presence of alkaline phosphatase, peroxidase and phagocytosis of latex beads. β-Hematin can also be easily synthesized and phagocytosed by monocytes. Canine and human monocytes were used for all the experiments and in all cases the results obtained were similar.

CHAPTER 4

RAISING ANTIBODIES AGAINST PEPTIDES FROM HEAT SHOCK PROTEIN 70 (HSP70/HSC70)

4.1 INTRODUCTION

Heat shock protein 70 and heat shock cognate protein 70 are part of a multi-gene family of chaperones, that have four distinct features: highly conserved sequences, molecular mass of approximately 70 kDa, ATPase activity and the ability to bind and release hydrophobic segments of an unfolded polypeptide chain (Feige and Polla, 1994). The N-terminal ATPase domain is the most conserved, with about 64% identity between eukaryotic HSP70s. The C-terminal domain is more variable where a protease sensitive domain joins it to the ATPase domain.

The response of cells to environmental stress such as heat or chemicals is to induce the production of heat shock proteins. Some HSPs, the heat shock cognate proteins, are constitutively expressed. The HSP proteins are also involved in important functions under normal conditions (Feige and Polla, 1994). Malaria is one of the stress conditions, which induces the production of heat shock proteins, where fever, prostaglandins and hydrogen peroxide stimulate HSP synthesis (Polla, 1988; Clerget and Polla, 1990). HSP 70 is involved in the regulation of the secondary effects of TNF-α, namely the secretion of PLA_2 (Jäättelä, 1993). In the case of severe malaria, the serum PLA_2 levels are between 40 – 1100 fold greater than in healthy individuals (Vadas *et al.*, 1993). As PLA_2 plasma levels are elevated during malaria and there is fever, it is of interest why the HSP response does not inhibit the production of PLA_2 as it does in other conditions. One possible explanation is that the expression of HSP70 is altered by hemozoin. Hemozoin may exert its effect in two ways. The first being when it is released into the blood when the infected red blood cells burst, and its presence induces the production of TNF-α and other inflammatory mediators and fever, ultimately the expression of HSP70 is altered. The second mechanism is when the monocytes phagocytose either the infected red blood cells and/or the released hemozoin and the cells become stressed and produce HSP 70.

An understanding of these mechanisms could be achieved using immunostaining on western blots using antibodies against heat shock proteins. Instead of using monoclonal antibodies that are extremely expensive, anti-peptide antibodies could be produced and used in the present study. Peptides were utilised in the production of anti-peptide antibodies in chickens, which are evolutionary distant to mammals and are likely to give a better response to the mammalian HSP peptides. The antibodies were purified using the Polson *et al.* (1985) PEG 6 000 technique as described by Goldring and Coetzer (2003) and affinity purified using a peptide linked affinity matrix. The titres were evaluated using ELISA and the recognition of the entire protein by the anti-peptide antibodies confirmed with western blotting.

4.2 SELECTION OF HEAT SHOCK PROTEIN PEPTIDES

The amino acid sequences of heat shock protein 70 (HSP70) and heat shock cognate protein 70 (HSC70) were aligned to determine amino acid regions in the sequences that contained similar sequences and amino acid regions that were different (Figure 4.1). The N-terminus shows a higher frequency of conserved amino acids between the two sequences than the C-terminus. Selecting peptides in regions of the sequences that are dissimilar would hence result in anti-peptide antibodies that are likely to be specific for each of the parental proteins. Regions of interest were determined from a range of criteria from the graphs obtained in the Predict 7 programme (Càrmenes *et al.*, 1989). Initially, the whole protein sequence was used to determine areas of increased flexibility, hydrophilicity, surface probability and antigenicity (Figure 4.2A; Figure 4.3A).

Hydrophilicity is an important criterion in the selection of antigenic peptides as the hydrophilic residues are often on the exterior of the protein where they interact with water. The hydrophobic residues are frequently buried in the structure of proteins (Van Regenmortel *et al.*, 1988). The local maxima in a hydrophilicity plot have been correlated to regions that are exposed on the surface of the protein as well as parts of epitopes. Thus when predicting peptides it is preferable to consider the areas containing the highest peaks for all four criteria. Proteins as well as peptides are not rigid structures; they have dynamic conformational

variations that are linked to their functional activity. That is the proteins are flexible. There is a correlation between the peaks in the flexibility plot and the position of epitopes.

Van Regenmortel *et al.* (1988) state that although flexibility is not an absolute requirement for antigenicity, it has been associated with a greater than average antigenic reaction. Surface probability is linked to the ability of the antibody to bind to the epitope. Epitopes on the surface are more accessible than those buried deep within the tertiary structure of the protein (Van Regenmortel *et al.*, 1988). The last selection criteria was that of antigenicity, this is a computer generated plot that utilises all the prediction criteria mentioned previously to provide an educated guess as to where the most antigenic regions are. This is not an absolute prediction criterion, as the other three are more accurate, but in combination with them it is an effective tool. The regions of interest would hence be those where all four criteria had elevated levels.

Figure 4.2A shows four regions where there are maxima in all four criteria. The first section in the sequence (200 – 300 aa) was examined, but the sequence identity between HSP70 and HSC70 was 100%. The region from amino acids 500 – 600 (Figure 4.2B) was selected for further analysis (Figure 4.2B), as there are three peaks in all the plots (aa 503 – 516; 560 – 574; 586 – 598). The similarity of these regions to the human HSC 70 and chicken HSP 70 sequence was investigated, as well as the similarity to any other protein that may be encountered in the human, canine or chicken systems. The region of 503 – 516 amino acids was 93% similar to human HSC 70 and chicken HSP 70. The region of 560 – 574 was 65% similar to human HSC 70 and 82% similar to chicken HSP 70. The sequence of 586 – 598 was 73% similar to human HSC 70 and chicken HSP 70. The selected peptide sequence is CLAEKDEFEHKRKE (Table 2.4; Figure 4.1). The position of the selected peptide is shown in Figure 4.1 (amino acids 586 – 598) and the peptides selection criteria plot is shown in Figure 4.2C. Ultimately the lack of similarity between human HSP 70 and chicken HSP 70 was the deciding factor in choosing the HSP peptide.

HSC 70 has four regions where all four criteria are maximal (Figure 4.3A). The first maxima in the sequence (250 – 300 aa) were examined, but the sequence identity between HSC70 and

HSP70 was 99%. All other regions with possible peptides were examined by a similarity search and the sequence from 550 – 650 was selected to be examined further (Figure 4.3B). There are two peaks in all the plots (aa 561 – 574; 586 – 600). The similarity of the identified regions to the human HSC 70 and chicken HSP 70 sequence was determined. The region of 561 – 574 was 65% similar to human HSP 70 and 82% similar to chicken HSC 70. The sequence 586 – 598 was 73% similar to human HSP 70 and 85% similar to chicken HSC 70. The region with the lowest similarity was aa 561 – 574. Thus the peptide sequence KINDEDKQKILDKC (Table 2.4; Figure 4.1) was chosen. The position of the selected peptide is shown in Figure 4.1 and the peptides selection criteria plot is shown in Figure 4.3C.

```
HSP   1 MAKAAAIGIDLGTTYSCVGVFQHGKVEIIANDQGNRTTPSYVAFTDTERLIGDAAKNQVA
HSC   1 MSKGPAVGIDLGTTYSCVGVFQHGKVEIIANDQGNRTTPSYVAFTDTERLIGDAAKNQVA
          * *  * ************************************************

HSP  61 LNPQNTVFDAKRLIGRKFGDPVVQSDMKHWPFQVINDGDKPKVQVSYKGETKAFYPEEIS
HSC  61 MNPTNTVFDAKRLIGRRFDDAVVQSDMKHWPFMVVNDAGRPKVQVEYKGETKSFYPEEVS
         ** ************ * * ********** * **   ***** ****** ***** *

HSP 121 SMVLTKMKEIAEAYLGYPVTNAVITVPAYFNDSQRQATKDAGVIAGLNVLRIINEPTAAA
HSC 121 SMVLTKMKEIAEAYLGKTVTNAVVTVPAYFNDSQRQATKDAGTIAGLNVLRIINEPTAAA
         ****************  ***** ****************** ****************

HSP 181 IAYGLDRTGKGERNVLIFDLGGGTFDVSILTIDDGIFEVKATAGDTHLGGEDFDNRLVNH
HSC 181 IAYGLDKKVGAERNVLIFDLGGGTFDVSILTIEDGIFEVKSTAGDTHLGGEDFDNRMVNH
         ******     ******************** ******* ************** ***

HSP 241 FVEEFKRKHKKDISQNKRAVRRLRTACERAKRTLSSSTQASLEIDSLFEGIDFYTSITRA
HSC 241 FIAEFKRKHKKDISENKRAVRRLRTACERAKRTLSSSTQASIEIDSLYEGIDFYTSITRA
         *  *********** ************************** ***** ************

HSP 301 RFEELCSDLFRSTLEPVEKALRDAKLDKAQIHDLVLVGGSTRIPKVQKLLQDFFNGRDLN
HSC 301 RFEELNADLFRGTLDPVEKALRDAKLDKSQIHDIVLVGGSTRIPKIQKLLQDFFNGKELN
         *****  **** ** ************* **** ********** **********  **

HSP 361 KSINPDEAVAYGAAVQAAILMGDKSENVQDLLLLDVAPLSLGLETAGGVMTALIKRNSTI
HSC 361 KSINPDEAVAYGAAVQAAILSGDKSENVQDLLLLDVTPLSLGIETAGGVMTVLIKRNTTI
         ******************** *************** ***** ******** ***** **

HSP 421 PTKQTQIFTTYSDNQPGVLIQVYEGERAMTKDNNLLGRFELSGIPPAPRGVPQIEVTFDI
HSC 421 PTKQTQTFTTYSDNQPGVLIQVYEGERAMTKDNNLLGKFELTGIPPAPRGVPQIEVTFDI
         ****** ****************************** *** ******************

HSP 481 DANGILNVTATDKSTGKANKITITNDKGRLSKEEIERMVQEAEKYKAEDEVQRERVSAKN
HSC 481 DANGILNVSAVDKSTGKENKITITNDKGRLSKEDIERMVQEAEKYKAEDEKQRDKVSSKN
         ******** * ****** *************** **************** **  ** **

HSP 541 ALESYAFNMKSAVEDEGLKGKISEADKKKVLDKCQEVISWLDANTLAEKDEFEHKRKELE
HSC 541 SLESYAFNMKATVEDEKLQGKLSEADKQQLLDKCNEIINWLDKNQTAEKEEFEHQQKELE
         *********  **** * ***  ** * **** * * *** *  *** **** ****

HSP 601 QVCNPIISGLYQGAGG-PG--PGGF--GAQGPKGGSGSGPTIEEVD
HSC 601 KVCNPIITKLYQSAGGMPGGMPGGFPGGGAPPSGGASSGPTIEEVD
         ******  *** *** **  ****  *   * **  *********
```

Figure 4.1 Amino acid sequence alignment of human heat shock protein 70 with human heat shock cognate protein 70. The amino acid sequences of heat shock protein 70 (HSP) and heat shock cognate 70 (HSC) were aligned from the first amino acid to the last. * Indicates amino acids that are present on both sequences in the same position. Gaps in the sequence where no alignment is possible due to different numbers of amino acids is depicted by a -. The peptide sequences that were selected are included, HSP peptide is boxed in RED and the HSC peptide is boxed in BLUE.

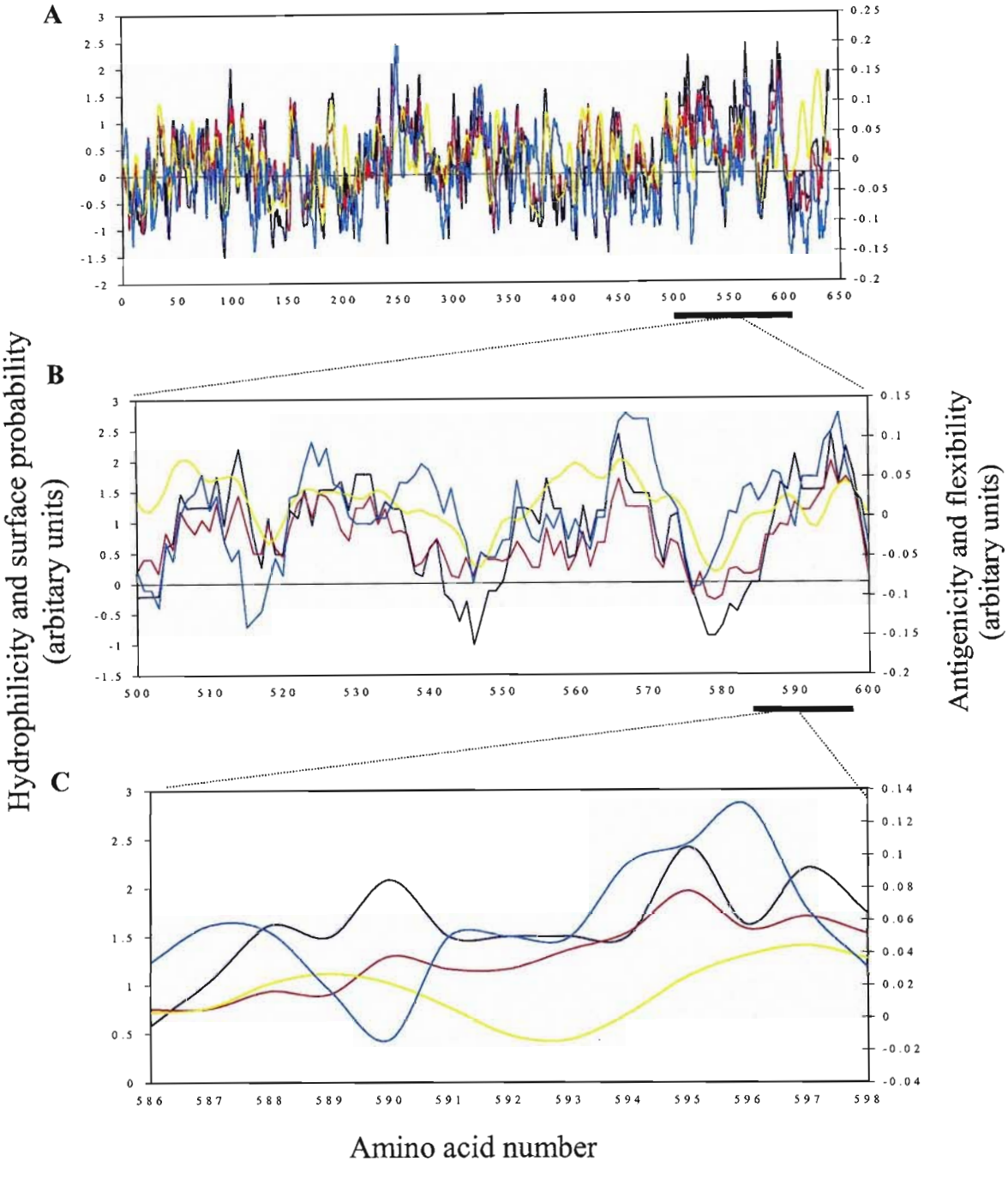

Figure 4.2 Prediction criteria used for the selection of an immunogenic peptide from human heat shock protein 70. The heat shock protein 70 sequence was used in the Predict7 programme and the following peptide selection criteria plotted: hydrophilicity (-), surface probability (-), antigenicity (-) and flexibility (-). **(A)** The entire HSP70 amino acid sequence (amino acid numbers 0 - 641). **(B)** A section of the HSP70 sequence from amino acid number 500 - 600. **(C)** The selected heat shock protein 70 peptide (HSP), amino acids 586 - 598, used to immunize chickens.

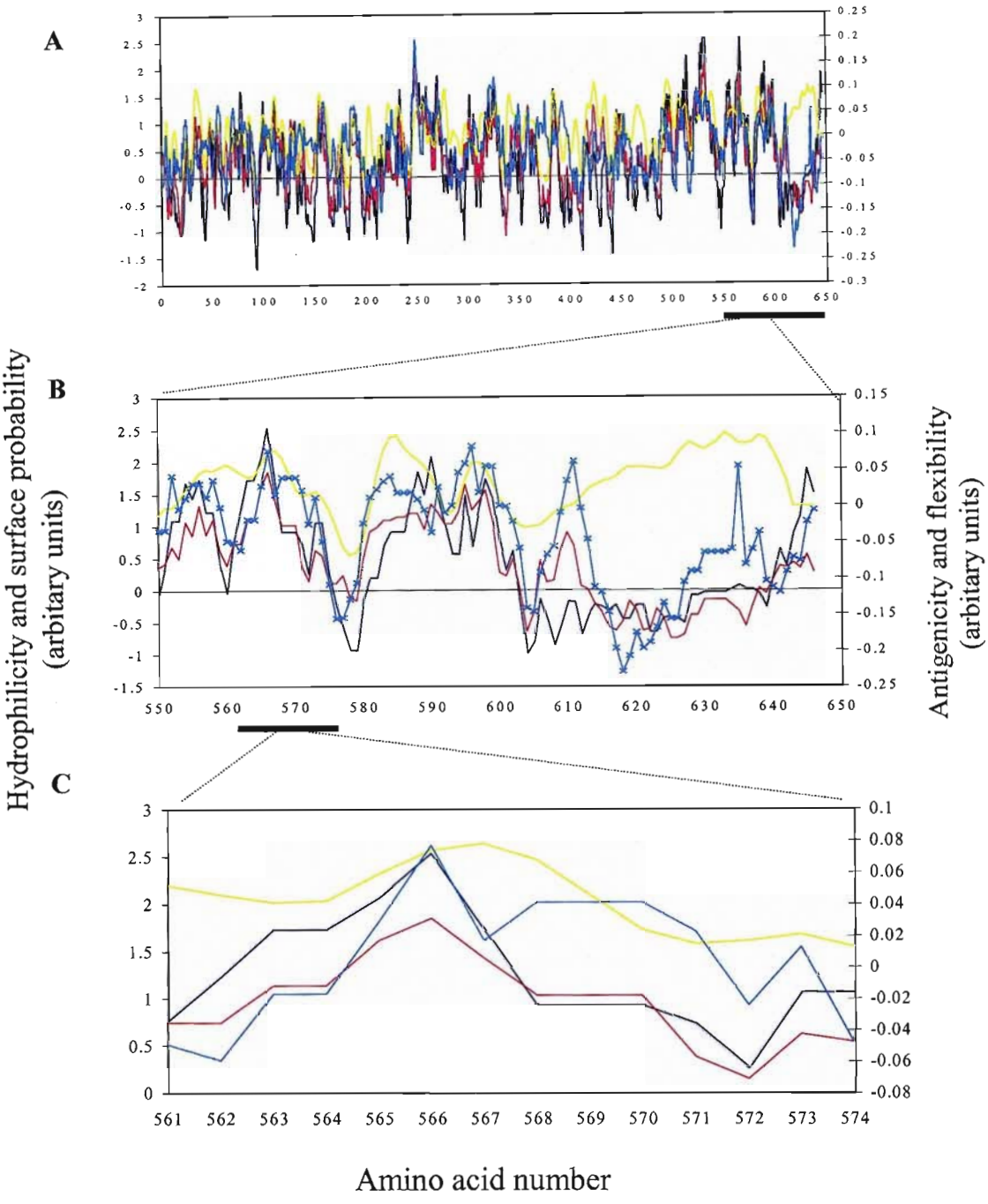

Figure 4.3 Prediction criteria used for the selection of an immunogenic peptide from human heat shock cognate protein 70. The heat shock cognate protein 70 sequence was used in the Predict7 programme and the following peptide selection criteria plotted: hydrophilicity (-), surface probability (-), antigenicity (-) and flexibility (-). **(A)** The entire HSC70 amino acid sequence (amino acid numbers 0 - 646). **(B)** A section of the HSP70 sequence from amino acid number 550 - 650. **(C)** The selected heat shock cognate protein 70 peptide (HSC), amino acids 561 - 574, used to immunize chickens.

As mentioned previously, heat shock protein 70 consists of two domains, the highly conserved N-terminal ATPase binding domain (Figure 4.4A) and the variable C-terminal peptide-binding domain (Figure 4.4B). The structures of the two domains are extremely different, the peptide-binding domain is similar to that of the MHC class I molecule. The peptide on the figure (Figure 4.4.B) is located on the outer α-helices of the peptide-binding domain. This confirms the surface probability selection criteria in Figure 4.2, and suggests that the anti-peptide antibodies are likely to bind to the peptide sequence in the native protein.

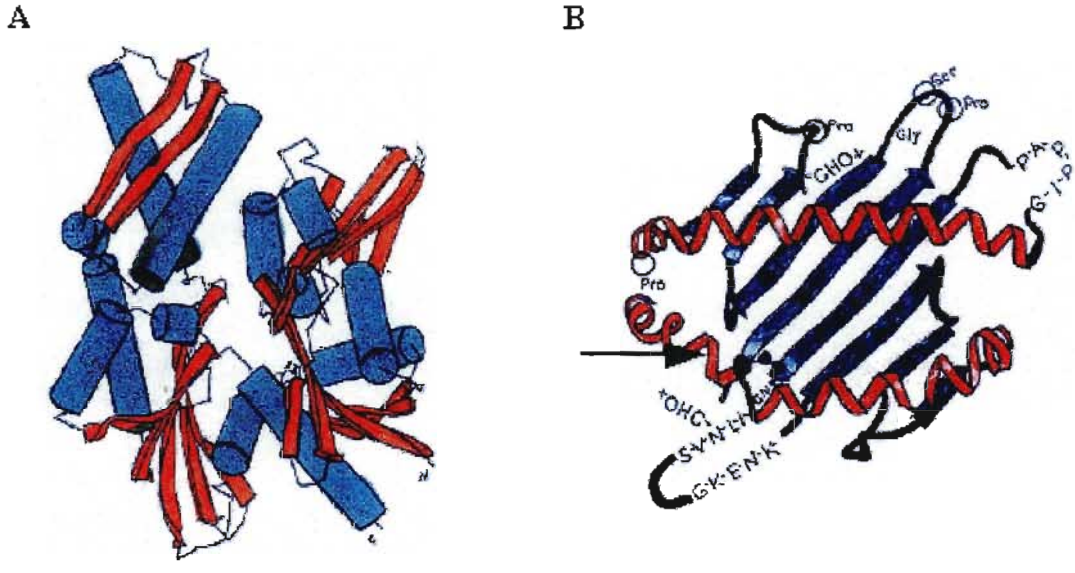

Figure 4.4 The structure of heat shock protein 70. HSP70 consists of two domains, the highly conserved N-terminal ATPase domain **(A)** and the less conserved C-terminal peptide-binding domain **(B)**. The ATPase domain structure was determined by X-ray crystallography and the peptide binding domain structure was modelled on the structure of human MHC Class I molecules. The arrow indicates the peptide position on the native protein. (Adapted from Feige and Polla, 1994).

4.3 ANTI-PEPTIDE ANTIBODY ISOLATION AND CHARACTERISATION

Anti-peptide antibodies were isolated from chicken eggs using the PEG 6 000 precipitation technique and the titres were determined using an ELISA. Antipeptide antibodies were separated from the anti-carrier antibodies and other antibodies using affinity chromatography. The efficiency of each step was evaluated using an ELISA. Finally, the ability of the anti-peptide antibodies to recognize the native heat shock proteins was evaluated using Western blotting.

4.3.1 Isolation of chicken anti-heat shock protein peptide antibodies.

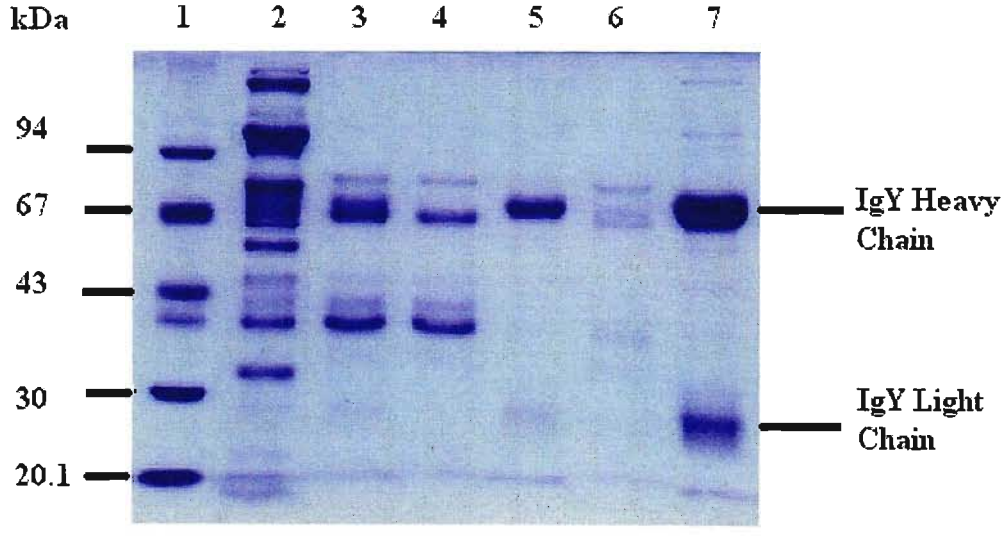

Figure 4.5 12.5 % Reducing SDS-PAGE showing the purification of chicken anti-peptide antibodies. Chicken antibodies were isolated from egg yolks using the PEG 6 000 precipitation technique. The samples were loaded onto a 12.5% Laemmli SDS-PAGE gel and stained with Coomassie brilliant blue. Lane 1: Pharmacia molecular mass markers; Lane 2: egg yolk mixed with 2 volumes of phosphate buffer; Lane 3: filtrate after the first centrifugation step; Lane 4: supernatant from the initial 12% PEG pellet; Lane 5: the redissolved initial 12% PEG pellet; Lane 6: supernatant from the second 12% PEG pellet; Lane 7: final purified IgY pellet.

Using the PEG 6 000 precipitation technique the average yield for the IgY was 20.48 mg/ml. The purification procedure was very successful as can be seen on Figure 4.5 and according to Schade *et al.* (1999) the purity of IgY using this method is greater than 90%. This has been recently confirmed by Goldring and Coetzer (2003) who routinely obtain yields of 90% purity using the same technique. The first sample (Lane 2) contains the egg yolk mixed with two volumes of 100 mM sodium phosphate buffer (pH 7.6), and there are many proteins present. Lane 3 contains the filtrate after the first centrifugation step that removes the vitellins and lipids and had approximately six proteins. Proteins were removed from the filtrate by the addition of 12% PEG as indicated in Lane 4 by the presence of two protein bands. It appears that all but two proteins have been removed by the 12% PEG. The pellet (Lane 5), however, still contains protein but there are fewer bands than in Lane 2. The IgY heavy and light chains are heavily stained, as their concentration in proportion to all the other proteins has increased. The second 12% precipitation removed more egg proteins (Lane 6) but less than the first 12% step (Lane 4).

The final IgY pellet is loaded at a higher concentration of protein compared to the other lanes and contains some minor bands. The bands represent the different reduced forms of the protein (Lane 7). The most prominent band is the heavy chain at approximately 66 000 Da, which compares favourably with published values (65 – 70 kDa; Schade *et al.*, 1999). It runs as a broad band, because of the presence of a substantial amount of carbohydrates and the antigen binding regions contain variable amino acids. The light chain is also prominent with an approximate molecular weight of 27 000 Da (22 – 30 kDa; Schade *et al.*, 1999). The minor protein bands present are: the unreduced protein of approximately 180 000 Da (Warr *et al.*, 1995), two heavy chains and one light chain of approximately 155 000 Da, two heavy chains of approximately 130 000 Da, a heavy and a light chain of approximately 90 000 Da, two light chains of approximately 55 000 Da. The IgY isolation was successful as there was a good yield and the SDS-PAGE data show the IgY to be pure (Figure 4.5).

4.3.2 Evaluation of chicken anti-heat shock protein peptide antibody and anti-rabbit albumin antibody titres using ELISA

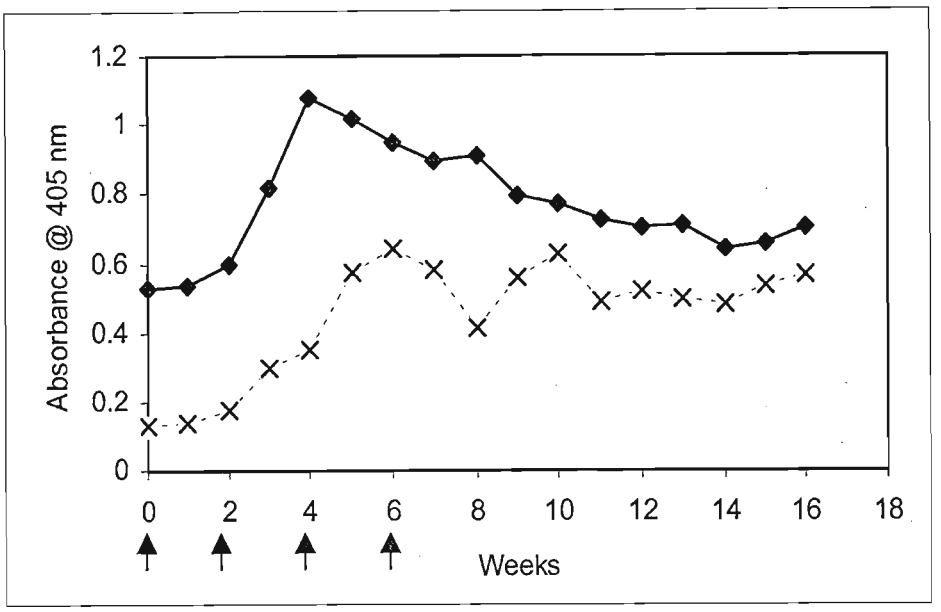

Figure 4.6 Progress of anti-peptide antibody production in chickens immunized with the HSP peptide conjugated to rabbit albumin. Two chickens were immunized with the HSP peptide conjugated to rabbit albumin: chicken 1 (◆) and chicken 2 (x). The HSP peptide was coated at a concentration of 1 μg/ml to microtitre plates and incubated with chicken anti-HSP peptide antibodies (200 μg/ml) collected from eggs. Binding was visualised with goat anti-chicken IgY horseradish peroxidase. Each point is the mean absorbance at 405 nm of duplicate samples. The arrows indicate when the chickens were immunized.

The two chickens injected with the HSP-peptide conjugated to rabbit albumin produced anti-peptide antibodies (Figure 4.6). The antibodies produced by chicken 1 were of higher titre than those produced by chicken 2, as indicated by the difference between the two curves. In both cases the titre increased slowly till week two. For chicken 1 the titre peaked during the 4^{th} week and for chicken 2 during the 6^{th} week post immunization. The titre then decreased slowly till week 16 where the titre was still higher than that of the non-immune control (data not shown). The titre of anti-peptide antibodies peaked twice in chicken 2, once at week 6 and again at week 10. In this chicken the titre remained high but constant after week 10 until week

16, where it was significantly higher than the non-immune control. Figure 4.6 shows the difference in the antibody response between two chickens kept under the same conditions and immunized with the same peptide conjugate.

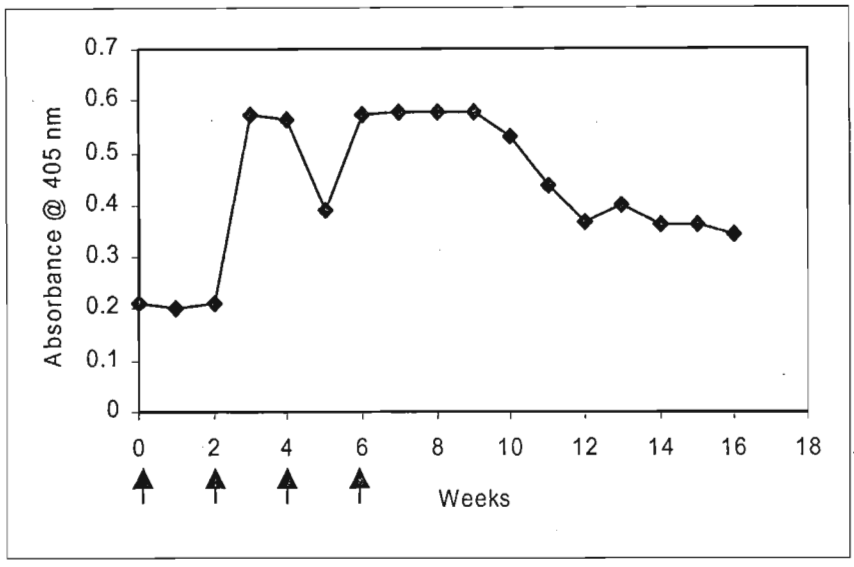

Figure 4.7 Progress of anti-peptide antibody production in chickens immunized with the HSC peptide conjugated to rabbit albumin. Three chickens were immunized with the HSC peptide conjugated to rabbit albumin: chicken A (◆), chicken B (died after four weeks) and chicken C (died after seven weeks). The microtitre plates were coated with the HSC peptide at a concentration of 1μg/ml and incubated with chicken anti-HSC peptide antibodies (200 μg/ml) collected from eggs. Binding was visualised with goat anti-chicken IgY horseradish peroxidase. Each point is the mean absorbance at 405 nm of duplicate samples. The arrows indicate when the chickens were immunized.

The chickens injected with the HSC peptide conjugated to rabbit albumin (Figure 4.7) had a completely different response to that of the chickens injected with the HSP-conjugate (Figure 4.6). Although three chickens were immunized, two chickens died after 4 weeks and 7 weeks, respectively, without producing any eggs and hence no antibodies. Chicken 1, however, had high antibody titres from week 3 to week 9. There was a decrease in titre at week 5. The titre tapered off from week 9 to week 16. The titre at week 16 was higher than that of the non-immune control (data not shown).

Both peptides elicited an immune response in the chickens immunized. The anti-peptide antibody titre in all three chickens was high irrespective of the peptide used. However, chicken 1 immunized with the HSP-peptide conjugated to rabbit albumin had the highest titre (Figure 4.6). Thus the selection of the peptides is considered to be successful as they both elicited an immune response in chickens with high titres of the antibodies.

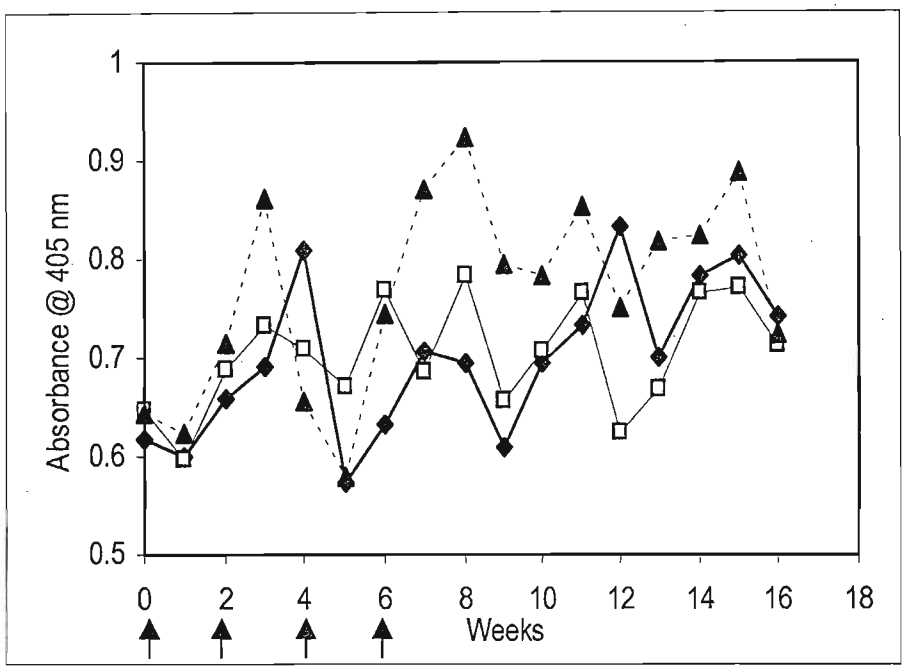

Figure 4.8 Progress of anti-carrier antibody production in chickens immunized with the HSP or HSC peptide conjugated to rabbit albumin. Two chickens were immunized with HSP peptide conjugated to rabbit albumin: chicken 1 (◆) and chicken 2 (□). One chicken was immunized with the HSC peptide conjugated to rabbit albumin (-▲-). Rabbit albumin was coated at a concentration of 1μg/ml to microtitre plates and incubated with chicken anti-rabbit albumin antibodies (200 μg/ml) collected from eggs. Binding was visualised with goat anti-chicken IgY horseradish peroxidase. Each point is the mean absorbance at 405 nm of duplicate samples. The arrows indicate when the chickens were immunized.

The titres of anti-carrier antibodies fluctuated during the immunisation period (Figure 4.8). With respect to the rabbit albumin conjugated to the HSP peptide, the titres had peaked at

weeks 4, 7, 12 and 15 in chicken 1 with the highest titres of antibody during weeks 4 and 12. In chicken 2 peak titres were observed during weeks 3, 6, 8, 11 and 15, at week 3 the peak was smaller than the subsequent peaks. The chicken immunized with the HSC peptide conjugated to rabbit albumin had anti-carrier antibody titre peaks at weeks 3, 8, 11 and 15. In all cases at week 16 the titre is higher than the non-immune control. The chicken immunized with the HSC70 peptide generally produced more antibodies against the carrier protein than the chickens immunized with the HSP70 peptide. Figure 4.8 shows that the chickens produced antibodies against the carrier protein, rabbit albumin, as well as the peptide of interest. The anti-carrier antibodies needed to be separated from the anti-peptide antibodies using affinity purification.

4.3.3 Affinity purification of chicken anti-heat shock protein peptide antibody

The anti-HSP peptide antibodies were pooled into four pools: weeks 1-7, weeks 8-11, weeks 12-14 and weeks 15 & 16. The anti-HSP peptide antibody titre peaked at week 3 and 7 (Figure 4.6), thus the weeks 1-7 pool would be expected to contain the most antibodies (Figure 4.9). The anti-peptide antibody elution profiles for both the HSC peptide and the HSP peptide were similar (Figure 4.9). The anti-HSP peptides isolated from chicken 1 have been previously shown to be in high titre between weeks 3 and 7 (Figure 4.6) and were eluted from the affinity column with a concentration of 15.2 mg/ml. The total yield for chicken 1 immunized with HSP was 98.27 mg. This yield was significantly higher (7.5 fold) than anti-HSP peptide antibodies isolated from chicken 2 which, yielded 13.21 mg. The yield of anti-HSC peptide antibodies was 3.73 mg, significantly lower than the yields for the anti-HSP peptide antibodies from both chickens utilized.

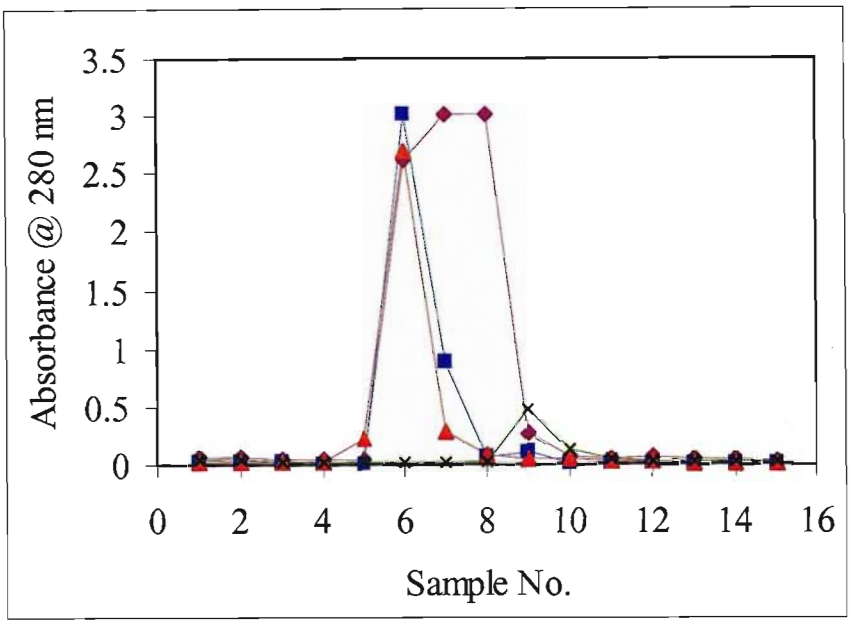

Figure 4.9 Elution profile of anti-HSP peptide antibodies from the HSP peptide affinity matrix. HSP peptide was coupled to the Sulfolink® affinity matrix. The isolated polyclonal chicken antibodies: weeks 1-7 (◆); weeks 8 – 11 (■); weeks 12 – 14 (▲) and weeks 15 – 16 (x) were allowed to circulate through the peptide affinity column overnight. The unbound antibodies were washed off the column and the bound antibodies were eluted using a low pH buffer (pH 2.8). The absorbance of the anti-peptide antibodies was measured at 280 nm. The samples with an absorbance greater the 0.2 were pooled. This is a representative elution profile of three peptide columns and anti-peptide antibodies.

4.3.4 Evaluation of affinity purified chicken anti-heat shock protein peptide antibody titre using ELISA

The anti-HSP peptide antibodies had a higher titre than the non-affinity purified antibodies (Figure 4.10) and both preparations of antibody are of high titre as they can be used at concentrations of 10 μg/ml to 100 μg/ml with very little difference in the absorbance obtained. There appears to still be some anti-peptide antibodies remaining in the antibody solution that had not bound to the column, as the titre is significantly higher than that of the non-immune control. The anti-HSP antibodies isolated from chicken 2 and the anti-HSC antibodies showed similar patterns to the anti-HSP antibodies isolated from chicken 1 (data not shown). The

affinity purification was successful as the anti-peptide antibodies were evidently separated from the anti carrier antibodies (Figure 4.10).

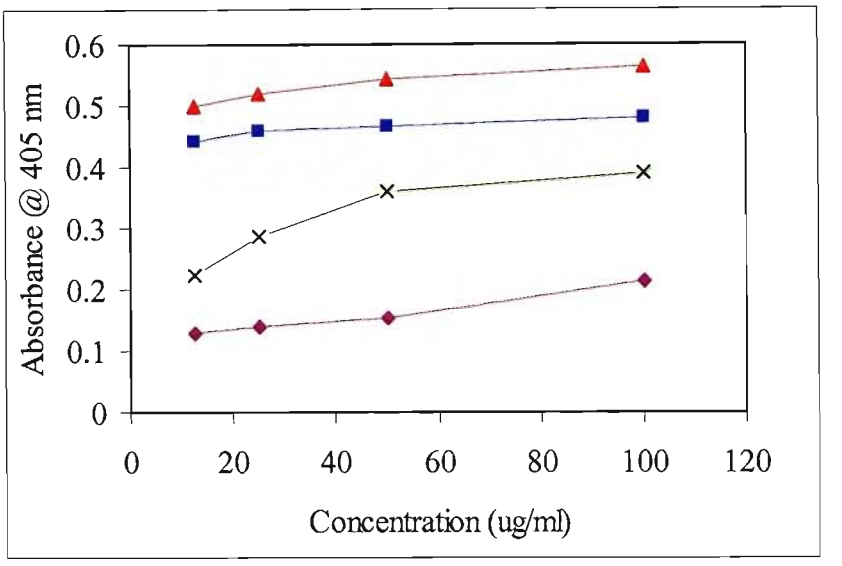

Figure 4.10 Evaluation of the affinity purification of chicken anti-HSP peptide antibodies. The HSP peptide was coated at a concentration of 1 µg/ml to microtitre plates and incubated with serial doubling dilutions of affinity purified chicken anti-HSP peptide antibodies from weeks 1-7: Non-immune (◆); non-affinity purified antibodies (■); affinity purified antibodies (▲) and the remaining antibodies after affinity purification (-x-). Binding was visualised with goat anti-chicken IgY horseradish peroxidase antibody. Each point is the mean absorbance at 405 nm of duplicate samples. All affinity purified anti-peptide antibodies showed similar trends.

4.3.5 Evaluation of affinity purified chicken anti-peptide antibody recognition of the native protein in lymphocyte lysates using western blotting

The affinity purification of the anti-peptide antibodies was accomplished as mentioned above (Section 4.3.4). Western blotting was used to determine the possible presence of residual anti-rabbit albumin as well as to show that the anti-peptide antibodies recognize the peptide conjugate after electrophoresis (Figure 4.11). The SDS-PAGE gel shows a number of light bands in Lane 2, but the main band is at 67 kDa which is rabbit albumin. The two peptide conjugates in Lanes 3 and 4 are not classic thin bands but more a large smear ranging from 68

kDa to well above 100 kDa. The 'smearing' is a result of between a minimum of one and a maximum of 40 peptides binding to each rabbit albumin molecule. At a size of 1762 Da for HSP and 1670 Da for HSC, the combinations can range from 68 kDa if only one peptide binds to 137 kDa if the calculated number of 40 HSP peptides bind. The affinity purified antibodies contain no rabbit albumin as there is only recognition of the peptide conjugates in Lane 3 for the anti-HSP antibodies and Lane 4 for the anti-HSC antibodies. No recognition of the large rabbit albumin band at 67 kDa, in Lane 2 is evident. Thus no anti-carrier antibodies remained in the affinity purified anti-peptide antibody preparation. The anti-HSP antibodies (Figure 4.11B) and the anti-HSC antibodies (Figure 4.11C) recognized the respective peptide conjugate in a western blot but to visualize the reaction, a higher concentration of the anti-peptide antibodies (100μg/ml) was needed compared to the ELISA, which required only 10 μg/ml.

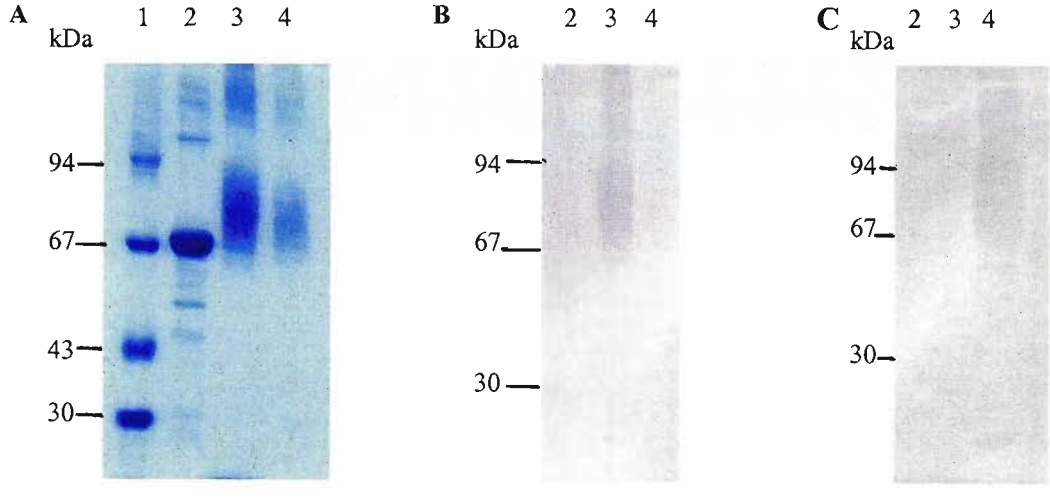

Figure 4.11 Evaluation of the affinity purification of the anti-peptide antibodies by western blotting. (A) Non-reducing SDS-PAGE of rabbit albumin and the peptide conjugates. The non-reduced samples were loaded onto a 12.5% Laemmli gel and stained with Coomassie brilliant blue. Lane 1: Pharmacia molecular mass markers; Lane 2: Rabbit albumin; Lane 3: HSP-peptide conjugated to rabbit albumin; Lane 4: HSC-peptide conjugated to rabbit albumin. After electrophoresis the proteins were electroblotted onto nitrocellulose and probed with **(B)** 100 μg/ml anti-HSP peptide antibody and **(C)** 100 μg/ml anti-HSC peptide antibody. Binding was visualised with goat anti-chicken IgY horseradish peroxidase antibody.

Both the anti-HSP antibodies and the anti-HSC antibodies (Figure 4.12) recognized the native heat shock proteins present in lymphocyte preparations. There is no visible difference on the SDS-PAGE gel between cells incubated at 37°C (Lane 1, Figure 4.12A) or 44°C (Lane 2; Figure 4.12A) for 2 h, although there are many bands present at different sizes (Figure 4.12A). In order to visualize any changes in the expression of heat shock proteins under stress conditions, SDS-PAGE is insufficient and inconclusive. However, western blotting and the use of specific antibodies, such as affinity-purified anti-peptide antibodies is likely to give information about the changes in expression.

The anti-HSP peptide antibody recognised approximately 10 proteins, in both the cells incubated at 37°C (Lane 1) or 44°C (Lane 2). The heat shock protein 70 band is present at 70 kDa in both Lane 1 and Lane 2 at the same intensity, which seems to indicate there is no change or increase in the expression of HSP70 under stress conditions (Figure 4.12B). The band present at 33 kDa is very intense and broad, which may be as a result of HSP70 being cleaved between the ATPase domain and the peptide binding domain by cathepsin D (Sehorn *et al.*, 2002). To determine if this is a possible explanation, a protease inhibitor cocktail can be incorporated with the cells prior to lysis. The anti-HSC antibodies only detected two proteins (Figure 4.12C), although both were present in the cells incubated at 37°C (Lane 1) and 44°C (Lane 2). The protein band at 70 kDa, is most likely heat shock cognate protein 70, but the protein of 100 kDa that was recognised is unknown. There are two possible explanations, the anti-peptide antibodies recognise a continuous epitope in a protein present in human lymphocytes that has not been sequenced yet or it may be another heat shock protein at 100 kDa.

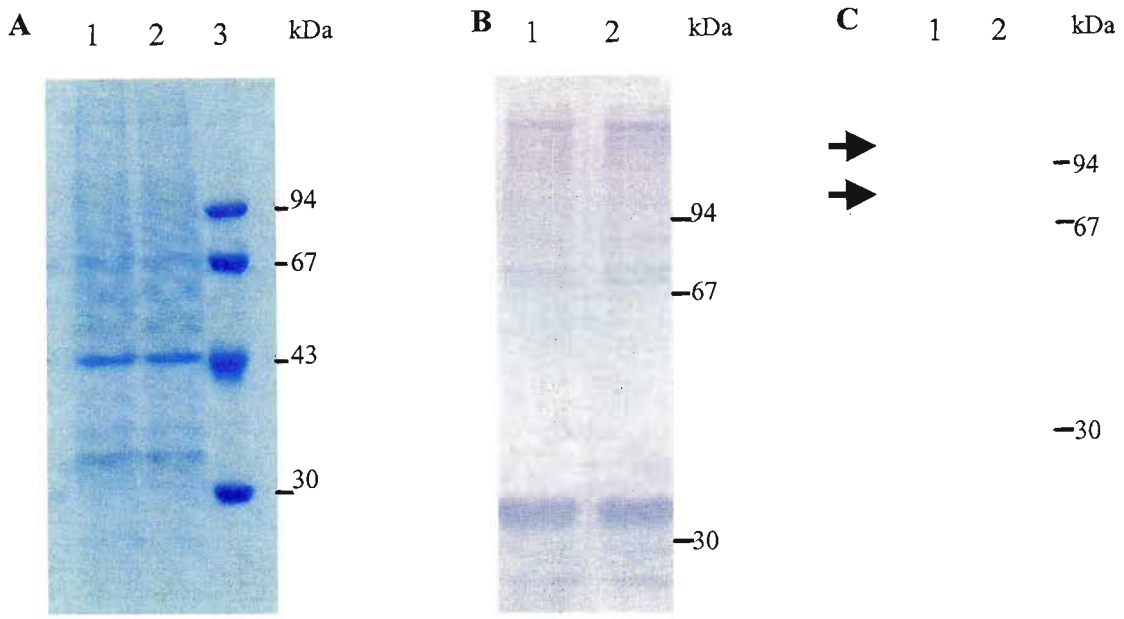

Figure 4.12 Detection of human heat shock proteins present in lymphocyte lysates with anti-peptide antibodies. (A) Lymphocytes were isolated, incubated at either 37°C or heat shocked at 44°C for 2 h followed by lysing using reducing buffer and SDS (10%). The reduced samples were loaded onto a 12.5% reducing Laemmli SDS-PAGE gel and stained with Coomassie brilliant blue. Similar numbers of cells were loaded in each lane. Lane 1: Lysates of lymphocytes at 37°C; Lane 2: Lysates of lymphocytes at 44°C; Lane 3: Pharmacia molecular mass markers. After electrophoresis, proteins were electroblotted onto nitrocellulose and probed with **(B)** 25 μg/ml anti-HSP peptide antibody and **(C)** 25 μg/ml anti-HSC peptide antibody. Binding was visualised with goat anti-chicken IgY horseradish peroxidase antibody. Arrows indicate position of bands recognized by anti-HSC peptide antibody.

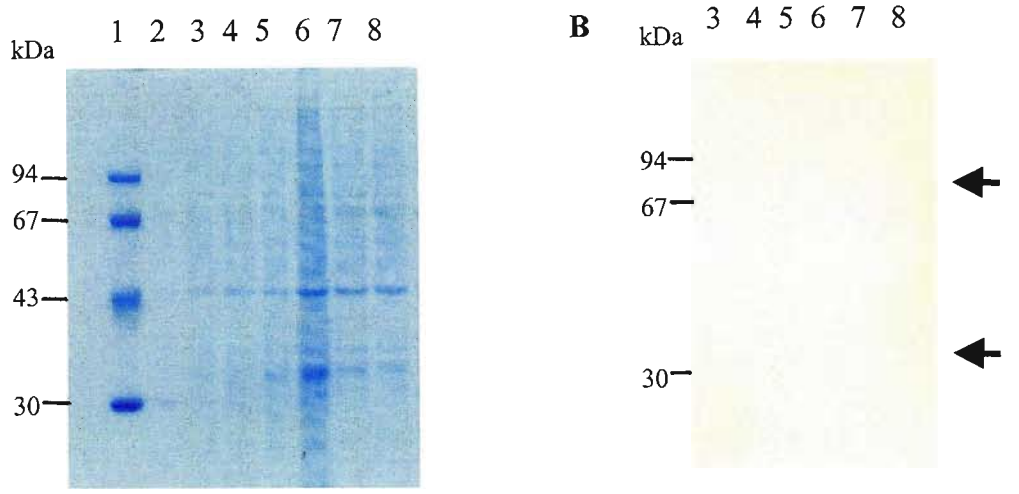

Figure 4.13 Detection of human heat shock proteins in lymphocyte lysates in the presence of protease inhibitors and monocyte lysates with anti-peptide antibodies. (A) Lymphocytes and monocytes were isolated, incubated at either 37°C or heat shocked at 44°C for 2 h followed by addition of a protease inhibitor cocktail to some samples and lysis of cells using reducing buffer and SDS (10%). The reduced samples were loaded onto a 12.5% reducing Laemmli SDS-PAGE gel and stained with Coomassie brilliant blue. Similar numbers of cells were loaded in each lane. Lane 1: Pharmacia molecular mass markers; Lane 2: Blank; Lane 3: Lysates of monocytes at 37°C; Lane 4: Lysates of monocytes at 44°C; Lane 5: Lysates of lymphocytes at 37°C; Lane 6: Lysates of lymphocytes at 44°C; Lane 7: Lysates of lymphocytes at 37°C with protease inhibitors; Lane 8: Lysates of lymphocytes at 44°C with protease inhibitors. **(B)** After electrophoresis the proteins were electroblotted onto nitrocellulose and probed with 25 μg/ml anti-HSP peptide antibody. Arrows indicate position of bands recognized by anti-HSP peptide antibody.

Monocyte lysates from cells incubated at 37°C (Lane 3; Figure 4.13B) and 44°C (Lane 4; Figure 4.13B) that do not have protease inhibitors, have insufficient protein when undiluted to be visualized on a Coomassie stained SDS-PAGE gel (Figure 4.13A) or to be detected by the anti-HSP antibodies on a western blot (Figure 4.13B). The lymphocyte lysates in Lanes 5 and 6, showed many bands as in Figure 4.12A, The anti-HSP antibodies detected the same two prominent bands as in Figure 4,12B, those being the HSP70 band at 70 kDa and the large

intense band at 33 kDa. There appears to be no difference in the intensity of the bands between the cells incubated at 37°C and 44°C.

The cells that were lysed in the presence of the inhibitor cocktail again had the same number of bands (Lanes 7 and 8; Figure 4.13B), but, although the 33 kDa band was present it appears to be thinner and less intense. In contrast the 70 kDa band is slightly more intense than in Lanes 5 and 6. There is again no difference between the cells incubated at 37°C and 44°C, even in the presence of inhibitors. The inhibitors may have inhibited some of the proteases as the intensity of the 33 kDa band has evidently decreased, thus in future experiments a higher concentration of pepstatin A may be required to inhibit the potential cathepsin D cleavage of HSP70.

During the selection of the peptides, similarity searches indicated that canine HSP70 and HSC70 are 100% similar to human HSP70 and HSC70 respectively. As canine cells were used for the X-ray microanalysis study, the possibility that the anti-human HSP70 peptide antibodies recognized canine HSP70 was determined. Analysis of canine lymphocytes, lysed in the presence of inhibitors (Lanes 1 and 2; Figure 4.14A) indicated no difference between the banding patterns at 37°C or 44°C. The same is true when the blots were probed with the anti-HSP antibodies; there were bands at 70 kDa and 33 kDa in both Lanes 1 and 2 (Figure 4.14B). These bands are the same as those encountered in the human lymphocyte lysates in Figures 4.12 and 4.13. The anti-HSC antibody detected two bands in both lanes containing canine lymphocyte lysates, one at 70 kDa and 100 kDa (Figure 4.14C), which again correspond to the bands seen in human lymphocyte lysates in Figure 4.12.

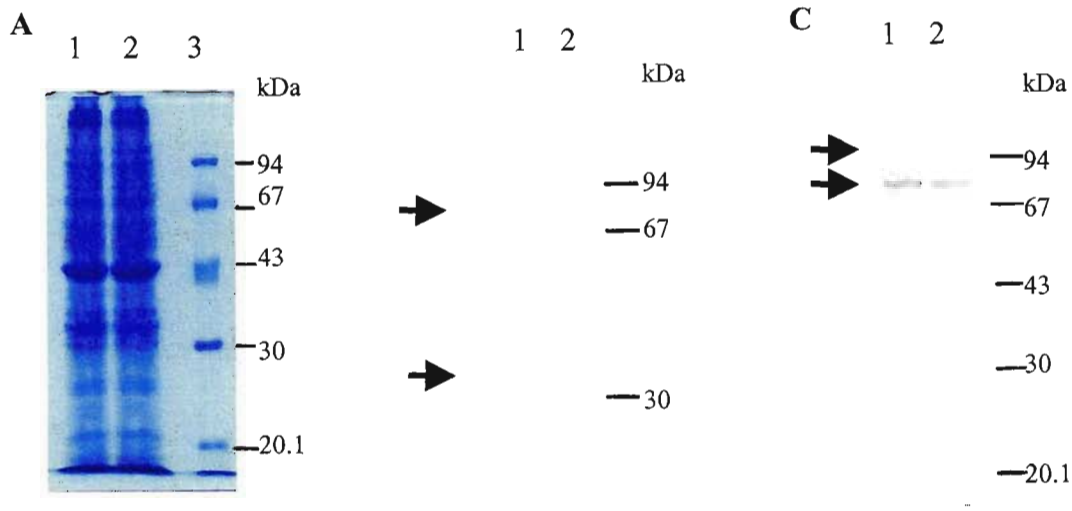

Figure 4.14 Detection of canine heat shock proteins in lymphocyte lysates with anti-peptide antibodies. (A) Lymphocytes were isolated, incubated at either 37°C or heat shocked at 44°C for 2 h followed by addition of an protease inhibitor cocktail and lysing of cells using reducing buffer and SDS (10%). The reduced samples were loaded onto a 12.5% reducing Laemmli SDS-PAGE gel and stained with Coomassie brilliant blue. Similar numbers of cells were loaded in each lane. Lane 1: Lysates of canine lymphocytes at 37°C; Lane 2: Lysates of canine lymphocytes at 44°C; Lane 3: Pharmacia molecular mass markers. After electrophoresis the proteins were electroblotted onto nitrocellulose and probed with 25 μg/ml anti-HSP peptide antibody **(B)** or 25 μg/ml anti-HSC peptide antibody **(C)**. Arrows indicate position of bands recognized by the anti-HSP peptide **(B)** antibody and the anti-HSC peptide antibody **(C)**.

4.4 DISCUSSION

When an organism is exposed to elevated temperatures it responds by rapidly expressing highly conserved proteins, known as heat shock proteins. The heat shock response is universal, occurring in every cell and species from eubacteria to humans (Lindquist, 1986). It is widely hypothesized that the purpose of the heat shock response is to protect the organism from the toxic effects of heat and other forms of stress. There are many other inducers of heat shock proteins, these include ethanol, sodium arsenite, cadmium, anaerobiosis, zinc, copper, mercury, sulfyryl reagents, calcium ionophores, steroids, chelating agents, glucosamine,

deoxyglucose and oxidative injury (Lindquist, 1986). The presence of the malaria parasite and its by-products in the bloodstream and in monocyte phagocytic vesicles induces fever and ultimately the expression of HSPs (Clerget & Polla, 1990). It has previously been mentioned that the heat shock proteins are unable to inhibit the production of phospholipase A_2 in malaria, whereas in most other situations the HSPs inhibit PLA_2 expression. Increased levels of phospholipase A_2 are associated with severe malaria (Vadas *et al.*, 1993).

HSP70 is the most highly conserved of the heat shock proteins, with the similarity between human HSP70 and the *Drosophila* protein being 73%. The majority of the differences can be accounted for by homologous substitutions (Lindquist, 1986). The antibody response to the malarial HSP70 proteins is mainly directed toward the non-conserved epitopes (Shinnick, 1991). However, human and monkey immune sera contain antibodies that recognize amino acid sequences conserved between *P. falciparum* and human HSP70 (Mattei *et al.*, 1989; Richman *et al.*, 1989). Pathogenic microorganisms can elicit a humoral and cellular response to epitopes shared with the hosts; this immunoreactivity may play a role in pathogenicity and in autoimmune consequences of infection (Shinnick, 1991; Winfield and Jarjour, 1991; Maresca and Kobayashi, 1994). To elicit an immune response in immunized chickens it was considered more appropriate to design and use synthetic peptides rather than utilizing the whole protein.

The sequences of human HSP70 and human HSC70 were aligned so that the regions where the amino acids are least conserved could be determined (Figure 4.1). One of the peptide selection criteria was that there be as little similarity between the alternative protein as possible, thus when the antibodies were produced the anti-HSP70 antibody would not recognize the HSC70 protein and *vice versa*. The C-terminal domains of the two proteins appeared to be the least conserved, which is also further confirmed by this region of HSP70 being reported to contain a variable peptide-binding domain (Feige and Polla, 1994). An alternative reason for using the C-terminus was that the commercially available anti-HSP70 monoclonal antibodies from Stressgen (www.stressgen.com) were produced against the region of amino acids 436 – 640, which is the C-terminal domain of HSP70.

The entire protein sequence was analysed using the Predict7 programme (Càrmenes *et al.*, 1989) to predict the location of epitopes. Thus HSP70 and HSC70 were analysed in terms of hydrophilicity (Hopp and Woods, 1981), surface probability (Emini *et* al., 1985; Janin *et* al., 1978), flexibility (Karplus and Schulz, 1985) and antigenicity (Welling *et* al., 1985). The C-terminus of both proteins contained regions with high peaks for the four selection criteria (Figure 4.2A; Figure 4.3A). From the predictions obtained for the whole proteins, smaller amino acid regions (Figure 4.2B; Figure 4.3B) and ultimately peptides (Figure 4.2C; Figure 4.3C) were selected. Individually, the peptide selection criteria are insufficient to determine epitopes suitable for eliciting an immune response in chickens. However, the combination of selecting regions of high hydrophilicity, surface probability, flexibility and antigenicity are a good indicator for predicting immunogenic peptides.

It has been observed that the locations of epitopes on the native protein also correspond to areas of high sequence variability i.e. low similarity (Van Regenmortel *et al.*, 1988). The regions selected, based on the Predict7 programme, were further analysed using similarity searches, to avoid cross reactivity with other proteins such as HSC70 in the case of anti-HSP70 peptide antibodies. Ultimately two peptides were selected because they showed relatively low similarity with the chicken proteins. Based on these percentage similarities the HSP peptide is most likely to elicit the better immune response. Since the peptides were able to elicit an immune response and the isolated antibodies recognized the native proteins in human and canine lymphocyte lysates, the criteria used to select the peptides were successful.

The three dimensional structure of HSP70 (Figure 4.4), suggests that the selected peptides are on the surface of the protein. More precisely, they are on the α-helix that lines the exterior of the peptide-binding groove of the variable substrate recognition domain (Feige and Polla, 1994). Thus the probability that the antibodies produced against the HSP70 and HSC70 peptides will be able to recognize the respective native proteins is high.

As discussed previously, chickens were used for the production of the anti-peptide antibodies. The immunization of the chickens with the HSP-rabbit albumin conjugate was successful and both chickens laid eggs until the collection of eggs was terminated. In the case of the three

chickens immunized with the HSC-rabbit albumin conjugate, the immunization was successful in one chicken but the other two chickens died.

The average yield of IgY isolated from eggs was 20.48 mg/ml, which corresponded to 45 mg per egg. Goldring and Coetzer (2003) routinely isolate 60 mg per egg, the difference in the amount of antibodies isolated depends on numerous factors influencing the chickens. SDS-PAGE was used to confirm the purity of the IgY isolated (Figure 4.5). The removal of proteins by each step in the isolation procedure is clearly visible until two major bands remain in the final pellet. These two bands are the heavy and the light chain of IgY. A number of minor bands were present in the final pellet, these are the different reduced forms of IgY as confirmed by Goldring and Coetzer (2003) using a western blot. The isolation of IgY was successful as there was a high yield and the antibodies were relatively pure.

ELISAs were used to monitor the antibody production in chickens by titrating test antibodies against the respective free peptide, HSP or HSC, coated as antigen. The antibodies raised against the peptides conjugated to rabbit albumin bound well to the free peptides. The antibodies raised against the HSP-rabbit albumin conjugate, bound well to the free HSP peptide (Figure 4.6). There were differences in the response of the antibodies from the different chickens with HSP chicken 1 having a higher titre than HSP chicken 2. The antibodies produced against the HSC-rabbit albumin conjugate bound well to the free HSC peptide (Figure 4.7).

The anti-carrier antibody titres for all the immunized chickens fluctuated from the first immunization till the termination of egg collection (Figure 4.8). The ELISA confirmed that the chickens immunized with the peptide-rabbit albumin conjugate made antibodies against both the peptide and the rabbit albumin. Of interest is that chicken immunized with the HSC-rabbit albumin conjugate produced higher titre anti-carrier antibodies than the two chickens immunized with the HSP conjugate. However, the reverse was true for the anti-peptide antibodies. Previously it was thought that the HSP peptide might elicit the better immune response, based on the percentage similarities between the human derived peptides and the chicken proteins. However, it would require a larger number of chickens to determine the

statistical relevance of the data presented, thus it is premature to draw any conclusions about the immunogenic performances of the peptides.

The isolated IgY contained both antibodies against the peptides and the carrier. The anti-peptide antibodies were purified from the anti-carrier antibodies and the remaining pool of polyclonal antibodies by affinity purification. The anti-HSP and anti-HSC antibodies showed similar elution profiles (Figure 4.9), however the yields of anti-peptide antibodies obtained were different. This difference is most likely due to differences exhibited by individual chickens. An ELISA was performed to confirm the affinity purification of the anti-peptide antibodies was successful (Figure 4.10). Both the anti-HSP and anti-HSC affinity purified antibodies showed similar trends. As expected the affinity purified antibodies had higher specific titres than the unpurified antibody pool. A minor portion of anti-peptide antibodies remained in the unbound affinity matrix eluant. As yields of antibodies were high it was not necessary to repeat the affinity purification. A western blot confirmed that the affinity purified anti-peptide antibodies no longer contained anti-carrier antibodies (Figure 4.11).

There appeared to be no visible difference in the protein banding between the human or canine lymphocytes incubated at 37°C or at 44°C, whether the lysates were in the presence of protease inhibitors (Figure 4.13A; Figure 4.14A) or not (Figure 4.12A). It was expected that HSP70 expression would not occur at 37°C (Lindquist, 1986). However, in the western blot HSP70 was expressed at both 37°C and 44°C, and there was no apparent difference in the levels of expression. There may be many reasons why cells produce HSP70 at 37°C. The isolation of lymphocytes using the hypertonic density centrifugation method of by Boyum (1968) subjects the cells to physical stress, which results in spontaneous PGE_2 and IL-1 production (Thiem *et al.*, 1988). Cytokine production can induce intracellular HSP70 expression in peripheral blood mononuclear cells (Njemini *et al.*, 2002). HSP70 may also be stimulated by serum (Wu *et al.*, 1986). Since HSP70 expression has been induced at 37°C, it is suggested that an alternative isolation procedure be investigated. However, adherence should not be used as monocytes isolated by using this method are subject to transient activation (Fincato *et* al., 1991; Hall, 1994; De Almeida *et al.*, 2000) because adherence represents an activation signal (Njemini *et al.*, 2002). Clerget and Polla (1990) have shown

that activation of monocytes induces the expression of HSP70 and Njemini *et al.* (2002) found a significant increase in the production level of HSP70 by adherent cells incubated at 37°C. From western blots the possibility that the anti-HSP antibody may be cross-reacting with the HSC70 in those lysates cannot be ruled out. Pure HSC70 and HSP70 were not available at the time, to determine the level of cross-reactivity.

The anti-HSP antibodies recognized two major bands, one at 70 kDa and one at 33 kDa, in all lymphocyte lysates examined irrespective of incubation temperature, the presence or absence of protease inhibitors, or whether the blood was human or canine (Figure 4.12B; 4.13B and 4.14B). As has been mentioned before HSPs have relatively stable characteristic breakdown products, with HSP70 being reduced to doublets of 40 kDa and 22 kDa by proteolysis (Lindquist, 1986). As previously mentioned Sehorn *et al.* (2002) found that the cleavage of DnaK, by cathepsin D yielded fragments of the C-terminal binding domain with molecular weights greater than 20 kDa. The protein band of 33 kDa may be the result of HSP70 being cleaved between the ATPase domain and the peptide binding domain by cathepsin D. The HSP peptide was derived from the C-terminal domain of human HSP70, so the antibodies would recognize these cleavage products. There are a number of lighter bands that are greater than 20 kDa with the largest being 33 kDa. The anti-HSP antibodies recognized the native protein at 70 kDa. There were also a number of lighter bands in the region greater than 100 kDa, but the identity of these proteins was not confirmed.

The only major difference between the uninhibited and the protease inhibited lymphocyte lysates was the intensity of the bands, thus indicating there may have been partial inhibition of proteolysis. If cathepsin D, a ubiquitous aspartic protease that has an operating pH of 2.8 – 5.0 and a pI of 5.5 – 6.5 (Pillay *et al.*, 2002), was in fact cleaving the HSP70 then using an inhibitor cocktail containing a higher concentration of the cathepsin D inhibitor, pepstatin A, would likely lead to recognition of the 70 kDa protein by the anti-HSP antibodies. Although it appears that the inhibitor cocktail did not inhibit the action of proteases on the HSPs, this may be due to the cells being activated for a long period of time, and the natural breakdown of HSPs by the cell may already be underway. Thus as the inhibitors were added to the cell lysates the cellular cleavage products of HSP70 are likely to have been present.

The anti-HSC antibodies recognized two proteins in both the 37°C and 44°C lysates of human (Figure 4.12C) and canine lymphocytes (Figure 4.14C). One was 70 kDa, which was most likely HSC70, and the other was a band of 100 kDa which, as in the case of the anti-HSP blot, may be a related protein.

It was previously noted that there was 100% similarity between the human derived heat shock protein peptides and the same sequence in canine HSP70 and HSC70, thus both the anti-peptide antibodies should, and did, recognize any protein with the respective peptide sequences. Lindquist (1986) found that a monoclonal antibody produced against *Drosophila* HSP70, reacted with 70 kDa proteins found in *Drosophila*, sea urchins, nematodes, chickens and humans.

Further investigations into the difference in expression of HSP70 and HSC70 at 37°C or 44°C could be done using ^{35}S-methionine or [H]^{3}-amino acid labelling. Western blots could be made more sensitive using a chemiluminescent detection method. Alternatively, the expression of HSP70 mRNA in the cells of interest could be determined using northern blot analysis (Fincato *et* al., 1991). To determine the degree of cross-reactivity between the anti-peptide antibodies and HSP70 or HSC70, it would be necessary to obtain pure HSP70 and HSC70 to be used in ELISAs or competitive assays using western blots.

In summary, the anti-peptide antibodies raised recognized both the free peptide and an appropriate protein of 70 kDa in cell lysates.

CHAPTER 5

ELECTRON PROBE X-RAY MICROANALYSIS OF CANINE MONOCYTES

5.1 INTRODUCTION

Electron probe X-ray microanalysis (EPXMA) is a technique that enables determination of the elemental composition of a specimen (Warley, 1997). When the electron beam interacts with the specimen, X-rays are generated and these carry information about the elemental composition of the cell. The advantages of EPXMA are the simultaneous detection of elements, analysis at the individual cell level and the intracellular localization of elements. This technique is also unique in the fact that it combines the ability to undertake chemical analysis with the high resolution of the electron microscope, hence one is able to correlate chemical information with the ultrastructural aspect (Warley, 1997). As mentioned before, Warley *et al.* (1994) state that this is an ideal method for measuring elemental concentrations, elemental fluxes and for studying the effects of drugs on a given cell type. Elemental profiles of the monocytes may give insights into the mechanisms of action of each drug. Monocytes were incubated with therapeutic concentrations of the drugs, thus the results can be correlated to clinical observations (Goldring and Nemaorani, 1999). Incubations with the drugs were stopped after 0 min, 10 min and 18 h. The 10 min time point used in the present study was chosen as Warley *et al.* (1994) found changes in elemental concentrations occur almost immediately, and the 18 h time point was utilised, as anti-malarial drugs were found to modulate the expression of monocyte surface receptors after 18 h (Goldring and Nemaorani, 1999). Air-drying was used, so although the specimen's structure is disrupted, the total elemental content of the cell can still be measured (Warley, 1997).

5.2 ELEMENTAL PROFILES OF CANINE MONOCYTES INCUBATED WITH ANTI-MALARIAL DRUGS

Monocytes were incubated with therapeutic concentrations of the eight anti-malarial drugs: quinine, chloroquine, primaquine, artemisinin, pyrimethamine, tetracycline, doxycycline and dapsone and suramin, a trypanocidal drug. Figure 5.1 shows a spectrum of a canine monocyte

incubated in medium only, this spectrum is representative of all the control spectra obtained. The peaks visible are Na, P, S, Cl, K, Ca and Au. The Au peak is from the grid and the remaining elements are from the monocyte. It should be noted that a spectrum only shows the number of counts obtained for each element and thus is qualitative data. Quantitative data is obtained by using correction factors and removing the background as mentioned in Sections 2.6.9).

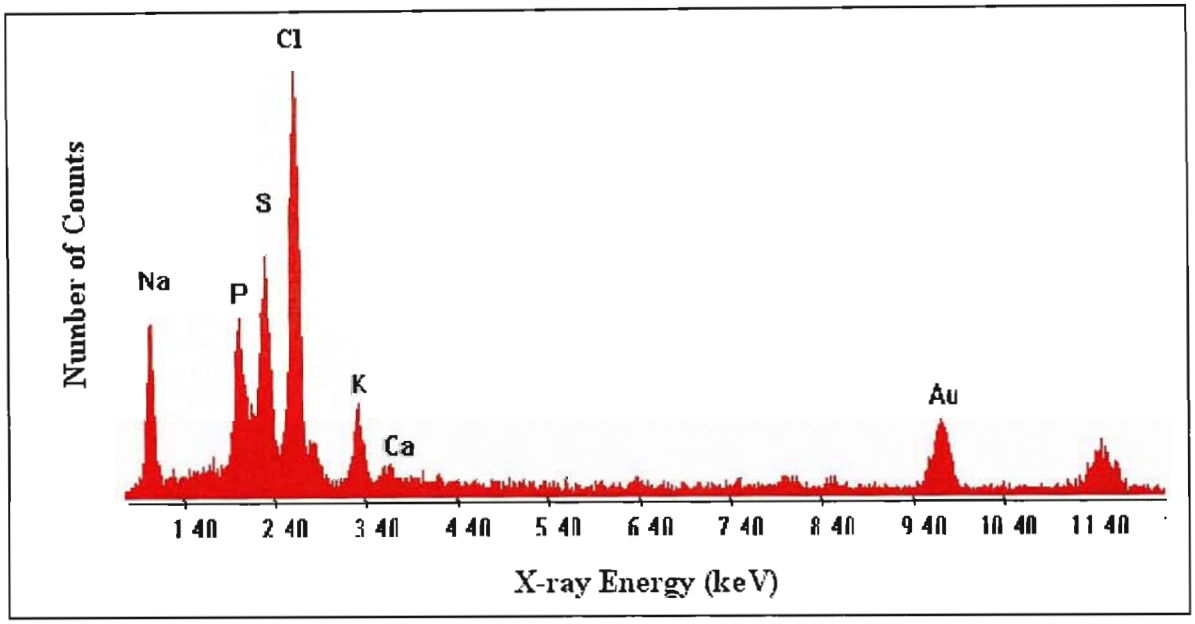

Figure 5.1 A typical elemental X-ray spectrum produced by EPXMA of canine monocytes. Canine monocytes were allowed to adhere to gold electron microscope grids. The grids were removed from the medium, washed and airdried. Spectra were obtained in a Philips CM120 transmission electron microscope equipped with an EDAX detector.

5.2.1 Elemental profiles of canine monocytes incubated with chloroquine, primaquine, tetracycline, dapsone and pyrimethamine

Chloroquine, primaquine, tetracycline, doxycycline and dapsone have been grouped together due to similarities in the elemental profiles, but it must be noted that the profiles are unique for each drug (Figure 5.2). There was no significant difference in the concentration of Na after 10 min incubation with chloroquine, primaquine, tetracycline, pyrimethamine and dapsone (Figure 5.2A; B; C; D and E; $P>0.05$). Between 10 min and 18 h there is a large increase in

Na for all the drugs, which is statistically significant. Chloroquine, tetracycline and pyrimethamine did not significantly affect the Mg concentration at either of the two time points (Figure 5.2A; C and D; P>0.05). Primaquine induces a significant decrease in the Mg concentration between 10 min and 18 h (Figure 5.2B; P>0.05). There was a significant increase in the Mg concentration after 18 h incubation with dapsone (Figure 5.2E; P>0.05).

There was a significant increase in the P concentration after 10 min incubation with chloroquine (Figure 5.2A; P>0.05). Primaquine and pyrimethamine do not alter the P concentration after 10 min, but after 18 h the concentration was significantly decreased below that of the control in the monocytes incubated with chloroquine, primaquine and pyrimethamine (Figure 5.2A; B and D; P>0.05). Tetracycline and dapsone did not significantly alter the P concentration at any time point (Figure 5.2 C and E; P>0.05).

The concentration of S remains constant after 10 min incubation with chloroquine, primaquine, pyrimethamine and dapsone (Figure 5.2A; B; D and E; P>0.05), but there is a significant decrease upon incubation with tetracycline (Figure 5.2C; P>0.05). After 18 h incubation with all five drugs there is a significant increase in the concentration of S (Figure 5.2; P>0.05).

There was no significant difference in the concentrations of Cl after 10 min incubation with primaquine, tetracycline, pyrimethamine and dapsone (Figure 5.2 B; C; D and E; P>0.05), but there is a significant increase upon incubation with chloroquine, (Figure 5.2A; P>0.05). After 18 h incubation with all five drugs there is a significant increase in the concentration of Cl (Figure 5.2; P>0.05).

The K concentration remains constant after 10 min of incubation of monocytes with chloroquine, primaquine, tetracycline and dapsone (Figure 5.2A; B; C; E; P>0.05). There was a significant decrease in the K concentration after 10 min incubation with pyrimethamine (Figure 5.2D; P>0.05). Monocytes incubated with tetracycline and dapsone after 18 h showed a significant decrease in the K concentration (Figure 5.2C and E; P>0.05). The cells incubated with chloroquine for 18 h showed a significant increase in the concentration of K.

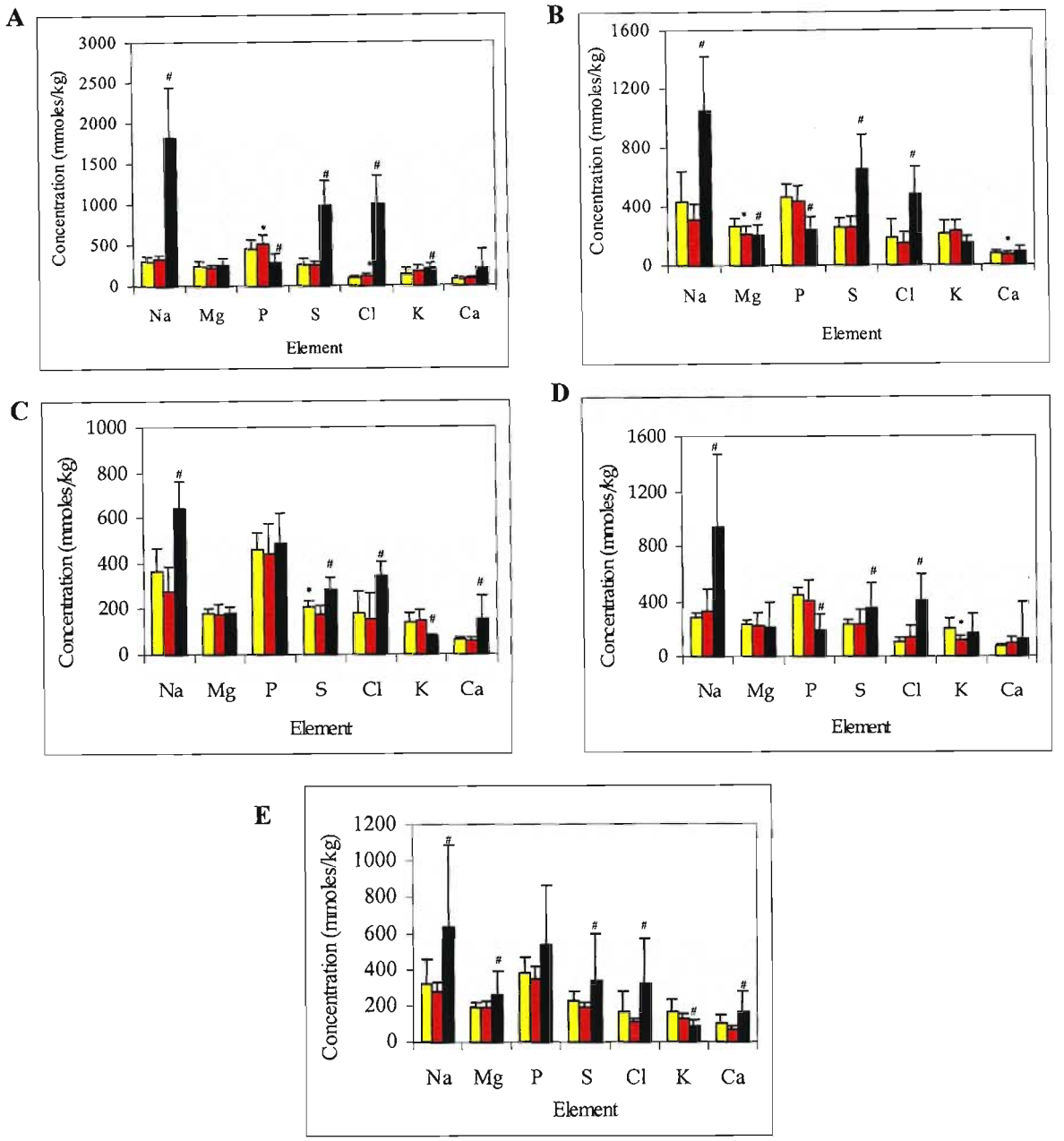

Figure 5.2 Elemental composition of canine monocytes incubated with chloroquine, primaquine, tetracycline, pyrimethamine and dapsone. Canine monocytes on gold electron microscope grids were incubated with therapeutic concentrations of (**A**) chloroquine, (**B**) primaquine, (**C**) tetracycline, and (**D**) pyrimethamine and (**E**) dapsone. The grids were removed, washed and airdried after 0 min (■), 10 min (■) and 18 h (■). Analysis took place in a Philips CM120 transmission electron microscope equipped with an EDAX detector. Spectra were obtained and the concentrations determined using the continuum method. The significant difference was determined using the Mann-Whitney U-test ($P>0.05$; statistical difference between 0 min and 10 min* or 18 h#). Bars represent the standard error of the mean

There was no significant difference in the Ca concentration of cells incubated with chloroquine and pyrimethamine for any length of time (Figure 5.2A and D; P>0.05). The Ca concentration was unaffected after 10 min of exposure to tetracycline and dapsone (Figure 5.2 C and E; P>0.05). There was a significant decrease in the Ca concentration in cells incubated with primaquine. Tetracycline and dapsone induced a significant increase in the concentration of Ca after 18 h. (Figure 5.2C and E; P>0.05).

All the drugs mentioned increased the concentrations of Na, S, and Cl. Differences between the drugs are seen in their effects on Mg, P, K and Ca. Chloroquine is the only drug to decrease P and increase K. Primaquine and pyrimethamine both decrease P. Primaquine was the only drug to decrease Mg and Ca. Tetracycline and dapsone have no effect on P but decrease K and increase Ca. Dapsone increases Mg concentrations. Thus even though these dugs appear to alter the elemental profiles in a similar way, each drug induces individual alterations in unique ways.

5.2.2 Elemental profiles of canine monocytes incubated with quinine and artemisinin

Artemisinin (Figure 5.3A) and quinine (Figure 5.3B) appear to influence the majority of the elemental concentrations determined, in a similar manner. The concentrations of Na, S and Cl at 10 min are significantly decreased in monocytes incubated with both drugs. After 18 h the concentrations of the Na and Cl are significant increased upon incubation with artemisinin (Figure 5.3A; P>0.05) but are unaffected by quinine (Figure 5.3B; P>0.05). The concentration of S returns to the levels of the control. There is a significant increase in the Mg concentrations after 10 min but no significant difference after 18 h in the case of both drugs. The P concentration is unaffected by the presence of artemisinin at 10 min and 18 h (Figure 5.3A; P>0.05). Quinine brings about a significant increase in the P concentration at 10 min. (Figure 5.3B; P>0.05). Artemisinin significantly increased the concentration of K at 10 min, the concentration decreases significantly to levels below that of the control after 18 h (Figure 5.3A; P>0.05). Quinine causes a significant decrease in the K concentration within 10 min, but the concentration was at pre-incubation levels after 18 h (Figure 5.3B; P>0.05).

Artemisinin had no significant effect on the concentration of Ca at any time point studied, whereas quinine induced a significant increase after 18 h (Figure 5.3; P>0.05).

Although these two drugs have completely different structures they seem to influence the concentrations of certain elements in canine monocytes in a similar manner. Both drugs significant decrease the concentrations of Na, S and Cl after 10 min and significantly increase the concentration of Mg after 10 min. With respect to P, K and Ca they influence the concentrations in of the drugs in different ways.

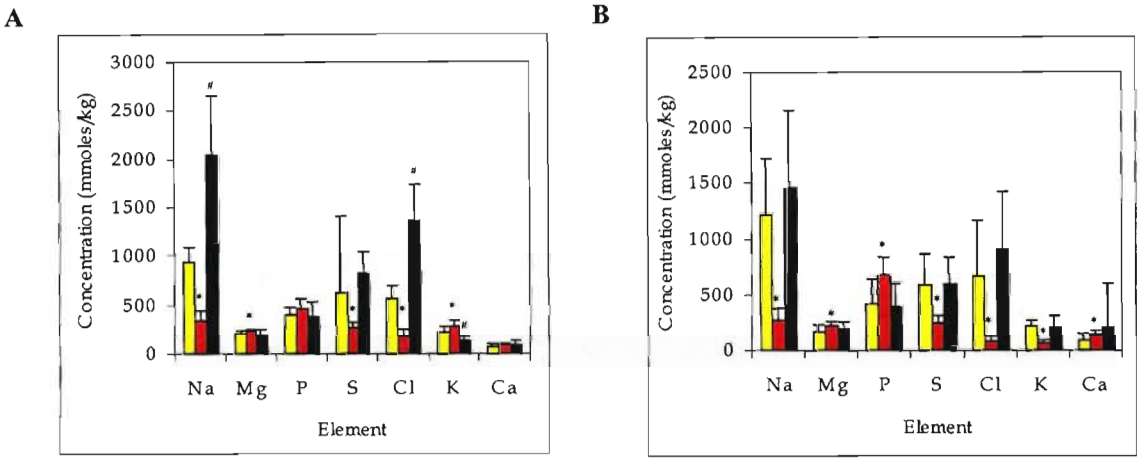

Figure 5.3 Elemental composition of canine monocytes incubated with artemisinin and quinine. Canine monocytes on gold electron microscope grids were incubated with therapeutic concentrations of (**A**) artemisinin and (**B**) quinine. The grids were removed, washed and airdried after 0 min (■), 10 min (■) and 18 h (■). Analysis took place in a Philips CM120 transmission electron microscope equipped with an EDAX detector. Spectra were obtained and the concentrations determined using the continuum method. The significant difference was determined using the Mann-Whitney U-test (P>0.05; statistical difference between 0 min and 10 min* or 18 h#). Error bars represent the standard error of the mean.

The monocytes incubated with quinine were subjected to a high concentration of DMSO. Thus to determine if DMSO contributed to the elemental concentration changes, the monocytes were incubated with DMSO at the same concentration. The elemental profiles observed for DMSO was very different to that observed in the monocytes incubated with quinine (data not

shown). The concentrations of Na, P, S, Cl and K were unaltered after 10 min but significantly decreased after 18 h. The concentration of Mg was not affected at all by DMSO. Ca concentrations decreased significantly after 10 min and increased to pre-control levels after 18 h. Quinine altered the concentrations of elements after only 10 min whereas DMSO altered the concentrations after 18 h. It is most likely that quinine overrides elemental changes induced by the DMSO.

5.2.3 Elemental profiles of canine monocytes incubated with doxycycline

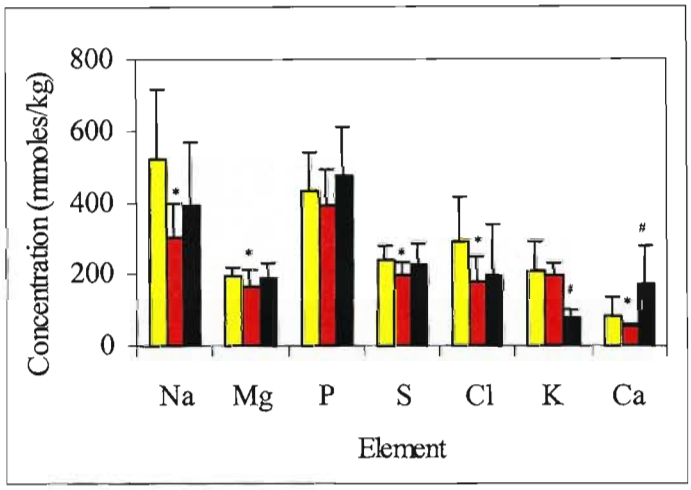

Figure 5.4 Elemental composition of canine monocytes incubated with doxycycline. Canine monocytes on gold electron microscope grids were incubated with therapeutic concentrations of doxycycline. The grids were removed, washed and airdried after 0 min (■), 10 min (■) and 18 h (■). Analysis took place in a Philips CM120 transmission electron microscope equipped with an EDAX detector. Spectra were obtained and the concentrations determined using the continuum method. The significant difference was determined using the Mann-Whitney U-test ($P>0.05$; statistical difference between 0 min and 10 min* or 18 h#). Error bars represent the standard error of the mean.

Doxycycline is unique amongst the anti-malarial drugs tested and produced unique alterations in monocyte elemental concentrations (Figure 5.4). Doxycycline significantly decreased the concentrations of Na, Mg, S and Cl at 10 min, the concentrations increased at 18 h to the

levels of the controls (Figure 5.4; P>0.05). The concentration of P is not significantly altered at any time points measured. The concentraion of K remains constant after 10 min but significantly decreases after 18 h. Doxycycline significantly decreased the concentration of Ca at 10 min, the concentration significantly increased at 18 h to levels higher than the control (Figure 5.4; P>0.05). The major difference between the trends seen for doxycycline and the drugs previously mentioned in Figures 5.2 and 5.3, is at 10 min the elemental concentration of Na, S, Cl and Ca was decreased, and the [Ca] increased after 18 h.

5.2.4 Elemental profiles of canine monocytes incubated with suramin

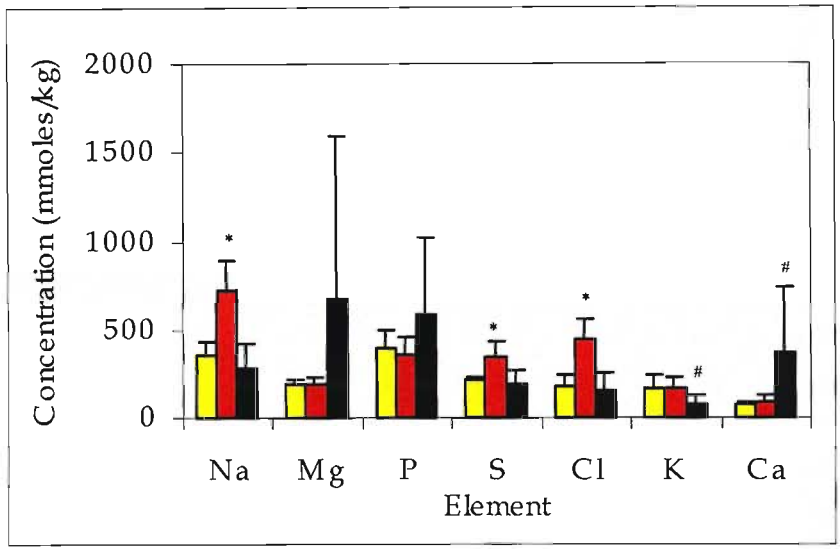

Figure 5.5 Elemental composition of canine monocytes incubated with suramin. Canine monocytes on gold electron microscope grids were incubated with therapeutic concentrations of suramin. The grids were removed, washed and airdried after 0 min (■), 10 min (■) and 18 h (■). Analysis took place in a Philips CM120 transmission electron microscope equipped with an EDAX detector. Spectra were obtained and the concentrations determined using the continuum method. The significant difference was determined using the Mann-Whitney U-test (P>0.05; statistical difference between 0 min and 10 min* or 18 h#). Error bars represent the standard error of the mean.

Suramin causes a significant increase in the concentrations of Na, S and Cl after 10 min, but after 18 h the concentrations return to pre-control levels (Figure 5.5; P>0.05). There is no

significant difference in the concentrations of Mg and P for the time points measured. In the case of K, the concentration remains constant until 10 min and thereafter it decreased significantly. There is a significant increase in the concentration of Ca after 18 h. The profile of this trypanocidal drug is different to any of the anti-malarial drugs previously discussed in this chapter.

5.2.5 Summary

This is a brief summary pointing out the similar effects of drugs on the individual elements (Table 5.1). The relevance of these effects will be discussed later at the end of the chapter (Section 5.6). All the drugs altered the concentrations of sodium significantly (Table 5.1). However, there were differences in the time when the changes occurred and whether there was an increase or a decrease. Suramin was the only drug that increased the concentration of Na after 10 min (Figure 5.5), where as chloroquine, primaquine, tetracycline, pyrimethamine, dapsone (Figure 5.2) and artemisinin (Figure 5.3A) increased the concentration after 18 h. The concentration of Na was decreased by artemisinin, quinine (Figure 5.3) and doxycycline (Figure 5.4) after 10 min. It was interesting to note that artemisinin decreased the concentration of Na rapidly but after 18 h the concentration was increased above that of the control. Artemisinin was the only drug to induce two changes in the Na concentration at the two time points measured with respect to the control.

The concentration of Mg was affected by a few drugs (Table 5.1). Artemisinin and quinine increased the concentration after 10 min (Figure 5.3), whereas only dapsone increased the concentration after 18 h (Figure 5.2E). Doxycycline (Figure 5.4) decreased the concentration immediately and primaquine (Figure 5.2B) decreased the concentration after 10 min and 18 h, suggesting that the Mg concentration stays at a lowered level for the full 18 h.

Table 5.1 Anti-malarial drugs inducing significant alterations in elemental concentrations in canine monocytes. Drugs inducing different effects at 10 min and 18 h[#] (P>0.05); drugs inducing similar effects at 10 min and 18 h* (P>0.05).

Element	Time	Increase	Decrease
Na	10 min	Suramin	Artemisinin[#] Quinine Doxycycline
	18 h	Chloroquine Primaquine Tetracycline Pyrimethamine Dapsone Artemisinin[#]	
Mg	10 min	Artemisinin Quinine	Primaquine* Doxycycline
	18 h	Dapsone	Primaquine*
P	10 min	Chloroquine[#] Quinine	
	18 h		Chloroquine[#] Primaquine Pyrimethamine
S	10 min	Suramin	Tetracycline[#] Artemisinin Quinine Doxycycline
	18 h	Chloroquine Primaquine Tetracycline[#] Pyrimethamine Dapsone	
Cl	10 min	Chloroquine* Suramin	Artemisinin[#] Quinine Doxycycline
	18 h	Chloroquine* Primaquine Tetracycline Pyrimethamine Dapsone Artemisinin[#]	
K	10 min	Artemisinin[#]	Pyrimethamine Quinine
	18 h	Chloroquine	Tetracycline Dapsone Artemisinin[#] Doxycycline Suramin
Ca	10 min	Quinine	Primaquine Doxycycline[#]
	18 h	Tetracycline Dapsone Doxycycline[#] Suramin	

In Table 5.1 the concentration of P was increased by chloroquine (Figure 5.2A) and quinine (Figure 5.3B) immediately, but after 18 h the concentration was decreased by chloroquine, primaquine and pyrimethamine (Figure 5.2A; B and D). It was interesting to note that chloroquine increased the concentration of P after 10 min but after 18 h the concentration was decreased below control levels.

Suramin (Figure 5.5) was the only drug that increased the concentration of S rapidly (Table 5.1), however after 18 h the concentration was increased by chloroquine, primaquine, tetracycline, pyrimethamine and dapsone (Figure 5.1). Tetracycline (Figure 5.2C), artemisinin, quinine (Figure 5.3) and doxycycline (Figure 5.4) decreased the concentration of S after 10 min. Tetracycline had a dual effect by decreasing the concentration after 10 min and then increasing it above control levels after 18 h.

The chlorine concentration was increased after 10 min by chloroquine (Figure 5.2A) and suramin (Figure 5.5), and after 18 h by chloroquine, primaquine, tetracycline, pyrimethamine, dapsone (Figure 5.2) and artemisinin (Figure 5.3A). Chloroquine induced what appears to be a permanent increase in the Cl concentration, this may be due to the presence of a chlorine group in the structure but it is premature to draw any conclusions. Artemisinin, quinine (Figure 5.3) and doxycycline (Figure 5.4) decreased the Cl concentration after 10 min. Artemisinin again shows a dual effect where after 10 min it induces a decrease but after 18 h it causes an increase of the Cl concentration above the control level (Table 5.1).

Potassium was increased in concentration after 10 min by artemisinin (Figure 5.3A) and after 18 h by chloroquine (Figure 5.2A). Pyrimethamine (Figure 5.2D) and quinine (Figure 5.3B) decreased the concentration of K immediately, where as tetracycline, dapsone (Figure 5.2 C and E), artemisinin (Figure 5.3A), doxycycline (Figure 5.4) and suramin (Figure 5.5). Again artemisinin induced a dual effect by increasing the K concentration after 10 min and then decreasing it with respect to the control after 18 h.

Quinine (Figure 5.3B) increased the concentration of calcium after 10 min and after 18 h, tetracycline, dapsone (Figure 5.2 C and E), doxycycline (Figure 5.4) and suramin (Figure 5.5)

increased the concentration. The concentration was decreased after 10 min by primaquine (Figure 5.2B) and doxycycline (Figure 5.4). In this case doxycycline induced a dual effect on the Ca concentration, by decreasing it after 10 min and increasing it after 18 h.

The reported dual effects (Table 5.1) are interesting and unexpected, especially where at one time point the concentration of the element is decreased significantly below the control and then after 18 h the concentration is increased above the control, or *vice versa*. Artemisinin is interesting in that it affects three elements in this dual manner: Na and Cl with a decrease after 10 min and an increase after 18 h, and K where the opposite happens. Tetracycline and doxycycline also exhibit dual effects on S and Ca respectively i.e. decrease after 10 min and increase after 18 h. Chloroquine exhibits two types of dual effect: P is increased after 10 min and decreased after 18 h; and Cl is increased over both time points. Primaquine decreases the Mg concentration at both time points measured.

An interesting occurrence to note is all of the elemental concentrations altered by quinine occurred after 10 min, thereafter the concentrations returned to normal levels. Dapsone induced its effects after 18 h on all the elements where the concentrations were altered. All the other drugs measured altered the concentrations of elements at both 10 min and 18 h. All the drugs used in this study induced both increases and decreases in the elemental concentrations.

As important as the increases and decreases in the elemental concentrations may be, the drugs that do not induce any effect on specific elements may also be important (Table 5.2). Mg concentration was unaltered by chloroquine, tetracycline, pyrimethamine (Figure 5.2A, C and D) and suramin (Figure 5.5). Tetracycline, dapsone (Figure 5.2 C and E), artemisinin (Figure 5.3A), doxycycline (Figure 5.4) and suramin (Figure 5.5) did not alter the concentration of P in canine monocytes. The concentration of K was only unaffected by one drug, primaquine (Figure 5.2B). Calcium concentrations were unaltered by incubation of canine monocytes with chloroquine, pyrimethamine (Figure 5.2A and D) and artemisinin (Figure 5.3A).

Table 5.2 Anti-malarial drugs that do not induce significant alterations in elemental concentrations in canine monocytes.

Element	Drugs not altering concentration of element
Mg	Chloroquine Tetracycline Pyrimethamine Suramin
P	Tetracycline Dapsone Artemisinin Doxycycline Suramin
K	Primaquine
Ca	Chloroquine Pyrimethamine Artemisinin

It was interesting to note that although some of the drugs altered the concentrations of specific elements in a similar manner, none of the drugs altered the concentrations in the same way as any other drug. The similarities and the differences can most likely be accounted for by the similarities or differences in the structures of the drugs and their modes of action.

5.3 PHOSPHOROUS / POTASSIUM (P/K) RATIOS OF CANINE MONOCYTES INCUBATED WITH ANTI-MALARIAL DRUGS

Although the elemental profile gives a lot of information about the effects of the various drugs, the P/K ratios give information about fluxes within the cell, such as the opening and closing of K channels. K channels also maintain the [K] and exist in either a closed or open conformation depending on the voltage across the membrane (Karp, 1996). When the K channel opens, more than a million K ions can flow through in one second, thus changes in intracellular K concentration are extremely rapid. The opening of a small number of K channels impacts significantly on the electrical properties of the cell. There may be a variety of different K channels in a single cell that open and close in response to different voltages (Karp, 1996). P concentrations remain fairly constant in cells, as the majority of the element is present in DNA. However, this is not an infallible rule as there are proteins which contain P. The concentration is also dependent on the stage of the cell cycle, i.e. a cell undergoing division is likely to have a much higher concentration of P than a cell not dividing. In

comparison to all the other elements P is the best to use as a constant in a ratio (Skepper *et al.*, 1999).

5.3.1 P/K ratios of canine monocytes incubated with chloroquine and primaquine

The P/K ratios of cells incubated with chloroquine (Figure 5.6A) and primaquine (Figure 5.6B) are similar in profile. There is no significant difference (P>0.05) in the P/K ratios for both drugs after 10 min. However, after 18 h there is a significant decrease (P>0.05) in the P/K ratios of both drugs. The K concentration is increased with respect to the P concentration, which indicates the closing of K channels.

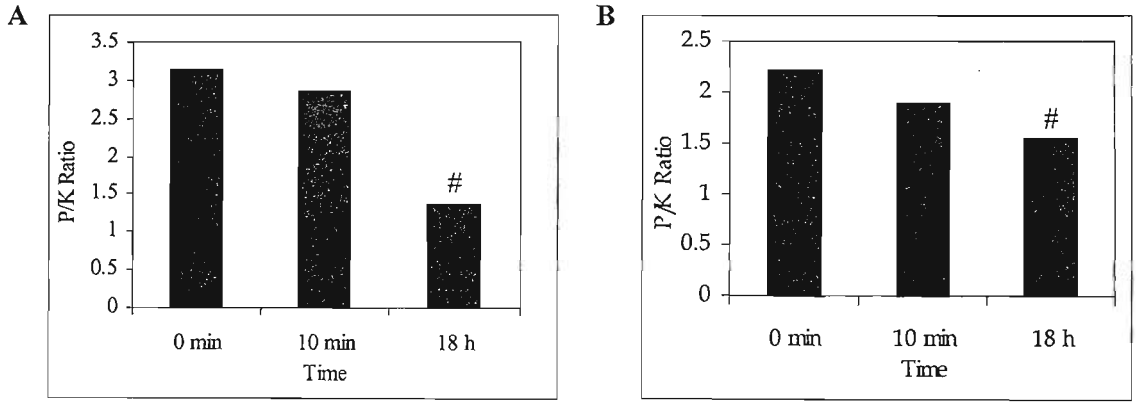

Figure 5.6 P/K ratios of canine monocytes incubated with chloroquine and primaquine. Canine monocytes on gold electron microscope grids were incubated with therapeutic concentrations of (**A**) chloroquine and (**B**) primaquine for 0 min, 10 min and 18 h. Once the spectra were obtained and the concentrations determined the P/K ratio was calculated. The significant difference was determined using the Mann-Whitney U-test (P>0.05; statistical difference between 0 min and 18 h#).

5.3.2 P/K ratios of canine monocytes incubated with tetracycline, doxycycline, artemisinin, suramin and dapsone

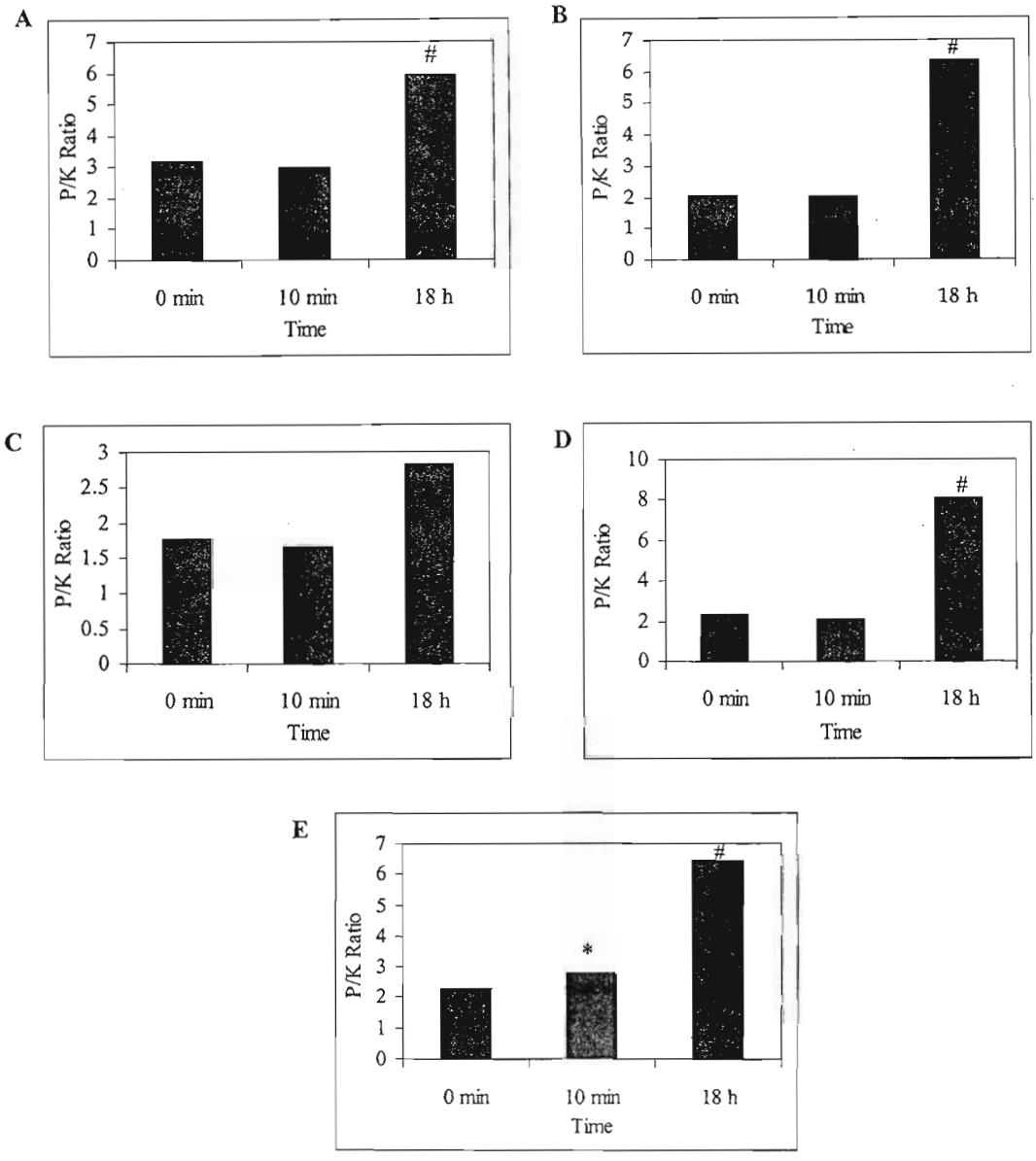

Figure 5.7 P/K ratios of canine monocytes incubated with tetracycline, doxycycline, artemisinin, suramin and dapsone. Canine monocytes on gold electron microscope grids were incubated with therapeutic concentrations of (**A**) tetracycline, (**B**) doxycycline, (**C**) artemisinin, (**D**) suramin and (**E**) dapsone for 0 min, 10 min and 18 h. Once the spectra were obtained and the concentrations determined the P/K ratio was calculated. The significant difference was determined using the Mann-Whitney U-test ($P>0.05$; statistical difference between 0 min and 10 min* or 18 h#).

The P/K ratios of tetracycline (Figure 5.7A), doxycycline (Figure 5.7B), artemisinin (Figure 5.7C), suramin (Figure 5.7D) and dapsone (Figure 5.7E) show a similar trend. After 10 min there is a significant increase in the P/K ratio of cells incubated with dapsone only (Figure 5.7D; P>0.05). After 18 h there is a significant increase in the P/K ratios of cells incubated with tetracycline, doxycycline, suramin and dapsone (Figure 5.7A; B; D and E; P>0.05). Although artemisinin appears to have a similar trend to the other four drugs, there is in fact no significant difference in the P/K ratios at both the time points studied. Thus K concentration was decreased with respect to the P concentration, which indicates the opening of K channels. The channels were open after 10 min and 18 h in cells incubated with dapsone, but opened only after 18 h in cells incubated with tetracycline, doxycycline and suramin. The only exception was artemisinin where the channels were unaffected.

5.3.3 P/K ratios of canine monocytes incubated with pyrimethamine

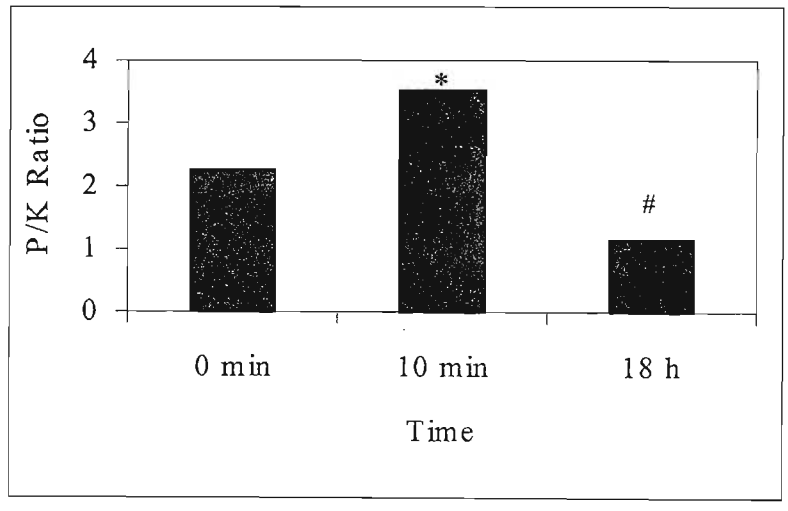

Figure 5.8 P/K ratios of canine monocytes incubated with pyrimethamine. Canine monocytes on gold electron microscope grids were incubated with therapeutic concentration of pyrimethamine for 0 min, 10 min and 18 h. Once the spectra were obtained and the concentrations determined the P/K ratio was calculated. The significant difference was determined using the Mann-Whitney U-test (P>0.05; statistical difference between 0 min and 10 min* or 18 h#).

The P/K ratios of monocytes incubated with pyrimethamine show a large fluctuation (Figure 5.8). After 10 min the P/K ratio was significantly increased (P>0.05), however after 18 h it had decreased significantly to below control values. In this case it is possible that after 10 min where the K concentration is decreased with respect to the P concentration, the K channels may be opening. But after 18 h the K channels may be closed as K is increased with respect to P.

5.3.4 P/K ratios of canine monocytes incubated with quinine

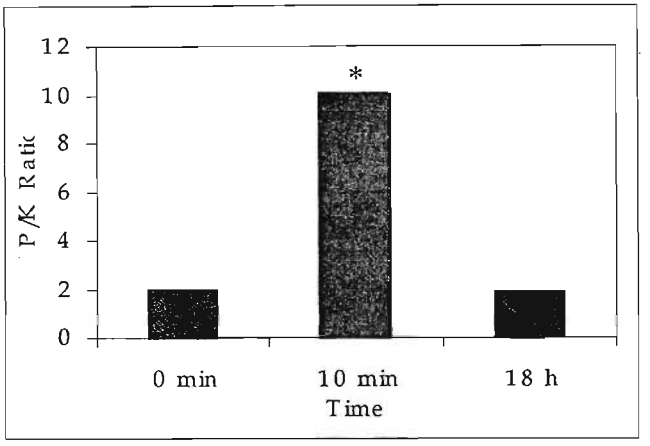

Figure 5.9 P/K ratios of canine monocytes incubated with quinine. Canine monocytes on gold electron microscope grids were incubated with therapeutic concentration of quinine for 0 min, 10 min and 18 h. Once the spectra were obtained and the concentrations determined the P/K ratio was calculated. The significant difference was determined using the Mann-Whitney U-test (P>0.05; statistical difference between 0 min and 10 min* or 18 h#).

Quinine (Figure 5.9) shows a profile similar to pyrimethamine (Figure 5.8) with the ratios after 10 min significantly elevated (P>0.05) to a ratio of 10.04. After 18 h the ratio has returned to pre-incubation levels. Thus after 10 min the K channels are opening, as [K] is decreased with respect to [P], but after 18 h the K channels have closed and returned to the normal state. Monocytes incubated with DMSO at the high concentration used to solubilize quinine, showed no significant difference in the P/K ratio after 10 min, but increased

significantly (P>0.05) to a ratio of 5.2 after 18 h. This indicates that a K channels was opening after 18 h. There were differences in the trends and the P/K ratio values where significant increases were observed in monocytes incubated with quinine and DMSO.

5.3.5 Summary

This is a brief summary pointing out the similar effects of drugs on the P/K ratios of canine monocytes (Table 5.3). The relevance of these effects will be discussed later at the end of the chapter (Section 5.6).

Table 5.3 Anti-malarial drugs inducing significant alterations in the P/K ratios of canine monocytes.

Time	Drugs inducing a	
	Increase (K channels opening)	**Decrease (K channels closing)**
10 min	Dapsone Pyrimethamine Quinine	
18 h	Tetracycline Doxycycline Suramin Dapsone	Chloroquine Primaquine Pyrimethamine

An increase in the P/K ratio i.e. the K concentration is decreased with respect to the P concentration indicates that K channels is opening and *vice versa*. The P/K ratios (Table 5.3) of canine monocytes were increased significantly above pre-incubation levels by dapsone (Figure 5.7E; P>0.05), pyrimethamine (Figure 5.8; P>0.05) and quinine (Figure 5.9; P>0.05) after 10 min and by tetracycline, doxycycline, suramin and dapsone (Figure 5.7 A, B, D and E; P>0.05). There was a significant decrease in the P/K ratios after 18 h, induced by chloroquine, primaquine (Figure 5.6; P>0.05) and pyrimethamine (Figure 5.8; P>0.05). Artemisinin (Figure 5.7C; P>0.05) had no effect at all on the P/K ratios of the canine monocytes at any of the time points measured. As noted in the elemental concentrations, there are also dual effects in the alterations of the P/K ratios. However, these dual effects are exerted by drugs that altered the elemental concentrations at one time point only. Dapsone increased the P/K ratio after 10 min and 18h. Pyrimethamine increased the P/K ratio after 10 min and then after 18 h decreased the ratio below the pre incubation levels.

5.4 ELECTRON PROBE X-RAY MICROANALYSIS OF PHAGOCYTICALLY ACTIVE CANINE MONOCYTES

Previous chapters have shown that the monocytes are phagocytically active with 72% and 70.5% phagocytosing latex beads and β-hematin respectively. Thus the chances that phagocytically active cells were analysed were high. β-Hematin has been shown to disrupt the normal functioning of human monocytes (Arese and Schwarzer, 1997) in an unknown way. EPXMA may unlock the mechanism of how β-hematin disrupts further phagocytic activity of monocytes.

5.4.1 Elemental profiles of canine monocytes that phagocytosed latex beads or β-hematin

Monocytes that have phagocytosed latex beads (Figure 5.10A) or β-hematin (Figure 5.10B) have different elemental profiles. Latex beads do not significantly alter the Na concentration at 10 min or after 18 h, whereas β-hematin causes a significant decrease in Na concentration after 10 min, followed by a return to control levels after 18 h. Mg concentration was significantly increased by latex beads after 10 min , but after 18 h the concentration returned to control levels. There was no significant difference in the concentration of Mg in cells phagocytosing β-hematin for 10 min but there was a significant increase after 18 h. Latex beads do not alter the P concentration at any of the time points used (Figure 5.10A; $P>0.05$). The P concentrations of monocytes after phagocytosis of β-hematin were significantly increased after 10 min and after 18 h. The S concentrations were not significantly affected by either latex bead or β-hematin phagocytosis. Cl concentrations remained within pre-incubation levels at 10 min and at 18 h after phagocytosis of latex beads. β-hematin induced a significant decrease in the Cl concentration at 10 min but after 18 h the concentration returned to control values (Figure 5.10B; $P>0.05$). Latex beads had no significant effect on the concentration of K at 10 min, but after 18 h there was a significant decrease in its concentration. β-hematin had no significant effect on the K concentration at all time points examined. The Ca concentration was unaffected after 10 min but after 18 h there was a significant increase in concentration in

cells phagocytosing latex beads and β-hematin. There are no similarities between the elemental profiles of monocytes that phagocytosed latex beads or β-hematin, with the exception of the effects on the concentration of Ca. The latex beads stimulate the normal processes that occur after phagocytosis, such as the generation of reactive oxygen intermediates, whereas β-hematin has a completely different effect on the elemental composition of the cell.

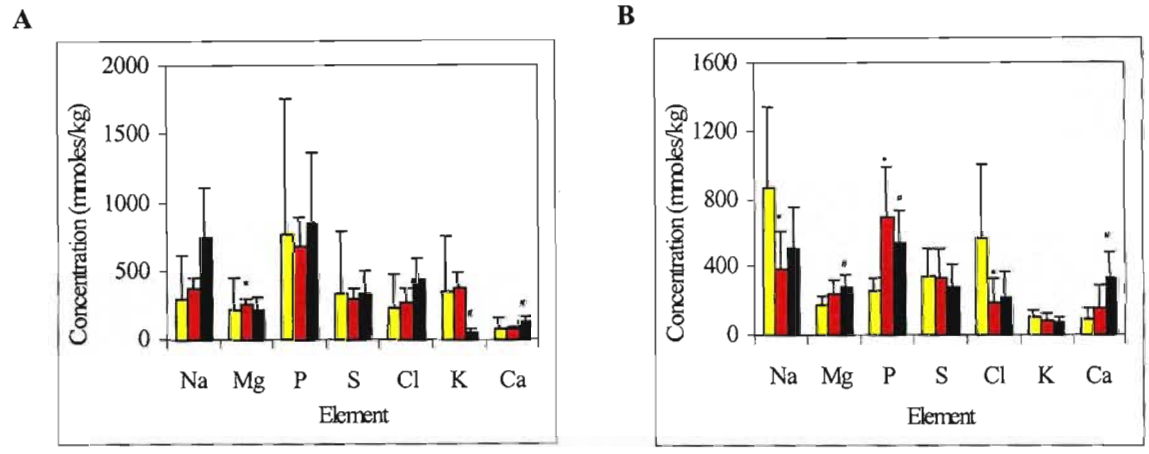

Figure 5.10 Elemental composition of canine monocytes that phagocytosed latex beads or β-hematin. Canine monocytes on gold electron microscope grids were allowed to phagocytose (**A**) latex beads and (**B**) β-hematin. The grids were removed, washed and air dried after 0 min (■), 10 min (■) and 18 h (■). Analysis took place in a Philips CM120 transmission electron microscope equipped with an EDAX detector. Spectra were obtained and the concentrations determined using the continuum method. The significant difference was determined using the Mann-Whitney U-test ($P>0.05$; statistical difference between 0 min and 10 min* or 18 h#). Error bars represent the standard error of the mean.

5.4.2 P/K ratios of canine monocytes that phagocytosed latex beads or β-hematin

After 10 min the P/K ratio of the monocytes that had phagocytosed latex beads was not significantly altered, but there was a significant increase in the ratio after 18 h (Figure 5.11A; $P>0.05$). This indicates that the K channels may be opening. In the case of β-hematin, the P/K ratio is significantly elevated above the control value after 10 min and after 18 (Figure

5.11B; P>0.05), indicating the opening of K channels after 10 min, and maybe after 18 h a small number of the K channels have closed. As was seen in the elemental profiles there is a difference between the P/K ratios of monocytes that had phagocytosed either latex beads or hemozoin. The only similarity that can be drawn between the two is that after 18 h the K channels appear to be fully open.

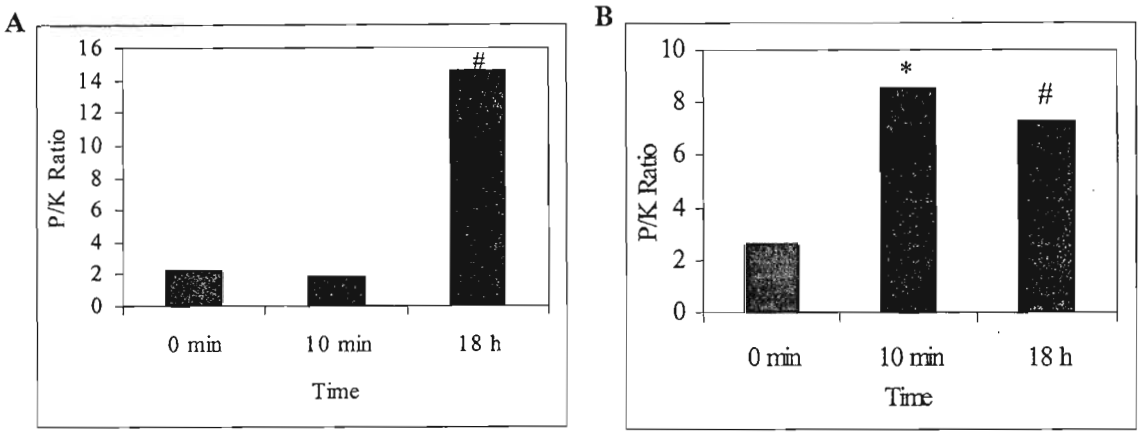

Figure 5.11 P/K ratios of canine monocytes that have phagocytosed latex beads and β-hematin. Canine monocytes on gold electron microscope grids were allowed to phagocytose (**A**) latex beads and (**B**) β-hematin. The grids were removed, washed and air dried after 0 min, 10 min and 18 h. Once the spectra were obtained and the concentrations determined the P/K ratio was calculated. The significant difference was determined using the Mann-Whitney U-test (P>0.05; statistical difference between 0 min and 10 min* or 18 h#).

5.4.3 Summary

When latex beads or β-hematin are phagocytosed they will activate the monocytes, but because of their physical characteristics the type of activation is likely to be different. In Table 5.4, the differences between the effects of the latex bead and β-hematin phagocytosis on the elemental concentrations are summarised. The only similarities are that both of these compounds increase the concentration of Ca after 18 h, and both have no effect on the concentration of S; all other effects are completely different. Na is only altered by β-hematin after 10 min. The concentration of Mg is increased after 10 min by latex beads and decreased

after 18 h with β-hematin. The P concentration was increased by β-hematin for the duration of the study. β-hematin decreased the concentration of Cl after 10 min and the latex beads decreased the concentration of K after 18 h. The P/K ratio of canine monocytes that have phagocytosed β-hematin were increased after 10 min and 18 h, where as the cells that phagocytosed latex beads, the P/K ratio was increased after 18 h only (Figure 5.11).

Table 5.4 Phagocytosis of latex beads or β-hematin inducing significant alterations in elemental concentrations in canine monocytes. Similar effect exerted by one condition* (P>0.05).

	Time	Elemental concentration significantly	
		Increased	**Decreased**
Latex Beads	10 min	Mg	
	18 h	Ca	K
β-Hematin	10 min	P*	Na Cl
	18 h	Mg P* Ca	

5.5 ELECTRON PROBE X-RAY MICROANALYSIS OF HEAT SHOCKED CANINE MONOCYTES

One of the symptoms of malaria is high fever. All living organisms have developed mechanism to deal with the stress of elevated temperatures, in fact as mentioned before the proteins involved are the most conserved proteins in animals. However, in the present study the proteins are not the focus but rather the question addressed was how does the elemental composition change between monocytes incubated at 37°C and those cells incubated under heat shock or stress conditions at 44°C?

5.5.1 Elemental profile of heat shocked canine monocytes

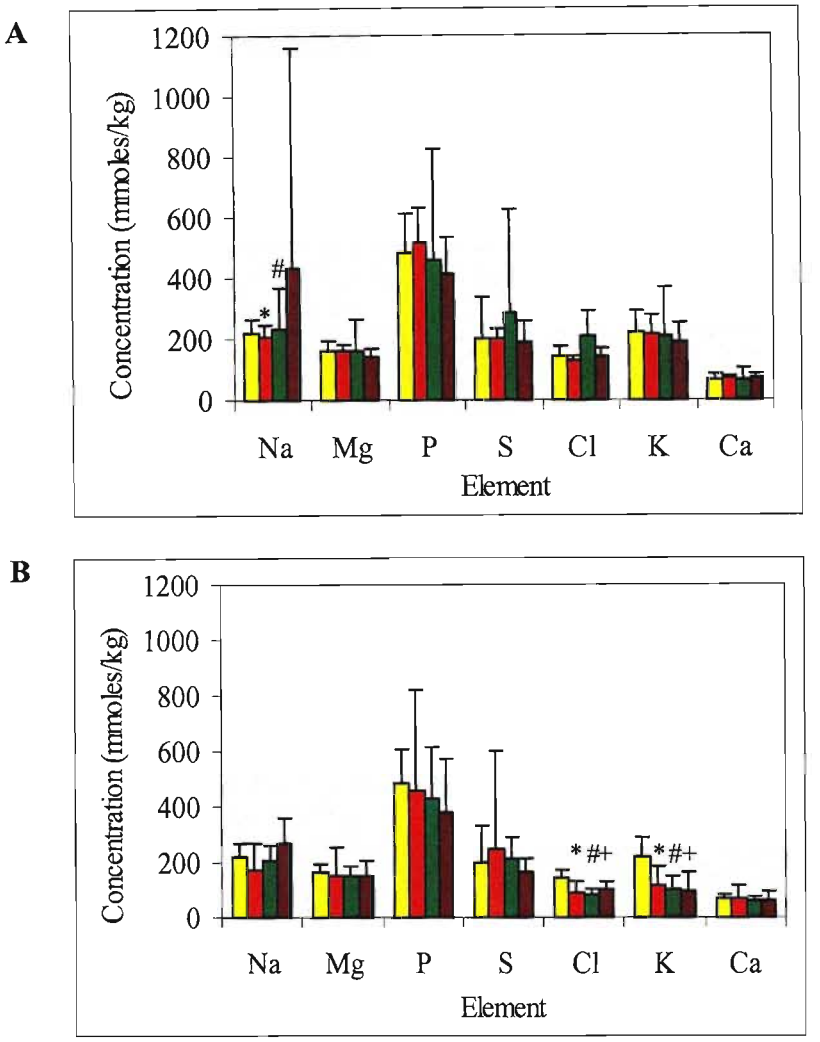

Figure 5.12 Elemental composition of canine monocytes incubated at 37°C or 44°C. Canine monocytes on gold electron microscope grids were incubated at (**A**) 37°C and (**B**) 44°C. The grids were removed, washed and air dried after 0 min (■), 10 min (■), 30 min (■) and 2 h (■). Analysis took place in a Philips CM120 transmission electron microscope equipped with an EDAX detector. Spectra were obtained and the concentrations determined using the continuum method. The significant difference was determined using the Mann-Whitney U-test ($P>0.05$; statistical difference between 0 min and 10 min*, 30 min# or 2 h+). Error bars represent the standard error of the mean.

As described in Chapter 4, the monocytes were incubated for 2 h and grids were removed after 0, 10 and 30 min, as well as 2 h. These incubation times are different from those used in the drug study as continued heat shock for 18 h would be ultimately detrimental to the integrity and viability of the cells. The Na concentration at 37°C (Figure 5.12A; P>0.05) was significantly decreased after 10 min but after 30 min there was a significant increase above the value of the control, the concentration then returned to normal levels after 2 h. The Na concentration was not affected, at any time by incubation at 44°C (Figure 5.12B; P>0.05).

Incubation at 37°C and 44°C at the times stipulated had no significant effect on the Mg, P, S and Ca concentration. The Cl and K concentrations were not significantly altered after incubation at 37°C for all the time points measured. The concentration of Cl and K after incubation at 44°C was significantly decreased below that of the control after 10 min and remained at the same concentration at 30 min and 2 h.

5.5.2 P/K ratios of heat shocked canine monocytes

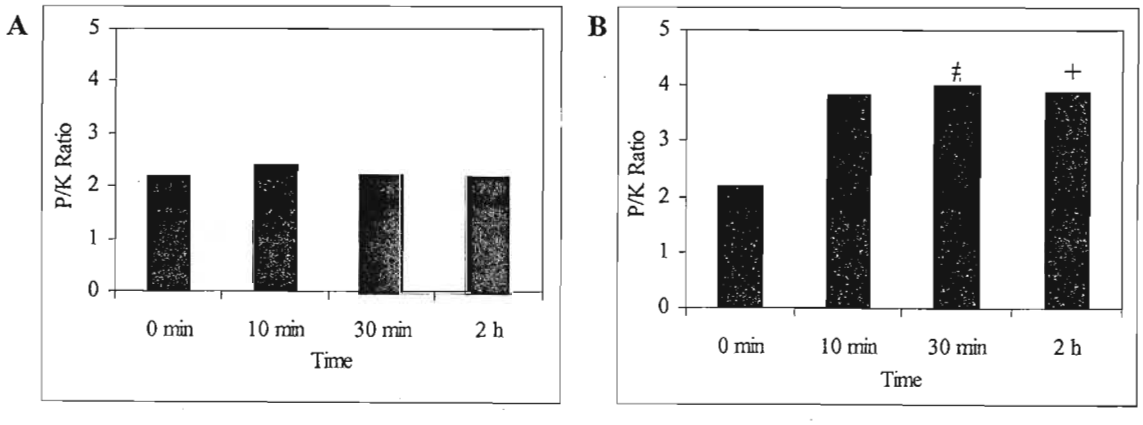

Figure 5.13 P/K ratios of canine monocytes incubated at 37°C or 44°C. Canine monocytes on gold electron microscope grids were incubated at (**A**) 37°C and (**B**) 44°C. The grids were removed, washed and air dried after 0 min, 10 min, 30 min and 2 h. Once the spectra were obtained and the concentrations determined the P/K ratio was calculated. The significant difference was determined using the Mann-Whitney U-test (P>0.05; statistical difference between 0 min and 10 min*, 30 min# or 2 h+).

Incubation at 37°C for all time points resulted in no significant difference in the P/K ratio (Figure 5.13A; P>0.05). The P/K values for the monocytes incubated at 44°C was not significantly altered after 10 min, but significantly increased after 30 min and 2 h (Figure 5.13B; P>0.05). Thus K channels have opened after 30 min and remained open for the 2 h. There is a difference between the P/K ratios of cells incubated at 37°C and 44°C after 30 min and 2 h.

5.5.3 Summary

The control cells incubated at 37°C exhibited a dual change in the concentration of Na; after 10 min the concentration was decreased but after 30 min the concentration was increased above that of the control. These effects at 37°C were unexpected. Incubation at 44°C did not alter the cells' Na concentration but, the concentrations of Cl and K were decreased for a the duration of the study. Mg, P, S and Ca concentrations were unaffected by incubation at 37°C or 44°C (Figure 5.12). The P/K ratios of the canine monocytes incubated at 37°C were unaltered for the duration of the study, whereas the ratios of the cells incubated at 44°C were increased after 30 min and 2 h (Figure 5.13).

5.6 DISCUSSION

There was very little difference between the spectra of human monocytes and canine monocytes (data not shown). However, the spectra of normal human monocytes obtained by Fishman *et al.* (1985) were different to the spectra obtained in this study (Figure 5.1). The discrepancies between the spectra are most likely due to the preparation techniques used, as in this study the monocytes were air dried whereas Fishman *et al.* (1985) fixed and embedded the cells in resin. It is likely that the spectra obtained in this study are more representative of the elemental concentrations in the monocyte as air-drying only removes the water whereas fixing and resin embedding would alter the elemental concentrations considerably.

Mammalian cells contain twenty different chemical elements, and the distribution of these elements is controlled by highly organised mechanisms (Williams and Fraústo da Silva, 2000). There are intense feedback mechanisms that maintain the distribution and the homeostasis of each element. The distribution of an element has two characteristics: one is the incorporation of the element in certain compounds (e.g. DNA) and the second is the disposition of the compound in different compartments (e.g. DNA in the nucleus) and parts of a cell or organism (Williams and Fraústo da Silva, 2000).

The major chemical elements in the cell are C, H, O and N. These elements form kinetically stable organic molecules such as proteins, fatty acids, polynucleotides and polysaccharides (Williams and Fraústo da Silva, 2000). In this study, however, these were not measured, as the X-rays emitted by these elements are below the detection limits of the beryllium window used.

The concentration of sulfur in canine monocytes in this study was altered by all the drugs tested but in different ways and at different times (Table 5.1). Monocytes phagocytosing latex beads and β-hematin, as well as those incubated at 37°C and 44°C, showed no alterations in the [S] at the time points studied. The distribution of S is described as 'peculiar' by Williams and Fraústo da Silva (2000). This element is dominantly situated in the metabolic pathways of all organisms such as the pathway of oxidative phosphorylation. Many coenzyme structures and activities are based on thiol (cysteine) and thioethers (methionine). The intracellular pool of methionine is low and carefully regulated, which is why S^{35}-methionine labelling is successful in determining the expression of new proteins. The extracellular saccharides of higher organisms contain sulphate. S is essential for the production of ATP by aerobic cellular respiration (Tortora and Grabowski, 2000). Bouchot *et al.* (1999) found an increase in the [S] in the nucleus of THP-1 cells infected with *Toxoplasma gondii*, which may be due to an increase in DNA transcription and protein synthesis. The increase in [S] brought about in this study by chloroquine, suramin, primaquine, tetracycline, pyrimethamine and dapsone, may be due to the same process. The relevance of and the reason for the decrease in the [S] brought about by tetracycline, artemisinin, quinine and doxycycline, is unknown in some instances as

is the reason why tetracycline induces a decrease in [S] at 10 min followed by an increase at 18 h.

Phosphorous exists in an organism in one oxidation state, phosphate. The distribution of P is in irreversible covalent compounds such as phospholipids, DNA, RNA and ATP (Tortora and Grabowski, 2000), which are connected to transcription factors and membrane pumps. It has been observed that the levels of nucleotide phosphates, e.g. ATP are fixed for a specific metabolic state of the cell. Williams and Fraústo da Silva (2000) mention that the distribution of P is extremely complex and influenced by numerous control mechanisms.

The [P] was increased by chloroquine and quinine at 10 min, and decreased by chloroquine, primaquine and pyrimethamine after 18 h (Table 5.1). Phagocytosis of β-hematin induced an increase in [P] at the time points studied (Table 5.4). Skepper *et al.* (1999) also observed unexpected changes in the [P], which they considered difficult to explain, but suggest that the fluctuations observed in [P] may be related to the cellular region analysed. These regions will contain both the cytoplasm and nucleoplasm, so any variations in the shape of the cell may alter the ratio of cytoplasm to nucleoplasm. However, this is unlikely to be the case in this study as not all the drugs examined altered the [P] and several cells were measured per experimental condition, statistically reducing this likelihood.

THP-1 cells infected with *Toxoplasma gondii* showed lower [P] in the nucleus than the uninfected cells (Bouchot *et al.*, 1999). Bouchot *et al.* (1999) mentions that the [P] may be correlated with phosphorylation of the nuclear components and this is most likely the reason for the changes in [P]. It is unknown why chloroquine initially triggers the cell in a way that decreases the [P], but after prolonged exposure there is a change in the cells response by increasing [P]. The cells that have phacogytosed β-hematin have increased [P] after 10 min and 18 h, suggesting that the β-hematin exerts both an immediate and a prolonged effect.

The majority of the elements studied cations (Na, Mg, K and Ca) but there are a few anions (Cl). These elements are handled by simple ionic transport processes and their distribution is directly related to the concentration of their respective free ions in equilibrium with the bound

forms. Concentrations of these elements in the extracellular and intracellular environments are generally uneven, which is directly related to the pumps, exchangers and channels which control them (Beames Jr., 1971; Eckert, 1988; Williams and Fraústo da Silva, 2000). Immediately after addition of the drugs to the monocytes, major fluctuations in the elemental concentrations may occur as a result of the pumps being activated. However, after 18 h of incubation the cells are likely to reach equilibrium, thus giving an indication as to the prolonged increases and decreases brought about by the drugs.

Sodium ions represent approximately 90% of the extracellular cations (Tortora and Grabowski, 2000). The most abundant cation in the intracellular fluid is K. Na/K ATPase actively maintains the concentrations of K and Na in the cell. The pump actively transports Na out of the cell and K into the cell to maintain a balance in the concentrations: because the ions are able to diffuse back across the membrane the pumps operate continually (Tortora and Grabowski, 2000). The sodium pumps are also responsible for maintaining normal cell volume. Glucocorticoids exert their effect by increasing the cell volume in U937 macrophages (Gamper *et al.*, 2000). The activation of Na conductance into the cell by osmotic shrinkage is thought to depolarise the cell membrane, which then facilitates the entry of Cl and ultimately increases the volume of the cell (Gamper *et al.*, 2000).

Cl ions are the most abundant extra cellular anions (Tortora and Grabowski, 2000). Fluxes in [Cl] have been implicated in apoptosis, where the CD95 receptor is triggered to activate an outwardly rectifying chloride channel (ORCC). The efflux of Cl in staurosporine-induced apoptosis activates Ced-3/ICE proteases (Fernández-Segura *et al.*, 1999). If the decrease in [Cl] brought about by incubation corresponded to cell death, then it would be expected that cells that show low levels after 10 min would show even lower levels after 18 h, but this was not the case. Artemisinin induced the opposite effect by producing high levels of Cl after 18 h, even though the [Cl] was low after 10 min. The [Cl] remains elevated after 10 min and 18 h incubation with chloroquine. This may just be due to the presence of the Cl in the structure of the drug, but a significant difference was noted between the [Cl] at 10 min and at 18 h which suggests that this is unlikely to be the case.

Decreases in [K] and [Cl] and increases in [Na] precede the appearance of apoptosis markers, but these changes were not associated with loss of membrane integrity (Fernández-Segura *et al.*, 1999; Skepper *et al.*, 1999). Warley (2002, pers. comm.*) found that K channels were activated early in apoptosis, while the exposure of apoptotic cells to high [K] attenuates apoptosis. K has been implicated in the activation of caspase-1 and caspase-3 (CPP32)-like proteases. The loss of K is crucial for the activation of endonucleases in intact cells, which are thought to be involved in phagocytosis. With regard to the drugs used in this study, none induced decreases in [K] and [Cl] or increases in [Na], suggesting that they did not induce apoptosis.

Nkamgueu *et al.* (2000) found that human monocytes challenged with microorganisms or alumina particles manifested an increase in [Na] and [Cl] and a decrease in [K]. Canine monocytes incubated with tetracycline, dapsone and artemisinin for 18 h showed similar results. β-Hematin induced an increase in [Na] and a decrease in [Cl] at all the time points measured, and had no effect on the [K]. The phagocytosis of latex beads induced a decrease in the [K] concentration after 18 h. Drugs induced similar effects, but the increases of [Na] and [Cl] and the decrease in [K] occurred at different time points. Suramin increased [Na] and [Cl] after 10 min, and decreased [K] after 18 h, whereas pyrimethamine increased [Na] and [Cl] after 18 h and decreased [K] after 10 min. Primaquine increased the concentrations of Na and Cl after 18 h, but had no effect on the concentration of K at any of the time points measured.

Artemisinin-treated malaria-infected red blood cells have lower [K] and [P], and higher [Na], in the early stage parasites than the late stage parasites. These effects are most likely due to the drug acting on membrane transport and phosphorous metabolism (Lee *et al.*, 1988). Unlike the infected red blood cells, canine monocytes incubated with artemisinin showed no significant change in the [P]. Chloroquine induces a decrease in [K] and an increase in [Na] in the late stage parasites (Lee *et al.*, 1988). In canine monocytes chloroquine increased the concentrations of Na, Cl and K. The [K] is decreased and the [Na] increased in red blood

* Dr A. Warley, Division of Physiology, United Medical and Dental Schools, St Thomas's Hospital Campus, Lambeth Palace Road, London, SE1 7EH, United Kingdom.

cells infected with late stage parasites, whereas the parasites have high [K] and low [Na] (Lee *et al.*, 1988). After 20 h of infection the [Na] decreased and the [K] increased in THP-1 cells infected with *Toxoplasma gondii* (Bouchot *et al.*, 1999). The only drug to induce high [K] and low [Na] in canine monocytes was artemisinin after 10 min.

Cells that are subjected to heat shock showed depressed levels of K and Cl at all time points measured. There are numerous changes in the physiology of a cell after heat shock (Welch *et al.*, 1991). These include alterations in the activity of the Na/K ATPase, thus altering the levels of intracellular Na and K (Welch *et al.*, 1991). There may be a role for K and K channels in heat shock. Separate activation of K and Cl transporters during heat shock, oxidative injury or other inducers of the stress response (Polla *et al.*, 1991).

Quinine decreased the concentrations of Na, Cl and K after 10 min, doxycycline decreased the concentrations of Na and Cl after 10 min, and K after 18 h. At present there is no literature available which describes any situations where the concentrations of Na, K and Cl are all depressed.

Skepper *et al.* (1999) mention that a small but significant fall in the [Na] of the control over the experimental period indicated a healthy Na/K ATPase mechanism and viable cells. The canine monocytes incubated at 37°C in this study showed decreased [Na] after 10 and 30 min. Adams and Hamilton (1992) noticed that with the addition of IFNγ to macrophages there was an immediate rise in the concentration of Na. IFNγ activates macrophages *in vivo* thus an immediate increase in the [Na] may indicate the activation of the cells. In this study suramin was the only drug to increase the [Na] immediately. Thus suramin may be activating the monocytes or inducing the secretion of IFNγ.

If the P/K ratio is close to unity in the control but significantly elevated or depressed on treatment with drugs, this indicates a relatively stable P contribution and a large contribution to the P/K ratio from changes in the K concentration (Skepper *et al.*, 1999). However, in the case of this study the P/K ratios of the controls were not close to unity but the majority had a ratio of 2, indicating that the [P] was not stable in the monocytes studied and further indicating

a contribution from both [K] and [P]. Until further studies are performed on normal canine monocytes to determine the normal P/K ratios, no conclusions can be made from these data. The canine monocyte P/K ratios in this study were increased by dapsone, pyrimethamine, quinine and β-hematin phagocytosis after 10 min, and by tetracycline, doxycycline, suramin, dapsone, β-hematin and latex bead phagocytosis after 18 h. The P/K ratios were decreased after 18 h by chloroquine, primaquine and pyrimethamine. It was interesting to note that cells incubated at 37°C and 44°C, and with artemisinin, showed no significant change in the P/K ratio at all the time points studied. β-hematin phagocytosis resulted in an elevated P/K ratio at both 10 min and 18 h, which indicated the opening of K channels. Pyrimethamine increased the P/K ratio after 10 min and then decreased it after 18 h, indicating the K channels were open and then closed. Quinine is able to block K channels in a concentration dependent manner from 50 to 200 μM (Maruyama *et al.*, 1994), which was much higher than the therapeutic concentration (15 μg/ml ≅ 40 μM) used in this study. Quinine appeared to induce the rapid opening of the K channels in this study, but after 18 h they appeared to be closing which may indicate that quinine is blocking the K channels.

In this study the concentration of Mg was increased by artemisinin, quinine and phagocytosis of latex bead after 10 min and after 18 h by dapsone and phagocytosis of β-hematin. A decrease was induced by doxycycline and primaquine after 10 min and primaquine after 18 h (Table 5.1). The concentration was unaltered by chloroquine, tetracycline, pyrimethamine and suramin (Table 5.2). Approximately 46% of all Mg ions occur in the intracellular fluid. Mg is able to bind directly to highly charged substances such as DNA, RNA, ATP, ADP, citrate and proteins, which is thought to affect the activity of the cell (Günther, 1990; Williams and Fraústo da Silva, 2000). Mg is found bound and free in the cytosol, nucleus, ribosomes, mitochondria and the cell membrane. When [Mg] is depleted, numerous cellular functions are altered such as glycolysis, respiration, DNA, RNA and protein synthesis (Günther, 1990). The intracellular [Mg] is tightly regulated, thus it is thought that it has a regulatory function in the cell (Maguire, 1990). Mg has been shown to be involved in the activation or inhibition of a number of enzymes, such as acetyl CoA synthetase, 5'-nucleotidase, phosphorylase kinase, phosphoribosyl pyrophosphate transferase, phosphoglucomutase, malic enzyme, Na/K ATPase, Ca ATPase, DNA polymerase, glutamine synthase, adenylate cyclase and channels

such as the Ca release channel and the inward rectifying K channel (Maguire, 1990). As mentioned for the other elements, little is known about the influences of increases and decreases in the concentration of Mg induced by the anti-malarial drugs in monocytes.

Ca has been studied by numerous groups because it is a secondary messenger and is involved in apoptosis. Ca exchanges rapidly across the cell membrane, but the concentration in the cytoplasm of cells remains low due to the activity of the Na/Ca antiporters (Tortora and Grabowski, 2000). The extracellular levels of Ca are thought to be linked to the level of phosphate and the pH (Williams and Fraústo da Silva, 2000). Calcium is a well-known secondary messenger; because its fast entry into the cell generates a novel and temporary state of the cell. The calcium messenger may act almost simultaneously on as many as 40 proteins, such as mechanical switches (troponins), membrane adjusters (annexins), transcription factors (calcineurin) and metabolic switches (calmodulins and S100) (Williams and Fraústo da Silva, 2000). Thus Ca acts as a coordinating agent for short durations in exited cells and as a homeostatic agent for longer alterations of state. In this study, elevated calcium levels were found in canine monocytes incubated with quinine after 10 min, and with tetracycline, dapsone, doxycycline, suramin, latex bead and β-hematin phagocytosis after 18 h. A decrease in the [Ca] was induced by primaquine and doxycycline after 10 min. The intracellular mobilization of Ca is essential for monocyte responses to chemotactic factors, which result in dose-dependent increases in the cytosolic Ca concentration (Verghese and Snyderman, 1989). Apoptosis is mediated primarily by the release of Ca into the cytosol (Karp, 1996). Doxycycline induced a dual effect by decreasing the [Ca] after 10 min and increasing it after 18 h.

The [Ca] was increased in canine monocytes after 18 h incubation with suramin. Suramin induces multiple effects on the homeostasis of Ca in cells (Emmick *et al.*, 1994). It induces Ca release from skeletal muscle sarcoplasmic reticulum vesicles in a concentration-dependent manner. Suramin inhibits the Ca-ATPase and the Ca release channel. Suramin has also been found to cause concentration-dependent inhibition of ADP-induced increases in [Ca] in platelets (Hall and Hourani, 1994). Serum calcium levels in human cancer patients are depleted after suramin administration (Walther *et al.*, 2000). The calcium concentration is

elevated in numerous cells by the presence of suramin, thus the canine monocytes incubated with suramin would be expected to show increased levels of Ca. In fact suramin increased the [Ca] substantially in this study and, of all the drugs to elevated the [Ca], suramin increased it the most. Thus the other drugs that elevate the [Ca] at the same time points as suramin may inhibit the Ca-ATPase and the Ca release channel but this could only be proven with further investigations. The [Ca] was unaltered in cells incubated with chloroquine, pyrimethamine and artemisinin.

Phagocytosed β-hematin affects monocyte functionality. Changes in the concentration of cytosolic Ca in macrophages have been measured using a calcium sensitive fluorescent dye. Hishikawa *et al.* (1991) found that, prior to phagocytosis of an IgG-coated latex bead, there is a dramatic rise in [Ca]. Calcium plays a major role in phagocytosis and is involved at different stages in the lead-up to the ingestion of the particle. Calcium is a prerequisite for the activation of *c-fos* expression, which is an important candidate for the induction of the heat shock response during phagocytosis (Donati *et al.*, 1991). The [Ca] was found to be elevated in cells phagocytosing latex beads and β-hematin after 18 h, but not after 10 min. Prior to phagocytosis there is likely to be an increase in [Ca] but after 10 min the majority of the particles have either been ingested or are attached to the monocyte, thus the [Ca] will have returned to normal. After 18 h, phagocytosis will be complete and the increase in [Ca] is most likely the result of the presence of the latex beads and the β-hematin in the phagosome. An early consequence of heat shock is a decrease in intracellular pH, reduced levels of ATP, and an increase in cytosolic Ca levels (Welch *et al.*, 1991). This change in [Ca] was not detected in this study. However, Polla *et al.* (1991) found no increase in the [Ca] in U937 cells during heat shock. The binding of extracellular HSP70 leads to intracellular Ca fluxes and the induction of pro-inflammatory cytokines (Pockley, 2001).

Table 5.5 Anti-malarial drugs inducing the greatest alterations in elemental concentrations in canine monocytes.

Element	Time	Increase		Decrease	
		Drug	%	Drug	%
Na	10 min	Suramin	41	Quinine	47
	18 h	Artemisinin	291		
Mg	10 min	Artemisinin	21	Doxycycline	16
	18 h	Dapsone	30		
P	10 min	Quinine	52		
	18 h			Pyrimethamine	56
S	10 min	Suramin	8	Tetracycline	44
	18 h	Chloroquine	212		
Cl	10 min	Suramin	59	Quinine	70
	18 h	Artemisinin	389		
K	10 min	Artemisinin	38	Quinine	67
	18 h	Chloroquine	2	Suramin	64
Ca	10 min	Quinine	72	Doxycycline	36
	18 h	Suramin	356		

Although no conclusions can be made from the changes in elemental concentrations induced by the various drugs, the drugs that induce the greatest changes are worth considering further (Table 5.5). The percentage increase or decrease in the concentration of the respective element was determined using the baseline levels determined for the canine monocytes from all the control samples used in this study. The baseline concentrations of the elements in canine monocytes, as analysed in 150 cells were: 518.2 mmoles/kg for Na; 199.1 mmoles/kg for Mg; 439.7 mmoles/kg for P; 316.3 mmoles/kg for S; 279.7 mmoles/kg for Cl; 204 mmoles/kg for K and 81.3 mmoles/kg for Ca.

Suramin increased the concentrations of Na by 41%, S by 8 %, and Cl by 59 % after 10 min and Ca by 356% after 18 h. The drug substantially decreased [K] by 64% after 18 h. Quinine decreased [Na] by 47%, [Cl] by 70% and [K] by 67% and increased [P] by 52% and [Ca] by 72% after 10 min. Artemisinin induced small increases in Mg (21%) and K (38%) concentrations within 10 min and massive increases in [Na] (291%) and [Cl] (389%) after 18 h. Doxycycline decreased [Mg] by 16% and [Ca] by 36% after 10 min. The concentrations of [S] and [K] were maximally increased by chloroquine after 18 h by 212% and 2% respectively. After 18 h dapsone maximally increased [Mg] by 30% and pyrimethamine

decreased [P] by 56%. Tetracycline decreased the concentration of [S] after 10 min by 44%. Suramin, quinine and artemisinin induced numerous changes in the elemental concentrations and the majority of these changes were larger than any of the other drugs used. However, quinine induced these changes after 10 min whereas artemisinin and suramin induced these changes after 18 h. Although artemisinin did increase the concentrations of certain elements after 10 min, it was by much smaller amounts than after 18 h. Chloroquine was the only other drug to induce a large increase in S, which was increased by 212%. Interestingly, quinine and artemisinin at present are only used in the treatment of malaria and not for prophylaxis due to the severity of the side affects if administration is not controlled (Raynes, 1999 Van Agtmael *et al.*, 1999). The same applies for suramin in the treatment of trypanosomiasis, AIDS and cancer (Schiller *et al.*, 1994).

Drugs that altered the P/K ratios by the greatest margin were: quinine, suramin and pyrimethamine. The P/K ratio was increased by quinine by 348% after 10 min and suramin by 261% after 18 h. Pyrimethamine decreased the P/K ratio after 18 h by 49%. Interestingly although artemisinin has a great influence on the concentrations of other elements it had no detectable effect on the P/K ratio.

Interestingly, Cl and Ca are likely to be important in chloroquine resistance in the malaria parasite. Chloroquine susceptibility was increased two–three fold in resistant and susceptible parasites in Cl-free media (Martiney *et al.*, 1999). The exact mechanism of the Cl modulation of chloroquine susceptibility is unknown. The calcium channel blockers, verapamil, desipramine, chlorpromazine, ketotifin, tetrandrine, cyproheptidine and fluoxetin, are able to reverse chloroquine resistance in *P. falciparum* isolates *in vitro* (De *et* al., 1993; Agrawal *et al.*, 2002).

The individual changes in the elemental concentrations of the cells under different conditions may be important, but changes in the concentration of one element may be linked to changes in the concentrations of other elements. Digitalis is a drug given to patients with heart failure; it exerts its effect by altering the intracellular concentrations of elements. Specifically, digitalis slows down the Na/K ATPase thus allowing Na to accumulate in the cells and

reducing the concentration gradient across the cell membrane. The Na/Ca anti-porters slow down causing Ca to accumulate in the cell (Tortora and Grabowski, 2000). None of the drugs used in this study effect the same elemental changes brought about by digitalis. However, this example serves to highlight that there are many factors involved in the elemental changes and to try to explain what is happening in 14 experimental conditions, each with different time points, requires more investigation and a complete knowledge of all the processes under elemental regulation. This study was unique as no others of its kind have been undertaken. The changes in the elemental concentrations in canine monocytes induced by drugs, phagocytosis and heat shock are evidence that further investigations are required. These will enable development of a fuller understanding of the mechanisms for the increases and decreases of the elemental concentrations in canine monocytes, as well as the cellular responses to the changed concentrations. Once this greater understanding has been achieved, the results could be extrapolated to the mechanisms of action of the various drugs on monocytes. Further analysis of each individual drug at different time points or analysis of a simpler cell such, as the red blood cell may give further insight into the changes that are occurring. Due to the complexity of the monocyte it may be better to study the effects of the various drugs on red blood cells first to determine the relationships between the elements. Not much is known about the influence of elemental changes within red blood cells but numerous investigators have studied the transport of ions across the red blood cell membrane as well as across the parasitophorous membrane surrounding the malaria parasite (Kirk, 2001).

CHAPTER 6

GENERAL DISCUSSION

Plasmodium falciparum malaria is a globally and economically important disease. Peripheral blood monocytes are the first line of defence during infection (Asch, 1991) and perform many immunomodulatory functions, such as phagocytosis, intracellular and extracellular killing by the generation of reactive oxygen intermediates (Schwarzer *et al.*, 1992; Fiori *et al.*, 1993) and the production of cytokines (Thuma *et al.*, 1996). However, in the case of malaria some of these functions are suppressed or induced to a greater extent by hemozoin phagocytosis (Francis *et al.*, 1997; Sherry *et* al., 1995; Schwarzer *et al.*, 1998; Scorza *et al.*, 1999), the presence of malaria glycosylphosphatidylinositol (GPI) in blood (Schofield *et al.*, 1996; Tachado *et al.*, 1996), fever conditions (heat shock) (Clerget and Polla, 1990; Polla and Kantengwa, 1991; Jäättelä, 1993; Vadas *et* al., 1993) and the presence of anti-malarial drugs in the bloodstream of the patient (Schwartz *et al.*, 1985; Gabay *et al.*, 1994; Goldring *et* al., 1999; Goldring and Nemaorani, 1999; Goldring and Ramoshebi, 1999).

Canine monocytes were isolated in this study using the Histopaque®-1077 density gradient centrifugation method followed by adherence to glass coverslips (Goldring *et al.*, 1992). The morphology (Auger and Ross, 1992), presence of peroxidase (Krakowka and Wallace, 1983; Stachura, 1989) and alkaline phosphatase (Van Noorden and Frederiks, 1992) as well as the ability of the cells to phagocytose latex beads and β-hematin (Auger and Ross, 1992; Schwarzer *et* al., 1999) confirmed the identity and viability of the isolated monocytes. β-Hematin was synthesized from hematin using a protocol used by Slater *et al.* (1991) and Taramelli *et al.* (1995). In further studies, it may be interesting to look at the effects of the various anti-malarial drugs on monocyte phagocytosis of latex beads, β-hematin, hemozoin and malaria infected red blood cells.

Antigenic peptides were selected from the highly conserved human HSP70 and HSC70 proteins using the Predict7 programme (Càrmenes *et al.*, 1989) and protein similarity searches performed on the Swiss Prot website using BLAST2.0. The anti-peptide antibodies raised in chickens immunized with the peptide rabbit albumin conjugate, were able to recognise the free

peptide in an ELISA and the native 70 kDa proteins in human and canine heat shocked lymphocyte lysates on western blots. HSP70 was not expected to be expressed at 37°C (Lindquist, 1986), but in this study it was expressed at both 37°C and 44°C. The lymphocytes were most likely activated by the isolation (Wu *et* al., 1986; Thiem *et al.*, 1988, Njemini *et al.*, 2002) thus for future experiments alternative isolation methods need to be investigated.

The anti-HSP peptide recognized approximately 10 proteins in the isolated lymphocyte lysates; these may be products of cathepsin D cleavage of HSP70 (Sehorn *et* al., 2002) or normal breakdown products of HSP70 (Lindquist, 1986). Further investigations would require the use of a higher concentration of the cathepsin D inhibitor, pepstatin A or using numerous increments in time and/or temperature. As mentioned in Chapter 4, ^{35}S-methionine or [H]^{3}-amino acid labelling or northern blot analysis of the HSP70 mRNA, would provide information about the expression of new proteins at the onset of heat shock. In this study the possibility that the anti-HSP antibody was also cross-reacting with HSC70 in the lymphocyte lysates could not be ruled out. Unfortunately, pure HSP70 and HSC70 were unavailable but for future studies have both proteins will be required for an extensive study on HSP expression. Another possibility would be to obtain numerous lymphocyte or monocyte lysates, to use the anti-peptide antibodies to affinity purify the proteins, and determine if they are fragments of HSP70 or represent other proteins recognized by the antibodies. If these problems are resolved then the effects of anti-malarial drugs on the expression of heat shock proteins in the presence or absence of β-hematin or hemozoin could be undertaken.

The X-ray microanalysis study showed that all the drugs, the phagocytosis of latex beads and β-hematin as well as heat shock altered the elemental concentrations and the P/K ratios of canine monocytes in unique ways. However, there were differences in the time when the changes occurred and whether there was an increase, a decrease or no change in the elemental concentrations. Although the mechanisms for these changes and the cellular responses to them are as yet uncharacterised, the data obtained in this study can be compared to a certain extent with other studies. The comparisons must be conservatively approached as the present study was performed using canine monocytes whereas most other studies examined human monocytes. Thobakgale (2002) detected primaquine in the cytoplasm and granules of canine

monocytes, thus confirming that this drug is present within the cell. The other anti-malarial drugs used in this study are also likely to be internalized in the monocytes.

The most influential drugs on the concentrations of elements were suramin, quinine and artemisinin as the alterations they induced were greater than any of the other drugs used. Quinine was the only drug to influence the concentrations of all the elements, with the exception of Mg after 10 min; suramin and artemisinin affected the concentrations at 10 min and 18 h. As mentioned previously suramin and quinine altered the P/K ratios by the greatest margins but artemisinin had no effect. In future studies it may be interesting to investigate these three drugs further, as altering the concentrations of elements may in part lead to a better understanding of how these three drugs act on normal cellular metabolism.

Goldring and Nemaorani (1999) examined the modulation of human monocyte surface receptors by anti-malarial drugs (quinine, artemisinin, chloroquine, primaquine, pyrimethamine), the trypanocidal drug, suramin, and a protein kinase C inhibitor, staurosporine. All the drugs used were found to reduce the expression of monocyte receptors at therapeutic doses in unique ways. The most effective drug in reducing receptor expression after 18 h was quinine (65% reduction), followed by pyrimethamine (60% reduction). After 18 h incubation in this study, both quinine and pyrimethamine had no effect on the concentrations of K and Ca. However, artemisinin (40% reduction) was the least effective anti-malarial drug in reducing receptor expression and suramin reduced expression by only 7%. These two drugs showed only one similarity in altering the elemental concentrations in monocytes, they decreased the concentration of K after 18 h. Primaquine and chloroquine reduced receptor expression to a lesser degree than pyrimethamine, but primaquine had no effect on the concentration of K whereas chloroquine increased it. This indicates that changes in the K concentration may be involved in the regulation of the expression of monocyte receptors. However, it must be remembered that there are many other contributing factors that will alter the expression of monocyte receptors. Staurosporine was found to reduce monocyte receptor expression by 98% (Goldring and Nemaorani, 1999), as well as prevent the adherence of malaria infected erythrocytes to human monocytes (Goldring and Ramoshebi, 1999). This may be related to the efflux of Cl found by Fernández-Segura *et al.* (1999) in staurosporine-

induced apoptosis, but the alteration of the other elements may be involved in monocyte receptor expression.

Although western blots showed no apparent difference in the expression of HSP70 and HSC70 at 37°C and 44°C, X-ray microanalysis showed that there were differences in the way the elemental concentrations were altered at 37°C and 44°C. However, it must be noted that the cells were isolated and treated very differently and therefore direct comparisons are not valid.

In future studies the alterations in the elemental concentrations induced by the anti-malarial drugs on the monocyte phagocytosis of latex beads, β-hematin, hemozoin and malaria infected red blood cells could be investigated. The effects of anti-malarial drugs on the elemental concentrations in heat shocked human or canine monocytes in the presence or absence of β-hematin, hemozoin or malaria infected red blood cells could also be investigated. These results could be compared to the phagocytic indices and the expression of heat shock proteins previously mentioned. Other avenues to explore using X-ray microanalysis are the effects on the elemental concentrations in the malaria parasite in the red blood cell, brought about by therapeutic concentrations of anti-malarial drugs. Although other investigators have examined the membrane transport in the red blood cell as well as in malaria infected red blood cells, no one fully understands the implications for the cells of increases and decreases in the concentrations of elements (Kirk, 2001). Other methods could be utilized, such as fluorescent ion-sensitive indicators, which can be used to monitor the intracellular elemental concentrations in time course studies (Kirk, 2001). At present fluorescent indicators are available for Na, H, K, Ca, Mg and Cl. The elemental concentrations could also be measured using atomic absorption spectroscopy or electron energy loss spectroscopy (EELS) (Jeanguillaume *et al.*, 1996). In order to utilize X-ray microanalysis to its fullest potential in a study such as that presented here, it would be preferable to plunge freeze the grids in liquid nitrogen or propane and then freeze dry the samples. This would give clearer ultrastructural details within the cell and would enable the investigator to determine the elemental concentrations in the different intracellular organelles. Unfortunately, the samples could not be prepared in this way because the equipment required was unavailable.

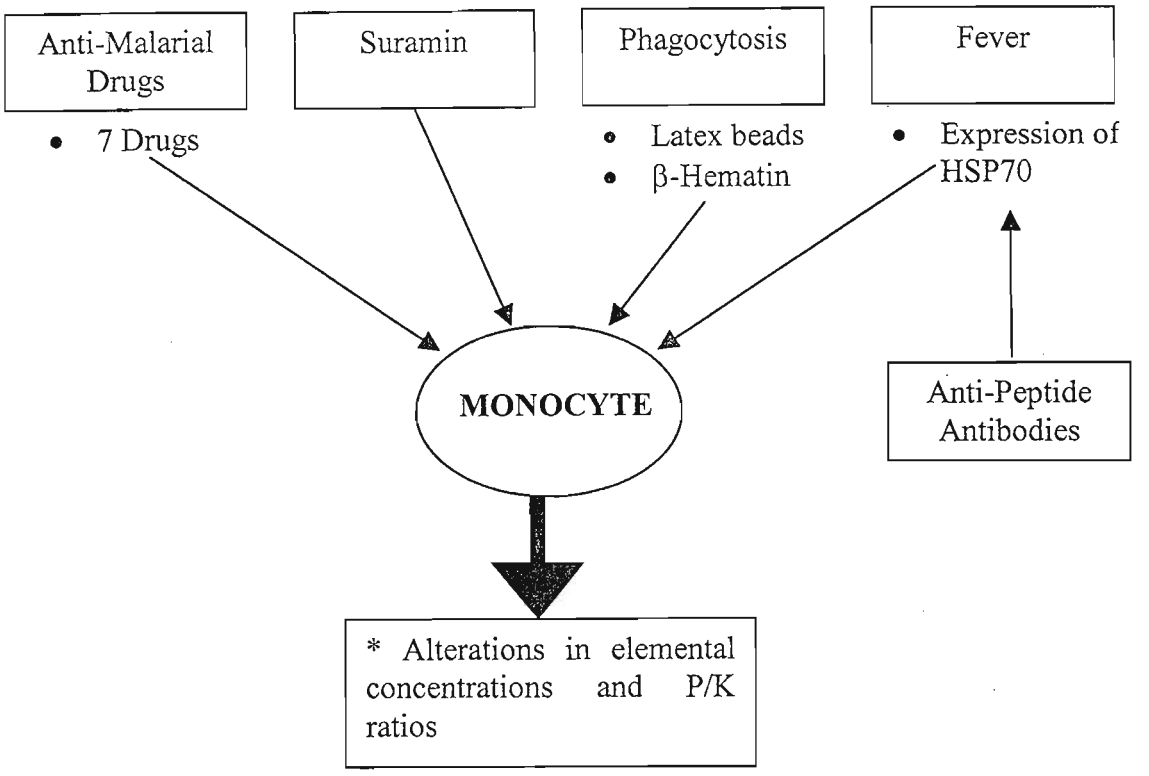

Figure 6.1 Diagrammatic representation of the present study on the effects of anti-malarial drugs, suramin, fever and phagocytosis on the concentrations of elements in canine monocytes.

This study was a preliminary investigation into the effects of anti-malarial drugs and heat shock on the elemental concentrations in canine monocytes, as well as the effects of heat shock on the expression of HSPs. Although the results at present are inconclusive in light of the current lack of knowledge with regard to elemental homeostasis in monocytes, each anti-malarial drug and experimental condition induced a unique response in the monocytes. The baseline elemental concentrations in canine monocytes have been conclusively determined in this study and will aid in further work in this field. Monocytes are complex cells, and in this unique study we have identified that various anti-malarial drugs, fever and hemozoin alter the concentrations of elements in different ways (Figure 6.1). Further investigations will hopefully increase understanding of the implications of these changes on monocytes.

REFERENCES

Abdalla, S. H. and Wickramasinghe, S. N. (1985). Human monocyte activation by supernatants from continuous cultures of *Plasmodium falciparum*. *Transactions of the Royal Society of Tropical Medicine and Hygiene* **79**: 657 – 662.

Absolom, D. R. (1986). Basic methods for the study of phagocytosis. *Methods in Enzymology* **132**: 95 – 180.

Adams, D. O. and Hamilton, T. A. (1992). Molecular basis of macrophage activation: diversity and its origin. *In*: C. E. Lewis and J. O'D. McGee (eds), *The Natural Immune System: The Macrophage*, pp 77 – 114. Oxford University Press, Oxford.

Agrawal, R.; Tripathi, R.; Tekwani, B. L.; Jain, S. K.; Dutta, G. P. and Shukla, O. P. (2002). Haem polymerase as a novel target of antimalarial action of cyproheptadine. *Biochemical Pharmacology* **64**: 1399 – 1406.

Akompong, T; Ghori, N. and Haldar. K. (2000). *In vitro* activity of riboflavin against the human malaria parasite *Plasmodium falciparum*. *Antimicrobial Agents and Chemotherapy* **44**: 88 – 96.

Alzani, R.; Corti, A.; Grazioli, L.; Cozzi, E.; Ghezzi, P. and Marcucci, F. (1993). Suramin induces deoligomerization of human tumor necrosis factor alpha. *Journal of Biological Chemistry* **268**: 12526 – 12529.

Arese, P. and Schwarzer, E. (1997). Malarial pigment (haemozoin): a very active 'inert' substance. *Annals of Tropical Medicine and Parasitology* **91**: 501 – 516.

Asch, C. (1991). Macrophages at the center of infection. *Parasitology Today* **7**: 2 – 3.

Asea, A.; Kraeft, S. T.; Kurt-Jones, E. A.; Stevenson, M. A.; Chen, L. B.; Finberg, R. W.; Koo, G. C. and Calderwood, S. K. (2000). HSP70 stimulates cytokine production through a CD14-dependent pathway, demonstrating its dual role as chaperone and cytokine. *Nature Medicine* **6**: 435 – 442.

Auger, M. J. and Ross, J. A. (1992). The biology of the macrophage. *In*: C. E. Lewis and J. O'D. McGee (eds), *The Natural Immune System: The Macrophage*, pp 1 – 74. Oxford University Press, Oxford.

Austin, D. R.; Chan, S. C.; Malley, A.; Hanifin, J. M. and Hirshman, C. A. (1985). Enrichment of dog leukocyte subpopulations using density gradients. *Journal of Clinical Laboratory Immunology* **17**: 53 – 57.

Basco, L. K. and Le Bras, J. (1993). *In vitro* activity of artemisinin derivatives against african isolates and clones of *Plasmodium falciparum. American Journal of Tropical Medicine and Hygiene* **49**: 301 – 307.

Basco, L. K.; Ramiliarisoa, O. and Le Bras, J. (1994). *In vitro* activity of pyrimethamine, cycloguanil, and other antimalarial drugs against african isolates and clones of *Plasmodium falciparum. American Journal of Tropical Medicine and Hygiene* **50**: 193 – 199.

Beames Jr., C. G. (1971). Cellular Biology. *In*: J. E. Breazile (ed), *Textbook of veterinary physiology*, pp 28 – 29. Lea & Febiger, Philadelphia.

Beelen, R. H. J.; Bos, H. J.; Kamperdijk, E. W. A. and Hoefsmit, E. C. M. (1989). Ultrastructure of monocytes and macrophages. *In*: M. Zembala and G. L. Asherson (eds), *Human monocytes*, pp 8 – 16. Academic Press, London.

Bendrat, K.; Berger, B. J. and Cerami, A. (1995). Haem polymerization in malaria. *Nature* **378**: 138 - 139.

Berger, B. J.; Bendrat, K. and Cerami, A. (1995). High-performance liquid chromatographic analysis of biological and chemical heme polymerization. *Analytical Biochemistry* **231**: 151 – 156.

Biswas, S.; Karmarkar, M. G. and Sharma, Y. D. (2001). Antibodies detected against *Plasmodium falciparum* haemozoin with inhibitory properties to cytokine production. *FEMS Microbiology Letters* **194**: 175 – 179.

Bloland, P. B. and Ettling, M. (1999). Making malaria-treatment policy in the face of drug resistance. *Annals of Tropical Medicine and Parasitology* **93**: 5 – 23.

Bloland, P.B.; Ettling, M. and Meek, S. (2000). Combination therapy for malaria in Africa: hype or hope? *Bulletin of the World Health Organisation* **78**: 1378 - 1388.

Bohle, D. S.; Dinnebier, R. E.; Madsen, S. K. and Stephens, P. W. (1997). Characterization of the products of the heme detoxification pathway in malarial late trophozoites by X-ray diffraction. *The Journal of Biological Chemistry* **272**: 713 – 716.

Bouchot, A.; Zierold, K.; Bonhomme, A.; Kilian, L.; Belloni, A.; Balossier, G.; Pinon, J. M. and Bonhomme, P. (1999). Tachyzoite calcium changes during cell invasion by *Toxoplasma gondii*. *Parasitology Research* **85**: 809 – 818.

Boyer, R. F. (1993). *Modern Experimental Biochemistry,* 2nd ed., pp 81 – 143, 249 – 250. Benjamin/Cummings, San Francisco, CA.

Boyum, A. (1968). Isolation of mononuclear cells and granulocytes from human blood. Isolation of mononuclear cells by one centrifugation and of granulocytes by combining centrifugation and sedimentation at 1 *g*. *Scandinavian Journal of Clinical and Laboratory Investigation*, **21**: 77 – 89.

Bradley, D. (2000). Dimeric malarial drugs for enhanced activity. *Drug Discovery Today* **5**: 44 – 45.

Bray, P. G.; Mungthin, M.; Ridley, R. G. and Ward, S. A. (1998). Access to hematin: the basis of chloroquine resistance. *Molecular Pharmacology* **54**: 170 –179.

Bray, P. G.; Ward, S. A. and Ginsburg, H. (1999). Na^+/H^+ antiporter, chloroquine uptake and drug resistance: inconsistencies in a newly proposed model. *Parasitology Today* **15**: 360 – 363.

Breckenridge, A. M. and Winstanley, P. A. (1997). Clinical pharmacology and malaria. *Annals of Tropical Medicine and Parasitology* **91**: 727 – 733.

Brewer, T. G.; Grate, S. J.; Peggins, J. O.; Weina, P. J.; Petras, J. M.; Levine, B. S.; Heiffer, M. H. and Schuster, B G. (1994). Fatal neurotoxicity of arteether and artemether. *American Journal of Tropical Medicine and Hygiene* **51**: 251 – 259.

Burrin, D. (1994). Immunochemical techniques. *In*: K. Wilson and J. Walker (eds), *Principles and techniques of practical biochemistry,* 4th ed., pp 65 -101. Cambridge University Press, Cambridge.

Bussolino, F.; Turrini, F. and Arese, P. (1987). Measurement of phagocytosis utilizing [^{14}C]cyanate-labelled human red cells and monocytes. *British Journal of Haematology* **66**: 271 – 274.

Butler, D.; Maurice, J. and O'Brien, C. (1997). Time to put malaria control on the global agenda. *Nature* **386**: 535 – 536.

Cármenes, R. S,; Freije, J. P.; Molina, M. M. and Martín, J. M. (1989). Predict7, a program for protein structure prediction. *Biochemical and Biophysical Research Communications* **159**: 687 – 693.

Carosi, G. and Castelli, F. (1997). Introduction. *In*: G. Carosi and F. Castelli (eds), *Handbook of Malaria infection in the tropics. Quaderni di cooperazione sanitaria, no. 15*, pp 11-13. Organizazione per la Cooperazione Sanitaria Internazionale, Bologna, Italy.

Chandler, J. A. (1977). X-ray microanalysis in the electron microscope. *In*: A. M. Glauert, (ed), *Practical methods in electron microscopy*, pp 392 - 393. North-Holland Publishing Company, Amsterdam.

Clark, M. A.; Chen, M. J.; Crooke, S. T. and Bomamlaski, J. S. (1988). Tumour necrosis factor (cachectin) induces phospholipase A_2 activity and synthesis of a phospholipase A_2-activating protein in endothelial cells. *Biochemical Journal* **250**: 125 – 132.

Clerget, M. and Polla, B. S. (1990). Erythrophagocytosis induces heat shock protein synthesis by human monocytes-macrophages. *Proceedings of the National Academy of Sciences of the United States of America* **87**: 1081 – 1085.

Coetzee, M.; Craig, M and le Sueur, D. (2000). Distribution of African malaria mosquitoes belonging to the *Anopheles gambiae* complex. *Parasitology Today* **16**: 74 – 77.

Coleman, M. D. (2001). Dapsone-mediated agranulocytosis: risks, possible mechanisms and prevention. *Toxicology* **162**: 53 – 60.

Collins, F. H. and Paskewitz, S. M. (1995). Malaria: current and future prospects for control. *Annual Review of Entomology* **40**: 195 – 219.

Cribb, A. E.; Miller, M.; Tesoro, A. and Spielberg, S. P. (1990). Peroxidase-dependent oxidation of sulfonamides by monocytes and neutrophils from humans and dogs. *Molecular Pharmacology* **38**: 744 – 751.

Crum, N. F. and Gable, P. (2000). Quinine-induced hemolytic-uremic syndrome. *Southern Medical Journal* **93**: 726 – 728.

David, P. H.; Handunneti, S. M.; Leech, J. H.; Gamage, P. and Mendis, K. N. (1988). Rosetting: a new cytoadherence property of malaria-infected erythrocytes. *American Journal of Tropical Medicine and Hygiene* **38**: 289 – 292.

De, D.; Bhaduri, A. P. and Milhous, W. K. (1993) A novel pyrrolidonoalkaneamine (WR268954) that modulates chloroquine resistance of *Plasmodium falciparum in vitro*. *American Journal of Tropical Medicine and Hygiene* **49**: 113 – 120.

De Almeida, M. C.; Silva, A. C.; Barral, A. and Barral Netto, M. (2000). A simple method for human peripheral blood monocyte isolation. *Memórias do Instituto Oswaldo. Cruz* **95**: 221 – 223.

Deans, J. A. and Cohen, S. (1983). Immunology of malaria. *Annual Review of Microbiology* **37**: 25 - 49.

Dhingra, V.; Vishweshkar Rao, K. and Lakshmi Narasu, M. (2000). Current status of artemisinin and its derivatives as anti-malarial drugs. *Life Sciences* **66**: 279 – 300.

Diccianni, M. B.; Mistry, M. J.; Hug, K. and Harmony, J. A. K. (1990). Inhibition of phospholipase A_2 by heparin. *Biochimica et Biophysica Acta* **1046**: 242 – 248.

Donati, Y. R. A.; Kantengwa, S. and Polla, B. S. (1991). Phagocytosis and heat shock response in human monocyte-macrophages. *Pathobiology* **59**: 156 – 161.

Dorn, A.; Stoffel, R.; Matile, H.; Bubendorf, A. and Ridley, R. G. (1995). Malarial haemozoin / β-haematin supports haem polymerization in the absence of protein. *Nature* **374**: 269 – 271.

Dua, V. K.; Gupta, N. C.; Kar, P. K.; Nand, J.; Edwards, G.; Sharma, V. P. and Subbarao, S. K. (2000). Chloroquine and desethylchloroquine concentrations in blood cells and plasma from Indian patients infected with sensitive or resistant *Plasmodium falciparum*. *Annals of Tropical Medicine and Parasitology* **94**: 565 – 570.

Duc, D. D.; De Vries, P. J.; Khanh, N. X.; Binh, L. K.; Kager, P. A. and Van Boxtel, C. J. (1994). The pharmokinetics of a single dose of artemisinin in healthy Vietnamese subjects. *American Journal of Tropical Medicine and Hygiene* **51**: 785 – 790.

Dunn, M. J. (1987). Two dimensional polyacrylamide gel electrophoresis. *In*: A. Chrambach; M. J. Dunn and B. J. Radola (eds), *Advances in Electrophoresis, Volume 1*, pp 1 - 93. VCH Verlagsgesellschaft, Weinheim, Germany.

Eckert, R. (1988). *Animal Physiology: Mechanisms and adaptations, 3rd Ed.* pp 76 – 77. W. H. Freeman and Company, New York.

Edwards, G. (1997). Haem-mediated decomposition of artemisinin and its derivatives: pharmacological and toxicological considerations. *Journal of Pharmacy and Pharmacology* **49**: 49 – 53.

Egan, T. J.; Hunter, R.; Kaschula, C. H.; Marques, H. M.; Misplon, A. and Walden, J. (2000). Structure-function relationships in aminoquinolines: effect of amino and chloro groups on quinoline-hematin complex formation, inhibition of β-hematin formation, and antiplasmodial activity. *Journal of Medicinal Chemistry* **43**: 283 – 291.

Egan, T. J.; Mavuso, W. W. and Ncokazi, K. K. (2001). The mechanism of β-hematin formation in acetate solution. Parallels between hemozoin formation and biomineralization processes. *Biochemistry* **40**: 204 – 213.

Egan, T. J.; Ross, D. C. and Adams, P. A. (1994). Quinoline anti-malarial drugs inhibit spontaneous formation of β-haemitin (malaria pigment). *FEBS Letters* **352**: 54 –57.

Eggleson, K. K.; Duffin, K. L. and Goldberg, D. E. (1999). Identification and characterization of falcilysin, a metallopeptidase involved in hemoglobin catabolism within the malaria parasite *Plasmodium falciparum*. *The Journal of Biological Chemistry* **274**: 32411 – 32417.

Emini, E. A.; Hughes, J. V.; Perlow, D. S. and Boger, J. (1985). Induction of hepatitis A virus-neutralizing antibody by virus-specific synthetic peptide. *Journal of Virology* **55**: 836 – 839.

Emmick, J. T.; Kwon, S.; Bidasee, K. R.; Besch, K. T. and Besch Jr., H. R. (1994). Dual effect of suramin on calcium fluxes across sarcoplasmic reticulum vesicle membranes. *Journal of Pharmacology and Experimental Therapeutics* **269**: 717 – 724.

Feige, U. and Polla, B. S. (1994). Hsp70 – a multi-gene, multi-structure, multi-function family with potential clinical applications. *Experientia* **50**: 979 – 986.

Fernández-Segura, E.; Cañizares, F. J.; Cubero, M. A.; Warley, M. A. and Campos, A. (1999). Changes in elemental content during apoptotic cell death studied by electron probe x-ray microanalysis. *Experimental Cell Research* **253**: 454 – 462.

Fincato, G.; Polentarutti, N.; Sica, A.; Mantovani, A. and Colotta, F. (1991). Expression of a heat-inducible gene of the HSP70 family in human myelomonocytic cells: regulation by bacterial products and cytokines. *Blood* **77**: 579 – 586.

Fiori, P. L.; Rappelli, P.; Mirkarimi, S. N., Ginsburg, H.; Cappuccinelli, P. and Turrini, F. (1993). Reduced microbicidal and anti-tumor activities of human monocytes after ingestion of *Plasmodium falciparum*-infected red blood cells. *Parasite Immunology* **15**: 647 – 655.

Fishman, P.; Hart, J. and Djaldetti, M. (1985). X-ray microanalysis of normal human neutrophils, lymphocytes, monocytes and platelets. *Biomedicine and Pharmacotherapy* **39**: 389 – 392.

Foley, M. and Tilley, L. (1997). Quinoline antimalarials: mechanisms of action and resistance. *International Journal for Parasitology* **27**: 231 – 240.

Foley, M. and Tilley, L. (1998). Quinoline antimalarials: mechanisms of action and resistance and prospects for new agents. *Pharmacological Therapy* **79**: 55 – 87.

Francis, S. E.; Sullivan Jr., D. J. and Goldberg, D. E. (1997). Hemoglobin metabolism in the malaria parasite *Plasmodium falciparum. Annual Review of Microbiology* **51**: 97 – 123.

Gabay, T.; Krugliak, M.; Shalmiev, G. and Ginsburg, H. (1994). Inhibition by anti-malarial drugs of haemoglobin denaturation and iron release in acidified red blood cell lysates – a possible mechanism of their anti-malarial effect? *Parasitology* **108**: 371 – 381.

Gamper, N.; Huber, S. M.; Badawi, K. and Lang, F. (2000). Cell volume-sensitive sodium channels upregulated by glucocorticoids in U937 macrophages. *Pflugers Arch: European Journal of Physiology* **441**: 281 – 286.

Ginsburg, H.; Ward, S. A. and Bray, P. G. (1999). An integrated model of chloroquine action. *Parasitology Today* **15**: 357 –360.

Goldie, P.; Roth Jr., E. F.; Oppenheim, J. and Vanderberg, J. P. (1990). Biochemical characterization of *Plasmodium falciparum* hemozoin. *American Journal of Tropical Medicine and Hygiene* **43**: 584 - 596.

Goldring, J. P. D. and Coetzer, T. H. T. (2003). Isolation of chicken immunoglobulins (IgY) from egg yolk. *Biochemistry and Molecular Biology Education* **31**: 185 – 187.

Goldring, J. P. D and Nemaorani, S. (1999). Antimalarial drugs modulate the expression of monocyte receptors. *International Journal of Immunopharmacology* **21**: 599 – 607.

Goldring, J. P. D. and Ramoshebi, L. N. (1999). Glucocorticoids, antioxidants and staurosporine modulate the adherence between monocytes and malaria infected erythrocytes. *Inflammation Research* **48**: 657 – 661.

Goldring, J. D.; Molyneux, M. E.; Taylor, T.; Wirima, J. and Hommel, M. (1992). *Plasmodium falciparum*: diversity of isolates from Malawi in their cytoadherence to melanoma cells and monocytes *in vitro*. *British Journal of Haematology* **81**: 413 – 418.

Goldring, J. P. D.; Padayachee, T. and Ismail, I. (1999). *Plasmodium falciparum* malaria: rosettes are disrupted by quinine, artemisinin, mefloquine, primaquine, pyrimethamine, chloroquine and proguanil. *Memórias do Instituto Oswaldo. Cruz* **94**: 667 – 674.

Good, M. F. and Doolan, D. L. (1999). Immune effector mechanisms in malaria. *Current Opinion in Immunology* **11**: 412 – 419.

Grazioli, L.; Alzani, R.; Ciomei, M.; Mariani, M.; Restivo, A.; Cozzi, E. and Marcucci, F. (1992). Inhibitory effect of suramin on receptor binding and cytotoxic activity of tumor necrosis factor alpha. *International Journal of Immunopharmacology* **14**; 637 – 642.

Günther, T. (1990). Funtional compartmentation of intracellular magnesium. *In*: H. Sigel and A. Sigel (eds), *Metal ions in biological systems: Compendium on magnesium and its role in biology, nutrition, and physiology, Volume 26*, pp 194 - 231. Marcel Dekker, New York.

Gurr, E. (1960). *Encyclopedia of microscopic stains*, pp 217 – 219, 273 – 275, 397 – 398. Leonard Hill [Books] Limited, London, UK.

Guyton, A. C. (1982). *Human Physiology and Mechanisms of Disease*, 3rd Edition, pp 40 – 50. W. B. Saunders Company, Philadelphia, USA.

Hall, D. A. and Hourani, S. M. O. (1994). Effects of suramin on increases in cytosolic calcium and on inhibition of adenylate cyclase induced by adenosine 5'diphosphate in human platelets. *Biochemical Pharmacology* **47**: 1013 – 1018.

Hall, T. J. (1994). Role of hsp70 in cytokine production. *Experientia* **50**: 1048 – 1053.

Harlow, E. and Lane, D. (1988). *Antibodies: A laboratory manual*, pp 55 – 87. Cold Spring Harbour Laboratory, New York, USA.

Hawley, S. R.; Bray, P. G.; Mungthin, M.; Atkinson, J. D.; O'Niell, P. M. and Ward, S. A. (1998). Relationship between antimalarial drug activity, accumulation, and inhibition of heme polymerization in *Plasmodium falciparum in vitro*. *Antimicrobial Agents and Chemotherapy* **42**: 682 – 686.

Health Systems Trust news article. (2001). SA spends R90-million a year on malaria control: MRC. http://new.hst.org.za/news/index.php/20010520.

Hermanson, G. T. (1996). *Bioconjugate Techniques*, pp 132 – 133; 237 – 239. Academic Press, Inc., San Diego, USA.

Hien, T. T. and White, N. J. (1993). Qinghaosu. *Lancet* **341**: 603 – 608.

Hightower, L. E. and Leung, S. M. (1997). Mammalian HSC70 and HSP70 proteins. *In*: M. J. Gething (ed), *Guidebook to molecular chaperones and protein folding catalysts*, pp 53 - 58. Oxford University Press, Oxford.

Hishikawa, Y.; Cheung, J. Y.; Yelamarty, R. V. and Knutson, D. W. (1991). Calcium transients during Fc receptor-mediated and nonspecific phagocytosis by murine peritoneal macrophages. *Journal of Cell Biology* **115**: 59 - 66.

Hoeck, W. G.; Ramesha, C. S.; Chang, D. J.; Fan, N. and Heller, R. A. (1993). Cytoplasmic phospholipase A_2 activity and gene expression are stimulated by tumor necrosis factor: dexamethasone blocks the induced synthesis. *Proceedings of the National Academy of Sciences of the United States of America* **90**: 4475 – 4479.

Hong, Y. L.; Yang, Y. Z. and Meshnick, S. R. (1994). The interaction of artemisinin with malarial hemozoin. *Molecular and Biochemical Parasitology* **63**: 121 – 128.

Hopp, T. P. and Woods, K. R. (1981). Prediction of protein antigenic determinants from amino acid sequences. *Proceedings of the National Academy of Sciences of the United States of America* **78**: 3824 – 3828.

Hopp, T. P. and Woods, K. R. (1983). A computer program for predicting protein antigenic determinants. *Molecular Immunology* **20**: 483 – 489.

Jäättelä, M. (1993). Overexpression of major heat shock protein hsp70 inhibits tumor necrosis factor-induced activation of phospholipase A_2. *Journal of Immunology* **151**: 4286 – 4294.

Janin, J.; Wodak, S.; Levitt, M. and Maigret, M. (1978). The conformation of amino acid side chains in proteins. *Journal of Molecular Biology* **125**: 357 – 386.

Jacquier-Sarlin, M. R.; Fuller, K.; Dinh-Xuan, A. T.; Richard, M. J. and Polla, B. S. (1994). Protective effects of hsp70 in inflammation. *Experientia* **50**: 1031 – 1038.

Jacquier-Sarlin, M. R.; Jornot, L. and Polla, B. S. (1995). Differential expression and regulation of hsp70 and hsp90 by phorbol esters and heat shock. *Journal of Biological Chemistry* **270**: 14094 – 14099.

Jeanguillaume, C.; Tence, M.; Zhang, L. and Ballongue, P. (1996). Practical aspects of electron energy loss spectroscopy (EELS) in biology. *Cellular and Molecular Biology* **42**: 439 – 450.

Jones, A.; Reed, R. and Weyers, J. (1994). *Practical skills in biology*, pp 111 – 119. Longman Scientific and Technical, Harlow, UK.

Juckett, G. (1999). Malaria prevention in travellers. *American Family Physician* **59**: 2523 – 2538.

Jung, M. (1994). Current developments in the chemistry of artemisinin and related compounds. *Current Medicinal Chemistry* **1**: 35 – 49.

Karp, G. (1996). *Cell and molecular biology: Concepts and experiment*, pp 152 – 153, 664 – 668. John Wiley & Sons, New York.

Karplus, P. A and Schulz, G. E. (1985). Prediction of chain flexibility in proteins: a tool for the selection of peptide antigens. *Naturwissenschaften* **72**: 212 – 213.

Karres, I.; Kremer, J. P.; Dietl, I.; Steckholzer, U.; Jochum, M. and Ertel, W. (1998). Chloroquine inhibits proinflammatory cytokine release into human whole blood. *American Journal of Physiology* **274**: R1058 – R1064.

Kemeny, D. M. and Chantler, S. D. (1988). An introduction to ELISA. *In*: D. M. Kemeny and S. J. Challacombe (eds), *ELISA and other solid phase immunoassays,* pp 1 – 29. John Wiley & Sons Ltd, Chichester, UK.

Kirk, K. (2001). Membrane transport in the malaria-infected erythrocyte. *Physiological Reviews* **81**: 495 – 537.

Klein, N. C. and Cunha, B. A. (2001). New uses of older antibiotics. *The Medical Clinics of North America.* **85**: 125 – 132.

Knell, A. J. (1991). *Malaria: A publication of the tropical programme of the welcome trust*, pp 1 – 89. Oxford University Press, Oxford.

Krakowka, S. and Wallace, A. L. (1983). *In vitro* properties of diffuse cytoplasmic esterase-positive canine mononuclear leukocytes. *Veterinary Immunology and Immunopathology* **5**: 1 – 13.

Kremsner, P. G.; Neifer, S.; Rasenack, T. and Bienzle, U. (1993). Interference by antimalarial drugs with the *in-vitro* production of reactive nitrogen intermediates by murine macrophages. *Journal of Antimicrobial Chemotherapy* **31**: 385 – 392.

Kuppner, M. C.; Gastpar, R.; Gelwer, S.; Nössner, E.; Ochmann, O.; Scharner, A. and Issels, R. D. (2001). The role of heat shock protein (hsp70) in dendritic cell maturation: hsp70 induces the maturation of immature dendritic cells but reduces DC differentiation from monocyte precursors. *European Journal of Immunology* **31**: 1602 – 1609.

Kwiatkowski, D. (1993). TNF-inducing malaria toxin: a sheep in wolf's clothing? *Annals of Tropical Medicine and Parasitology* **87**: 613 – 616.

Laemmli, U. K. (1970). Cleavage of structural proteins during the assembly of the head of bacteriophage T4. *Nature* **227**: 680 – 685.

Lee, P.; Ye, Z.; Van Dyke, K. and Kirk, R. G. (1988). X-ray microanalysis of *Plasmodium falciparum* and infected red blood cells: effects of qinghaosu and chloroquine on potassium, sodium, and phosphorous composition. *American Journal of Tropical Medicine and Hygiene* **39**: 157 – 165.

Leitner, W. W. and Krzych, U. (1997). *Plasmodium falciparum* malaria blood stage parasites preferentially inhibit macrophages with high phagocytic activity. *Parasite Immunology* **19**: 103 – 110.

Leskovac, V. and Peggins III, J. O. (1992). Hepatic metabolism of artemisinin drugs-III. Induction of hydrogen peroxide production in rat liver microsomes by artemisinin drugs. *Comparative Biochemistry and Physiology C: Comparative Physiology* **101**: 203 – 208.

Lindquist, S. (1986). The heat shock response. *Annual Review of Biochemistry* **55**: 1151 – 1191.

Lloyd, A. W. (1999). Monitor: molecules and profiles. *Drug Discovery Today* **4**: 568 – 570.

López-Antuñano, F. J. (1999). Is primaquine useful and safe as true exo-erythrocytic merontocidal, hypnozoitocidal and gametocidal antimalarial drug? *Salud Pública de México* **41**: 410 – 419.

Mackenzie, A. H. (1983). Pharmacologic actions of 4-aminoquinoline compounds. *American Journal of Medicine* **75**: 5 – 10.

Macreadie, I.; Ginsburg, H.; Sirawaraporn, W. and Tilley, L. (2000). Antimalarial drug development and new targets. *Parasitology Today* **16**: 438 – 444.

Magowan, C.; Brown, J. T.; Liang, J.; Heck, J.; Coppel, R. L.; Mohandas, N. and Meyer-Ilse, W. (1997). Intracellular structures of normal and aberrant *Plasmodium falciparum* malaria parasites imaged by soft x-ray microscopy. *Proceedings of the National Academy of Sciences of the United States of America* **94**: 6222 – 6227.

Maguire, M. E. (1990). Magnesium: A regulated and regulatory cation. *In*: H. Sigel and A. Sigel (eds), *Metal ions in biological systems: Compendium on magnesium and its role in biology, nutrition, and physiology, Volume 26*, pp 135 - 153. Marcel Dekker, New York.

Maresca, B. and Kobayashi, G. S. (1994). Hsp70 in parasites: as an inducible protective protein and as an antigen. *Experientia* **50**: 1067 – 1076.

Markovic, O. T.; Young, D. S. and Markovic, N. S. (1988). Quinidine-induced inhibition of leukocyte esterases. *Clinical Chemistry* **34**: 518 – 524.

Martel, J. L.; Jaramillo, S.; Allen Jr., F. H. and Rubinstein, P. (1974). Serology for automated cytotoxicity assays. *Vox Sanguinis* **27**: 13 – 20.

Martiney, J. A.; Ferrer, A. S., Cerami, A.; Dzekunov, S. and Roepe, P. (1999). Chloroquine uptake, altered partitioning and the basis of drug resistance: evidence of chloride-dependent ionic regulation. *Novartis Foundation Symposium 226*, pp 265 – 280.

Martiney, J. A.; Sherry, B.; Metz, C. N.; Espinoza, M.; Ferrer, A. S.; Calandra, T.; Broxmeyer, H. E. and Bucala, R. (2000). Macrophage migration inhibitory factor release by macrophages after ingestion of *Plasmodium chabaudi*-infected erythrocytes: possible role in the pathogenesis of malarial anaemia. *Infection and Immunity* **68**: 2259 – 2267.

Maruyama, N.; Kakuta, Y.; Yamauchi, K.; Ohkawara, Y.; Aizawa, T.; Ohrui, T.; Nara, M.; Oshiro, T.; Ohno, I.; Tamura, G.; Shimura, S.; Sasaki, H.; Takishima, T. and Shirato, K. (1994). Quinine inhibits production of tumor necrosis factor-α from human alveolar macrophages. *American Journal of Respiratory Cell and Molecular Biology* **10**: 514 – 520.

Mattei, D.; Scherf, A.; Bensaude, O. and Pereira da Silva, L. (1989). A heat shock-like protein from the human malaria parasite *Plasmodium falciparum* induces autoantibodies. *European Journal of Immunology* **19**: 1823 – 1828.

McGilvray, I. D.; Serghides, L.; Kapus, A.; Rotstein, O. D. and Kain, K. (2000). Nonopsonic monocyte/macrophage phagocytosis of *Plasmodium falciparum*-parasitized erythrocytes: a role for CD36 in malarial clearance. *Blood* **96**: 3231 – 3240.

Meshnick, S. R.; Thomas, A.; Ranz, A.; Xu, C. M. and Pan, H. Z. (1991). Artemisinin (qinghaosu): the role of intracellular hemin in its mechanism of antimalarial action. *Molecular and Biochemical Parasitology* **49**: 181 – 190.

Meshnick, S. R. (1996). Is haemozoin a target for antimalarial drugs? *Annals of Tropical Medicine and Parasitology* **90**: 367 – 372.

Metzger, W. G.; Mordmüller, B. G. and Kremsner, P. G. (1995). Malaria pigment in leucocytes. *Transactions of the Royal Society of Tropical Medicine and Hygiene* **89**: 637 – 638.

Miao, B.; Davis, J. and Craig, E. (1997). The HSP70 family – and overview. *In*: M. J. Gething (ed), *Guidebook to molecular chaperones and protein folding catalysts*, pp 3 - 13. Oxford University Press, Oxford.

Miller, P. J. and Stevenson, H. C. (1986). Suspension culture of human monocytes. *Methods in Enzymology* **132**: 243 – 250..

Miyachi, Y. (2000). Pharmacologic modulation of neutrophil functions. *Clinics in Dermatology* **18**: 369 – 373.

Mohan, K.; Dubey, M. L.; Ganguly, N. K. and Mahajan, R. C. (1995). *Plasmodium falciparum*: Role of activated blood monocytes in erythrocyte membrane damage and red cell loss during malaria. *Experimental Parasitology* **80**: 54 – 63.

Moore, G. E.; Gerner, R. E. and Franklin, H. A. (1967). Culture of normal human leukocytes. *Journal of the American Medical Association* **199**: 519 –524..

Murata, T.; Inoue, M.; Kanoe, M.; Kono, Y.; Ishida, M.; Horio, M.; Shimada, M.; Yokoyama, M.; Taura, Y. and Nakama, S. (1993). Ultrastructure and cytochemical characteristics of leuckocyte infected with *Hepatozoon canis*. *The Journal of Veterinary Medical Science* **55**: 1043 – 1045.

Na Bangchang, K., Karbwang, J. and Back, D. J. (1992). Primaquine metabolism by human liver microsomes: effect of other antimalarial drugs. *Biochemical Pharmacology* **44**: 587 – 590.

Newton, C. R. J. C.; Hien, T. T. and White, N. (2000). Cerebral malaria. *Journal of Neurology Neurosurgery and Psychiatry* **69**: 433 – 441.

Newton, P. and White, N. (1999). Malaria: new developments in treatment and prevention. *Annual Review of Medicine* **50**: 179 – 192.

Njemini, R.; Lambert, M.; Demanet, C.; Vanden Abeele, M.; Vandebosch, S. and Mets, T. (2003). The induction of heat shock protein 70 in peripheral mononuclear blood cells in elderly patients: a role for inflammatory markers. *Human Immunology* **64**: 575 – 585.

Njemini, R.; Vanden Abeele, M.; Demanet, C.; Lambert, M.; Vandebosch, S. and Mets, T. (2002). Age-related decrease in the inducibility of heat-shock protein 70 in human peripheral blood mononuclear cells. *Journal of Clinical Immunology* **22**: 195 – 205.

Nkamgueu, E. M.; Adnet, J.J.; Bernard, J.; Zierold, K.; Kilian, L.; Jallot, E.; Benhayoune, H. and Bonhomme, P. (2000). *In vitro* effects of zirconia and alumina particles on human blood monocyte-derived macrophages: X-ray microanalysis and flow cytometric studies. *Journal of Biomedical Materials Research* **52**: 587 – 594.

Noble, E. R. and Noble, G. A. (1982). *Parasitology: the biology of animal parasite,* 5Th ed, pp 87 – 112. Lea and Febiger, Philadelphia, USA.

O'Brien, P. J. (2000). Peroxidases. *Chemico-Biological Interactions* **129**: 113 – 139.

Olliaro, P. L. and Goldberg, D. E. (1995). The *Plasmodium* digestive vacuole: metabolic headquarters and choice drug target. *Parasitology Today* **11**: 294 – 297.

Olliaro, P. L.; Haynes, R. K.; Meunier, B. and Yuthavong, Y. (2001). Possible modes of action of the artemisinin-type compounds. *Trends in Parasitology* **17**: 122 – 126.

Omodeo-Salè, F.; Basilico, N.; Folini, M.; Olliaro, P. and Taramelli, D. (1998). Macrophage populations of different origins have distinct susceptibilities to lipid peroxidation induced by β-haematin (malaria pigment). *FEBS Letters* **433**: 215 – 218.

Oppenheim, J. J. and Leonard, E. J. (1989). Introduction. *In*: M. Zembala and G. L. Asherson (eds), *Human monocytes*, pp 1 – 16. Academic Press, London.

Orjih, A. U. and Fitch, C. D. (1993). Hemozoin production by *Plasmodium falciparum*: variation with strain and exposure to chloroquine. *Biochimica et Biophysica Acta* **1157**: 270 – 274.

Padmanaban, G. and Rangarajan, P. N. (2000). Heme metabolism of *Plasmodium* is a major antimalarial target. *Biochemical and Biophysical Research Communications* **268**: 665 – 668.

Page, M. and Thorpe, R. (1998). IgG purification. *In*: J. D. Pound (ed), *Immunochemical Protocols*, 2nd ed., pp 95 – 111. Humana Press, Totowa, New Jersey, USA.

Pagola, S.; Stephens, P. W.; Bohle, D. S., Kosar, A. D. and Madsen, S. K. (2000). The structure of malaria pigment β-haematin. *Nature* **404**: 307 – 310.

Pandey, A. V. and Chauhan, V. S. (1998). Heme polymerization by malarial parasite: A potential target for antimalarial drug development. *Current Science* **75**: 911 – 918.

Pandey, A. V.; Tekwani, B. L.; Singh, R. L. and Chauhan, V. S. (1999). Artemisinin, an endoperoxide antimalarial, disrupts the hemoglobin catabolism and heme detoxification systems in malarial parasite. *The Journal of Biological Chemistry* **274**: 19383 – 19388.

Paniker, U. and Levine, N. (2001). Dapsone and sulfapyridine. *Dermatologic Clinics* **19**: 79 – 86.

Patnaik, J. K.; Das, B. S.; Mishra, S. K.; Mohanty, S.; Satpathy, S. K. and Mohanty, D. (1994). Vascular clogging, mononuclear cell margination, and enhanced vascular permeability in the pathogenisis of human cerebral malaria. *American Journal of Tropical Medicine and Hygiene* **51**: 642 – 647.

Patz, J. A. and Reisen, W. K. (2001). Immunology, climate change and vector-borne diseases. *Trends in Immunology* **22**: 171 – 172.

Pelassy, C.; Cattan, N. and Aussel, C. (1992). Changes in phospholipid metabolism induced by quinine, 4-aminopyridine and tetraethylammonium in the monocytic cell line THP1. *Biochemical Journal* **282**: 443 – 446.

Petney, T. N. (2001). Environmental, cultural and social changes and their influence on parasite infections. *International Journal for Parasitology* **31**: 919 – 932.

Phillips, R. S. (2001). Current status of malaria and potential for control. *Clinical Microbiology Reviews* **14**: 208 – 226.

Phu, N. H.; Day, N.; Diep, P. T.; Ferguson, D. J. P. and White, N. J. (1995). Intraleucocytic malaria pigment and prognosis in severe malaria. *Transactions of the Royal Society of Tropical Medicine and Hygiene* **89**: 200 – 204.

Pichyangkul, S.; Saengkrai, P. and Webster, H. K. (1994). *Plasmodium falciparum* pigment induces monocytes to release high levels of tumor necrosis factor-α and interleukin-1β. *American Journal of Tropical Medicine and Hygiene* **51**: 430 – 435.

Pichyangkul, S.; Saengkrai, P.; Yongvanitchit, K.; Heppner, D. G.; Kyle, D. E. and Webster, H. K. (1997). Regulation of leukocyte adhesion molecules CD11b/CD18 and leukocyte adhesion molecule-1 on phagocytic cells activated by malaria pigment. *American Journal of Tropical Medicine and Hygiene* **57**: 383 – 388.

Picot, S.; Peyron, F.; Donadille, A.; Vuillez, J. P.; Barbe, G. and Amboise-Thomas, P. (1993). Chloroquine-induced inhibition of the production of TNF, but not of IL-6, is affected by disruption of iron metabolism. *Immunololgy* **80**: 127 – 133.

Pillay, C. S.; Elliott, E. and Dennison, C. (2002). Endolysosomal proteolysis and its regulation. *Biochemical Journal* **363**: 417 – 429.

Plebanski, M. and Hill, A. V. S. (2000). The immunology of malaria infections. *Current Opinion in Immunology* **12**: 437 – 441.

Pockley, A. G. (2001). Heat shock proteins in health and disease: therapeutic targets or therapeutic agents? *Expert Reviews in Molecular Medicine.* 21 September, http://www-ermm.cbcu.cam.ac.uk/01003556h.htm.

Polla, B. S. (1988). A role for heat shock proteins in inflammation? *Immunology Today* **9**: 134 – 137.

Polla, B. S. (1991). Heat shock proteins in host-parasite interactions. *Immunology Today* **12**: A38 – A41.

Polla, B. S. and Kantengwa, S. (1991). Heat shock proteins and inflammation. *Current Topics in Microbiology and Immunology* **167**: 93 – 105.

Polla, B. S.; Mili, N. and Kantengwa, S. (1991). Heat shock and oxidative injury in human cells. *In*: B. Maresca and S. Lindquist (eds), *Heat Shock*, pp 279 – 290. Springer-Verlag, Berlin.

Polla, B. S.; Stubbe, H.; Kantengwa, S.; Maridonneau-Parini, I. and Jacquier-Sarlin, M. R. (1995). Differential induction of stress proteins and functional effects of heat shock in human phagocytes. *Inflammation* **19**: 363 – 378.

Polson, A.; Coetzer, T.; Kruger, J.; von Maltzahn, E. and van der Merwe, K. J. (1985). Improvements in the isolation of IgY from the yolks of eggs laid by immunized hens. *Immunological Investigations* **14**: 323 – 327.

Polson, A.; Potgieter, G. M.; Largier, J. F.; Mears, G. E. F. and Joubert, F. J. (1964). The fractionation of protein mixtures by linear polymers of high molecular weight. *Biochimica et Biophysica Acta* **82**: 463 – 475.

Polson, A.; von Wechmar, M. B. and Fazakerley, G. (1980). Antibodies to proteins from yolk of immunized hens. *Immunological Communications* **9**: 495 – 514.

Pradines, B.; Spiegel, A.; Rogier, C.; Tall, A.; Mosnier, J.; Fusai, T.; Trape, J. F. and Parzy, D. (2000). Antibiotics for prophylaxis of *Plasmodium falciparum* infections: *in vitro* activity of doxycycline against Senegalese isolates. *American Journal of Tropical Medicine and Hygiene* **62**: 82 – 85.

Prasad, R. N.; Ganguly, N. K.; Mahajan, R. C. and Garg, S. K. (1984). Effect of quinine on phagocytic functions of normal rhesus monkey (*Macaca mulatta*) monocytes. *The Indian Journal of Medical Research* **79**: 550 – 553.

Price, R.; Van Vugt, M.; Phaipun, L.; Luxemburger, C.; Simpson, J.; McGready, R.; Kuile, F. T.; Kham, A.; Chongsuphajaisiddhi, T.; White, N. J. and Nosten, F. (1999). Adverse effects in patients with acute *falciparum* malaria treated with artemisinin derivatives. *American Journal of Tropical Medicine and Hygiene* **60**: 547 – 555.

Pruzanski, W. and Vadas, P. (1991). Phospholipase A_2 – a mediator between proximal and distal effectors of inflammation. *Immunology Today* **12**: 143 – 146.

Raynes, K. (1999). Bisquinoline antimalarials: their role in malaria chemotherapy. *International Journal for Parasitology* **29**: 367 – 379.

Riches, D. W. H.; Morris, C. J. and Stanworth, D. R. (1981). Induction of selective acid hydrolase release from mouse macropahges during exposure to chloroquine and quinine. *Biochemical Pharmacology* **30**: 629 – 634.

Richman, S. J.; Vedvick, T. S. and Reese, R. T. (1989). Peptide mapping of conformational epitopes in human malaria parasite heat shock protein. *Journal of Immunology* **143**: 285 – 292.

Ridley, R. G.; Dorn, A.; Matile, H. and Kansy, M. (1995). Haem polymerization in malaria. *Nature* **387**: 138 – 139.

Ridley, R. G.; Dorn, A.; Vippagunta, S. R. and Vennerstrom, J. L. (1997). Haematin (haem) polymerization and its inhibition by quinoline anti-malarials. *Annals of Tropical Medicine and Parasitology* **91**: 559 – 566.

Roitt, I. M. (1997). *Roitt's Essential Immunology*, 9th Edition, pp 6 – 16. Blackwell Science Ltd, Oxford, UK.

Rook, G. A. W. (1989). Intracellular killing of microorganisms. *In*: M. Zembala and G. L. Asherson (eds), *Human monocytes*, pp 291 – 302. Academic Press, London.

Rosenblatt, J. E. (1999). Antiparasitic agents. *Mayo Clinic Proceedings* **74**: 1161 – 1175.

Rosenthal, P. J.; Wollish, W. S.; Palmer, J. T. and Rasnick, D. (1991). Antimalarial effects of peptide inhibitors of a *Plasmodium falciparum* cysteine proteinase. *Journal of Clinical Investigation* **88**: 1467 – 1472.

Sadick, M. D. (1992). Macrophages in parasitic infection. *In*: C. E. Lewis and J. O'D. McGee (eds), *The natural immune system: The macrphage*, pp 267 – 284. Oxford University Press, Oxford, UK.

Salvesen, G. and Nagase, H. (1989). Inhibition of proteolytic enzymes. *In*: R. J. Beynon and J. S. Bond (eds), *Proteolytic enzymes: a practical approach*, pp 83 – 104. Oxford University Press, Oxford, UK.

Schade, R.; Staak, C.; Hendrikson, C.; Erhard, M.; Hugl, H.; Koch, G.; Larsson, A.; Pollmann, W.; van Regenmortel, M.; Rijke, E.; Spielmann, H.; Steinbusch, H. and Straughan, D. (1999). The production of avian (egg yolk) antibodies: IgY. *ATLA* **24**: 925 – 934. www://altweb.jhsp.edu/publications/EVCAM21.htm.

Schiller, C.; Spittler, A.; Willheim, M.; Szépfalushi, Z.; Agis, H.; Köller, M.; Peterlik, M. and Boltz-Nitulescu, G. (1994). Influence of suramin on the expression of Fc receptors and other markers on human monocytes and U937 cells, and on their phagocytic properties. *Immunology* **81**: 598 – 604.

Schmidt, G. D. and Roberts, L. S. (1989). *Foundations of Parasitology*, 4Th ed, pp 139 – 166. Times Mirror / Mosby College Publishing, St. Louis, USA.

Schofield, L.; Novakovic, S.; Gerold, P.; Schwartz, R. T.; McConville, M. J. and Tachado, S. D. (1996). Glycosylphosphatidylinositol toxin of *Plasmodium* upregulates intracellular adhesion molecule-1, vascular cell adhesion molecule-1, and E-selectin expression in vascular endothelial cells and increases leukocyte and parasite cytoadherence via tyrosine kinase-dependent signal transduction. *Journal of Immunology* **156**: 1886 – 1896.

Schwartz, A. L.; Strous, G. J. A. M.; Slot, J. W. and Geuze, H. J. (1985). Immunoelectron microscopic localization of acidic intracellular compartments in hepatoma cells. *The EMBO Journal* **4**: 899 – 904.

Schwarzer, E. and Arese, P. (1996). Phagocytosis of malarial pigment hemozoin inhibits NADPH-oxidase activity in human monocyte-derived macrophages. *Biochimica et Biophysica Acta* **1316**: 169 – 175.

Schwarzer, E.; Alessio, M.; Ulliers, D. and Arese, P. (1998). Phagocytosis of the malarial pigment, hemozoin, impairs expression of major histocompatibility complex class II antigen, CD54, and CD11c in human monocytes. *Infection and Immunity* **66**: 1601 – 1606.

Schwarzer, E.; Bellomo, G.; Giribaldi, G.; Ulliers, D. and Arese, P. (2001). Phagocytosis of malarial pigment haemozoin by human monocytes: a confocal microscopy study. *Parasitology* **123**: 125 – 131.

Schwarzer, E.; De Matteis, F.; Giribaldi, G.; Ulliers, D.; Valente, E. and Arese, P. (1999). Hemozoin stability and dormant induction of heme oxygenase in hemozoin-fed human monocytes. *Molecular and Biochemical Parasitology* **100**: 61 – 72.

Schwarzer, E.; Müller, O.; Arese, P.; Siems, W. G. and Grune, T. (1996). Increased levels of 4-hydroxynonenal in human monocytes fed with malarial pigment hemozoin: a possible clue for hemozoin toxicity. *FEBS Letters* **388**: 119 – 122.

Schwarzer, E.; Turrini, F.; Giribaldi, G.; Cappadoro. M. and Arese, P. (1993). Phagocytosis of *P. falciparum* malarial pigment hemozoin by human monocytes inactivates monocyte protein kinase C. *Biochimica et Biophysica Acta* **1181**: 51 – 54.

Schwarzer, E.; Turrini, F.; Ulliers, D.; Giribaldi, G.; Ginsburg, H. and Arese, P. (1992). Impairment of macrophage functions after ingestion of *Plasmodium falciparum*-infected erythrocytes or isolated malarial pigment. *Journal of Experimental Medicine* **176**: 1033 – 1041.

Scorza, T.; Magez, S.; Brys, L. and De Baetselier, P. (1999). Hemozoin is a key factor in the induction of malaria-associated immunosuppression. *Parasite Immunology* **21**: 545 - 554.

Segal, A. W. (1989). The respiratory burst in monocytes and macrophages. *In*: M. Zembala and G. L. Asherson (eds), *Human monocytes*, pp 89 – 100. Academic Press, London.

Sehorn, M. G.; Slepenkov, S. V. and Witt, S. N. (2002). Characterization of two partially unfolded intermediates of the molecular chaperone DnaK at low pH. *Biochemistry* **41**: 8499 – 8507.

Senaldi, G.; Vesin, C.; Chang, R.; Grau, G. E. and Piguet, P. F. (1994). Role of polymorphonuclear neutrophil leukocytes and their intergrin CD11a (LFA-1) in the pathogenesis of severe murine malaria. *Infection and Immunity* **62**: 1144 – 1149.

Seth, P.; Mani, H.; Singh, A. K.; Banaudha, K. K.; Madhavan, S.; Sidhu, G. S.; Gaddipati, J. P.; Vogel, S. N. and Maheshwari, R. K. (1999). Acceleration of viral replication and up-regulation of cytokine levels by antimalarials: implications in malaria-endemic areas. *American Journal of Tropical Medicine and Hygiene* **61**: 180 – 186.

Shalmiev, G.; Krugliak, M.; Turrini, F. and Ginsburg, H. (1996). Antimalarial drugs inhibit the phagocytosis of erythrocytes infected with *Plasmodium falciparum*. *Transactions of the Royal Society of Tropical Medicine and Hygiene* **90**: 558 – 562.

Shaw, S. E. and Anderson, N. V. (1984). Isolation and functional analysis of normal canine blood monocytes and alveolar macrophages. *American Journal of Veterinary Research* **45**: 87 – 90.

Sherry, B. A.; Alava, G.; Tracey, K. J.; Martiney, J.; Cerami, A. and Slater, A. F. G. (1995). Malaria-specific metabolite hemozoin mediates the release of several potent endogenous pyrogens (TNF, MIP-1α and MIP-1β) *in vitro*, and altered thermoregulation *in vivo*. *Journal of Inflammation* **45**: 85 - 96.

Shinnick, T. M. (1991). Heat shock proteins as antigens of bacterial and parasitic pathogens. *Current Topics in Microbiology and Immunology* **167**: 145 – 160.

Skepper, J. N.; Karydis, I.; Garnett, M. R.; Hegyi, L.; Hardwick, S. J.; Warley, A.; Mitchinson,, M. J. and Cary, N. R. B. (1999). Changes in elemental concentrations are associated with early stages of apoptosis in human monocyte-macrophages exposed to oxidises low-density lipoprotein: an x-ray microanalytical study. *Journal of Pathology* **188**: 100 – 106.

Skinner, T. S.; Manning, L. S.; Johnston, W. A. and Davis, T. M. E. (1996). *In vitro* stage-specific sensitivity of *Plasmodium falciparum* to quinine and artemisinin drugs. *International Journal for Parasitology* **26**: 519 – 525.

Skinner-Adams, T. and Davis, T. M. E. (1999). Synergistic *in vitro* antimalarial activity of omeprazole and quinine. *Antimicrobial Agents and Chemotherapy* **43**: 1304 – 1306.

Slater, A. F. G.; Swiggard, W. J.; Orton, B. R.; Flitter, W. D.; Goldberg, D. E.; Cerami, A. and Henderson, G. B. (1991). An iron-carboxylate bond links the heme units of malaria pigment. *Proceedings of the National Academy of Sciences of the United States of America* **88**: 325 – 329.

Smilack, J. D. (1999). The tetracyclines. *Mayo Clinic Proceedings* **74**: 727 – 729.

Stachura, J. (1989). Cytochemistry of monocytes and macrophages. *In*: M. Zembala and G. L. Asherson (eds), *Human monocytes*, pp 27 – 36. Academic Press, London.

Sullivan, A. D.; Ittarat, I. and Meshnick, S. R. (1996). Patterns of haemozoin accumulation in tissue. *Parasitology* **112**: 285 – 294.

Sullivan, D. J. (2002). Theories on malarial pigment formation and quinoline action. *International Journal for Parasitology* **32**: 1645 – 1653.

Sullivan Jr., D. J.; Gluzman, I. Y. and Goldberg, D. E. (1996a). Plasmodium hemozoin formation mediated by histidine-rich proteins. *Science* **271**: 219 – 222.

Sullivan Jr., D. J.; Gluzman, I. Y.; Russel, D. G. and Goldberg, D. E. (1996b). On the molecular mechanism of chloroquine's antimalarial action. *Proceedings of the National Academy of Sciences of the United States of America* **93**: 11865 – 11870.

Tachado, S. D.; Gerold, P.; McConville, M. J.; Baldwin, T.; Quilici, D.; Schwarz, R. T. and Schofield, L. (1996). Glycosylphosphatidylinositol toxin of *Plasmodium* induces nitric oxide synthase expression in macrophages and vascular endothelial cells by a protein tyrosine kinase-dependent and protein kinase C-dependent signaling pathway. *The Journal of Immunology* **156**: 1897 – 1907.

Taramelli, D.; Basilico, N.; De Palma, A. M.; Saresella, M; Ferrante, P.; Mussoni, L. and Olliaro, P. (1998). The effect of synthetic malaria pigment (β-haematin) on adhesion molecules expression and interleukin-6 production by human endothelial cells. *Transactions of the Royal Society of Tropical Medicine and Hygiene* **92**: 57 – 62.

Taramelli, D.; Basilico, N.; Pagani, E.; Grande, R.; Monti, D.; Ghione, M. and Olliaro, P. (1995). The heme moiety of malaria pigment (β-hematin) mediates the inhibition of nitric oxide and tumor necrosis factor-α production by lipopolysaccharide-stimulated macrophages. *Experimental Parasitology* **81**: 501 – 511.

Taylor, W. R. J.; Widjaja, H.; Richie, T. L.; Basri, H.; Ohrt, C.; Tjitra; Taufik, E.; Jones, T. R.; Kain, K. C. and Hoffman, S. L. (2001). Chloroquine/doxycycline combination versus chloroquine alone, and doxycycline alone for the treatment of *Plasmodium falciparum* and *Plasmodium vivax* malaria in northeastern Irian Jaya, Indonesia. *American Journal of Tropical Medicine and Hygiene* **64**: 223 – 228.

Thiem, P. A.; Halper, L. K. and Bloom, J. C. (1988). Techniques for assessing canine mononuclear phagocyte function as part of an immunotoxicologic evaluation. *International Journal of Immunopharmacology* **10**: 765 – 771.

Thobakgale, C. F. (2002). Evaluation of antibodies raised in chickens against antimalarial drugs. MSc Thesis, University of Natal, Pietermaritzburg.

Thorpe, S. J. and Kerr, M. A. (1994). Common immunological techniques: ELISA, blotting, immunohistochemistry and immunocytochemistry. *In*: M. A. Kerr and R. Thorpe (eds), *Immunochemistry Labfax*, pp 175 – 189. BIOS Scientific Publishers Limited, Oxford, UK.

Thuma, P. E.; Weiss, G.; Herold, M. and Gordeuk, V. R. (1996). Serum neopterin, interleukin-4, and interleukin-6 concentrations in cerebral malaria patients and the effect of iron chelation therapy. *American Journal of Tropical Medicine and Hygiene* **54**: 164 – 168.

Tingle, M. D.; Mahmud, R.; Maggs, J. L.; Hawley, S.; Coleman, M. D.; Ward, S. A. and Park, B. K. (1998). The effect of 2,2'-substitution on the metabolism and toxicity of dapsone *in vitro* and *in vivo*. *Environmental Toxicology and Pharmacology* **5**: 145 – 153.

Tortora, G. J. and Grabowski, S. R. (2000). *Principles of anatomy and physiology, 9th Ed,* pp 69 – 76, 903 – 965. John Wiley & Sons, New York.

Towbin, H.; Staehelin, T. and Gordon, J. (1979). Electrophoretic transfer of proteins from polyacrylamide gels to nitrocellulose sheets: procedure and some applications. *Proceedings of the National Academy of Sciences of the United States of America* **76**: 4350 – 4354.

Turrini, F.; Schwarzer, E. and Arese, P. (1993). The involvement of hemozoin toxicity in depression of cellular immunity. *Parasitology Today* **9**: 297 – 300.

Vadas, P. and Pruzanski, W. (1986). Biology of disease: role of secretory phospholipase A_2 in the pathobiology of disease. *Laboratory Investigation* **55**: 391 – 404.

Vadas, P.; Keystone, J.; Stefanski, E.; Scott, K. and Pruzanski, W. (1992). Induction of circulating group II phospholipase A_2 expression in adults with malaria. *Infection and Immunity* **60**: 3928 – 3931.

Vadas, P.; Pruzanski, W.; Stefanski, E.; Ellies, L. G.; Aubin, J. E.; Sos, A. and Melcher, A. (1991). Extracellular phospholipase A_2 secretion is a common effector pathway of interleukin-1 and tumour necrosis factor action. *Immunology Letters* **28**: 187 – 193.

Vadas, P.; Taylor, T. E.; Chimsuku, L.; Goldring, D.; Stefanski, E.; Pruzanski, W. and Molyneux, M. E. (1993). Increased serum phospholipase A_2 activity in Malawian children with *falciparum* malaria. *American Journal of Tropical Medicine and Hygiene* **49**: 455 – 459.

Van Agtmael, M. A.; Eggelte, T. A. and van Boxtel, C. J. (1999). Artemisinin drugs in the treatment of malaria: from medicinal herb to registered medication. *Trends in Pharmcological Sciences* **20**: 199 – 205.

Van Beek, M. J. and Piette, W. W. (2001). Antimalarials. *Dermatologic Clinics* **19**: 147 – 160.

Van den Borne, B. E. E. M.; Dijkmans, B. A. C.; de Rooij, H. H.; le Cessie, S. and Verweij, C. L. (1997). Chloroquine and hydroxychloroquine equally affect tumor necrosis factor-α,

interleukin-6, and interferon-γ production by peripheral blood mononuclear cells. *The Journal of Rheumatology* **24**: 55 – 60.

Van Noorden, C. J. F. and Frederiks, W. M. (1992). *Microscopy Handbooks 26, Enzyme histochemistry: a laboratory manual of current methods*, pp 21 – 23, 65, 89. Oxford University Press, Oxford.

Van Oss, C. J. (1986). Phagocytosis: an overview. *Methods in Enzymology* **132**: 3 – 15.

Van Regenmortel, M. H. V.; Briand, J. P.; Muller, S. and Plaué, S. (1988). Synthetic polypeptides as antigens. *In*: R. H. Burdon and P. H. van Knippenberg (eds), *Laboratory techniques in biochemistry and molecular biology: Volume 19*, pp 1 – 39; 95 – 111; 131 - 158. Elsevier, Amsterdam.

Van Weert, A. W. M.; Geuze, H. J.; Groothuis, B. and Stoorvogel, W. (2000). Primaquine interferes with membrane recycling from endosomes to the plasma membrane through a direct interaction with endosomes which does not involve neutralisation of endosomal pH nor osmotic swelling of endosomes. *European Journal of Cell Biology* **79**: 394 – 399.

Velazquez, J. M.; DiDomenico, B. J. and Lindquist, S. (1980). Intracellular localization of heat shock proteins in *Drosophila*. *Cell* **20**: 679 – 689.

Verghese, M. W. and Snyderman, R. 1989). Signal transduction and intracellular messengers. *In*: M. Zembala and G. L. Asherson (eds), *Human monocytes*, pp 101 – 112. Academic Press, London.

Walther, M. M.; Rehak, N. N.; Venzon, D.; Myers, C. E.; Linehan, W. M. and Figg, W. D. (2000). Suramin administration is associated with a decrease in serum calcium levels. *World Journal of Urology* **18**: 388 – 391.

Warhurst, D. C. (1998). Antimalarial drug discovery: development of inhibitors of dihydrofolate reductase active in drug resistance. *Drug DiscoveryToday* **3**: 538 – 546.

Warley, A. (1990). Standards for the application of X-ray microanalysis to biological specimens. *Journal of Microscopy* **157**: 135 – 147.

Warley, A.; Cracknell, K. P. B.; Cammish, H. B.; Twort, C. H. C; Ward, J. P. T. and Hirst, S. J. (1994). Preparation of cultured airway smooth muscle for study of intracellular element concentrations by X-ray microanalysis: comparison of whole cells with cryosections. *Journal of Microscopy* **175**: 143 – 153.

Warley, A. (1997). X-ray microanalysis for biologists. *In*: A. M. Glauert, (ed.), *Practical methods in electron microscopy series : Volume 16,* pp 1 – 246. Portland Press, London.

Warley, A. and Skepper, J. N. (2000). Long freeze-drying times are not necessary during the preparation of thin sections for X-ray microanalysis. *Journal of Microscopy* **198**: 116 – 123.

Warr, G. W.; Magor, K. E. and Higgins, D. A. (1995). IgY: clues to the origins of modern antibodies. *Immunology Today* **16**: 392 – 398.

Warrell, D. A. (1997). Cerebral malaria: clinical features, pathophysiology and treatment. *Annals of Tropical Medicine and Parasitology* **91**: 875 – 884.

Weakley, B. S. (1981). A beginner's handbook in biological transmission electron microscopy, pp 24 – 26, 69 – 75. Churchill Livingstone, Edinburgh.

Weber, S. M.; Levitz, S. M. and Harrison, T. S. (2000). Chloroquine and the fungal phagosome. *Current Opinion in Microbiology* **3**: 349 – 353.

Welch, W. J.; Kang, H. S.; Beckmann, R. P. and Mizzen, L. A. (1991). Response of mammalian cells to metabolic stress; changes in cell physiology and structure/function of stress proteins. *Current topics in Microbiology and Immunology* **167**: 31 – 52.

Welling, G. W.; Weijer, W. J.; van der Zee, R. and Welling-Webster, S. (1985). Prediction of sequential antigenic regions in proteins. *FEBS Letters* **188**: 215 – 218.

Wernsdorfer, W. H. (1980). The importance of malaria in the world. *In:* J. P. Kreier (ed), *Malaria. Volume 1. Epidemiology, chemotherapy, morphology, and metabolism,* pp 1 – 93. Academic press, New York.

Wernsdorfer, W. H. (1997). Antimalarial drugs. *In*: G. Carosi and F. Castelli (eds), *Handbook of Malaria infection in the tropics. Quaderni di cooperazione sanitaria, no. 15*, pp 151-198. Organizzazione per la Cooperazione Sanitaria Internazionale, Bologna, Italy.

White, N. J. (1996). The treatment of malaria. *New England Journal of Medicine* **355**: 800 – 806.

Wickramasinghe, S. N. and Abdalla, S. H. (2000). Blood and bone marrow changes in malaria. *Balliere's: Best Practice and Research: Clinical Haematology* **13**: 277 – 299.

Williams, R. J. P. and Fraústo da Silva, J. J. R. (2000). The distribution of elements in cells. *Coordination Chemistry Reviews* **200 – 202**: 247 – 348.

Wilson, M. E. and Britigan, B. E. (1998). Iron acquisition by parasitic protozoa. *Parasitology Today* **14**: 348 – 353.

Winfield, J. B. and Jarjour, W. N. (1991). Stress proteins, autoimmunity, and autoimmune disease. *Current Topics in Microbiology and Immunology* **167**: 161 – 189.

Winstanley, P. A. (2000). Chemotherapy for *falciparum* malaria: the armoury, the problems and the prospects. *Parasitology Today* **16**: 146 – 153.

Wright, S. D. (1986). Methods for the study of receptor-mediated phagocytosis. *Methods in Enzymology* **132**: 204 – 221.

Wolf, R.; Tüzün, B. and Tüzün, Y. (2000a). Dapsone: unapproved uses or indications. *Clinics in Dermatology* **18**: 37 – 53.

Wolf, R.; Wolf, D. and Ruocco, V. (2000b). Antimalarials: unapproved uses or indications. *Clinics in Dermatology* **18**: 17 – 35.

Wu, B. J.; Kingston, R. E. and Morimoto, R. I. (1986). Human HSP70 promoter contains at least two distinct regulatory domains. *Proceedings of the National Academy of Sciences of the United States of America* **83**: 629 – 633.

Wynne, K. M. and Moore, M. (1982). Small-scale isolation and characterisation of human peripheral blood monocytes. *Journal of Pathology* **138**: 1 – 16.

Zhang, J.; Krugliak, M. and Ginsburg, H. (1999). The fate of ferriprotorphyrin IX in malaria infected erythrocytes in conjunction with the mode of action of anti-malarial drugs. *Molecular and Biochemical Parasitology* **99**: 129 – 141.

Ziegler, J.; Linck, R. and Wright, D. W. (2001). Heme aggregation inhibitors: antimalarial drugs targeting an essential biomineralization process. *Current Medicinal Chemistry* **8**: 171 – 189.